Recombinant protein production in the chloroplast of microalgae: a systems biology approach

A thesis submitted to the University of Manchester for the degree of Doctor of Philosophy

In the Faculty of Engineering and Physical Sciences

2014

Oluwafemi Davies

School of Chemical Engineering and Analytical Science

List of Contents

Word Count: 60,812

List of Figures

List of Tables

Abbreviations and symbols

ATP	adenosine triphosphate
atpβ	chloroplast ATP synthase *β*-subunit gene
atpA	chloroplast ATP synthase α-subunit gene
$CaCl_2.2H_2O$	calcium chloride dihydrate
CO_2	carbon dioxide
$CoCl_2.6H_2O$	cobalt (II) chloride hexahydrate
$CuSO_4.5H_2O$	copper sulphate pentahydrate
$FeSO_4.7H_2O$	iron (II) sulphate heptahydrate
g	grams
g dry wt	gram dry cell weight
g	acceleration due to gravity
h	hour
Hg	millimetre mercury
H_3BO_3	boric acid
IPTG	isopropyl-*β*-D-thiogalactopyranoside
$K_2HPO_4.3H_2O$	dipotassium hydrogen phosphate trihydrate
kb	kilo base pair
kDa	kilo dalton
KH_2PO_4	potassium dihydrogen phosphate
KOH	potassium hydroxide

K_S	substrate saturation constant
l	length
L	litre
Ln	natural logarithm
M	molar
m^2	square metre
m^3	cubic metre
mg	milligram
$MgSO_4.7H_2O$	magnesium sulphate heptahydrate
ml	millilitre
mM	millimolar
mm	millimetre
$MnCl_2.4H2O$	manganese (II) chloride tetrahydrate
mRNA	messenger ribonucleic acid
mt-	paternal mating type
mt+	maternal mating type
Na_2EDTA	disodium ethylene diamine tetra acetic acid
ng	nanogram
NH_4Cl	ammonium chloride
$(NH_4)_6Mo_7O_{24}.4H_2O$	ammonium heptamolybdate
nm	nanometre
O_2	oxygen
^oC	degree Celsius

psbA	chloroplast photosystem II protein D1 gene
psbD	chloroplast photosystem II protein D2 gene
rbcL	ribulose bisphosphate carboxylase gene
rrnL	*large subunit rRNA sequence*
rrnS	*16S rRNA sequence*
rpm	revolutions per minute
s	second
sd	standard deviation
TAP	tris acetate phosphate
tris	tris (hydroxymethyl) aminomethane
tRNA	transfer RNA
TSG6	tumour necrosis factor stimulated gene 6
UV	ultra violet light
$UV_{254\ nm}$	ultra violet light at 254 nm
$ZnSO_4.7H_2O$	zinc sulphate heptahydrate
ε	molar extinction coefficient
μ	specific growth rate
µg	microgram
µl	microlitre
µm	micrometre
µM	micromolar
μ_{max}	maximum specific growth rate
µmol	micromole

% (v/v)	percentage volume per volume
% (w/w)	percentage weight per weight
~	approximate to
>; >>	greater than; far greater than
<; <<	less than; far less than
≠	not equal
≤	less than or equal to
≥	greater than or equal to

Abstract

The University of Manchester

Oluwafemi Davies

Doctor of Philosophy

Recombinant protein production in the chloroplast of microalgae: a systems biology approach

19 September 2014

Several expression systems for recombinant protein production, essentially cells or whole organisms are currently in use today. Recently, research into recombinant protein production revealed a more attractive expression system based on the microalgae, *C. reinhardtii*, for significant savings in cost and production of correctly folded recombinant proteins. However, protein yield in the microalgae remain very low, non-predictable and whether this was due to limitations in the system was unclear. Using the expression of *E. coli β*-glucuronidase (gus) in *C. reinhardtii* chloroplast, the overall aim of the project was to address if the low recombinant gus yield in *C. reinhardtii* was due to limitations that affect growth and protein production, and if the fluxes for recombinant gus production were suboptimal (limiting). The finding was used to implement a strategy for a more predictable recombinant protein yield in *C. reinhardtii*. The research involved a range of experiments, analysis, and Flux Balance Analysis (FBA) modelling.

The growth of *C. reinhardtii* cultures were characterized in autotrophic, heterotrophic and mixotrophic conditions to identify factors that limit growth and recombinant gus yields. These factors were availability of light, carbon and nitrogen substrates, pH changes, protein burden and energetic limitation (ATP). The highest biomass was obtained in autotrophic and mixotrophic cultures (>1 g/litre), the lowest biomass was in heterotrophic cultures (~0.4 g/litre). The recombinant gus yields on the basis of dry cell weight were: mixotrophic cultures (0.038%), autotrophic cultures (0.032%), heterotrophic cultures (0.026%). No detectable protein burden was observed for expression of recombinant gus in autotrophic and mixotrophic conditions, but protein burden was significant in heterotrophic condition (15 – 18% reduction in growth rate). A strategy that significantly increased growth and cell productivity (>3 fold) in heterotrophic condition was identified. FBA was used to identify suboptimal amino acid steady state fluxes (bottlenecks) that limited the gus yield. Using FBA modelling, model verifications and corrections, a strategy that significantly increased the yield of recombinant gus in each cell (~2 fold) was identified. Put together, the total increase represents a 6 fold increase in recombinant gus yield. Furthermore, this research presented a framework for identifying, analysing and understanding the effect of the uptake of individual amino acid towards recombinant protein yield.

Declaration

I declare that no portion of this work referred to in this thesis has been submitted in support of an application for another degree or qualification of this or any other university or other institute of learning.

Candidate Name: Oluwafemi Davies

Faculty: Engineering and Physical Sciences

Thesis Title: Recombinant protein production in the chloroplast of microalgae: a systems biology approach

Signed: Date:

Copyright Statement

i. The author of this thesis (including any appendices and/or schedules to this thesis) owns certain copyright or related rights in it (the "Copyright") and s/he has given The University of Manchester certain rights to use such Copyright, including for administrative purposes.

ii. Copies of this thesis, either in full or in extracts and whether in hard or electronic copy, may be made **only** in accordance with the Copyright, Designs and Patents Act 1988 (as amended) and regulations issued under it or, where appropriate, in accordance with licensing agreements which the University has from time to time. This page must form part of any such copies made.

iii. The ownership of certain Copyright, patents, designs, trademarks and other intellectual property (the "Intellectual Property") and any reproductions of copyright works in the thesis, for example graphs and tables ("Reproductions"), which may be described in this thesis, may not be owned by the author and may be owned by third parties. Such Intellectual Property and Reproductions cannot and must not be made available for use without the prior written permission of the owner(s) of the relevant Intellectual Property and/or Reproductions.

iv. Further information on the conditions under which disclosure, publication and commercialisation of this thesis, the Copyright and any Intellectual Property and/or Reproductions described in it may take place is available in the University IP Policy (see http://www.campus.manchester.ac.uk/medialibrary/policies/intellectual-property.pdf), in any relevant Thesis restriction declarations deposited in the University Library, The University Library's regulations (see http://www.manchester.ac.uk/library/aboutus/regulations) and in The University's policy on presentation of Theses.

Acknowledgement

I would like to acknowledge and thank my colleagues in Anil Day's lab and in the plant sciences' groups for their help and support throughout this project. Particularly I would mention Julio, Leopoldo, Elena, Xun, Mohamed, Liz, Chuks, Chapman, Beth, Matty, Aniefon, Mayowa, Pete, Andy, Tom, Helena, Nick and Yaomin. Thank you all for the help and company we had in the groups which helped to create a friendly study environment. I extend my thanks to Dr. Giles Johnson, Dr Jon Pittman and Dr. Patrick Gallois for their support. In addition, many thanks to Cathy Winder, Samrina Rehman, Joseph French and other colleagues in the Manchester Centre for Integrative Systems Biology. Studying with you all has been enlightening, rich and blessed experiences for me.

My deepest gratitude goes to my supervisors, Prof. Hans Westerhoff and Dr. Anil Day. Many thank to Anil, not only for the close supervision but also for the constant motivation, encouragements and advices. My special thanks go to Hans for giving me the opportunity to work on this project, and also for providing the support framework to study at the University of Manchester. Many thanks also to my co-supervisors, Dr. Malkhey Verma and Prof Jacky Snoep. Special thanks to Malkhey and Dr. Ettore Murabito for reviewing this work. I would also like to acknowledge the EPSRC for their funding support through the School of Chemical Engineering and Analytical Sciences/Doctoral Training Centre grant.

Finally, I give many thanks to my family for their constant love, support and understanding through the years. They have been with me all along and helped to make this journey really worthwhile.

Chapter 1 – Introduction

1.1 Research background and problem

The production of recombinant proteins for applications such as therapeutic agents (biopharmaceutical proteins), diagnostic and analytical agents (enzymes and proteins) in industries and tools for scientific research constitutes a rapidly growing market (Fischer et al., 1999, Dove, 2002, Mayfield and Franklin, 2005). Recombinant proteins can only be produced in living cells, yet the production of recombinant proteins in cells is subject to many challenges because living cells are difficult to manipulate (Dove, 2002). For example, the ability to produce correctly folded and fully functional complex recombinant proteins in host cells can be a challenge (Dove, 2002). In addition, the high capital and operational costs for the production and recovery of recombinant proteins of sufficient quality presents other challenges (Dove, 2002). Different recombinant protein expression system such as bacteria cells, yeast cells, insect cells, mammalian cell cultures and animals exists (Fischer et al., 1999, Dove, 2002). All the systems have different levels of limitations ranging from high costly production operations, to incorrect protein folding, protein misfolding, protein aggregation, or poor protein yield (Dove, 2002).

Plants and microalgae have been identified for a more useful application for the production of recombinant proteins (Hiatt et al., 1989, Staub et al., 2000, Boynton et al., 1988, Ishikura et al., 1999, Franklin et al., 2002). Plants and microalgae may be attractive because they are photosynthetic leading to relatively inexpensive growth requirements with light used for their energetics. Therefore, in terms of capital and operational costs they are significantly cheaper (Dove, 2002, Fischer, 1999). They may be instructed to produce correctly folded and biologically active recombinant proteins in the chloroplast (Chebolu and Daniell, 2009, Franklin and Mayfield, 2004). Additionally, the proteins produced from plants and microalgae are generally regarded as safe (GRAS) for oral consumption or use as biopharmaceuticals (Fischer et al., 1999, Chebolu and Daniell, 2009, Franklin and Mayfield 2004). This is because proteins expressed in plants or microalgae chloroplasts are free from pathogenic contaminations and are correctly folded (Chebolu and Daniell, 2009,

Franklin and Mayfield 2004). However for plants, the disadvantage is that they typically require longer period of time to grow (usually many months to years) before the stable expression of recombinant proteins is achieved (Fletcher et al., 2007) following their transformations. This shortcoming does not occur in microalgae. Microalgae have relative fast growth rates meaning that stable expression of recombinant proteins can be achieved within few weeks after their transformation (Walker et al., 2005, Fletcher et al., 2007).

For recombinant protein production, the microalga that has been best characterized biochemically is *Chlamydomonas reinhardtii* (Harris, 1989, Merchant et al., 2007, Maul et al., 2002, Popescu and Lee, 2007). The expression of recombinant proteins including human growth factors (Devinoy et al., 1994), vaccines epitomes (Rasala et al., 2010), antibodies and enzymes in *C. reinhardtii* chloroplast has been demonstrated (Mayfield et al., 2003, Mayfield and Franklin, 2005, Ishikura et al., 1999). Despite these successes, the yields of recombinant proteins expressed in *C. reinhardtii* remain consistently very low, typically about 0.01 – 0.1% of total soluble proteins (Ishikura et al., 1999, Komine et al., 2002, Franklin et at., 2002, Mayfield et al., 2003, Surzycki et al., 2009, Rasala et al., 2010). These authors used combinations of molecular biology approaches involving genetic modifications, design of promoter constructs and combinations, codon optimization, and chloroplast transformations in order to generate transgenic strains of capable of increasing the expression yield for the recombinant protein of choice. However, the low recombinant protein yield persists for *C. reinhardtii*. This low yield presents challenge that must be addressed if the expression system based on *C. reinhardtii* may achieve large-scale production potential for biopharmaceutical proteins. Only a Few reports of protein yield of higher than 2% total soluble proteins exists (Surzycki et al., 2009, Rasala et al., 2010).

1.1.1 Research approach

In general, living cells are difficult to manipulate. For example, it is possible to modify, engineer or transform cells to produce a certain protein, but cells are robust systems. They are able to adapt and respond to perturbations in their metabolic, genetic or hierarchical

organization and maintain their homeostasis to ensure their survival (Kell and Westerhoff, 1986, Snoep et al., 2002, ter kuile and Westerhoff, 2001). Cells can invoke complex responses involving metabolic, genetic and signalling capacities to regulate and elicit control mechanisms that maintain their homeostasis in the presence of such perturbations (Kell and Westerhoff, 1986, Snoep et al., 2002, ter kuile and Westerhoff, 2001). The cell is likely to experience the recombinant protein production as such a perturbation and its homeostatic responses will then tend to counteract the perturbation. The likely result is that recombinant protein yield, may be far lower than the yield that was expected, and in many cases erratic and unpredictable because the cell may not always engage in the same homeostatic response (ter kuile and Westerhoff, 2001).

Therefore, in the current study a different approach (one that may complement and significantly move forward the recombinant protein research in microalgae, but also inspire new approaches to protein production in other systems) is presented. This system biology approach will be used to shine light on the growth and recombinant protein production in *C. reinhardtii*, to identify and understand limitations. The understanding will be used to identify and understand strategies that are predictive of a significantly increased recombinant protein yield. Systems biology studies how life arises in otherwise dead matter, or how living systems (cells, tissues, organs, whole organisms) function through non-linear interactions of their molecular components (Westerhoff and Alberghina 2005). This also includes the study of how biological forms, structures, functions and processes that sustain life arise through interactions of the components of biological systems, and therefore their responses to the external environment. In the last decade, systems biology has developed as an inter-disciplinary area of research that studies complex networks of living organisms, and integrates quantitative experimental (biological) data and theoretical analysis including modelling approaches (Navlakha and Bar-Joseph, 2011). Systems biology is being implemented to understanding the function of living cells and to make biology more predictable. For example, system biology approaches have been applied to drug target identification (Oberhard et al., 2013), and to metabolic engineering (Ranganathan et al., 2010), but has not yet been implemented to predict a robust and increased recombinant protein production in the microalgae.

In the current study, a range of experiments, analysis, flux balance analysis (FBA) modelling, model predictions and verifications was used to identify major factors affecting growth, the limitations to growth and recombinant protein yield. The model of recombinant protein production studied in this work was the expression of *E. coli* β-glucuronidase (gus) in the chloroplast of *C. reinhardtii*. The expression of this recombinant protein was previously demonstrated in *C. reinhardtii* (Ishikura et al., 1999) with a very low yield (0.01 – 0.08% total soluble protein).

1.1.2 Project aims and objective

The main aim of this project was to address whether the low recombinant protein yield in *C. reinhardtii* was due to limitations that affect growth, and if the fluxes for recombinant protein production were suboptimal (limiting). This included the implementation of integrated approaches involving quantitative experimentations, analysis of growth, recombinant protein production, and FBA modelling for a more predictable and higher recombinant protein yield in *C. reinhardtii*. The objectives include:

1. To understand and characterize the growth of *C. reinhardtii* strains under various growth conditions (autotrophic, heterotrophic and mixotrophic).

2. To identify and characterize limitations that affect the growth and recombinant protein yields.

3. To use flux balance analysis on the genome scale model of algae metabolism (AlgaGEM) to study steady state distribution of fluxes associated with maximal protein production, and to identify fluxes that limit protein production.

4. To gain understanding of the effect of the suboptimal fluxes on the recombinant protein yield.

5. Identification, understanding and the design of strategy for improved microalgae growth, predictable and optimized yield for the recombinant protein.

1.2 Key results and major contributions

1. Identification of a growth strategy that significantly increased the growth of *C. reinhardtii* heterotrophic cultures (> 3 fold increase), and of a strategy that significantly increased recombinant gus yield in each cell (~2 fold increase). Put together, this represents a 6 fold increase in amount of recombinant gus. The combination of the quantitative experiments, analysis and the FBA modelling was a first in the field of recombinant protein expression research for the microalgae. These approaches may be applied to other recombinant proteins expressed in microalgae.

2. Recombinant protein yield was limited by availability of light and carbon, limited also by protein burden, and by suboptimal amino acid fluxes in the metabolic network.

3. The protein burden or protein cost represents the fractional reduction in growth rate due to expression of recombinant gus. No detectable protein cost was detected for cultures grown in autotrophic or mixotrophic condition, but in heterotrophic condition the protein burden was high (15 – 18% reduction in growth rates). No protein cost data has been published for the expression of foreign proteins in microalgae (although data exist for bacteria and yeast). Therefore, this finding was a milestone. The protein cost may be useful to study and understand the yield of recombinant protein that may be allowed by the cell without cessation of growth.

4. An approach was established for identifying, analysing and understanding the effect of the uptake of individual amino acids on recombinant protein yield. Upon understanding the effect of the assimilation of an amino acid on the yield, growth cultures may be supplemented with the amino acid or combinations of amino acid so as to optimize the recombinant protein yield.

5. Based on these results, other strategies that may further increase recombinant protein yield were identified, and proposed for future work towards recombinant protein research. These include the identification, characterization and optimization of the expression of specific transporters for amino acids or processes for the uptake of amino acids into cells.

1.3 Thesis organization

The thesis was organized into seven chapters. Chapter 1 which is the current chapter is the introduction of the PhD project. This introduction starts with the background to the research and the research problem, and then summarizes the research approach, the research aims, objectives and the key results. Chapter 2 is a detailed literature review of the topic highlighting previous and the current state of knowledge in the research area. This review begins with a brief description of the *Chlamydomonas reinhardtii*, aspects of its nutrition, laboratory-scale and large-scale cultivation of the microalgae. Thereafter, we discuss the various applications of recombinant proteins, the different platforms used for expressing them, and the techniques used to generate transgenic strains capable of expressing recombinant proteins. Then we present a brief look into applications of systems biology approaches that may facilitate an understanding of the recombinant protein research in microalgae.

Chapter 3 presents the materials and detailed methods used in the current work (both experimental and FBA modelling). In Chapters 4 and 5, the experimental results are presented, analysed and discussed. Here the limitations to growth and protein yield such as availability of light, carbon, pH, nitrogen, protein cost and ATP limitations are presented. The strategy that significantly increased the growth of *C. reinhardtii* was identified and presented here. In Chapter 6, the FBA modelling and prediction of the metabolic steady state fluxes was used to identify a solution for maximal protein yield. In addition, suboptimal amino acid steady state fluxes that limited the yield of protein were identified. The effect of the uptake of individual amino acid on the FBA predicted gus yield was presented. The FBA predictions were verified by quantitative experiments and the results of these experiments are also discussed in this chapter. The strategy that significantly increased the yield of the recombinant protein in cells was presented and discussed.

In Chapter 7, the summary of the results of Chapters 4, 5 and 6 was presented and the conclusions were made. In addition, suggestions for further work and future scope that may significantly move the recombinant protein research forward were presented.

Chapter 2 - Literature Review

2.1 The *Chlamydomonas* species

Algae are a diverse group of eukaryotic and autotrophic organisms ranging from the unicellular green algae (microalgae) to the multicellular algae or macroalgae (Rosenberg et al., 2008). Generally, microalgae are microscopic and well known examples include *Chlamydomonas, Chlorella, Dunaliella*, and *Haematococcus* (Harris, 1989). Microalgae show great adaptations and are widely distributed in different habitats such as soils, fresh-water, sea-water and sewage ponds (Harris, 1989). *Chlamydomonas* species are motile single-cell organisms propelled in liquid medium by aid of a pair of flagella (Harris, 1989). Several species of the *Chlamydomonas* including *C. reinhardtii, C.eugametos, C. moewusii, C. smithii, C. britannica* and *C. frankii* are well described and commonly studied.

Among the *Chlamydomonas* species, *C. reinhardtii* (Figure 2.1) has attracted more attention as a model for studying biological systems because this organism is the most biologically characterized *Chlamydomonas* (Harris, 1989). The study of *C. reinhardtii* has been used to gain understanding about the evolution of cells, formation of cellular structures (such as cilia, flagella) and organelles (chloroplast and mitochondrion) many cellular functions in eukaryotes (Harris, 1989). As a eukaryotic model organism, cellular functions such as cell motility, cell growth, reproduction, genetics, cellular respiration and photosynthesis have been well studied using *C. reinhardtii* (Harris, 1989). Studies such as the adaptations of cells to their environment (Collins and Bell, 2004), and the effects of mutations on cell fitness (deVisser et al., 1996) have been demonstrated using *C. reinhardtii*. The genomes in *C. reinhardtii* (chloroplast, nuclear and mitochondrion) are well characterized (Maul et al., 2002, Merchant et al., 2007, Popescu and Lee, 2007), and provides wealth of information for genetic manipulation and studies of this microalgae.

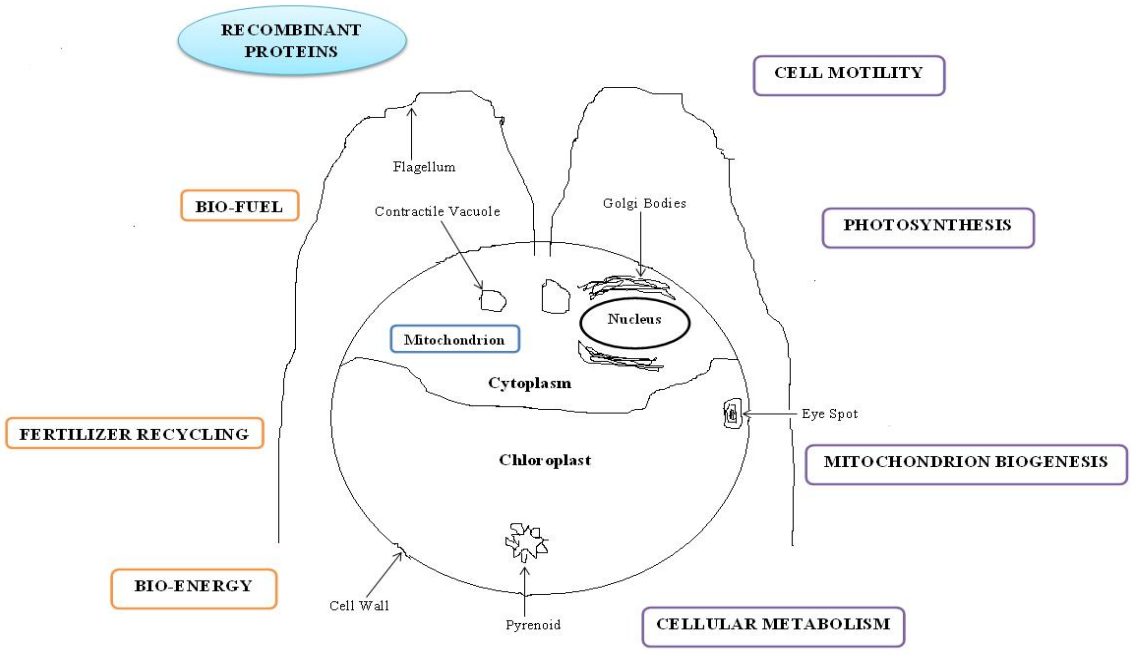

Figure 2.1: *Chlamydomonas reinhardtii* cell showing prominent cellular features (chloroplast, mitochondrion, eyespot, pyrenoid, flagellum, contractile vacuoles, nucleus and golgi body) and some applications of the *C. reinhardtii* model in research.

Today, *C. reinhardtii* continue to attract increasing research attention in other areas related to the cell metabolism. These includes the research into alternative fuel production such as biodiesel and bio-ethanol production (Mitra and Melis, 2008), and studies for alternative energy production such as bio-hydrogen and bio-methane production using *C. reinhardtii* (Cournac et al., 2002, Melis and Happe, 2004). Since the last two decades, research into recombinant protein production such as the expression of enzymes, proteins, human growth factors, antibodies, and vaccine in *C. reinhardtii* has attracted increasing attention (Ishikura et al., 1999, Mayfield et al., 2003, Purton, 2007, Rasala et al., 2010).

2.1.1 Microalgae culture collections.

Many strains of *Chlamydomonas* species studied in the laboratory are currently obtained from major algae culture collection centres in the world where they are grown and maintained. One of such algae collection centres includes the Chlamydomonas Resource Centre (formerly called Chlamydomonas Culture Collections) at the University of

Minnesota, Minnesota, USA. The centre holds more than 2400 strains of *Chlamydomonas* (wild type and mutants strains), hundreds of plasmids and several cDNA libraries (http://www.chlamy.org). Another is the culture collection of Algae at Goettingen University (SAG), Germany that maintains a huge diversity of microalgae (http://www.uni-goettingen.de/en/184982.html). In the United Kingdom, the Culture Centre of Algae and Protozoa (CCAP) maintain thousands of algae and protozoa strains (http://www.ccap.ac.uk). The collection centres provide useful resources, links and information regarding maintaining cultures and tools for *Chlamydomonas* research.

2.1.2 Maintaining *C. reinhardtii* cultures in the laboratory

The wild-type *C. reinhardtii* cells are either mating-type plus (*mt+*) for the maternal parent, or mating type minus (*mt-*) representing the paternal parent (Harris, 1989). Both parents are strictly controlled in the population of vegetative cells so that the population contain only *mt+* or only *mt-* but not both (Harris, 1989). This is very important to the cell population as they can only propagate by asexual cell division (Harris, 1989)). The maintenance of *C. reinhardtii* cultures is easy to achieve but contamination problems may arise if aseptic, sterile techniques and good laboratory practises are not followed. The cultures are susceptible to bacteria, fungi and yeast contaminations, and these could be seriously difficult to eradicate without losing the cultures. The requirements for growth of *C. reinhardtii* cultures include water, source of carbon and nitrogen (Sager and Granick, 1953), and trace elements (Hutner, 1949). There are a number of culture media available to grow *C. reinhardtii* cultures. Three commonly used laboratory culture media for *C. reinhardtii* are listed on Table 2.1. These include tris-acetate-phosphate medium or TAP (Gorman and Levine, 1965), minimal medium (Gorman and Levine, 1965) and Sueoka high-salt medium (Sueoka, 1960).

The minimal medium lacks organic carbon source and is used for autotrophic growth. On the other hand, TAP and Sueoka high-salt media are rich in organic carbon and may be used for growing the cultures under heterotrophic or mixotrophic conditions. For example, the use of TAP or Sueoka high-salt media makes it possible to grow and study photosynthetic-mutant strains in dark condition (heterotrophic), which otherwise are unable to grow in light conditions (autotrophic or mixotrophic conditions). Despite the

availability of many organic carbon compounds, only a few (mainly simple organic carbon compounds) have proved successful for heterotrophic growth of *Chlamydomonas* (Harris, 1989). For *C. reinhardtii*, these include acetate, monoacetin, acetyl methyl acetate and acetyl methyl carbinol (Sager and Granick, 1953, Harris, 1989). Use of carbon sources such as glucose, sucrose, lactose, galactose, mannose, D-xylose, L-arabinose, ribose, starch, mannitol, glycerophosphate, propionate, ethanol, glycerol, butyrate, formaldehyde, formate, oxalate, tartrate, pyruvate, malate, fumarate, succinate, citrate, α-ketoglutarate, trans-aconitate, glutamate, aspartate, asparagine, glycine and glutamine fail to support heterotrophic growth of *C. reinhardtii* (Sager and Granick, 1953, Harris, 1989). However, the metabolic pathways and enzymatic reactions utilizing and producing many of these carbon compounds exist within the *C. reinhardtii* cellular metabolism (Kanehisa et al., 2014).

Table 2.1: Common types of media used to grow *Chlamydomonas* cultures.

Media type	**Description of medium**
Minimum medium (Gorman and Levine, 1965).	A carbon-free medium used for autotrophic growth. A selective medium against photosynthetic-mutant strains.
Sueoka high-salt medium (Sueoka, 1960).	A medium containing acetate, higher concentration of ammonium and phosphate salts for growth of cultures
Tris-Acetate- Phosphate Medium (Gorman and Levine, 1965).	TAP is widely used for growing *C. reinhardtii* cultures, and contains acetate, ammonium, phosphate salts and tris buffer.

Inorganic carbon sources such as CO_2 or dissolved as HCO_3^- ions support the autotrophic and mixotrophic growth of *Chlamydomonas* (Collins and Bell, 2004, Moroney and Ynalvez, 2007). The availability of CO_2 for growth depends on the environment, and the

availability may be limited by the diffusion of the gaseous CO_2 in water (Moroney and Ynalvez, 2007). As part of the adaptation to very low CO_2 (Collins and Bell, 2004), *C. reinhardtii* has been shown to elaborate, operate very efficient carbon transport into cells, and to efficiently concentrate carbon internally within the cell (Moroney and Ynalvez, 2007).

Simple inorganic nitrogen sources such as ammonium, nitrate and nitrite (Syrett, 1962, Thacker and Syrett, 1972) support the growth of *Chlamydomonas*. But *Chlamydomonas* species carrying *nit1* and *nit2* mutations for nitrate reductase are unable to grow on nitrate or nitrite as nitrogen source, and would require alternative nitrogen source such as ammonium (Harris, 1989). Organic nitrogen sources such as urea (Hodson et al., 1975), glutamine (Sager and Granick, 1953), acetamide (Gresshoff, 1981), adenine, guanine, urate, hypoxanthine, xanthine, allantoin (Pineda et al., 1984) have been found useful nitrogen source for the growth of *Chlamydomonas*.

2.1.3 Factors that affect large-scale microalgae growth

Large-scale cultivation of microalgae may be possible by scaling up cultures from the laboratory-scale (culture flasks of several hundred millilitres) to large-scale growth facilities of thousands of litres. Currently, large-scale facilities for growing microalgae are either open-culture system (Terry and Raymond, 1985, Weissman et al., 1988) or closed-culture system (Grima et al., 1999, Weissman et al., 1988). In both facilities, the cultivation of microalgae is by continuous culture method in which fresh growth medium is continuously fed into the facility and the used broth is removed at constant rates.

An open-culture system is a pond open to the environment often called a raceway pond (Terry and Raymond, 1985). Raceway ponds are designed for easy operation, low capital and low operational costs (Weissman et al., 1988). However, the disadvantage of the system is its unsuitability for growing pure cultures of microalgae for expressing recombinant proteins due to contamination issues (Weissman et al., 1988). Other typical problems include poor temperature control, high evaporative water losses, poor mixing effects, low efficiency in use of CO_2 and lowered cell productivity (Weissman et al., 1988).

Closed-culture system is one that is closed from the environment. Typical example of such a system is the photo-bioreactor (Terry and Raymond, 1985, Weissman et al., 1988). The photo-bioreactor is used for the growth of cultures to avoid contamination problems, and as such maybe used for the growth of microalgae for recombinant protein production. Other advantages include improved temperature control, good mixing effects, low water losses, high efficiency in the use of CO_2 use and high cell productivity (Weissman et al., 1988). Nevertheless, the drawback is the higher capital, maintenance and operational cost (Weissman et al., 1988). Design and operational parameters that could be optimized in order to improve microalgae growth are discussed in the next sub-sections.

2.1.3.1 The availability of light, light intensity and light wavelength

The availability of light affects the growth of microalgae (Harris, 1989, Lien and Knutsen, 1976, Mihara and Chase 1971). For autotrophic cultures cultivated in light and dark cycle periods, growth was shown to depend on the availability of light. For example, *C. reinhardtii* cultures were shown to require no less than 8 h light duration in order to grow (Harris, 1989). Generally, longer light duration periods more than 8 h are used to grow cultures (Harris, 1989, Lien and Knutsen, 1976, Mihara and Chase 1971), with 12 h light and 12 h dark commonly used (Mihara and Chase, 1971, Harris 1989) to grow cultures sychronously. In the photo-bioreactor, adequate provision of light within all areas of the vessel is essential for growth.

Light intensity affects photosynthetic rates, and therefore, the growth and cell productivity of autotrophic or mixotrophic cultures (Brown and Geen, 1974, Lee and Low, 1992). Higher microalgae growth could be achieved by increasing light intensity to the optimum value as well as improving availability of light to cultures. Nonetheless, the effective penetration of light into the photo-bioreactor becomes a limiting factor, particularly, in dense cultures where different amount of light are received in different zones in the photo-bioreactor (Apt and Behrens, 1999). The problem of light penetration can be made worse by poor design of the growth facility. On the other hand, supplying excessive light or light intensity, could cause photo-inhibition of growth (Grima et al., 1999, Grima et al., 1996).

The wavelength of the supplied light is another parameter that affects growth since photosynthetic active radiations only occurs within 400 – 700 nm (Brown and Geen, 1974).

2.1.3.2 Temperature and pH control

Temperature and pH are important variables that affect cell growth because extremes of these parameters denature cell proteins and enzymes (Sinclair, 1987). *C. reinhardtii* would grow over pH range 6.5 – 8.0 but not at pH 5 (Sager and Granick, 1953). *Chlamydomonas* grow over the range of 15 – 30^{o}C with optimum temperature around 20 – 25^{o}C (Harris, 1989). Besides, the growth of microalgae cultures generates heat and requires effective control in order to avoid temperature rises and heat gradients within the growth facility. Effective temperature control may be employed through the use of temperature controlled thermostat device or use of heat exchangers (Chisti, 2007, Pulz, 2001).

2.1.3.3 Gaseous exchange limitations

Gaseous exchange problems arise within the culture facility due to diffusional limitations of gases such as air, CO_2 into the liquid medium and affect microalgae growth (Apt and Behrens, 1999). The diffusion of gases into the medium may be improved by increasing the cross-sectional surface area of the liquid medium. To do this adequate stirring and mixing within the cultures could be required (Grobbelaar, 2010). This improves aeration, mass transfer, diffusion of gases in the culture facility (Harris, 1989, Grobbelaar, 1994, Grobbelaar, 2010). This may also be achieved by bubbling air into the photo-bioreactor (Weissman et al., 1988), and excessive O_2 generated from photosynthesis must be removed from the photo-bioreactor to prevent photo-oxidative damage to microalgae cells (Weissman et al., 1988).

2.1.3.4 Mixing and turbulent flow

Good mixing of the culture would be to prevent the sedimentation of microalgae cells, and formation of deficient zones for nutrients, gases, temperature and pH gradients (Grobbelaar, 2010). Adequate mixing creates turbulent flow that aid to move the cells

uniformly through different zones with in the photo-bioreactor and enhance uniform light profile within the culture (Grobbelaar, 1994, Grobbelaar, 2010), thereby improving cell growth and productivity. In spite of this, excessive mixing can produces strong turbulence that may lead to cell damages and death. For that reason, the degree of mixing, mixing time, as well as the energy input and the energy transfer efficiency of mixers are important parameters that need to be optimized in order to achieve optimal microalgae growth (Grobbelaar, 1994, Grobbelaar, 2010).

2.2 Recombinant protein expression systems

The production of proteins by recombinant technology of sufficient quantity and good quality is important to biopharmaceutical, biotechnology industries and to research using recombinant proteins (Fischer et al., 1999, Dove 2002, Mayfield and Franklin, 2005). Proteins can only be produced in cells, meaning that a variety of host cell types may be used for the expression and recovery of recombinant proteins (Fischer et al., 1999, Dove, 2002, Mayfield and Franklin). Recombinant therapeutic proteins (biopharmaceutical proteins) such human growth hormone (Devinoy et al., 1994), antibodies (Mayfield and Franklin, 2005, Mayfield et al., 2003), and vaccines (Chebolu and Daniell, 2009, Rasala et al., 2010) find applications in treatment of disease conditions or disease prevention (Dove, 2002). These biopharmaceutical proteins have demonstrated advantages over chemically synthesized drugs. These include their higher selectivity, higher specificity and greater effectiveness on biological targets leading to fewer side effects but greater successes in the treatment of diseases (Dove, 2002). These advantages are possible if the proteins are in their stable, functional, and biologically active form (Dove, 2001). Cells are difficult to manipulate for recombinant protein production because different cellular regulatory controls exist (Kell and Westerhoff, 1986, Snoep et al., 2002, ter kuile and Westerhoff, 2001), cellular limitations and bottlenecks abound making recombinant protein production a very costly venture (Dove, 2002). Today, research aimed at identifying and the development of cost-effective processes for producing biologically active therapeutic protein make up substantial investment in biopharmaceutical and biotech industries (Dove, 2002).

Furthermore, proteins made by recombinant technology find applications as enzymes, proteins and analytical agents research (Fischer et al., 1999, Mayfield et al., 2007). The applications for recombinant proteins will continue to increase in the near future as new recombinant proteins are produced. Currently, recombinant technology uses molecular biology techniques involving cloning a foreign gene into a vector, and the transformation of host cells to express the foreign gene product (recombinant protein). Some examples of host used to express recombinant proteins include mammalian cells, insect cells, yeast cells, bacteria cells, animals and plants (Fischer et al., 1999). These expression systems were compared by Fischer et al. (1999) in terms of the cost of operation, the type of recombinant protein that could be produced, protein yield, risks and safety of the processes. The summary of the comparisons are shown on Table 2.2.

Table 2.2: Some features of recombinant protein expression systems in bacteria cells, yeast cells, mammalian cells, animals, and plant (Fischer et al., 1999).

Cost of Operation:	Bacteria cell	Yeast cell	Mammalian cell	Animals	Plants
Production	Medium	Medium	High	High	Low
Scale-up	High	High	High	High	Low
Storage	Cheap	Cheap	Expensive	Expensive	Cheap
Recombinant protein:					
Glycosylated	Absent	Incorrect	Correct	Correct	Not always
Complex Protein	No	No	No	Yes	Yes
Protein yield:	Medium	High	Medium	High	High
Risky:	Yes	Unknown	Yes	Yes	Unknown
Safety level:	Low	Unknown	Medium	High	High

The different expression systems listed on Table 2.2 have distinct limitations and advantages. For example, the production and capital costs involved with the expression of recombinant proteins in mammalian cells or animals are generally higher than the costs incurred using plants. However, if the proteins are needed in a fully glycosylated state, then the mammalian cell culture or animal may be better alternatives since glycosylation is always guaranteed to occur in these systems. If the criteria are the production of correctly folded, functional complex proteins, and at relatively cheap costs, then the plant expression system has distinct advantages over the others (Hiatt et al., 1989, Staub et al., 2000, Dove, 2002). As well as these, there are no risks of prion contamination for recombinant proteins expressed in plants (Chebolu and Daniell, 2009), making the system more attractive for production of biopharmaceutical proteins, or proteins met for oral consumption as food.

2.2.1 Microalgae as an expression system for recombinant proteins.

The successful expression of recombinant proteins in the chloroplast of *C. reinhardtii* has been achieved (Ishikura et al. 1999, Mayfield et al., 2003, Rasala et al., 2010). Like plants, the opportunity for recombinant protein production in the microalgae offers several advantages. *Chlamydomonas reinhardtii* possesses the cellular machinery to correctly fold recombinant protein in the chloroplast (Franklin and Mayfield, 2004), and the ability to assemble complex mammalian proteins in the chloroplast (Mayfield et al., 2003, Rasala et al., 2010). Additionally, the proteins expressed in microalgae are free from prion (which may be concern for protein expressed in transgenic animal), and free of pathogenic contaminations, which may be concerns for proteins expressed in bacteria cells (Chebolu and Daniell, 2009, Franklin and Mayfield, 2004, Manuell et al., 2007). Besides, microalgae are generally regarded as safe (GRAS) for food consumption, and this GRAS status extends to recombinant protein produced in the cells (Franklin and Mayfield, 2004, Gantar and Svircev, 2008). Another advantage is that microalgae including *C. reinhardtii* are photosynthetic and grow cheaply using light, water, CO_2, simple nitrogenous sources, and trace elements (Harris, 1989). Consequently, the anticipated cost of expressing recombinant proteins in the microalgae may be a fraction of those incurred in mammalian cell culture, transgenic animals, bacteria or yeast cells. Moreover, the chloroplast offer high level of biological containment (Ruf et al., 2007) thereby highly reducing the risk for loss of the transgenes to the environment.

Microalgae have some advantages over plants for use in recombinant protein expression. Firstly, microalgae have faster growth rates than plant (Walker et al., 2005). Therefore, the time taken from the transformation of microalgae cells to the stable expression of recombinant proteins is relatively shorter (usually a few weeks). For plants, the stable expression of the recombinant proteins may take years to achieve after the transformation event (Fletcher *et al.*, 2007). Secondly, microalgae could be grown in a closed-culture system such as the photo-bioreactor (Walker et al., 2005), and this would not displace agricultural land met to grow food crops (Fletcher et al., 2007). Thirdly, the photo-bioreactor ensures that the microalgae is physically separated from the environment and do not contaminate the environment. The spread of pollen from plants poses regulatory concerns for the environment, since such flow guarantees that transgenes may contaminate and affect the environment (Ellstrand, 2001, Quist and Chapela, 2001). This is not the case for microalgae (*C. reinhardtii*) since they propagate through asexual cell division, making it impossible to spread genes (endospores) to the environment (Harris, 1989). For the unicellular green algae, the cost of protein extraction and purification may be relatively lower than those incurred from multicellular plant tissues (Walker et al., 2005). Therefore, the microalgae may potentially offer a lower cost production platform for the production of recombinant proteins. However, a bottleneck for recombinant protein production in *C. reinhardtii* is the inherent low yield (typically, about 0.01 – 0.1% of total soluble protein) of recombinant protein in the chloroplast (Mayfield and Franklin, 2005, Mayfield et al., 2003, Rasala et al., 2010, Wang et al., 2008).

2.2.2 *Chlamydomonas reinhardtii* genomes

Three distinct genomes have been identified in *C. reinhardtii*: chloroplast genome (Maul et al., 2002), mitochondrion genome (Popescu and Lee, 2007), and the nuclear genome (Merchant et al., 2007). The nuclear genome is the largest genome (~121 Mb) and contains about 15,000 genes (Merchant et al., 2007). Genetic inheritance of nuclear genes occurs by mendelian crosses of the maternal gametes (*mt+*) and paternal gametes (*mt-*) in *C. reinhardtii* (Harris, 1989). The chloroplast genome was reported by Rochaix (1995) as ~200 kb circular DNA molecule. There are about 80 copies of the genome per cell (Rochaix, 1995). The chloroplast genes are inherited only from the maternal gamete (Corriveau and Coleman, 1988). The mitochondrion genome is the smallest ~16 kb and is a

linear DNA molecule (Grant and Chiang, 1980) containing about 12 genes (Gray and Boer, 1988, Michaelis et al., 1990). Mitochondrial genes are inherited only from the paternal gamete (Boynton et al., 1987).

The different transformation methods for the *C. reinhardtii* genomes are listed on Table 2.3. The biolistic particle bombardment and glass-bead methods are popular and effective for transforming the chloroplast and nuclear genomes. The transformation of the mitochondrion genome is difficult to achieve but was reported with extremely low efficiency (Randolphanderson et al., 1993).

Table 2.3: Transformation methods for *C. reinhardtii* genomes.

Transformation Method	**Genome**	**References**
Biolistic particle Bombardment	Nuclear	(Debuchy et al., 1989)
	Chloroplast	(Boynton et al., 1988)
	Mitochondrial	(Randolphanderson et al., 1993)
Glass-bead	Nuclear	(Kindle, 1990)
	Chloroplast	(Kindle et al., 1991)
Silicon carbide whiskers	Nuclear	(Dunahay, 1993)
Electroporation	Nuclear	(Shimogawara et al., 1998)

2.2.3 Chloroplast and nuclear genome transformations

Transformation of a *C. reinhardtii* genome involves the integration of a cloned foreign DNA (transgene) into the genome. Transformation of the nuclear genome has been reported, but with extremely lowered expression yield for the recombinant protein (Casas-Mollano et al., 2007, Neupert et al., 2009, Rochaix, 2002). A number of factors have been cited to account for the extremely lowered expression level and recombinant protein yield from a transformed nucleus. The occurrences of intron sequences in the nuclear genes have been cited (Rochaix, 2002). The operation of gene silencing mechanisms in the nucleus (Casas-Mollano et al., 2007, Neupert et al., 2009) and RNA interference (Bock, 2007) have been demonstrated to significantly reduce the yield of recombinant proteins expressed from the nuclear genome. Thirdly, nuclear genome transformation occurs by illegitimate recombination events (Kindle et al., 1989). In illegitimate recombination, the transgene are inserted randomly in the genome resulting in unpredictable outcomes such as rearrangements and gene mutations (Kindle et al., 1989, Tam and Lefebvre, 1993). The result is an unstable, unpredictable and extremely low expression for the transgene in the nucleus.

Conversely, the chloroplast transformed with a transgene provides a higher expression level and yield for recombinant protein than the transformed nucleus (Rochaix, 2002). This is because chloroplast lacks gene-silencing and RNA interference that reduce the level of transgene expression (Bock, 2007). Moreover, chloroplast transformation occurs by homologous recombination events (Day and Goldschmidt-Clermont, 2011, Purton, 2007). In homologous recombination, the transgene is integrated at specific sites on the genome, and the insertion sites are regions of sequence homology with the genome (Day and Goldschmidt-Clermont, 2011). The result is that the transformation event is specific, precise (gene targeting), and more predictable. These factors contribute to a more uniform, stable and hence higher transgene expression levels achieved from a transformed chloroplast. Since gene targeting is possible, chloroplast transformation allows the possibility to insert a gene cassette into the genome, and hence, express multiple genes simultaneously using a single promoter (Bock, 2007, Su et al., 2005). The expression of multiple genes could allow for example, the synthesis of multi-subunit proteins or protein complexes in the chloroplast.

2.2.4 Chloroplast transformation by biolistic particle bombardment method.

A key feature of chloroplast genome is that the genome is very rich in adenine and thymine nucleotides (Rochaix, 1995), and exhibits codon bias for these nucleotides (Nakamura et al., 1999). This means that adenine or uracil nucleotides are favoured in the third position of a codon over guanine or cytosine nucleotides (Nakamura et al., 1999). As a result, genes that match the codon bias are expressed very much higher than those that do not. For instance, codon optimization of the *gfp* gene to match the codon bias of *C. reinhardtii* chloroplast genome was shown to greatly improve the expression of recombinant green fluorescent protein (GFP) in the chloroplast (Franklin et al., 2002). Hence, the first step in the transformation of the chloroplast genome requires that the transgene (foreign gene) must be codon optimized to match the codon usage of the *C. reinhardtii* chloroplast genome (Mayfield et al., 2007, Puigbo et al., 2007) for higher recombinant protein yield. The codon-optimized transgene is cloned into a plasmid DNA (vector) and amplified.

The methods used in chloroplast transformation are listed on Table 2.3. A method that delivers the vector through the cell wall, cell membrane into the chloroplast is vital for the success of transformation. This is most effectively achieved by biolistic particle bombardment (Boynton et al., 1988). An alternative to this method is the glass bead method (Kindle et al., 1991). The glass bead method involves the agitation of a suspension of cells and foreign DNA with glass beads by vortex. A limitation of the glass bead method is that it is only effective for cell-wall deficient strains. Generally, the transformation frequency of the chloroplast is extremely low and less efficient than the particle bombardment method. In spite of this, the glass bead method is relatively cheap, easy to operate and does not require specialized equipment (Kindle et al., 1991).

A typical biolistic particle bombardment device is shown in Figure 2.2. This is expensive and specialized equipment for delivering the cloned vector into a plant or microalgae chloroplast. The equipment incorporates a high-pressure and vacuum system, and is connected to a dedicated gas storage tank delivering helium (gas) for the operation. The component parts for the biolistic operation such particle disk, rupture disk and accessories must first be sterilized and assembled aseptically. A simple diagram illustrating the basic

operation of the device is shown in Figure 2.3. The plasmid DNA (cloned vector) is coated onto 1 µm sized gold particles and fired at high pressure (1100 psi) into a lawn of microalgae cells spread on selective, solid medium plate (Boynton et al., 1988). After firing, the device is again de-pressurized to -0.54 psi before the plate is removed. Bombarding cells with high velocity particle projectiles at ~400 m/s kills some of the cells but most cells survive. The transgene integrate into specific regions on the chloroplast genome by homologous recombination (Day and Goldschmidt-Clermont, 2011, Purton, 2007). The actual mechanistic characterization of the process has not be achieved, however homologous recombination is thought to involve sequence homology (~1 kb sequence homology) between the left and right targeting arm of the vector and the integration site on the genome (Day and Goldschmidt-Clermont, 2011, Purton, 2007).

The biolistic particle bombardment of 10^7 microalgae cells yields ~100 heteroplasmic transformants (Day and Goldschmidt-Clermont, 2011). In some cases, selective marker genes may be cloned to the vector and used to efficiently select the transformants from the non-transformed cells under selective pressures. In these instances, the basis of selection would be the expression of traits of the selective marker gene. Some selective marker genes and the criterion of the selections are listed in Table 2.4. The presence of ~80 copies of chloroplast genomes per cell (Rochaix, 1995), means that the early transformants contains a mixed population of non-transgenic and transgenic chloroplast genomes known as heteroplasmic state. Thus the transformants are propagated under selective pressure, so that by selections, cell divisions and several propagation steps leads to a uniform population of transgenic chloroplast genomes in cells or homoplasmic state (Day and Goldschmidt-Clermont, 2011). The homoplasmic state usually takes about four to six weeks to achieve**.**

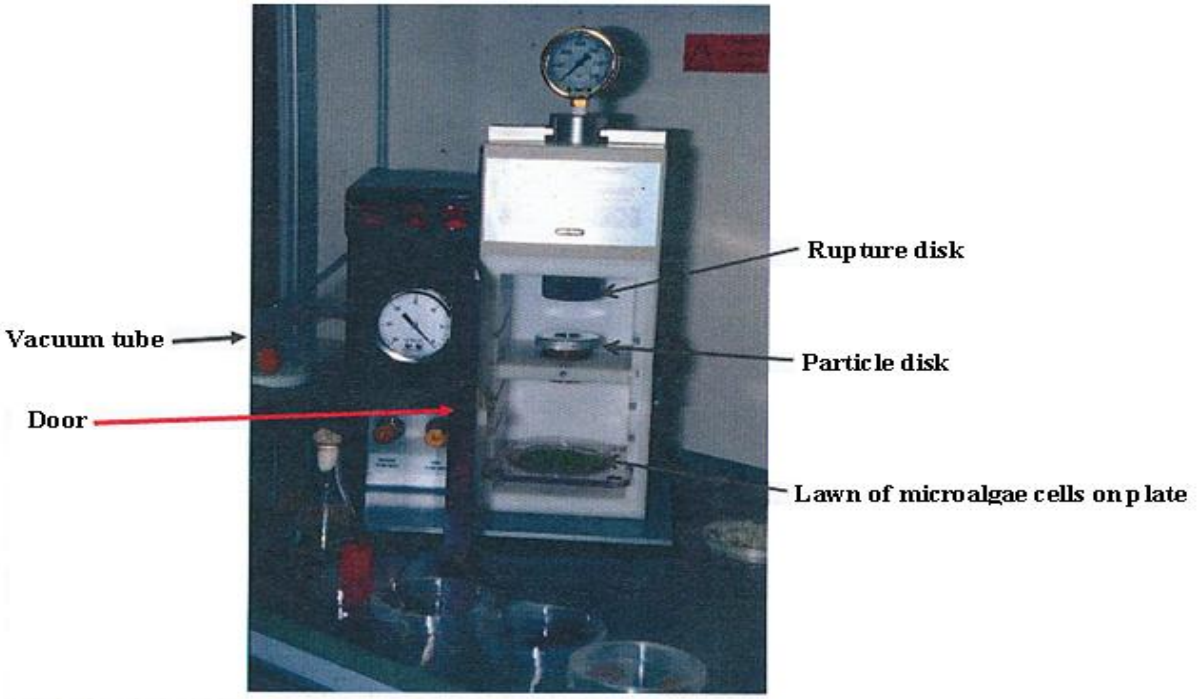

Figure 2.2: A common type of biolistic particle bombardment device (particle gun) used in chloroplast transformation (PDS-1000/He Biolistic particle device, Biorad, USA).

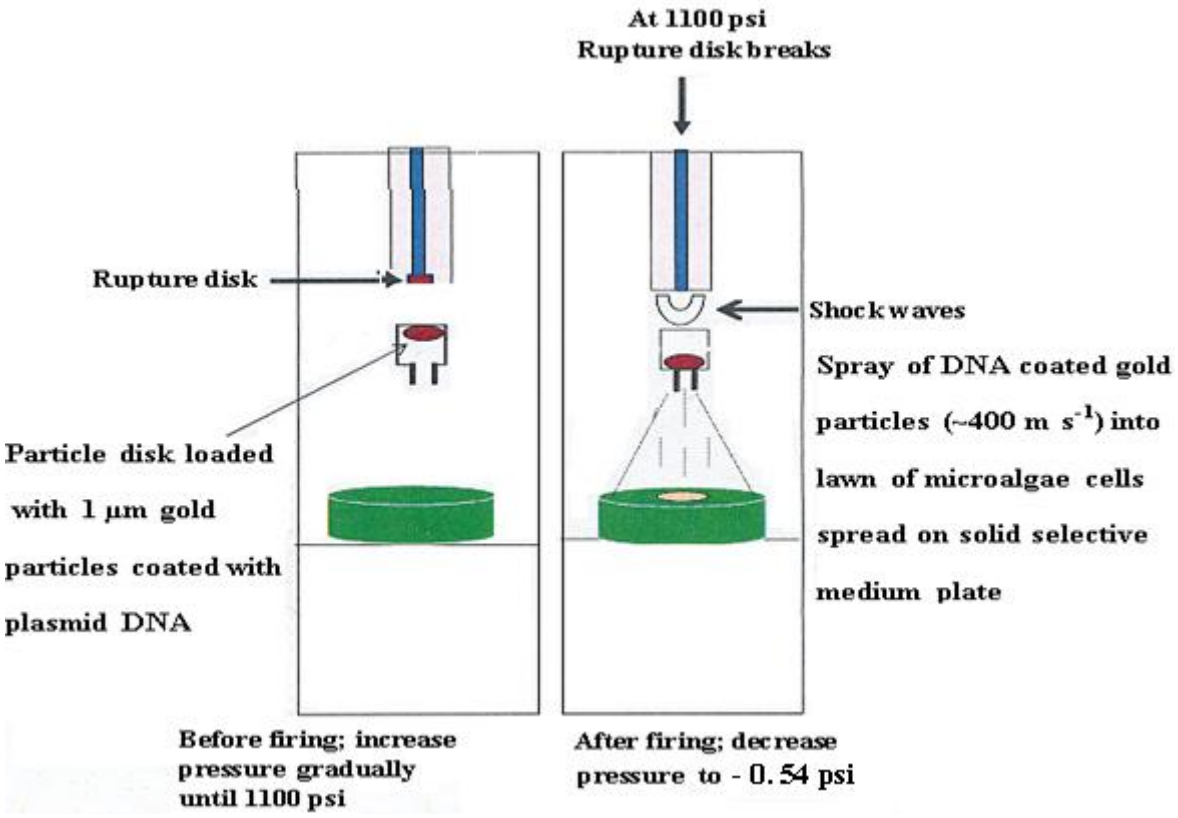

Figure 2.3: Schematic diagram of the operation of the biolistic device.

Table 2.4: Some selective marker genes used in chloroplast transformation.

Marker gene	**Selection criterion**	**References**
tscA	Photosynthetic transformants	(Kindle et al., 1991)
rrnS	Transformants resistant to Spectinomycin and streptomycin (Antibiotics)	(Kindle et al., 1991)
rrnL	Transformants resistant to erythromycin (antibiotic)	(Newman et al., 1990)
psbA	Transformants resistant to metribuzin (herbicide)	(Newman et al., 1991)

2.2.5 Factors that affect recombinant protein yield in the chloroplast.

In simple representation though the process is much more complex, the process of gene expression will involve the transcription of the gene of interest into mRNA transcript, and the translation of mRNA transcript into protein (see Figure 2.4).

The expression of chloroplast genes are affected by number of factors. Firstly, gene promoters have been shown to affect the level of transcription of genes into mRNA transcripts (Klein et al., 1994, Manuell et al., 2004). These promoters are endogenous genes of the chloroplast, some of which include *atpβ, atpA, psbD, psbA, rbcL* (Harris, 1989), and several researchers (Barnes et al., 2005, Fletcher et al., 2007, Manuell et al., 2004, Manuell et al., 2007, Surzycki et al., 2009) have succeeded to drive the level of chloroplast gene expression for recombinant proteins using these promoters.

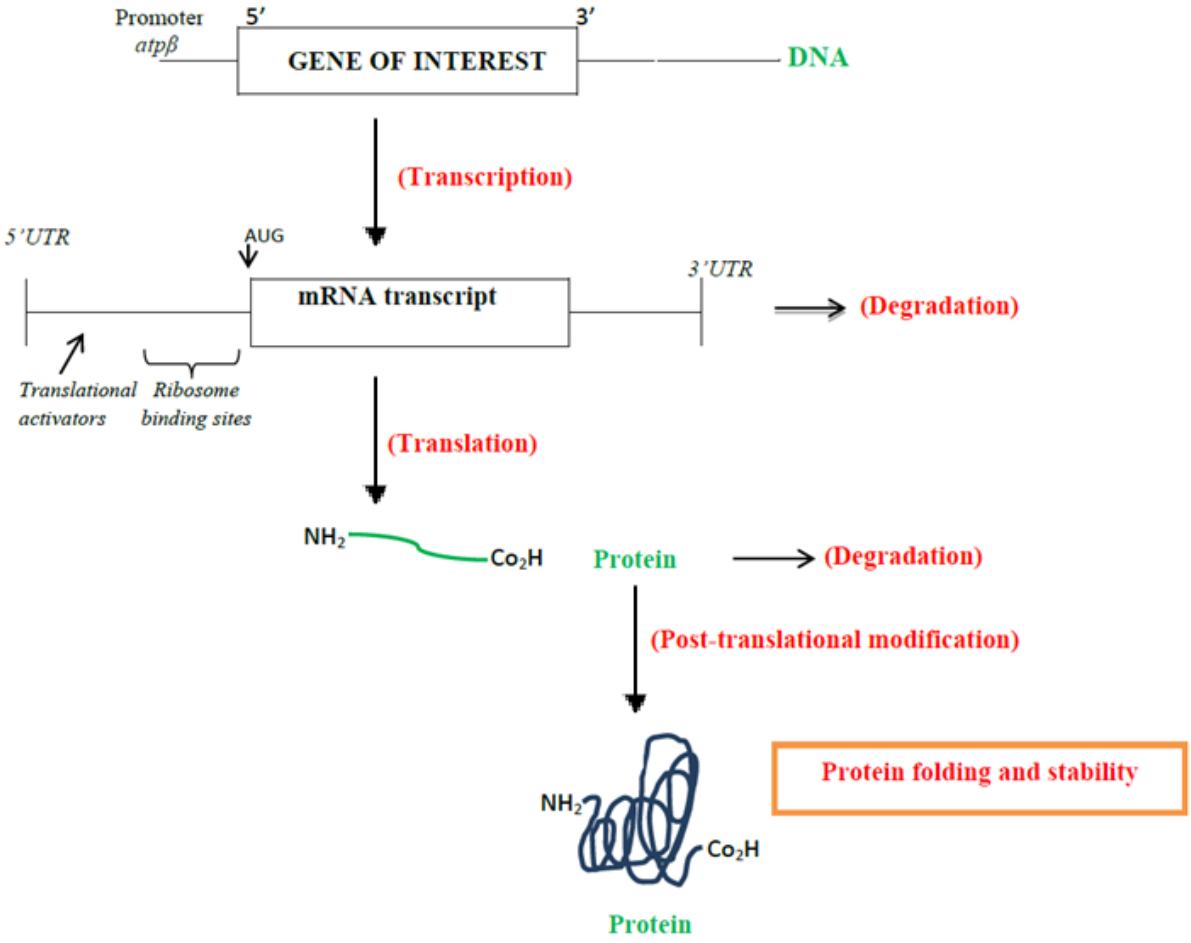

Figure 2.4: A simple illustration of gene expression involving endogenous promoter (*atpβ*) that drive expression of a gene of interest in chloroplast DNA.

In addition to using strong gene promoters, more researchers (Barnes et al., 2005, Salvador et al., 2004, Suay et al., 2005, Vaistij et al., 2000) have demonstrated the regulatory effects of sequences contained within the untranslated regions (UTR) on the mRNA. These workers showed that the regulatory sequences in UTR determine the initiation of mRNA translation (protein synthesis), and that interactions that occur within the sequences affect mRNA stability and degradation. These findings were important because the stability of mRNA or its degradation affects mRNA abundances, and mRNA abundance may affect protein yields. From these reports, one can infer that the use of strong gene promoters (increase transcription rates and the level of mRNA transcripts), and the UTRs affects translation of mRNA into protein. More workers (Barnes et al., 2005, Mayfield et al., 1995, Puigbo et al., 2007) have shown that recombinant protein yield may be increased by best combination of strong gene promoters and UTRs arrangement.

Another factor which has been identified to affect chloroplast gene expression is the availability of ribosome binding sites on the mRNA transcripts (Manuell et al., 2004). The ribosomes binding sites are sequences upstream from the start codon of the mRNA transcript, and they are required for the binding of ribosomes with sequences within the 5'UTR in order for the translation of mRNA into proteins to occur (Manuell et al., 2004). This means that if the ribosomes binding sites are unavailable, protein synthesis would not take place. Factors that interact with the ribosomes and the regulatory sequences in 5'UTR to enable the initiation of mRNA translation to protein to occur have been identified. These are the nuclear-encoded translational activators or *trans*-acting factors (Manuell et al., 2004, Mayfield et al., 1994) which migrate from the nucleus into the chloroplast to affect protein synthesis. These interactions of *trans*-acting factors reveal the effects of the nucleus on the yield of proteins expressed in chloroplast (Manuell et al., 2004, Mayfield et al., 1994), reflecting the cross-talk between the nucleus and chloroplast.

In addition to these reports, the yield of recombinant protein in the chloroplast has been shown to be mainly regulated at the translational level (Eberhard et al., 2002, Rochaix, 1996, Coragliotti et al., 2011). Other levels for chloroplast gene expression regulation, could be at points such as mRNA stability, mRNA degradation, availability of ribosomes binding sites, effects of regulatory sequences in mRNA UTRs, and the interactions of *trans*-acting factors with ribosomes and UTRs sequences (Barnes et al., 2005, Coragliotti et al., 2011, Manuell et al., 2004, Salvador et al., 2004).

The post-translational processing of proteins such as protein folding and protein modifications affects the stability of protein and protein degradation. The stability of protein and protein degradation may affect the net yield of the proteins (Coragliotti et al., 2011, Gruissem and Tonkyn, 1993, Sugita and Sugiura, 1996). Proteases have been identified in the chloroplast which mediates degradation of proteins, particularly unstable proteins or those susceptible to the protease activity (Doran, 2006). These may likely affect protein yields in the chloroplast. However, whether a recombinant protein is expressed or the yield of the protein in the chloroplast has been shown to be protein-specific as well as strain-specific (Surzycki et al., 2009).

2.3 Systems biology approaches (bottom-up or top-down)

In simple terms, if we consider society to be 'the cell' and humans to be 'molecules', for society to function, humans must interact and follow rules. In living organisms, molecules do not exist in isolation but continually interacts and communicate with each other, and the interactions of the non-living molecules gives rise to living properties and functions (Westerhoff and Alberghina, 2005). Systems biology seeks to understand how the biological properties, functions, and behaviours that are characteristic of living organisms originate from the interactions of their components (Westerhoff and Alberghina, 2005). The aim of systems biology is to use integrated approaches involving computational modelling, statistical analysis, control theory, dynamic system theory, global network analysis or whole system analysis and quantitative experimentation to understand how biological properties and functions arise from non-linear interactions between components of the biological system (Kell and Westerhoff, 1986, Navlakha and Bar-Joseph, 2011, Westerhoff and Alberghina, 2005). These approaches go beyond the study of qualitative behaviour and provide quantitative descriptions of biological systems under given conditions, allowing testable predictions (models) of the system properties and behaviour to be understood for the set of conditions (Westerhoff and Alberghina, 2005).

The bottom-up or top-down system biology approach is often implemented to quantitatively describe biological systems. The bottom-up approach studies the local interactions (such as molecular interactions in reaction pathways) to gain understanding of the underlying mechanistic relationship between the interacting species with appropriate mathematical equations (Oliver, 2006). The requirement to obtain quantitative data to assign parameter values for each interaction and interacting species is imperative. When these interactions are well understood and characterized, testable mathematical descriptions for the reaction subnetworks may be constructed (Oliver, 2006). The goal of the approach is to combine the separate reaction subnetworks into a model of the system to describe its behaviour (Oliver, 2006). The top-down approach uses physiological observations and organism-wide data to create model of the biological system. The model is used to generate a hypothesis which can be rigorously tested by experiments (Oliver, 2006). Top-down approach allow the study of biological behaviours on whole system scale but lacks quantitative details for the interactions giving rise to the biological behaviours (Bruggemann and Westerhoff, 2007).

The main underlying principle of systems biology is that the whole system is greater than the sum of its parts i.e. biological functions cannot be understood just by studying the components of a system in isolation because functions arises from non-linear interactions between the components (Kitano, 2002; Westerhoff and Alberghina, 2005; Sauer et al., 2007). Systems biology approaches are inter-disciplinary, and involve working at the interface of engineering, computational, mathemathematical and science disciplines, with the premise that there is always something to be understood in biological systems which can not be completely discovered and understood by one field alone (Boogerad et al., 2007). Systems biology approaches are now increasingly being applied to obtain better understanding of biology and functional behaviours, and some examples are given in the preceeding paragraphs.

Systems biology approaches is widely used to improve metabolic engineering of different commercially important microorganisms (bacteria, yeast and fungi), for improved production of microbial-derived chemicals, specialty chemicals and high value products such as organic acids, primary metabolites, amino acids, proteins, enzymes, food supplements, and antibiotics (Papini et al., 2010, Nevoigt, 2008, Rokem et al., 2007). The use of microbial systems for production of chemicals is increasing, and has the advantages of being renewable, sustainable, reduces chemical wastes and emission of gaseous pollutants compared to traditional chemical processes (Papini et al., 2010).

Another area in which systems biology is widely used is in improvements to bioprocesses (fermentation processes) through microbial strain development (Park et al., 2008). The study and analyses of cellular networks and their interactions in microbial systems using systems biology approaches are used to gain insights of how biological networks are integrated, and to guide the metabolic engineering of microbial strains for fermentation processes (Park et al., 2008, Lee et al., 2005, Askenazi et al., 2003, Alper et al., 2005).

Systems biology has impacted on pharmaceutical, biomedical and clinical research. Approaches in system biology are used to study and gain improved understanding of non-pathogenic and multifactorial diseases to facilitate clinical treatments (Bielekova et al., 2014, Villoslada et al., 2009, Sookoian and Pirola, 2013, Leoncikas et al., 2014). These

approaches could be extended to include the study pathogen - host cell interaction networks to obtain improved understanding of pathogenic infections, and to find effective treatments for such diseases (Dozmorov et al., 2007, Tan et al., 2007). Dynamic analyses and integrated approaches of systems biology are implemented in the study of cellular networks (metabolic, signalling and gene regulatory networks) in order to understand biological behaviours to different perturbations which may include environmental, diseases or effects of drugs (Cho et al., 2006, Kreeger and Lauffenburger 2010, Liu et al., 2012). In these instances, the analyses can be used to identify intervention points in the networks that serve as effective drug targets against diseases and in drug discovery research (Cho et al., 2006, Kreeger and Lauffenburger, 2010, Liu et al., 2012, Butcher et al., 2004, Apic et al., 2005, Silver et al., 2007).

Additionally, network modelling and analysis together with inferences from experiments can be integrated together, and the biological understanding gained may be used to guide formulation of strategies to optimize the production of value products from microbial cell factories (Rokem et al., 2007, Albert, 2007, Khannapho et al., 2008).

2.3.1 Systems biology understanding for recombinant protein research

Current molecular biology approaches involving chloroplast genome transformation can result in targeted genetic modification, producing transgenic strains capable of expressing recombinant proteins (Boynton et al., 1988, Mayfield et al., 2007). Aspects of this literature review highlighted nutritional and environmental factors that are considered in the growth of the microalgae, design of culture systems, operational parameters for optimal growth, codon optimization, transformation of *C. reinhardtii*, and factors that affect the protein yield in the chloroplast. Despite decades of advances in these areas, the yield of recombinant proteins expressed in the *C. reinhardtii* chloroplast has been consistently low. The limitation is a challenge that must be overcome if large-scale recombinant protein production based on the microalgae is to be achieved.

Other factors more than those currently identified may contribute to the low yield. In addition, most of the previous research work into recombinant protein production in microalgae has largely been qualitative descriptions of the biological process. New quantitative approaches (system biology) that complements and significantly contributes to the understanding of recombinant protein production in microalgae may be needed (Westerhoff and Alberghina 2005). Such quantitative approach may allow the identification and understanding of bottlenecks in the metabolic and hierarchical regulations of the microalgae that determines the yield of recombinant proteins (Snoep et al., 1995, Snoep et al., 2002, ter Kuile and Westerhoff, 2001).

For example, systems biology approaches may be pursued to shed light, and understand how recombinant protein yield may be significantly increased than current yields in *C. reinhardtii*, with improved predictability for the expression system. The approach may be used to address if the low recombinant protein yield in the microalgae is due to a high protein burden, and if the fluxes for recombinant protein production are suboptimal (Snoep et al., 1995). The analysis may be extended to identify and understand metabolic, hierarchical and signalling regulations (Snoep et al., 2002, ter Kuile and Westerhoff, 2001) as these determines how a cell executes regulations and controls when perturbed. The cell is likely to experience the recombinant protein production as a perturbation. On the other hand, system biology approaches may be used to determine whether the low yields are due to metabolic stresses (such as ATP depletion, diversion of cellular resources such as amino acids and ribosomes) due to the synthesis of recombinant proteins not needed for growth (Dekel and Alon, 2005, Shachrai et al., 2010). Such stress may result as a protein burden (or protein cost) manifested as reduction on growth rates (Dekel and Alon, 2005, Shachrai et al., 2010). Protein burden has been demonstrated to be a significant determinant of the yield of a protein not needed for growth in a cell (Dekel and Alon, 2005, Dekel et al., 2005, Kalisky et al., 2007). The quantitative analysis of protein burden may be used to gain some understanding of the allowable yield of recombinant protein in a cell without cessation of growth (Dong et al., 1995), or aspects of the regulation which determine the protein yield under a given set of conditions (Kalisky et al., 2007). Protein cost data exists for bacteria (Novick and Weiner, 1957, Koch, 1983, Dong et al., 1995) but none has been determined for microalgae.

Recently, some models based on *C. reinhardtii* networks have been published. Examples include a metabolic model of glycolysis, tricarboxylic acid cycle and fermentative metabolism by Chang et al. (2007), and the genome scale model of primary metabolism in *C. reinhardtii* Boyle and Morgan, (2009). These models incorporated the cellular localizations of processes and the metabolic reactions, and were useful for predicting aspects of metabolism (hydrogen production) and the growth of *C. reinhardtii* under different conditions. However, the models were limited by size and incorporated fewer reactions and metabolites descriptions. More recently, a larger-scale model based on *C. reinhardtii* genome and metabolisms was published by Dal'Molin et al., (2011). Currently, algaGEM is the most up to date and comprehensive genome scale model of algae metabolism incorporating cellular compartments, the functions of over 800 open reading frames, >1800 metabolites and >1700 metabolic reaction in the microalgae. The model is a useful resource for studying, and making *in silico* predictions of metabolism, metabolic processes and the algae phenotypes (such as growth and hydrogen production). The utility of the model means it may be adapted and applied for the study of recombinant protein production, to identify limitations in the network, and understand strategies to overcome the metabolic limitations for protein production.

Chapter 3 - Materials and Methods

The materials and methods used for all the experiments are discussed in this chapter, beginning with the description of strains studied in the work.

3.1 Description of *Chlamydomonas reinhardtii* strains

Wild-type strain: cc621 mt- is a wild-type *C. reinhardtii* strain (Proschold et al., 2005) obtained from the Chlamydomonas Resource Centre, USA.

Mutant strain: cc373 mt+ strain is a photosynthetic mutant with the *ac-u-c-2-21* mutation (Shepherd et al., 1979, Woessner et al., 1984). The mutation is a 2.5 kb deletion in the chloroplast Bam 10 restriction fragment containing the *atpβ* gene (Boynton et al., 1988). The cc373 mt+ strain is non-photosynthetic and do not grow in light (Shepherd et al., 1979), hence making it a suitable recipient for transformation based on the rescue of the defective *atpβ* gene. The cc373 mt+ strain was obtained from the Chlamydomonas Resource Centre, USA.

Control strain: Bam10::cc373 mt+ strain was generated and provided by Julio Suarez (2013) for this study. Bam 10::cc373 mt+ is the photosynthetic-rescued strain obtained by transforming cc373 mt+ chloroplast, with plasmid pB10 (a Bam10-based plasmid) designed to rescue the mutant *atpβ* gene with an intact *atpβ* gene. Photosynthetic-rescue of cc373 mt+ without a foreign gene gave rise to the Bam10::cc373 mt+ control strain (i.e. lacking a foreign gene).

Transgenic strains: The photosynthetic-rescued strains transformed with human *TSG6 gene* (X6L and D6L) were generated and contributed by Julio Suarez (2013) to the study. In the X6L and D6L strains, gene expression for the recombinant human *TSG6* protein was constitutively driven by the endogenous chloroplast *atpA* and *psbD* promoters respectively. Both the transgenic constructs have an endogenous *rbcL* 3'UTR.

The photosynthetic strains with the gus gene *(gusA)* was obtained by transformation based on the rescue of the defective *atpβ* gene in cc373mt+ with the plasmid pB10 and *E. coli gusA* gene. Two transformants of the gus expressing strains (Gus12-2 and Gus12-B) were isolated from independent single cell colonies on plates. The Gus12-2 and Gus12-B strains were provided by Leopoldo Herrera Rodriguez (2013). In the Gus12-2 and Gus12-B strains, expression of recombinant *β*-glucuronidase (gus) was obtained by constitutive expression of the *gusA* gene using *atpA* promoter and *rbcL* 3'UTR (Ishikura et al., 1999).

3.1.1 Strain maintenance, storage and transfers

Materials: minimal agar solid medium, petri-plates (Thermo Fisher Scientific, UK), Class II laminar flow cabinet (Walker Safety Cabinet Ltd. UK) fitted with ultra-violet light ($UV_{254\ nm}$), 70% (v/v) ethanol, Sanyo growth cabinet (Sanyo Electric Co. Ltd. Japan), Innova illuminated refrigerated incubator shaker (New Brunswick Scientific Co. Inc. USA), sterile liquid medium (TAP or minimal).

All strains (except cc373 mt+) were grown on sterile minimal agar solid medium petri plates by incubating at 25^{o}C in 12 h light and 12 h dark cycles for four weeks in the Sanyo growth cabinet. The cc373 mt+ strain was grown on sterile TAP agar solid medium at 25^{o}C in the dark for 10 days.

All strain transfers were performed using aseptic techniques under the Class II laminar flow cabinet. Prior to the transfer, work surfaces were swabbed with 70% (v/v) ethanol and irradiated with UV-light (254 nm) for 20 minutes. Single cell colony was streaked into 50 ml of sterile liquid medium in a 250 ml shake flask to start the pre-growth culture. The pre-growth culture was incubated at 25^{o}C in the Innova illuminated refrigerated incubator shaker operating at 90 rpm. From the pre-growth cultures, cell cultures were transferred by pipette into fresh 50 ml liquid medium (growth culture).

3.1.2 Inoculum preparation and inoculum size

The pre-growth cultures were grown in shake flask containers with working volumes of 50 ml liquid medium, at 25^{o}C and 90 rpm until cells had reached 2.5 – 10 million cells per ml. An inoculum size of one ml pre-growth culture (not older than a week) was used to inoculate new 50 ml sterile liquid medium (growth culture) for the start of growth experiment.

3.2 Determination of cell density, optical density, and cell sizes

Materials: Haemocytometer (Weber Scientific Ltd. England), inverted light microscope (Leica DMIL, Portugal), spectrophotometer (Aquamate, UK), 1 cm light path length cuvette (Sarstedt, Germany), Cellometer Auto T4 (Nexcelom Biosciences, USA), Cellometer slides (Nexcelom Biosciences, USA), dense cultures, saturated iodine solution, sterile liquid medium, and reverse-osmosis water.

3.2.1 Determination of cell density (single cell count method)

Cultured cells were counted in the haemocytometer and the cell density (cells/ml) was determined. 5 ml of well-mixed dense culture was serially diluted (1, 2, 4, 8, 16, 32, 64, and 128-fold dilutions) with reverse osmosis water. 2 µl of iodine solution was added and mixed with 200 µl of diluted cultures to immobilize the cells. 10 µl of the diluted cultures was applied and allowed to flow by capillary action into the haemocytometer. The haemocytometer contain 25 large square areas (and each square area contains 16 grids). Immobilized cells were visualized with the inverted light microscope (100x resolution), and single cells within the 25 squares were counted manually. A grid has a depth of 0.1 mm and an area of 0.0025 mm^2, giving a volume of 0.00025mm^3 per grid. The total number of grids in the haemocytometer was 400. Therefore, the total grid volume was 0.1 mm^3 (0.0001 ml). The cell density (cells/ml) was calculated as the product of cell count and the multiplication factor (10^4).

3.2.2 Determination of optical density of cultures (Spectrophotometer method)

The optical density of 1 ml of well-mixed dilute cultures was quickly measured in the spectrophotometer at 600 nm using 1 cm light path length cuvette. 1 ml of sterile liquid medium was used as the blank. The absorbance of the blank was used to zero the spectrophotometer prior to measuring the absorbance of the cultures. The mean optical density was determined from three biological replicates and two technical replicate measurements.

3.2.3 Standard calibration curve of optical density and cell density

The mean optical density (at 600 nm) measurements were plotted against mean cell density to obtain the standard calibration curves. Figures 3.1, 3.2 and 3.3 are standard calibration curves for Bam10::cc373 mt+ cultures in mixotrophic, autotrophic and heterotrophic conditions respectively. For the standard calibration curves for cc621 mt-, cc373 mt+, D6L, X6L, Gus12-2 and Gus12-B strains refer to the Appendix I section of the thesis.

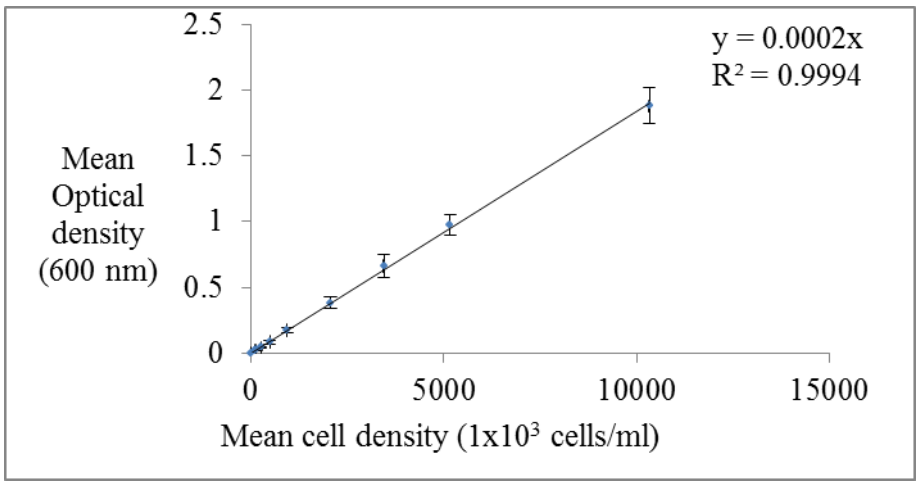

Figure 3.1: Standard calibration plot of optical density at 600 nm and cell density of Bam10::cc373 mt+ mixotrophic cultures. The mean values and standard deviation were determined from three biological replicates and two technical replicates.

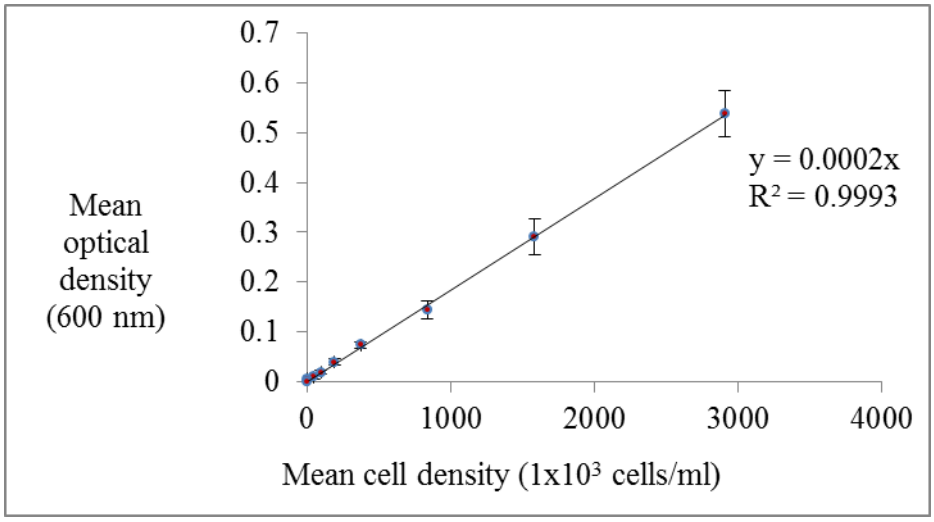

Figure 3.2: Standard calibration plot of optical density at 600 nm and cell density of Bam10::cc373 mt+ autotrophic cultures. The mean values and standard deviation were determined from three biological replicates and two technical replicates.

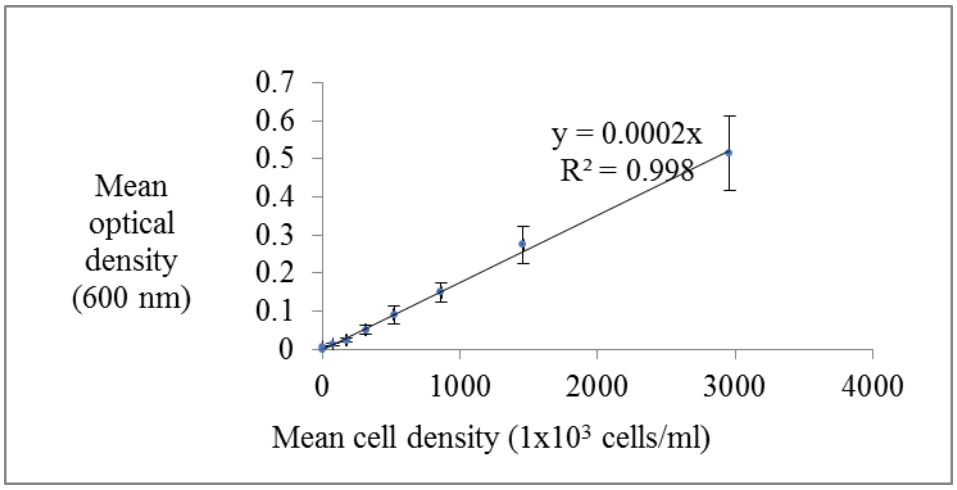

Figure 3.3: Standard calibration plot of optical density at 600 nm and cell density of Bam10::373 mt+ heterotrophic cultures. The mean values and standard deviation were determined from three biological replicates and two technical replicates.

The plots were linear with the slope equal to the correlation factor (2×10^{-7}) for converting optical density measurements into cell density (cells/ml). The standard calibration was constructed for cultures under autotrophic, heterotrophic and mixotrophic growth

conditions to provide an estimate of the cell density from optical density (at 600 nm) readings, using equation 3.1:

$$y = 0.0000002x \qquad (3.1)$$

Where, y is the measured optical density per ml of culture, and x is the cell density (number of cells per ml of culture).

3.2.4 The measurement of cell size

The cell sizes (cell diameter) were measured in the cellometer Auto T4 instrument. The cell diameters of exponential growth phase cultures growing in autotrophic, heterotrophic and mixotrophic conditions were measured. 20 µl of growth culture was applied into the cellometer slide and allowed to flow by capillary action. The mean cell diameter (µm) was determined from three biological replicates and two technical replicates.

3.3 Specific growth rates, doubling time, and cell productivity

Cultures were grown at a constant incubation temperature of 25^{o}C at 90 rpm in the Innova illuminated refrigerated incubator shaker. The cultures were grown in autotrophic condition in minimal medium (under continuous light); heterotrophic condition in TAP medium (under continuous dark); or mixotrophic condition in TAP medium (under continuous light), or synchronously in 12 h light and 12 h dark cycle periods in TAP medium (under mixotrophic condition). The optical density measurements (at 600 nm) were performed for cultures at regular intervals. The optical density was correlated into cell density (cells/ml) by dividing the measured optical density by the correlation factor (2 x 10^{-7}) according to equation 3.2:

$$Cell\ \ density\ \ = \left(\frac{Optical\ \ density\ \ of\ \ culture}{0.0000002} \right) \qquad (3.2)$$

Growth was monitored as optical density with respect to time, and the growth curves plotted as functions of cell density (cells/ml) against time (h) for each growth condition. The growth of cultures was characterized by an increase in cell density with time. Culture growth rate was described in terms of the specific growth rate (µ) with units of h^{-1}.

$$\mu = \frac{\ln(X_2 / X_1)}{t_2 - t_1} \qquad (3.3)$$

Where, t_2 and t_1 refer to different time intervals (with units of h) during the growth of culture. X_2 and X_1 represent cell concentrations (number of cells/ml), and ln represent the natural logarithm. X_2 is cell concentration at time t_2, and X_1 is the cell concentration at time t_1. Equation 3.3 describes the dependence of specific growth rate on time and cell concentrations. From equation 3.3, one can estimate that at the stationary phase there is no culture growth. The maximum specific growth rate was determined only during the exponential growth phase. The natural logarithm of cell density during the exponential growth phase was plotted against time. The gradient of the linear line (slope) was estimated as the maximum specific growth rate with units of h^{-1}.

The doubling time (t_d) represents the time taken for cells to double in number. The doubling time (h) was calculated using equation 3.4:

$$t_d = \frac{\ln(2)}{\mu_{max}} \qquad (3.4)$$

Where, μ_{max} is the maximum specific growth rate (h^{-1}). The cell productivity was calculated as the product of maximum specific growth rate and cell density. Cell productivity was expressed as gram dry cell weight per ml per h.

3.4 Preparation of growth media

Materials: Tris (hydroxymethyl) aminomethane (Fischer Scientific Ltd. UK), glacial acetic acid (Fischer Scientific Ltd. UK), hydrochloric acid (Fischer Scientific Ltd. UK), Hutner trace elements solution (Chlamydomonas Resource Centre USA), ammonium chloride (Sigma-Aldrich, Germany), calcium chloride dihydrate (Sigma-Aldrich Germany), magnesium sulphate heptahydrate (Sigma-Aldrich, USA), agar (Melford laboratories Ltd. England), dipotassium hydrogen phosphate trihydrate and potassium dihydrogen phosphate (BDH laboratory supplies Ltd. England), potassium hydroxide pellets (Hopkins and William, Essex, England), reverse-osmosis water, 15 amino acids including L-threonine, L-phenylalanine, L-histidine, L-glutamic acid, L-aspartic acid, L-serine, L-tyrosine, L-glutamine, L-arginine, L-cysteine, L-tryptophan, L-valine, L-isoleucine, L-leucine (Sigma-

Aldrich, Germany), L-proline (Duchefa Biochemies, Netherlands), and α-ketoglutaric acid sodium salt (Sigma-Aldrich, UK).

Preparation of tris acetate phosphate liquid medium (TAP)

A combination of salts, tris base, acetate and phosphates was used to formulate the TAP growth medium (Gorman and Levine, 1965) for *Chlamydomonas* cultures. 500 ml of reverse-osmosis water was measured into a clean measuring cylinder, and five ml of Beijerinck stock solution was added, 13.44 mM of phosphate buffer solution (pH 7), one ml of Hutner trace elements solution, and one ml of glacial acetic acid was added and mixed. The pH of the medium was adjusted to pH 7.30 with 2.42 g tris. The final volume was made up to one litre with reverse-osmosis water. The prepared TAP liquid medium was sterilised at 121^{o}C for 15 minutes, and then allowed to cool to room temperature.

Preparation of minimal medium

The medium was prepared as described above for TAP medium by omitting acetic acid and tris, as described by Gorman and Levine (1965). The pH of the medium was kept 7.0. The minimal medium was sterilised. The final concentration of components in TAP and minimal medium are presented on Table 3.1.

Preparation of tris-minimal medium

Tris-minimal medium was prepared by adjusting the pH of freshly prepared minimal medium to pH 7.30 with 0.46 g tris. The medium was sterilised.

Preparation of ammonium-free TAP medium

The ammonium-free TAP medium was prepared in the same method as the TAP medium, except that ammonium chloride was omitted from the medium

Preparation of ammonium-free, tris-free acetate medium

The ammonium-free, tris-free acetate medium was prepared with the same method as TAP medium (except that NH_4Cl and tris were omitted from the medium). The pH of the medium was adjusted to 7.30 by adding 2.25 ml 10 M potassium hydroxide.

Preparation of medium supplemented with amino acids, or with α-ketoglutarate

The liquid medium was prepared and supplemented with an amino acid, or the α-ketoglutarate. The pH of the medium was adjusted to 7.30 and the medium sterilised.

Table 3.1: TAP and minimal media compositions

	1 litre TAP medium (pH 7.30)		**1 litre minimum Medium (pH 7.0)**	
Chemical component	**Amount (mg)**	**Concentration (µM)**	**Amount (mg)**	**Concentration (µM)**
Tris	2420	19980	0	0
Beijerinck solution:				
NH_4Cl	500	9350	500	9350
$MgSO_4.7H_2O$	20	80	20	80
$CaCl_2.2H_2O$	10	90	10	90
Phosphates				
$K_2HPO_4.3H_2O$	1860	4080	1860	4080
KH_2PO_4	720	2640	720	2640
Glacial acetic acid	1050	17500	0	0
Hutner Trace elements solution:				
$FeSO_4.7H_2O$	4.99	17.95	4.99	17.95
$ZnSO_4.7H_2O$	22	76.50	22	76.50
$CuSO_4.5H_2O$	1.57	6.29	1.57	6.29
$MnCl_2.4H_2O$	5.06	25.56	5.06	25.56
$CoCl_2.6H_2O$	1.61	6.77	1.61	6.77
$(NH_4)_6Mo_7O_{24}.4H_2O$	1.10	6.2	1.10	6.2
H_3BO_3	11.40	184.36	11.40	184.36
Na_2EDTA	50	147.83	50	147.83
KOH	16	285	16	280

Preparation of TAP agar solid or minimal agar solid medium

10 g agar was added into one litre of the freshly prepared liquid medium. The medium was sterilised, and allowed to cool down to 50°C. 65 ml of the medium was transferred into sterile petri-plates, and allowed to solidify in the sterile environment of the Class II laminar flow hood (Walker Safety Cabinet). The solidified medium was sealed with sterile para-film and stored at 20°C.

3.5 Detection of recombinant *β*-glucuronidase (gus) in cultures

The enzymatic method described by Jefferson et al. (1987b) for the qualitative detection of gus activity in plant tissues and cultured cells was employed for the work. The method is highly sensitive, accurate and robust for the detecting *β*-glucuronidase activity in samples.

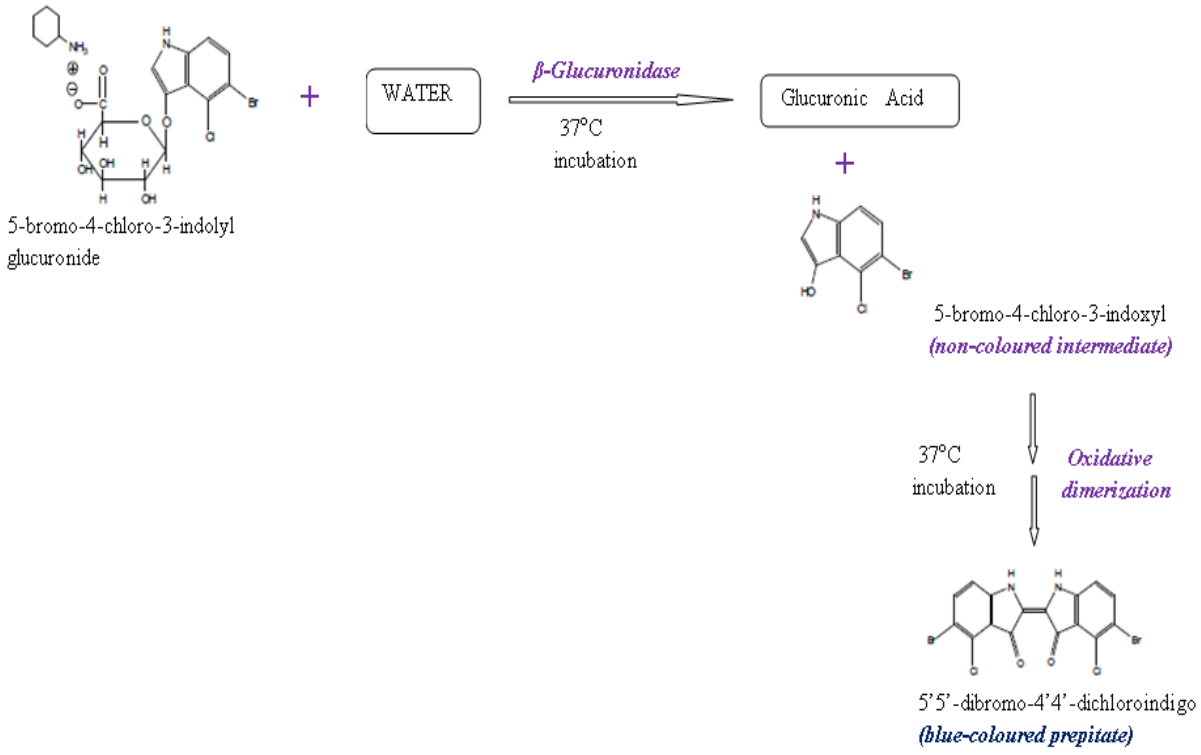

Figure 3.4: *β*-glucuronidase catalysed hydrolysis of 5-bromo-4-chloro-3-indoxyl glucuronide at 37°C to the 5-bromo-4-chloro-3-indoxyl intermediate; and oxidative dimerization of the intermediate to form insoluble blue-coloured 5'5'-dibromo-4'4'-dichloroindigo.

A schematic representation of steps in the test for gus activity in *C. reinhardtii* cultures is shown in Figure 3.4. In the reaction maintained at 37^{o}C, gus hydrolyses the substrate 5-bromo-4-chloro-3-indoxyl glucuronide (*X-gluc*) to produce a soluble non-coloured intermediate (5-bromo-4-chloro-3-indoxyl) and glucuronic acid. The non-coloured intermediate is unstable and undergoes oxidative dimerization to form the insoluble intense blue-coloured precipitate product (5'5'-dibromo-4'4'-dichloroindigo).

3.5.1 Cell culture preparation and cell harvest

Materials: Growth cultures, eppendorf centrifuge 5417R (Eppendorf AG Hamburg, Germany), 0.30% (w/v) 5-bromo-4-chloro-3-indolyl glucuronide solution (5.75 mM *X-gluc*), reverse osmosis water, temperature-controlled water bath (Grant Instruments Ltd. UK).

The cultures were propagated repeatedly under selective pressures (autotrophic growth in minimal medium at 54 µmol photons m^{-2} s^{-1}), 25^{o}C (90 rpm) to select the photosynthetic-rescued strains. The cell cultures of the photosynthetic-rescued strains (~2 million cells per ml) were harvested by centrifugation in the eppendorf centrifuge at *16100 x* ***g*** (14000 rpm) for five minutes. The cell pellets were immediately collected for qualitative detection of gus activity.

3.5.2 Qualitative detection of gus activity on 5.75 mM *X-gluc* substrate.

The cell pellets were re-suspended in 30 µl reverse osmosis water. 40 µl of the 5.75 mM *X-gluc* solution was mixed with the re-suspended cell sample and incubated overnight (24 h) at 37^{o}C, in the temperature-controlled water bath. The incubation assays with 5.75 mM *X-gluc*, was performed on the sterile minimal medium (blank control), Bam 10::cc373 mt+ samples (negative control), and on the gus transformants (Gus12-2 and Gus12-B). Detection of *β*-glucuronidase expression was confirmed by the enzymatic conversion of *X-gluc* to the insoluble blue-coloured precipitate.

3.6 Extraction and quantification of gus

Materials: Exponentially growing cultures (~2 x 10^6 cells/ml), Mistral 2000R refrigerated centrifuge (MSE, UK), sterile 0.22 µm filter (Merck Millipore Ltd. Ireland), gus extraction buffer (50 mM sodium phosphate buffer pH 7.0, 10 mM β-mercaptoethanol, 0.10 % (w/v) sodium laury sarcosine, 0.10% triton X-100, vivaspin 20 ultrafiltration spin concentrator (Sartorius Stedim Biotech GmbH, Germany), Heraeus multifuge X3R centrifuge (Thermo Fischer Scientific, Germany), Bandelin Sonoplus Sonicator (Bandelin Electronic, Berlin), Inverted light microscope (Leica DMIL, Portugal).

Recombinant gus was extracted from the cultured cells, measurements of gus activity and the gus yields were determined for autotrophic, heterotrophic, and mixotrophic cultures as described in the next sections.

3.6.1 Culture harvest and sample collections

The methods described by Rochaix et al. (1988), Jefferson (1987) and Jefferson et al. (1986) were employed for culture harvest, cell disruptions and sample collections.

Culture harvest and sample collections (cell pellets and supernatant fractions)

10 ml cultures of measured densities (~2 million cells per ml) were collected during the exponential growth phase, and centrifuged in the Mistral 2000R centrifuge at 2000 rpm for five minutes at 4^oC. The cell pellets were collected and re-suspended with 3 ml gus extraction buffer pH 7. The 10 ml supernatant fractions were collected, and filtered through a sterile 0.22 µm filter to remove suspended cells.

Concentration of culture supernatant fractions

The filtered supernatant fractions obtained as above were concentrated in vivaspin 20 unit using the instructions of the vivaspin 20 manufacturer. The 10 ml fractions were concentrated by ultra-filtration in the vivaspin 20 unit (with membrane molecular weight cut-off 10 kDa) and centrifugation at 6000 x ***g*** (10^oC) for five minutes in the Heraeus multifuge X3R centrifuge. The samples were concentrated by a factor of 10. The

supernatant concentrates were used in enzymatic assays to determine their gus activity, and in the Biorad protein assays to measure their proteins concentration.

Cell extractions (protein preparations) by sonication

The cell pellets suspended in the 3 ml gus extraction buffer (pH 7) were disrupted by sonication for 3 x 30 seconds (70-74% power) with one minute intervals on ice. The extracts were examined for cell lysis under the light microscope (Leica). The majority of the cells were disrupted by sonication. The crude cell extracts (protein preparations) were used for enzymatic assays to measure gus activity, and in the Biorad protein assays to measure proteins in the extracts.

3.6.2 Determination of gus activity (enzymatic assays)

Materials: 4-nitrophenyl β-D-glucuronide (Sigma-Aldrich, UK), gus extraction buffer (50 mM sodium phosphate buffer pH 7.0, 10 mM β-mercaptoethanol, 10 mM disodium EDTA, 0.10 % (w/v) sodium laury sarcosine, 0.10% triton X-100, 1 M sodium carbonate solution pH 10.30 (stop buffer), protein preparations (crude cell extracts or supernatant concentrates), 10 mg/ml BSA solution, spectrophotometer (Aquamate, UK), 1 cm light path length cuvette (Sarstedt , Germany), temperature-controlled water bath (Grant Instruments Ltd. UK), 4-nitrophenol sodium salt (Sigma-Aldrich GmbH, Germany).

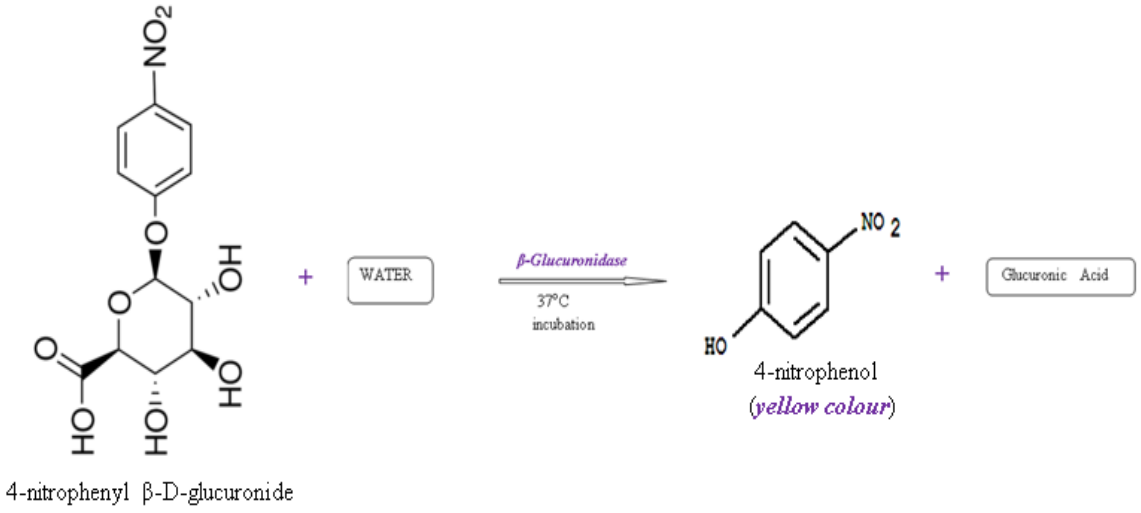

Figure 3.5: *β*-glucuronidase catalysed hydrolysis of 4-nitrophenyl β-D-glucuronide into 4-nitrophenol and glucuronic acid.

Enzymatic assays were performed on all samples (crude cell extracts and the supernatant concentrates) to measure the gus activity. The enzymatic hydrolysis of a glucuronide, followed by the spectrophotometric measurement of its product was used to quantify gus activity (Bowers et al., 1980). The assay is straightforward, highly sensitive, accurate and reproducible. Gus catalyse hydrolyses of 4-nitrophenyl β-D-glucuronide into 4-nitrophenol (a yellow coloured product), and glucuronic acid. A simple illustration of the reaction is shown in Figure 3.5.

The absorbance of light by 4-nitrophenol can be measured between 400 - 415 nm in a spectrophotometer (Bowers et al., 1980, Jefferson, 1987). 4-nitrophenol is mainly unionised at < pH 7 and exist as the conjugate acid (see Figure 3.6), with a low molar extinction coefficient at 405 nm. In the strongly alkaline condition such as pH >9.5, 4-nitrophenol is completely ionised, existing mainly as the 4-nitrophenolate salt (phenoxide ion) with high molar extinction coefficient at 400 - 415 nm (Bowers et al., 1980).

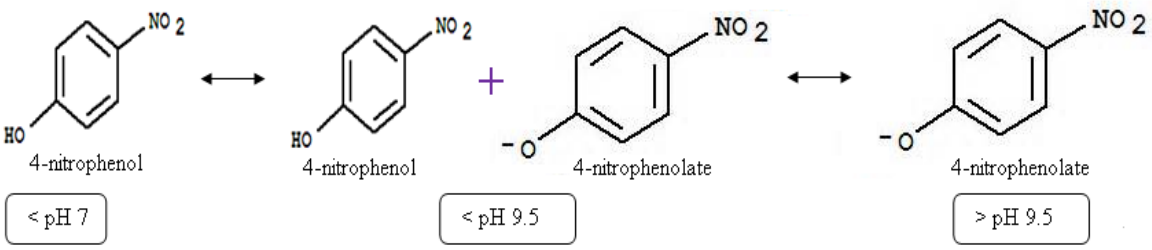

Figure 3.6: 4-nitrophenol and 4-nitrophenolate at different pH.

Thus the accurate spectrophotometric measurement of the 4-nitrophenol produced in assays requires that 4-nitrophenol must be completely ionised into the 4-nitrophenolate salt (Bowers et al., 1980). The requirement is achieved by stopping the gus catalysed reaction with a strong alkaline solution resulting in a final pH >9.5 (Bowers et al., 1980, Jefferson, 1987). Another requirement is that the molar extinction coefficient of the 4-nitrophenolate under the assay conditions must be experimentally determined (Bowers et al., 1980).

3.6.2.1 Enzymatic assay protocols.

Preparation of substrate

1 mM stock solution of 4-nitrophenyl β-D-glucuronide (substrate) was prepared by dissolving 157.6 mg of the substrate in 500 ml of the gus extraction buffer pH 7. 20 µl of 10 mg BSA/ml was added into a 1.6 ml of the 1 mM buffered substrate solution. The resulting 1.62 ml solution was pre-warmed in the temperature-controlled water bath at 37^{o}C. Bovine serum albumin (BSA) was included in the buffered substrate solution to stabilise gus during the reaction assay.

Reaction assay

The enzyme catalysed hydrolysis of the substrate was started by adding and mixing 0.2 ml of the enzyme sample (crude extract or concentrated supernatant fraction) into the 1.62 ml buffered substrate solution maintained at 37^{o}C. The dilution factor of gus in the solution was 9. The reactions were stopped at timed intervals of 2, 5, 10, 15, 20 minutes, by removing 0.2 ml of the reaction mixture into tubes containing 1 ml of 1 M sodium carbonate solution pH 10.30 (stop solution) at 20^{o}C. The final volume of the stopped reaction was 1.2 ml.

Blank

In the blank, 1.6 ml of 1 mM substrate solution (substrate and gus extraction buffer pH 7) was incubated at 37^{o}C to pre-warm. 0.2 ml of the blank mixture was mixed with 1 ml of 1 M sodium carbonate solution pH 10.30 at 20^{o}C. The final volume of the blank was 1.2 ml.

Control

The control was set up to measure any residual absorbance (at 405 nm) due to pigments or components in samples. In the control, 13 µl of 10 mg BSA/ml, 1.165 ml of gus extraction buffer (pH 7.0) and 22 µl of the enzyme (crude extract or concentrated supernatant fraction) were mixed together in the eppendorf tube at 20^{o}C. The final volume of the control was 1.2 ml.

The absorbance (at 405 nm) of the blank in a 1 cm light path length cuvette was used to zero the spectrophotometer. Thereafter, the absorbance (at 405 nm) of the stopped

reactions (2, 5, 10, 15, 20 minutes), and absorbance (at 405 nm) of the controls were measured. To obtain the corrected absorbance due to 4-nitrophenolate in the reactions, the absorbance of the controls were subtracted from absorbance of the stopped reactions.

Determination of 4-nitrophenolate concentration formed by reaction

The concentration of 4-nitrophenolate produced from the gus catalysed hydrolysis of the substrate at 37^{o}C at the different time intervals (2, 5, 10, 15, 20 minutes) was estimated using equation 3.5:

$$C = \left(\frac{(V * corrected\ \ absorbance\ of\ 4-nitrophenolate)}{\varepsilon * l * assay\ volume} \right) * dilution\ \ Factor \qquad (3.5)$$

Where C is concentration of 4-nitrophenolate (moles/litre), V is the final volume of the stopped reaction (1.2 ml), ε is molar extinction coefficient of 4-nitrophenolate (14453 L M^{-1} cm^{-1}) at 20^{o}C pH 10.3, l is the light path length (1 cm), and assay volume was 0.2 ml.

3.6.2.2 Molar extinction coefficient of 4-nitrophenolate at 405 nm

10 mM stock solution of 4-nitrophenolate was prepared by dissolving 161.09 mg of the salt with 10 ml reverse osmosis water. The 10 mM solution was serially diluted with gus extraction buffer (pH 7) to give 3.9 – 1000 µM 4-nitrophenolate (standard solutions). 0.2 ml of the 4-nitrophenolate standard solution was added and mixed with 1 ml of 1 M sodium carbonate solution (pH 10.3) at 20^{o}C. For the blank, 0.2 ml of gus extraction buffer (pH 7) was added to 1 ml of 1 M sodium carbonate solution pH 10.3 at 20^{o}C. The absorbance (at 405 nm) of the blank in a 1 cm light path cuvette was used to zero the spectrophotometer. Then the absorbancse (at 405 nm) of the 1.2 ml standard solutions were measured in the spectrophotometer.

The mean optical density (absorbance) of 4-nitrophenolate at 405 nm were plotted against the standard concentrations of 4-nitrophenolate in Figure 3.7. The plot was linear and the slope (14453) was determined. The value of the slope is the product of the molar extinction coefficient of 4-nitrophenolate and 1 cm light path length. Therefore, the molar extinction

coefficient of 4-nitrophenolate determined under the assay conditions (pH 10.3 and 20°C) at 405 nm was 14453 L M^{-1} $cm^{-}1$.

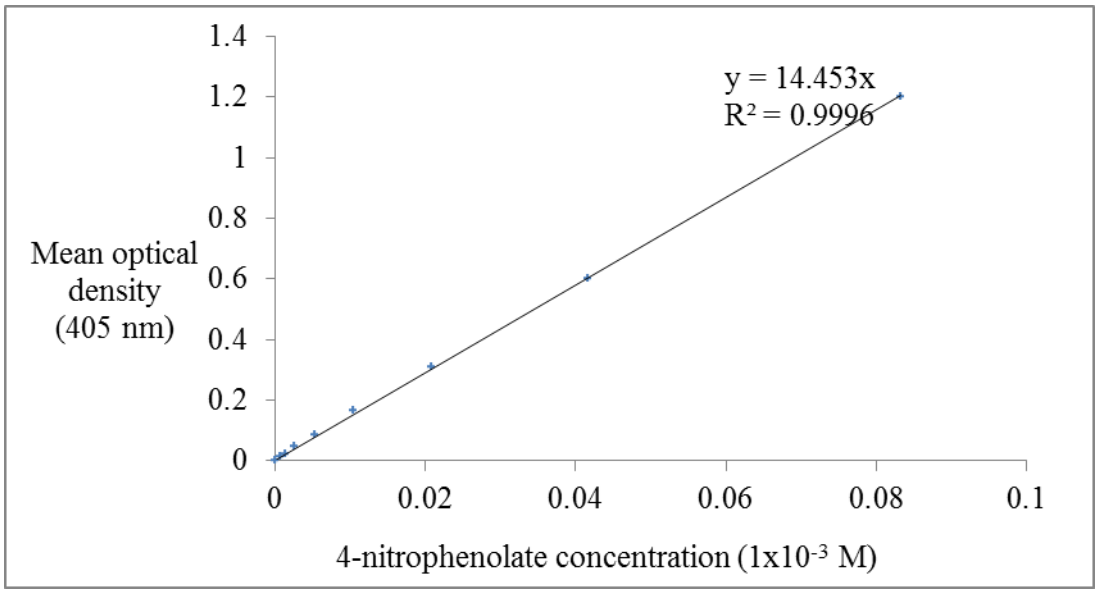

Figure 3.7: Standard calibration plot of optical density at 405 nm and 4-nitrophenolate concentrations (M) at pH 10.3 and 20°C. The mean and standard deviation were determined from 3 independent replicates and 2 technical replicates.

3.6.2.3 Reaction rates, gus activity, gus units, amount of gus and gus yield

Reaction rates

The Mean concentration (moles/litre) of the 4-nitrophenolate produced in the reaction was plotted against the time (minutes) giving the linear relationship between formation of product and time. The reaction rate (moles/litre/min) was calculated in equation 3.6:

$$\text{Reaction rate} = \left(\frac{(\text{Concentration of 4-nitrophenolate produced})}{\text{Time}} \right) \quad (3.6)$$

The reaction rate was also determined from the gradient of the slope in the linear plot of mean of 4-nitrophenolate concentration against time.

Gus activity

The gus activity was calculated as the number of moles of 4-nitrophenolate produced per minute at 37^{o}C. The optimum gus activity at 37^{o}C was calculated from equation 3.7:

$$Optimum\ gus\ activity\ in\ assay = \left(reaction\ rate * assay\ volume \right) \qquad (3.7)$$

Where, the assay volume was 0.2 ml. The gus activity in the samples (in units of nanomoles of 4-nitrophenolate formed/minute) was calculated using equation 3.8:

$$Gus\ activity\ in\ sample = \left(\frac{optimum\ gus\ activity\ in\ assay * extraction\ volume}{volume\ of\ enzyme} \right) \qquad (3.8)$$

Where the extraction volume was 3 ml for crude cell extract; 10 ml for the culture supernatant fractions (see method section 3.6.1); and volume of enzyme was 0.022 ml. The total gus activity was determined as the sum of gus activity in the crude cell extract and in the supernatant fraction.

Gus units, amount of gus, gus yield and gus productivity

The unit of an enzyme is the amount of the enzyme that catalyses the formation of one nanomole of the product per minute at 37^{o}C. The gus activity (nanomoles of 4-nitrophenolate formed/minute) was converted into enzyme units. The total enzyme unit was calculated as the sum of units of gus in the crude cell extracts and in the supernatant fractions. According to Jefferson, (1987), one unit of gus at 37^{o}C and pH 7 was approximately 5 ng of pure β-glucuronidase. The total amount of gus was estimated by multiplying the total units of gus by 5 ng. Gus yield was expressed as total amount of gus per cell (total ng gus/g dry cell weight). Gus productivity was expressed as the product of gus yield and maximum specific growth rate (total ng gus/g dry cell weight/h).

3.6.3 Determination of protein concentrations.

Materials: Biorad protein assay kit including 1 mg BSA/ml solution (Biorad laboratories GmbH, Germany), Spectrophotometer (Jasco V630, USA), 1 cm light path cuvette (Sarstedt, Germany), crude cell extracts and supernatant concentrates, Sorvall RC-5B refrigerated superspeed centrifuge (Du Pont, UK), Mistral 2000R refrigerated centrifuge

(MSE, UK), sterile 0.22 µm filter (Merck Millipore Ltd. Ireland), gus extraction buffer pH 7.

The protein concentration was determined using the Biorad protein assay method based on the principles of the Bradford assay (Bradford, 1976). The method is simple, straightforward, sensitive, and robust for measuring protein concentration in samples. The Biorad reagent is an acidic dye concentrate containing Coomassie brilliant blue G-250 dye, phosphoric acid and methanol. The free-dye solution is light brown with a maximum absorbance at 465 nm. When protein solution are added to the dye solution, binding of protein to the dye results in a colour change from light brown to blue colour, with a maximum absorbance that could be measured at 595 nm (Sedmak and Grossberg, 1977). The absorbance is proportional to the concentration of proteins present in the solution (Bradford, 1976).

3.6.3.1 Standard calibration curve of optical density and protein concentration

To correlate the absorbance of the blue colour solution formed to the concentration of proteins, a standard calibration curve for was first set up. Thereafter, assays were performed to measure the protein concentration in the samples.

Preparing dye reagent solution and standard BSA concentration

Five-fold dilution of the dye reagent concentrate was prepared by mixing 10 ml of the reagent to 40 ml reverse osmosis water. 1 mg BSA/ml stock solution was serially diluted with reverse osmosis water to obtain standard concentrations of 0.05 – 0.50 mg BSA/ml (standards).

Biorad protein assay protocol

The assay was started by mixing 0.02 ml of diluted BSA solutions (standards), 1 ml of dilute dye reagent and incubating at room temperature ($20^{o}C$) for five minutes. Gus extraction buffer (pH 7) was used as the blank. 0.02 ml of blank was mixed with 1 ml of dilute dye reagent and incubated at $20^{o}C$ for five minutes. After five minutes, the absorbance of the blank (at 595 nm) was used to zero the spectrophotometer (Jasco V630). After that, the absorbance of the blue colour solutions was measured. The mean

absorbance of the blue colour solutions was plotted against standard concentrations of BSA (mg/ml). The plot was linear (Figure 3.8), and the determined slope (correlation factor) was 1.15.

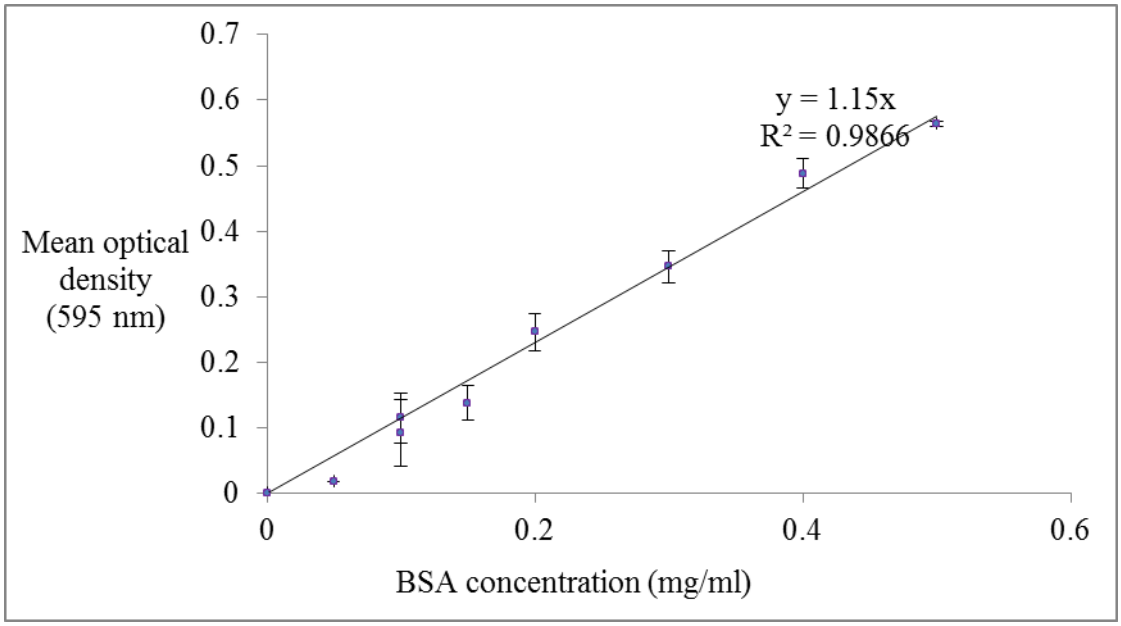

Figure 3.8: Standard calibration plot of optical density at 595 nm and BSA concentrations (mg/ml). The mean and standard deviation were determined from three independent replicates and two technical replicates.

3.6.3.2 Total protein yield (total cellular protein)

The samples (the 3 ml crude cell extracts and concentrated culture supernatant) were collected as described in section 3.6.1. Biorad protein assay method was performed on the concentrated supernatant fractions to determine the protein concentrations. 2.8 ml crude cell extracts were centrifuged in the sorvall centrifuge (SS34 rotor) at *25000 x* ***g*** (4^{o}C) for 30 minutes to sediment cellular and membranous debris. 2.8 ml supernatants (soluble fraction) were collected for protein estimation (Biorad protein assay method), leaving behind sediments (cellular debris) containing the insoluble protein fractions. The sediments were re-suspended with 2.8 ml of 1 M sodium hydroxide solution to dissolve and solubilise the fractions, and then kept overnight (16 h) at -20^{o}C. After 16 h, samples were thawed on ice and boiled for 10 minutes (100^{o}C) to ensure complete dissolution and solubilisation of

proteins. The Biorad protein assay method was also performed on the samples to determine the insoluble protein concentrations.

Assay for soluble and insoluble protein concentrations.

The Biorad protein assay method was performed as described in method section 3.6.3.1 with gus extraction buffer pH 7 as blank control. 0.02 ml of prepared samples were mixed with 1 ml of diluted Biorad reagent and kept at 20^{o}C for five minutes. After five minutes of blue colour development, the absorbance of the blank at 595 nm was used to zero the spectrophotometer, before the absorbance of the blue coloured solutions were measured. The protein concentration (mg/ml) was calculated from the measured absorbance and correlation factor (1.15) using equation 3.9:

$$Protein\ concentration = \left(\frac{Optical\ \ Absorbance\ \ (at\ 595\ nm)}{1.15} \right) * dilution\ \ factor \qquad (3.9)$$

Where, 1.15 is the correlation factor determined in Figure 3.8. Protein concentration was determined in the concentrated culture supernatant sample, the soluble fraction and the insoluble fraction samples concentrates. Soluble protein concentration was determined as the sum of protein concentration in the soluble fraction and in the concentrated culture supernatant. Insoluble protein concentration was determined in the insoluble protein fraction. The total protein concentration was determined as the sum of the soluble protein concentration and insoluble protein concentrations.

Total cellular protein (Total protein yield)

The total cellular protein was calculated by dividing the total protein concentration (mg/ml) by the cell concentration. The total cellular protein was expressed as total protein yield (mg total protein/g dry wt).

Protein productivity

Protein productivity was calculated as the product of total protein yield and maximum specific growth rate (mg total protein/g dry cell wt/h).

3.7 Determination of total carbohydrate

Materials: Phenol (Merck, Germany), 95% (v/v) sulphuric acid (Fischer scientific, UK), D-glucose (Fisher scientific, Uk), Spectrophotometer (Jasco V630, USA), 1 cm light path cuvette (Sarstedt, Germany), exponential phase cultures (~2 million cells per ml), Mistral 2000R centrifuge (MSE, UK), eppendorf centrifuge 5417 (Eppendorf AG, Hamburg).

The total carbohydrate in the strains was determined using the phenol sulphuric acid method described by Dubois et al. (1956). The method is simple, reproducible, sensitive and accurate for the detection and measurement of carbohydrates in samples. Carbohydrates react with a solution of phenol in concentrated sulphuric acid to produce orange-yellow complexes that are measured by spectrophotometry. The samples are first hydrolysed in concentrated sulphuric acid to break down polysaccharide to the corresponding monosaccharide units. The monosaccharides may become dehydrated by the acid to hydroxyl-methyl furfural and furfural derivatives. The complex mixture of sugars and their derivatives reacts with the phenol to form the orange-yellow coloured aromatic complexes. The orange-yellow colour is stable, allowing the amount of carbohydrates present to be determined by spectrophotometry at 490 nm. The absorbance of the orange-yellow colour is directly proportional to the amount of carbohydrates in the sample.

3.7.1 Standard calibration curve of optical density and amount of carbohydrate

The standard calibration curve was set up with glucose as the carbohydrate standard.

Preparing standard glucose concentrations and 5% (w/v) phenol solution

A stock solution of glucose (1 mg/ml) was prepared by dissolving 100 mg glucose in 100 ml reverse osmosis water. Different volumes of the standard glucose solution (0.01 – 0.15 ml) were diluted with reverse osmosis water to a final 0.5 ml (0.01 – 0.15 mg glucose respectively). The 5% (w/v) phenol solution was prepared by dissolving 1 g phenol into 20 ml reverse osmosis water.

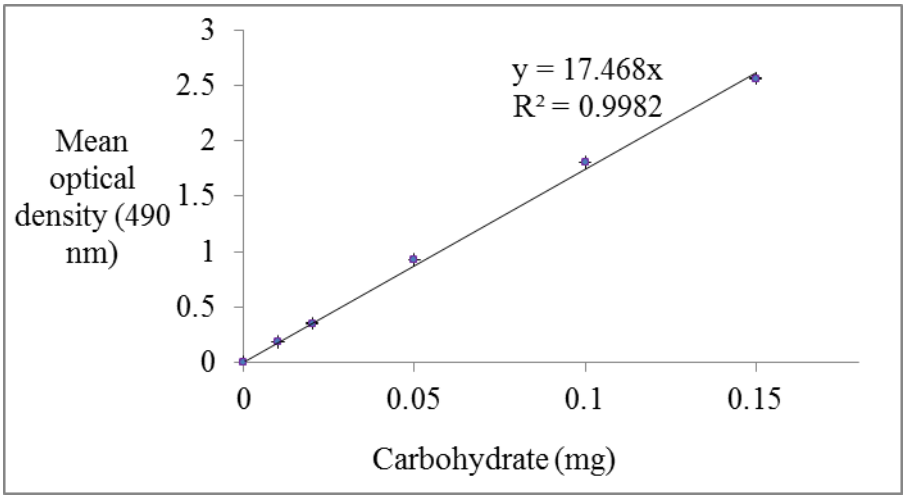

Figure 3.9: Standard calibration plot of optical density at 490 nm and amount of carbohydrate (mg). The mean and standard deviation were determined from three independent replicates and two technical replicates.

Phenol-sulphuric acid assay protocol **(Dubois et al., 1956)**

0.5 ml reverse osmosis was used as the blank. 0.5 ml of the 5% (w/v) phenol was added into 0.5 ml of the carbohydrate standard, and into the blank. 2.5 ml 95% (v/v) sulphuric acid was rapidly delivered (~3 s) into samples and blank respectively. The exothermic reaction was allowed to proceed for 10 minutes with orange-yellow colour development. The reaction mixture was then mixed by entry and exit from a pipette, and allowed to complete after another 20 minutes at 20^{o}C. The absorbance of blank (at 490 nm) was used to zero the spectrophotometer, and thereafter, the absorbance (at 490 nm) of the orange-yellow coloured solutions was measured. A calibration plot of mean absorbance against amount of carbohydrate (mg) was constructed as shown in Figure 3.9. The slope of the linear plot was determined to obtain the correlation factor 17.468 for correlating absorbance of orange-yellow complex at 490 nm into amount of carbohydrate (mg).

3.7.2 Determination of total cellular carbohydrate

7 ml of the exponential phase cultures (~2 million cells per ml) was harvested by centrifugation Mistral 2000R centrifuge at 2000 rpm for five minutes at 20^{o}C. The cell

pellets were washed twice with 7 ml reverse osmosis water by centrifugation at 2000 rpm for five minutes at 20^{o}C. The supernatants were discarded.

Cell harvest and acid-hydrolysis of cell pellets

The cell pellets were collected, re-suspended with 0.15 ml of 95% (v/v) sulphuric acid to hydrolyse the carbohydrates overnight (16 h) completely at room temperature (20^{o}C) to the corresponding sugars. After the 16 h incubation, reverse osmosis water was added to the acid-hydrolysed samples to a final 0.25 ml volume. The samples were centrifuged in the eppendorf centrifuge 5417 at *17000 x* ***g*** for 10 minutes at 20^{o}C. The supernatant fractions were collected for the phenol-sulphuric acid assay.

Phenol-sulphuric acid assay protocol

0.5 ml of the acid hydrolysed samples was prepared by adding 0.03 ml supernatant fractions to 0.47 ml reverse osmosis water. 0.5 ml reverse osmosis was used as the blank control. The phenol-sulphuric acid assay (described in section 3.7.1) was performed with 0.5 ml sample. After the reactions were completed, the absorbance of blank (at 490 nm) was used to zero the spectrophotometer. Then the absorbance (at 490 nm) of the orange-yellow colour solution formed was measured. The amount of carbohydrate (mg carbohydrate) in the samples was calculated according to equation 3.10:

$$Amount\ Carbohydrate\ (mg) = \left(\frac{(V * \ Absorbance\ (at\ 490\ nm))}{17.468\ *\ sample\ \ volume} \right) \qquad (3.10)$$

Where *V*, is the final volume of acid-hydrolysed sample (0.25 ml), *17.468* is the correlation factor, and sample volume in the phenol-sulphuric acid assay was 0.03 ml. The total cellular carbohydrate was calculated by dividing the amount of carbohydrate (mg) by the total number of cells harvested. Total cellular carbohydrate was expressed as total mg carbohydrate/g dry wt.

3.8. Determination of total cellular ATP concentration

Materials: exponential phase cultures (~2 million cells per ml), ammonium bicarbonate (Fisher chemical, UK), HPLC grade water (Sigma-Aldrich GmbH, Germany), 100% (v/v) HPLC grade methanol (Sigma-Aldrich GmbH, Germany), cellometer auto T4 instrument (Nexcelom Bioscience, USA) Sorvall RC-5B refrigerated superspeed centrifuge (Du Pont, UK), miVac centrifugal concentrator (Geneva Inc. USA), ATP bioluminescence Assay kit CLS II (Roche Diagnostics GmbH, Germany), Anthos Zenyth 3100 multimode detector (Anthos Labtec GmbH, Austria), Greiner flat bottom 96-well plate (Sigma-Aldrich, USA), multichannel pipette (Labnet International Inc. USA), Eppendorf refrigerated centrifuge 5415c (Eppendorf GmbH, Germany).

The total cellular ATP concentration was determined using the ATP bioluminescence assay kit CLS II (Roche Diagnostics GmbH, Germany) based on the luciferin-luciferase bioluminescence reaction (Crouch et al., 1993). In this method, luciferase catalyses the oxidation of luciferin to oxyluciferin and the luminescence from the reaction was measured in a microplate reader:

$$\text{ATP + D-luciferin } + O_2 \xrightarrow{\textit{luciferase}} \text{oxyluciferin + AMP + ppi + } CO_2 \text{ + light}$$

The amount of luminescence (emitted light) depends on the concentrations of ATP and luciferase present in the assay. The concentration of luciferase in the ATP bioluminescence assay kit CLS II (Roche Diagnostics GmbH, Germany) was constant and very low so that in the assay conditions, luminescence is directly proportional to ATP concentrations in the samples.

3.8.1 Quenching of metabolism and collection of metabolite samples

The method described by Lee and Fiehn (2008) and Winder et al. (2008) for quenching cellular metabolism and harvesting quenched cells was used. The quenching solution was prepared (60 ml 100% (v/v) HPLC grade methanol and 40 ml HPLC grade water containing 0.85 g ammonium bicarbonate) and stored at -48^{o}C. The ammonium

bicarbonate was added to minimize leakage of metabolites from the cells during the quenching procedure.

The cell density of exponential phase growth cultures was determined (~2 million cells per ml). The cell sizes were measured in the cellometer Auto T4 instrument. 2 ml of the cold -48^{o}C quenching solution was transferred into tubes pre-chilled at -80^{o}C on dry ice. 2 ml of the exponential growth phase cultures was rapidly quenched by plunging of the culture (~3 s) into the 2 ml cold quenching solution maintained on dry ice to inactivate metabolic activities in the cells. The quenched cultures were centrifuged at *16100 x* ***g*** for two minutes, at -15^{o}C in a sorvall refrigerated centrifuge (SS34 rotor) pre-chilled at -15^{o}C. 4 ml supernatant fractions (metabolite footprints) were collected, flash frozen in liquid nitrogen and stored at -80^{o}C. The quenched cell pellets were immediately flash frozen in liquid nitrogen and stored at -80^{o}C.

3.8.2 Cold methanol extraction of intracellular metabolites

The quenched cell pellets were re-suspended in 2 ml of cold -80^{o}C 100%v/v methanol (extraction solvent). The intracellular metabolites were extracted from the cells by freeze-thaw method (Winder et al., 2008). In each freeze-thaw cycle, the suspended cells in -80^{o}C extraction solvent were flash-frozen in liquid nitrogen, thawed on ice (0^{o}C), and vortex for 10 seconds followed by freezing in liquid nitrogen. 10 freeze-thaw cycles were performed in order to permeate the cells resulting in the leakage and extraction of intracellular metabolites into the -80^{o}C extraction solvent. The methanol extracted samples were centrifuged at -20^{o}C for eight minutes at *16100 x* ***g*** in the sorvall refrigerated centrifuge (SS34 rotor) pre-chilled at -20^{o}C. 2 ml supernatant fractions (metabolite fingerprints) were collected in tubes pre-chilled on dry ice (-80^{o}C), flash frozen in liquid nitrogen and stored at -80^{o}C.

3.8.3 Concentration of metabolite samples to dryness

0.5 ml of metabolite samples were collected into sterile tubes and kept at -80^{o}C. The 0.5 ml samples were concentrated to dryness in the miVac centrifugal concentrator operating

at 1000 rpm (30^{o}C) for one hour in order to the remove water and methanol from the sample. The dry metabolite sample was immediately collected on dry ice and stored at -80^{o}C before the ATP bioluminescence analysis.

3.8.4 Construction of the standard ATP calibration curve

A standard ATP calibration curve was first set up to correlate ATP bioluminescence to ATP concentrations under the assay conditions. A stock concentration of ATP (0.0165 M) was prepared by dissolving 10.3 mg ATP provided in the ATP bioluminescence assay kit with 1.03 ml reverse osmosis water. The 0.0165 M ATP solution was then serially diluted to give ATP standard concentrations in the range 5 x 10^{-8} M to 10^{-3} M solutions. The luciferase reagent was re-constituted by adding 10 ml reverse osmosis water to the luciferase reagent provided in the kit. The re-constituted reagent was carefully mixed to obtain homogenous solution and kept on ice (0^{o}C) prior to use.

ATP bioluminescence assay protocol

50 µl of the ATP standard samples were added to wells. 50 µl reverse osmosis water was used as the blank control. The luciferase catalysed reaction was started by adding 50 µl of the re-constituted luciferase reagent to the 50 µl ATP standard sample, and to 50 µl blank at 20^{o}C using a multichannel pipette. The reaction was maintained at 20^{o}C and the luminescence readings measured after 10 minutes in the Anthos Zenyth 3100 microplate reader calibrated to measure luminescence by endpoint assay at 20^{o}C. The ATP bioluminescence measurements were obtained by subtracting luminescence of blank from the luminescence of the ATP standard. A plot of the mean ATP bioluminescence against standard ATP concentrations was constructed. The plot was linear at the detection and sensitivity range of the assay for ATP concentrations (Figure 3.10). The slope was determined from the linear plot with a value of 2 x 10^{10} (the correlation factor) for correlating ATP bioluminescence units into ATP concentration (M) under the assay conditions.

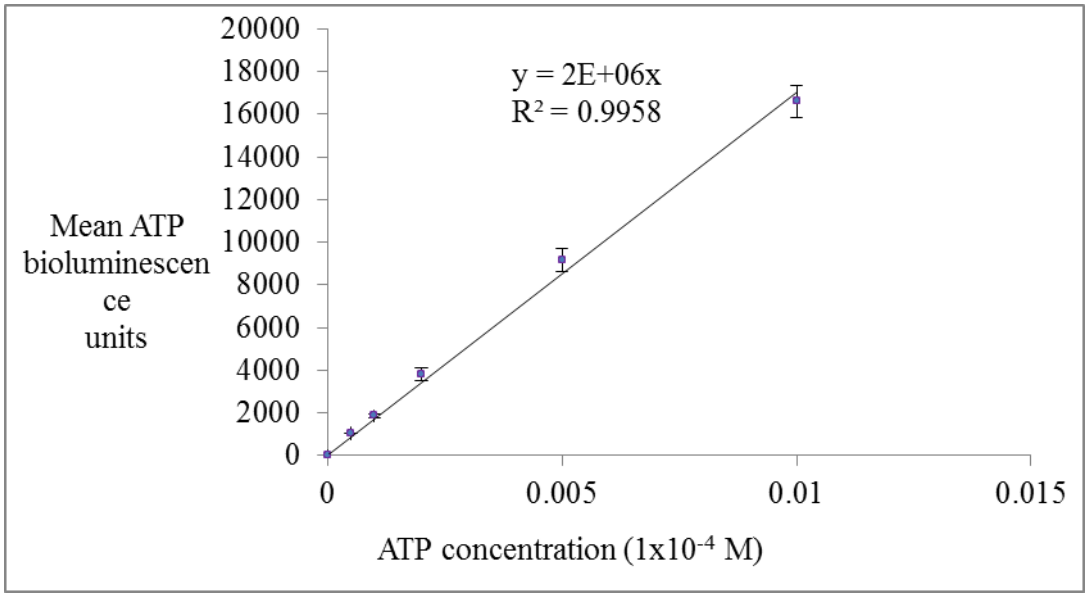

Figure 3.10: Standard calibration plot of ATP bioluminescence units and ATP concentrations (M). The mean and standard deviation were determined from three independent replicates and two technical replicates.

3.8.5 Determination of cellular ATP concentrations

The dry -80^{o}C metabolite sample from the footprint or fingerprint fractions was re-suspended with 0.5 ml reverse osmosis water to dissolve all metabolites completely into solution. The resulting solution was centrifuged at *17000 x* ***g*** for 10 minutes at 0^{o}C to sediment particulate matter and pigments. The supernatant fractions were collected for the ATP bioluminescence assay.

ATP bioluminescence assay protocol

The ATP bioluminescence assay was performed as described in section 3.8.1 with 50 µl of the sample. 50 µl reverse osmosis water was used as the blank control. At the end of the reaction (after 10 minutes) maintained at 20^{o}C, the luminescence readings were measured in the Anthos Zenyth 3100 microplate reader (endpoint assay). The ATP bioluminescence measurements were obtained by subtracting luminescence of the blank from the luminescence of the samples. The ATP concentration (M) was calculated using equation 3.11:

$$ATP\ concentrat\ ion\ (M) = \left(\frac{ATP\ biolu\ \min escence\ of\ \ sample}{2\ x10^{10}} \right) \qquad (3.11)$$

Where, 2 x 10^{10} is the factor for correlating ATP bioluminescence units into ATP concentration (M). The total ATP concentration was determined as the sum of ATP concentration measured in metabolite footprint and fingerprint fractions. Since two ml of cultures of known cell density was quenched for ATP analysis, the total number of ATP moles was calculated using equation 3.12:

$$Total\ ATP\ moles\ = 0.002 * Total\ \ ATP\ \ molar\ \ concentration \qquad (3.12)$$

C. reinhardtii cells are approximately spherical in shape, and the cell diameter (μm) was measured for the culture (see section 3.2.4). The cell volume (litre) was calculated using the formula for spherical volume according to equation 3.13:

$$spherical\ \ cell\ \ volume\ (L) = \left(\frac{4\pi\ X\ 10^{3}}{3\ X\ 10^{-18}} \right) * \left(\frac{d}{2} \right)^{3} \qquad (3.13)$$

Where π (*pi*) is approximately 3.14; *d* is the cell diameter (μm); the factor 10^{-18} in the denominator converts μm^3 into m^3. The factor 10^3 in the numerator, converts the volume unit into litre (L). The cellular ATP concentration (mM) was calculated taking into account the total number of ATP moles, total number of cells and the mean cell volume using equation 3.14:

$$Cellular\ \ ATP\ concentration = \left(\frac{Total\ \ ATP\ moles}{Total\ \ cells\ * Mean\ cell\ \ volume} \right) \qquad (3.14)$$

3.9 Determination of dry cell weight

The dry cell weight of cultures was determined after harvesting the cell pellets, and drying to constant dry weight as described by Neufeld and Zajic (1982) and Sonnleitner et al. (1992).

Materials: Exponential phase cultures, spectrophotometer (Aquamate, UK), Mettler AJ100 weight balance (Mettler-Toledo, UK), sterile polypropylene tubes (Corning Inc. USA),

temperature-controlled oven (Leader engineering Ltd., UK), Mistral 2000R centrifuge (MSE UK).

The weight of dry empty sterile polypropylene tube was first measured in the weight balance (Mettler AJ100) at room temperature (20^{o}C). Then the cell density (cells/ml) of the culture was measured. 12 ml of the culture was added into the weighed tube. The culture was centrifuged at 2000 rpm for five minutes in the Mistral 2000R centrifuge at 20^{o}C to sediment the cell pellets from the medium. The clear supernatant was carefully discarded. The wet cell pellets was collected and washed thrice with 8 ml reverse osmosis water by centrifugation at 2000 rpm for five minutes (20^{o}C) to remove salts and growth medium components from the cells. The supernatant was carefully discarded in order not to lose cells.

The weight of the wet cell pellets and tube was measured. After that, the wet cell pellets and tube was dried by heating at 60^{o}C for 12-14 h in the hot air oven (Leader engineering Ltd) until a constant dry weight was obtained. The dry cell pellet and tube (sample) was quickly weighed within a 3 minute time window at 20^{o}C, to prevent adsorption of moisture. The dry samples were weighted repeatedly over the 3 minute period to determine constancy of the measurements. The dry cell weight (g dry weight per cell) was calculated using equation 3.15:

$$Dry\ cell\ weight = \left(\frac{weight\ of\ dry\ cell\ pellets\ and\ tube - weight\ of\ dry\ empty\ tube}{Total\ number\ of\ cells\ in\ culture\ sample} \right) \quad (3.15)$$

3.10 Measurement of acetate consumption and uptake rates

Materials: Cultures, Mistral 2000R refrigerated centrifuge (MSE, UK), spectrophotomer (Aquamate, UK), 1 cm light path length cuvette (Sarstedt, Germany), sterile 0.22 μm syringe filter (Merck Millipore, USA), acetic acid assay reagents and enzyme kit (MegaEnzyme Ltd. Ireland), sterile liquid media (TAP or minimal).

The acetate concentration of media during growth was measured using the acetic acid assay method described by MegaEnzymes Ltd. (manufacturer of the acetic acid assay kit). The assay kit contains different enzyme preparations (acetate kinase, phosphotransacetylase, pyuruvate kinase and D-lactate dehydrogenase) and the reagent preparations (ATP, Coenzyme A, phosphoenol pyruvate, NADH). The reactions of the assay (shown in Figure 3.11) involve the enzymatic conversion of acetate (or acetic acid) into acetyl-phosphate and ADP, coupled to reactions that oxidize NADH to NAD^+. The amount of NAD+ produced is equivalent to the amount of NADH oxidised, and the amount of NADH converted equals the amount of acetate in the sample.

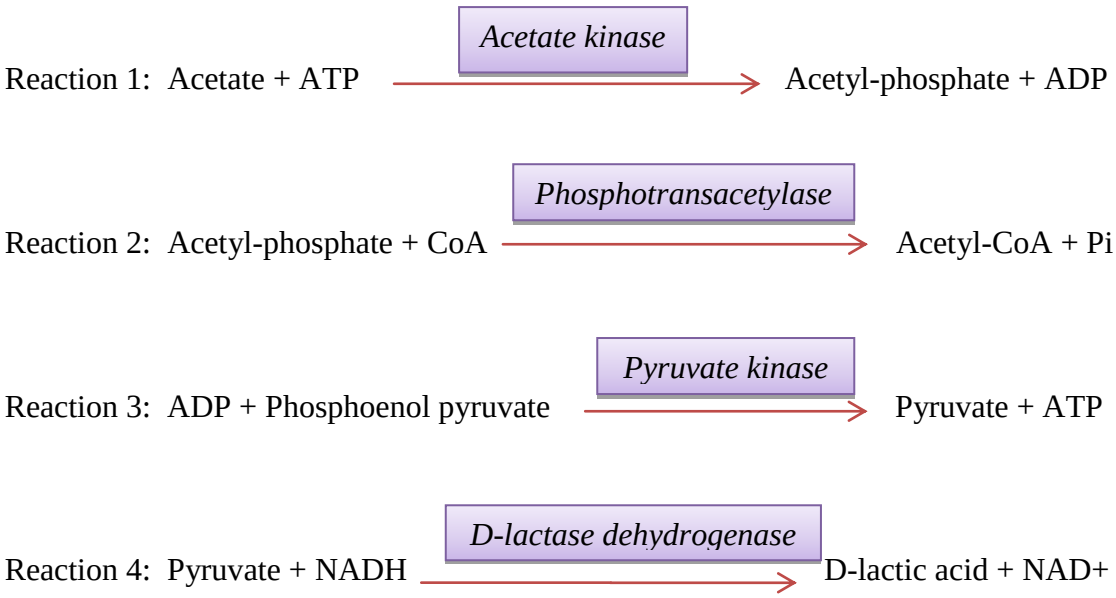

Figure 3.11: The enzymatic conversion of acetate to acetyl-CoA coupled to oxidation of NADH to NAD+.

The decrease in NADH concentration was measured by a decrease in absorbance of NADH at 340 nm. The assay is very sensitive, accurate and a robust method for determining the concentration of acetate in samples.

Sample collection

During growth the cell density of the culture was measured. 2 ml culture was collected and centrifuged at 2000 rpm for five minutes in the Mistral 2000R centrifuge to separate cells from the medium. The supernatant fraction was collected and immediately filtered through

a sterile 0.22 μm syringe filter (Merck Millipore) to remove any suspended cells. The filtrate sample contains the acetate concentration representative of the growth medium.

Acetic acid assay protocol on filtrate sample

The assay was performed according to the instruction of the manufacturer. 0.05 ml of the supernatant (sample), 1 ml of minimal medium (blank), 0.25 ml reagent solution 2 (mixture of NADH, ATP, phosphoenol pyruvate, polyvinylpyrrolidone buffer pH 7.4), 0.01 ml reagent solution 3 (Coenzyme A), and 0.01 ml enzyme solution 4 (containing D-lactate dehydrogenase, phosphotransacetylase, and pyruvate kinase) were added and mixed together. After two minutes incubation at 20^{o}C, the absorbance (at 340 nm) of NADH in the mixture was measured in the spectrophotometer using 1 cm light path cuvette. The reading provided the initial NADH absorbance at 340 nm. The enzymatic reactions were started by adding and mixing 0.01 ml acetate kinase preparation (solution 5) to the mixture. The final reaction volume was 1.33 ml. After four minutes incubation at 20^{o}C the reaction was completed and the absorbance of NADH (340 nm) was measured again. The reading provided the final NADH absorbance at the completion of the reaction.

Assay on sterile TAP

Sterile TAP medium contain the initial concentration of acetate. Acetic acid assay protocol on sterile TAP medium was used to measure the initial concentration of acetate in the medium at zero time before inoculation of cells. The acetic acid assay was performed as described previously using 0.05 ml sterile TAP as the sample. The final reaction volume was 1.33 ml.

Assay on sterile minimal medium (blank)

Sterile minimal medium (0 mM) acetate and was used as the blank control for the measurement. The acetic acid assay (as described above) was performed on blank using 1.05 ml of sterile minimal medium, and the final reaction volume was 1.33 ml.

3.10.1 Calculation of acetate concentration in growth medium

The decrease in NADH absorbance at 340 nm was measured by subtracting the initial and final NADH absorbance. The decrease in NADH absorbance was measured in the acetic acid assay on samples, sterile TAP media and the blank (minimal media). The correct

decrease in NADH absorbance in samples or sterile TAP was obtained by subtracting away the absorbance of blank from the absorbance of sample or sterile TAP values respectively. The acetate concentration was calculated using equation 3.16:

$$C = \left(\frac{(V * M * Correct\ decrease\ in\ NADH\ absorbance\ at\ 340\ nm)}{\varepsilon * l * \ sample\ \ volume} \right) * dilution\ \ \ factor \qquad (3.16)$$

Where C is the acetate concentration in g/litre, V is total reaction volume (1.33 ml), M is the molecular weight of acetic acid (60.05 g/mol), l is the light path length (1 cm); $\boldsymbol{\varepsilon}$ is the molar extinction coefficient of NADH at 340 nm (6300 L M^{-1} cm^{-1}), and the sample volume was 0.05 ml. The acetate consumed in the growth medium at any given time was determined using equation 3.17:

$$\text{Acetate consumed} = [\text{Acetate } (t0) \ - \ \text{Acetate } (t1)] \qquad (3.17)$$

Where, acetate (*t0*) refer to initial acetate concentration in the sterile medium prior to inoculation (zero time); acetate (*t1*) refer to acetate concentration in the medium after the given time of growth.

3.10.2 Estimation of specific acetate uptake rate

The specific acetate uptake rate was calculated as a function of concentration of acetate consumed, cell density and specific growth rate (Manichaikul et al., 2009). During growth, the specific acetate uptake rate depended on the concentration of acetate consumed, the specific growth rate and the increase in cell density according to equation 3.18:

$$U_{Acetic\ acid} = \left(\frac{Change\ in\ concentration\ of\ acetate\ \ during\ growth * \mu}{Increase\ in\ cell\ \ density\ \ during\ growth} \right) \qquad (3.18)$$

Where, $U_{Acetic\ acid}$ is the specific acetate uptake rate (mmoles acetate consumed/g dry cell weight/h), μ is the specific growth rate measured in the growth condition.

3.11 Measurement of ammonium consumption in growth medium

Materials: Ninhydrin reagent (Sigma-Aldrich, Germany), hydradantin (Sigma-Aldrich, Germany), dimethyl sulfuroxide (Sigma-Aldrich, Germany), 2-propanol (Fisher scientific, UK), 0.20 M sodium acetate buffer pH 4.50, spectrophotometer instrument (Jasco V630, USA), 1 cm light path cuvette (Sarstedt, Germany), sterile 0.22 µm syringe filter (Merck Millipore, USA), sterile TAP medium, sterile NH_4Cl-free TAP medium, cultures, spectrophotometer (Aquamate, UK).

The ammonium concentration was determined by measuring the concentration of NH_4Cl in the medium, using the ninhydrin method adapted from Jones et al. (2002) and Moore and Stein (1954). The principle of the assay is the reaction of ninhydrin reagent (a mixture of ninhydrin, hydradantin and dimethyl sulforoxide (DMSO)) with free amino groups or ammonium to form a stable purple-coloured complex solution:

(Ninhydrin + hydradantin + DMSO) + NH_4^+ ⟶ **Purple complex precipitate**

The absorbance of the purple-coloured solution at 570 nm is proportional to the intensity of the colour produced, and depends directly on the amount of ammonium in the sample. The method is accurate, sensitive, and reproducible and was simple to employ.

3.11.1 Standard calibration of optical density and ammonium concentrations

Preparation of ninhydrin reagent

1 g hydradantin was dissolved into 75 ml dimethyl sulfuroxide. 2 g of ninhydrin was mixed and dissolved into the solution. The final volume was adjusted to 100 ml with 25 ml of 0.20 M sodium acetate buffer (pH 4.5). The prepared ninhydrin reagent was used in the assay.

Preparation of ammonium standard solutions

Sterile TAP medium contain 500 µg NH_4Cl/ml of medium. Sterile TAP was used as the ammonium standard solution. 0.01 - 0.32 ml of the TAP medium was serially diluted with

reverse osmosis water to a final 1 ml to give concentrations of 5 - 160 µg NH_4Cl/ml (samples). Ammonium-free TAP medium was used as the blank. 0.01 ml of the blank was diluted to a final 1 ml volume with reverse osmosis water.

Ninhydrin assay protocol

The ninhydrin reaction was started by mixing 2 ml ninhydrin reagent with 1 ml of the ammonium containing TAP solutions (standards) resulting in purple colour change. In addition, 2 ml of the ninhydrin reagent was added into the 1 ml blank. The 3 ml reaction mixture was boiled (100^{o}C) for 15 minutes to complete the reaction and colour development. Thereafter, the solutions and blank were diluted by the addition of 5 ml 50% (v/v) 2-propanol.

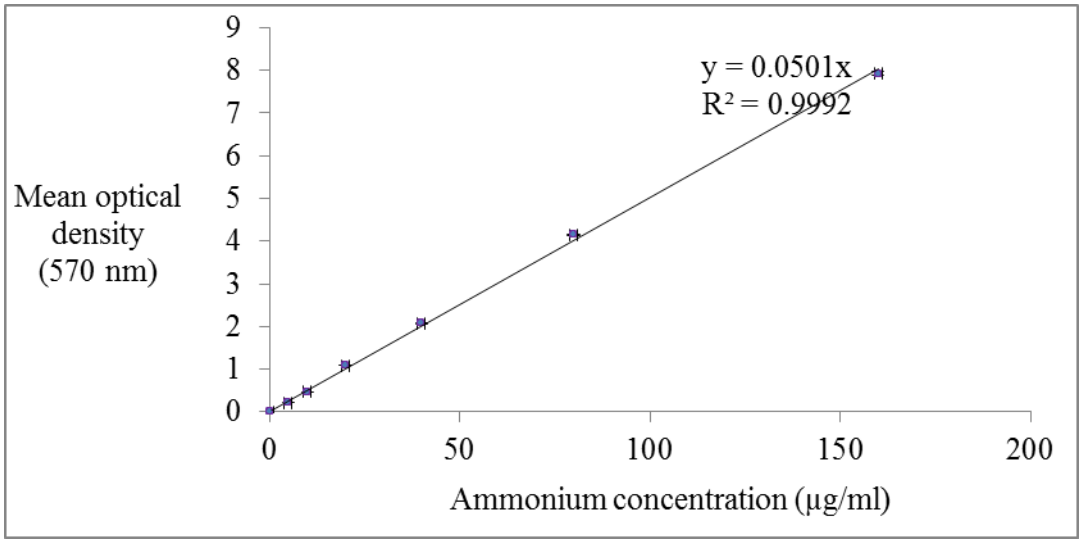

Figure 3.12: Standard calibration plot of optical density at 570 nm and ammonium concentrations (µg/ml). The mean and standard deviation were determined from three independent replicates and two technical replicates.

The absorbance of blank (at 570 nm) was used to zero the spectrophotometer instrument before absorbance (at 570 nm) of the purple colour solutions was measured. The plot of mean absorbance (at 570 nm) against standard NH_4Cl concentrations (µg/ml) was constructed. The plot was linear showing the relationship between the absorbance of the purple colour with ammonium concentrations. The slope of the linear plot was determined

(Figure 3.12). The slope value 0.0501 was obtained (factor for correlating optical density at 570 nm of the purple colour into ammonium concentration).

3.11.2 Ammonium concentration in growth media

During growth the cell density of the growth medium was measured. 2 ml culture samples were collected and centrifuged at 2000 rpm for five minutes in the Mistral 2000R centrifuge to sediment cell pellets from the medium. The supernatant fraction was collected and immediately filtered through a sterile 0.22 μm syringe filter (Merck Millipore) to remove any suspended cells. The clear filtrates (samples) was analysed for ammonium concentration.

Ninhydrin assay protocol

0.01 ml of blank (ammonium-free TAP), 0.01 ml sterile TAP, and 0.01 ml of the filtrate samples were each separately diluted to 1 ml with reverse osmosis water (100 dilutions of the samples). The ninhydrin assay was performed on the diluted sterile TAP samples (1 ml), diluted filtrate samples (1 ml), and on the diluted blank (1 ml), as described in section 3.11.1. The absorbance of the blank (at 570 nm) was used to zero the spectrophotometer instrument, before the absorbance (at 570 nm) of the purple colour solutions was measured in the samples. The concentration of ammonium in the filtrate samples or sterile TAP was calculated using equation 3.19:

$$C = \left(\frac{Absorbance\ of\ assay(at 570\,nm)}{0.0501} \right) * dilution\ \ factor \quad (3.19)$$

Where, *C* is ammonium concentration (μg/ml). The ammonium concentration (μg/ml) was converted into mM. The ammonium consumed at any given time was calculated using equation 3.20:

Ammonium consumed = [Ammonium (*t0*) – Ammonium (*t1*)] (3.20)

Where, ammonium (*t0*) refer to initial ammonium concentration in the sterile TAP medium prior to inoculation (zero time); ammonium (*t1*) refer to ammonium concentration in the medium after the given time of growth.

3.12 Measurement of chlorophyll concentrations and photosynthetic rates.

Materials: USB4000 UV/Visible light spectrophotomer (Ocean Optics; USA), acetone solution (80% (v/v) acetone, 2.50 mM sodium phosphate buffer pH 7.80), ependorf centrifuge 5415c (Ependorf GmbH; Germany), exponential phase growth cultures, DW2 Oxygen electrode instrument (Hansatech Instruments Ltd. England), Quantum sensor meter (Skye Instruments Ltd. UK), warm white LED light from Cree mc-e (Cree Inc. USA).

Chlorophyll concentrations were determined according to methods of Porra et al. (1989). The photosynthetic rates were measured using photosynthetic oxygen evolution as the indicator of photosynthetic activity. The photosynthetic rates were measured in the oxygen electrode instrument using the instructions of the manufacturer (Hansatech Instruments Ltd. England).

3.12.1 Estimation of chlorophyll concentration

The cell density (cells per ml) of cultures was first measured. The chlorophyll was extracted from the cultures using the acetone extraction method described by Porra et al. (1989). 1 ml culture was centrifuged at *16000 x* ***g*** in the eppendorf 5415c centrifuge for five minutes to completely sediment the cells. The supernatant was carefully discarded in order not to lose cells. The cell pellets were washed twice with reverse osmosis water to remove salts and growth medium components by quick spin at *16000 x g* for 30 seconds. The clear supernatants were carefully discarded and the cell pellet collected. The cell pellets were re-suspended, and homogenised with 1 ml 80% (v/v) acetone solution (buffered with 2.50 mM sodium phosphate pH7.80 to minimize degradation of chlorophylls) to extract and release chlorophyll pigments. The green extracts were

centrifuged at *16000 x* ***g*** for five minutes. 1 ml of the green supernatant fractions (acetone-extracted chlorophyll pigments) was collected.

Measurement of chlorophyll a and b concentrations

Chlorophyll *a* and *b* concentrations were measured in the USB 4000 UV/visible light spectrophotometer. 1 ml of buffered 80% (v/v) acetone was used as the blank to zero the spectrophotometer, before absorbance of the chlorophyll extracts were measured at 646.6 nm, 663.6 nm and 750 nm in the spectrophotometer. Chlorophyll *a* and *b* show peak maxima at 646.6 nm and 663.6 nm, and zero peak at 750 nm (Porra et al., 1989). The absorbance values were correlated into concentration units (nmol chlorophyll/ml) using the equations 3.21 and 3.22 by Porra et al. (1989):

$$Chyll\ a\ (nmol/ml) = 13.71*\Delta A_{(663.6nm - 750\ nm)} - 2.85*\Delta A_{(646.6nm - 750nm)} \quad (3.21)$$

$$Chyll\ b\ (nmol/ml) = 22.39*\Delta A_{(646.6nm - 750nm)} - 5.42*\Delta A_{(663.6\ nm - 750\ nm)} \quad (3.22)$$

ΔA represented the change in absorbance between a peak maxima and 750 nm. For the acetone extraction method, the values 13.71, 2.85, and 22.39, 5.42 are experimentally determined coefficients correlating the change in absorbance to chlorophyll *a,* and *b* concentrations, respectively (Porra et al., 1989). The molecular weights of chlorophyll *a* and chlorophyll *b,* are 893.489g/mole and 907.472 g/mole respectively. Therefore chlorophyll concentration was converted to mg chlorophyll/ml.

3.12.2 Measurement of photosynthetic rates

The DW2 oxygen electrode instrument was first calibrated before photosynthetic measurements were performed.

The DW2 oxygen electrode (Hansatech Instruments Ltd. England) comprises of a borosilicate vessel which houses the culture chamber containing the silver electrode disc (immersed in saturated potassium chloride solution). The electrode disc is separated from culture by a thin semi-permeable membrane that allows only the passage of dissolved

gases or ions to the electrode. Cultures placed in the chamber are continually stirred by a magnetic stirrer. The DW2 oxygen electrode has a control unit that digitizes electrical signals of the electrode measurements to computer screen output. An immersed electrode disc within the stirred borosilicate vessel measures the concentration of dissolved oxygen in cultures in the chamber. Since temperature fluctuations affect the concentration of dissolved gases, the temperature within the vessel is controlled and held constant at 20^{o}C by a thermostat, and also by controlled flow of cooling water through the jacket fitted on the vessel. Controlled stirring of cultures placed in the vessel eliminates thermal and diffusion gradient that may cause incorrect measurements. Electrochemical reactions occur at the electrode disc during oxygen-production (photosynthesis), and oxygen-consumption processes (respiration). The reactions produce electrical signals that are converted into digital signals by the control unit of the DW2 electrode instrument, and the output is subsequently displayed on a chart of signal intensity against time (s) on the computer screen.

The gross evolution of oxygen concentration with time (oxygen concentration balance with time) is the sum of oxygen consumption (respiration rate) and oxygen production (photosynthesis rate) processes. The gross evolution of oxygen was measured in the DW2 electrode instrument and expressed in (µmol O_2/ml/h). The respiration rate was measured in the DW2 electrode as (-µmol O_2/ml/h) indicating a consumption process. The photosynthetic rate was estimated by adding the respiration rate and the gross evolution of oxygen with time. The photosynthetic rate was expressed as µmol O_2/ml/h.

Determination of respiration rate

The cell density of the culture (cells/ml) was measured. Thereafter, 0.5 ml of culture was introduced into the stirred temperature-controlled (20^{o}C) borosilicate vessel. The measurement of oxygen consumption by the culture was performed in the dark. Real-time digital signal intensity plots against time were recorded by the control unit and displayed on the computer output screen. Measurements were taken for 3 – 4 minutes until signal intensity of dissolved oxygen decreases to a constant steady value due to oxygen depletion. The rate oxygen consumption was measured (respiration rate) and expressed in negative unit (-µmol O_2/ml/h).

Determination of gross oxygen evolution with time

After measuring the respiration rate, the 0.5 ml culture in the borosilicate vessel at 20^{o}C was immediately supplied with light. Warm-white light was supplied from the light emitting diode connected to the ports of the vessel at light intensity of 1200 µmol photons/m^2/s. The real-time signal intensity plots against time recorded by the control unit were displayed on the computer output screen showing a rapid increase in signal intensity of dissolved oxygen until a constant steady signal value was obtained after 10 minutes due to light-saturation. The increase in signal intensity with time for dissolved oxygen concentration reflected the unequal balance of oxygen production rate (photosynthesis) and oxygen consumption rate (respiration) i.e. photosynthesis rate greater than respiratory rate. The gross evolution of oxygen concentration with time was measured. (µmol O_2/ml/h). The constant steady signal value attained after 10 minutes reflected the equal balance of photosynthetic and respiration rates at the light intensity so that gross evolution of oxygen concentration with time was zero at this point.

Determination of photosynthetic rate

The photosynthetic rate was estimated by adding the respiration rate to the rate of gross evolution of oxygen. Theoretically, the ratio for the amount of CO_2 fixed into biomass by photosynthesis to the amount of O_2 produced by the process was unitary. Therefore, the photosynthetic rate was expressed as µmol CO_2 fixed/ml/h.

Estimation of specific photosynthetic rate

The specific photosynthetic rate was estimated by dividing the photosynthetic rate of the culture with the cell concentration (g dry wt/ml) in equation 3.23:

$$P_c = \left(\frac{Photosynthetic\ rate}{cell\ density} \right) \qquad (3.23)$$

Where P_C is the specific photosynthetic rate (µmol CO_2 fixed/g dry wt/h). This was also reported as the specific CO_2 fixation rate or specific CO_2 uptake rate.

3.13 Statistical methods

Data were presented as the mean of *n* number of biological (independent) replicates with standard deviation reflecting variability. The mean and standard deviation values were calculated using the statistics function in the Microsoft 2010 excel package. The standard error of mean values was calculated using equation 3.24:

$$SEM = \left(\frac{S\tan dard\ deviation}{\sqrt{n}} \right) \qquad (3.24)$$

Inferential statistical methods used were unpaired two-tailed *t* test. The *t* test statistics were performed using the statistics function in the Microsoft 2010 excel package.

3.14 Flux balance analysis of algaGEM model

In this study, flux balance analysis (FBA) was applied on the genome scale metabolic reconstruction algaGEM, based on the *Chlamydomonas reinhardtii* genome (Dal'Molin et al., 2011). FBA simulations on algaGEM were performed in the MatLab environment using the Constraint-Based Reconstruction and Analysis (COBRA) tool-box (Becker et al., 2007, Schellenberger et al., 2011). FBA was used to predict the maximal theoretical yield of recombinant *β*-glucuronidase (gus) in the three growth conditions. The heterotrophic condition (representing the limiting condition for growth and recombinant gus production) was simulated by applying appropriate constraints on the relevant reactions of the algaGEM model, based on the experimental flux values observed on *C. reinhardtii*. The *in silico* simulations were performed with the aim of: (a) identifying steady-state fluxes that limit gus production, (b) generating hypothesis for the optimization of gus yield (to be tested experimentally), (c) guiding the design of growth experiments and culture medium.

3.14.1 Basic concepts in flux balance analysis method

Flux balance analysis (FBA) is a constraint-based modelling technique widely used to analyse the flux distributions through a biochemical network under steady-state conditions (Orth et al., 2010). Typically, models of metabolic networks that are analysed by FBA methods will contain known metabolites, pathways, reactions, genes and the proteins

encoded in the system (Boyle and Morgan, 2009, Dal'Molin et al., 2011, Duarte et al., 2007, Edwards et al., 2001, Mo et al., 2007). The data used for constructing these models of biological systems can be derived from variety of sources including published literatures, databases sources (genomic, transcriptomics, proteomics, metabolomics, metabolic pathways,), cellular localization and interaction data sources, and information regarding the biochemical characterization of the networks in particular (Boyle and Morgan, 2009, Dal'Molin et al., 2011, Duarte et al., 2007, Mo et al., 2007).

In FBA the metabolic network is described in terms of its stoichiometric matrix ***N***, which summarizes in a computationally-friendly way the metabolites and metabolic reactions occurring in the system. The generic element (*i, j*) of ***N*** is the stoichiometric coefficient of metabolite *i* in reaction *j*.

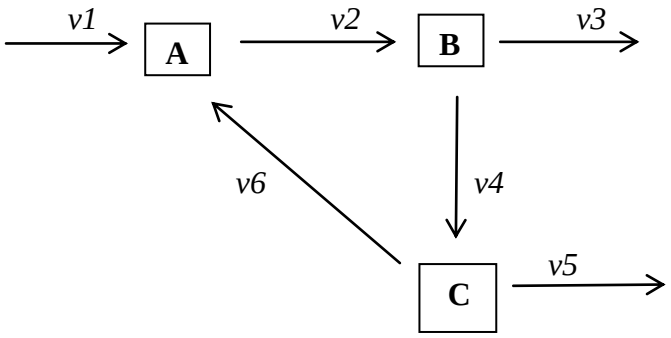

Figure 3.13: A simple network with three metabolites (A, B, C) and six reactions.

The sign of the entry (*i, j*) is positive or negative depending on whether the metabolite *i* is produced or consumed respectively, given the directionality of the reaction *j*. If metabolite *i* is not a substrate (reactant or product) in reaction *j*, the corresponding entry (*i, j*) is set to zero. For example, Figure 3.13 shows a simple network with three metabolites (A, B, C) and six reactions (*v1, v2, v3, v4, v5, v6*), where all the stoichiometric coefficients are assumed to be 1. The stoichiometric matrix ***N*** of the network in Figure 3.13 is:

$$\boldsymbol{N} = \begin{pmatrix} 1 & -1 & 0 & 0 & 0 & 1 \\ 0 & 1 & -1 & -1 & 0 & 0 \\ 0 & 0 & 0 & 1 & -1 & -1 \end{pmatrix} \qquad (3.25)$$

Where, the three rows (top to bottom) represents metabolites A, B, C respectively, while the six columns (left to right) represents reactions *v1* to *v6*. The time evolution of the metabolite concentrations in a network can be expressed as the product of the stoichiometric matrix ***N*** and the vector of fluxes ***v*** (Palsson 2006) according to equation 3.26:

$$\frac{dC}{dt} = N.v \qquad (3.26)$$

where *C* denotes the (column-) vector of metabolite concentrations, and v the (column-) vector of the fluxes. In the FBA formulation, equation 3.26 is equated to zero in order to constrain the system to the steady-state condition, where each molecular species is produced at the same rate as it is consumed:

$$\frac{dC}{dt} = N.v = 0 \qquad (3.27)$$

Other constrains are also introduced in FBA in order to define (if known) the maximal flux capacity of each reaction:

$$v_j^L \le v_j \le v_j^U \qquad (3.28)$$

Where, v_j^L and v_j^U are the lower and upper bound respectively of the flux v_j. The constraints expressed in equation 3.28 are also used to define the directionality of the different reactions (for example, if $v_j^L = 0$, and $v_j^U \neq 0$, then reaction j can only occur in the positive direction). Equations 3.27 and 3.28 define a linear problem in the variables, *v*. Any solution *v* of such problem represents a theoretically possible steady-state flux distribution through the underlying metabolic network. Since there are generally more reactions (variables) than metabolites (constraints), the problem defined by Equations 3.27 and 3.28 become underdetermined i.e. it has an infinite number of solutions. The entire collection of solutions is referred to as the null-space of *N* and represents the phenotype of the network (Orth et al., 2010). However, not all the mathematically possible solutions are biologically relevant. In order to identify one solution *v* that is biologically more representative than the others, FBA relies on the assumption that biological systems have evolved to optimize specific biological processes. FBA formalizes this assumption through

the introduction of an objective function *f*. The objective function is a mathematical expression that represents the criterion of optimality assumed to be fulfilled by the cell (for example production of biomass or ATP). The basic formulation of an FBA problem (Orth et al., 2010) is then given by equation 3.29:

maximize $f := \mathbf{c}^{T} . \mathbf{v}$

Subject to

$\boldsymbol{N}. v = 0$

$$v_j^L \leq v_j \leq v_j^U \qquad (3.29)$$

Where the objective function *f* to be maximized takes the form of a linear combinations of the flux variables $\boldsymbol{v}$ with coefficients $\boldsymbol{c}$ (in other terms the different fluxes $\boldsymbol{v_j}$ contribute to the objective function *f* with weights given by the coefficients $\boldsymbol{c_j}$). The equation 3.29 is an instance of a class of problems called linear programming (LP) problems (Orth et al., 2010). There are today a number of efficient algorithms that solves the LP problems using the accessible and low-cost computing power of common laptops. An FBA solution is an optimal solution of the LP problem as expressed in equation 3.29. The FBA solution is a flux distribution, *v* that maximizes the objective function *f* while satisfying the steady-state condition and the constraints imposed on the individual fluxes in equation 3.29 (Orth et al., 2010). For example, in order to predict the maximal theoretical yield of gus in algae and to study an optimal flux distribution leading to such yield, we can set the objective function *f* to represent the gus production. The maximal yield of the gus protein will then be given by the maximized value of *f*, while the flux distribution is given by the corresponding FBA solution *v*. This result can then be compared with experimentally measured gus yield to test the model prediction. The model can be further refined with experimental data and additional biological constraints where needed, until the predictions are compatible with experimental observations.

However, the optimal solution returned by FBA is not unique. There are in general an infinite number of solutions with the same degree of optimality (Orth et al., 2010), although only one is returned by the LP solver. Different algorithms have been proposed to

explore the space of the optimal solutions (Lee et al., 2000, Murabito et al., 2009), but they are computationally prohibitive when applied to genome-scale metabolic networks. A computationally affordable approach that is commonly used to gain some insight on the space of optimal solutions is flux variability analysis (FVA). Once the optimal value of the objective function f is determined by solving the FBA problem (equation 3.29), FVA is applied to assess the maximal and minimal range of values that each reaction flux, v_j, can assume compatibly with the optimal value previously found for f (Gudmundsson and Thiele, 2010, Mahadevan and Schilling, 2003).

The earliest use of FBA methods was reported by Papoutsakis (1984) to calculate the theoretical growth yield of butyric acid bacteria. Fell and Small (1986) used the approaches to study stoichiometric constraints on fat synthesis in adipocytes. FBA method has since been extended into other applications. For example, in metabolic engineering, FBA studies have been used to improve the yields of important bio-products derived from micro-organisms (Ranganathan et al., 2010). FBA is finding application in drug discovery studies and drug target identification (Oberhardt et al., 2013), in the study of interaction networks (Kim et al., 2012, Raghunathan et al., 2010), and in the design of optimized culture medium for cell growth (Yang et al., 2009). Today there is a number of genome-scale models designed for FBA (Boyle and Morgan, 2009, Dal'Molin et al., 2011, Duarte et al., 2007, Edwards et al., 2001, Mo et al., 2007). There are a variety of computational tools available to perform *in silico* analysis and these are reviewed by Lakshmanan et al., (2014). Some examples of computational tools for FBA include Cobra Toolbox (Becker et al al., 2007, Schellenberger et al., 2011), SurreyFBA (Gevorgyan et al., 2011), FASIMU (Hoppe et al., 2011), OptFlux (Rocha et al., 2010), FBA-SimVis (Grafahrend-belau et al., 2009), and FAME (Boele et al., 2012).

3.14.2 Simulation of AlgaGEM using Cobra tool box version 2.0

Flux balance analysis, a constraint-based reconstruction and analysis (COBRA) method, was used to simulate metabolism using the cobra toolbox (Schellenberger et al., 2011), freely available at http://opencobra.sourceforge.net/ in the MatLab environment. The

Cobra toolbox includes a linear programming solver (glpk), and a number of code sources for the analysis and simulation of models based on the system biology markup language (SBML) (Schellenberger et al., 2011). AlgaGEM is currently the most complete genome-scale metabolic network reconstruction model for algae and was freely downloaded from http://www.biomedcentral.com/1471-2164/12/S4/S5. The SBML model (algaGEM) was constructed by (Dal'Molin et al., 2011) using genomics, transcriptomics, proteomics and metabolomics data of *C. reinhardtii* obtained from literatures. The AlgaGEM consists of 1371 genes, 1734 metabolic reactions and 1863 metabolites. The model incorporates five cellular compartments: cytosol, mitochondrion, chloroplast, micro-body and extra-cellular environment. In the current work, FBA method was used to simulate recombinant protein production in the algaGEM. The commands for executing cobra scripts and the scripts for running FBA simulations on the SBML model are described and provided in Appendix IV.

3.14.3 Steps for performing FBA simulations of recombinant gus production

The model can be described in three layers. An external medium: representing an input layer (the *in silico* medium) from which light enters, and nutrients are transported into the model. The model structure (internal layer) receives the light input, nutrients and simulates *in silico* metabolism and growth (metabolic reactions). The third layer is the output layer: metabolic products reflecting model outputs are secreted away from the model into the external environment (output layer). The list of transport processes described by algaGEM is shown in Table (3.2).

All reactions of the model (transport processes and metabolic reactions) carry lower and upper flux bounds. The flux bounds define the minimal and maximal allowable flux through the reactions. Constraints representing experimentally measured reaction fluxes were used to constrain the corresponding reactions in the model. In particular, lower and upper bounds of the reactions were set to the corresponding experimental flux values. For example, flux for biomass formation (mmoles biomass/g dry wt/h) was set to the experimental measured value. Similarly, experimental constraints for light and nutrient uptake (acetate or CO_2) were applied on the model. For example in heterotrophic condition, cells grow in the dark using acetate as the only available carbon and energy

source, ammonia as nitrogen source and other nutrients in the medium such as phosphate, sulphates and trace elements.

Table 3.2: Transport (exchange) processes and corresponding reaction index numbers in the model.

Transport process	**reaction index**	**Transport process**	**reaction index**
CO_2 transport	35	Serine transport	1715
Water transport	36	Formate transport	1716
O_2 transport	37	Lactate transport	1717
Nitrate assimilation	38	Ethanol transport	1718
NH_3 transport	39	Arginine exhange	1720
H_2S transport	40	Asparagine exchange	1721
Sulphate transport	41	Cysteine exchange	1722
Glucose transport	42	Glycine exchange	1723
Starch transport	43	Histidine exchange	1724
Acetate transport	44	Isoleucine exchange	1725
Photon uptake	45	Leucine exchange	1726
Sucrose export	46	Lysine exchange	1727
Phosphate transport	47	Methionine exchange	1728
Glycolate excretion	49	Phenylalanine exchange	1729
Hydrogen production	50	Proline exchange	1730
Glutamate transport	1711	Threonine exchange	1731
Glutamine transport	1712	Tryptophan exchange	1732
Aspartate transport	1713	Tyrosine exchange	1733
Alanine transport	1714	Valine exchange	1734

To simulate heterotrophic growth, experimentally determined uptake rate of acetate (mmole/g dry wt/h) was assigned to the flux for acetate transport in the algaGEM model. Additionally, zero flux was assigned to photon transport, and zero flux for CO_2 transport.

Zero lower flux value was assigned to transport process that is not allowed to carry a nutrient into the model during simulation (such as described above for light and CO2 in heterotrophic condition). A zero lower and zero upper flux were assigned to transport reactions that do not participate in the model. Transport processes for the secretion of metabolites (or product) away from the model into the external environment have zero lower and positive upper fluxes.

For simulating the growth conditions, the following experimentally measured fluxes for transport processes were constrained on the model in addition to FBA constraints. Negative lower flux values signify uptake of nutrients into model.

HETEROTROPHIC:

- Fixed heterotrophic growth flux
  - Growth lower flux = 0.02446 mmole biomass/g dry wt/h
  - Growth upper flux = 0.02446 mmole biomass/g dry wt/h
- Carbon transport constraint
  - CO_2 lower uptake flux = 0
  - CO_2 upper uptake flux = +Infinity mmole CO_2/g dry wt/h
  - Acetate lower uptake flux = -1.70 mmole acetate/g dry wt/h
  - Acetate upper uptake flux = 0

- Photon transport flux
  - Photon lower flux = 0
  - Photon upper flux = 0

AUTOTROPHIC:

- Fixed autototrophic growth flux
  - Growth lower flux = 0.0309 mmole biomass/g dry wt/h
  - Growth upper flux = 0.0309 mmole biomass/g dry wt/h
- Carbon transport constraint
  - CO_2 lower uptake flux = -11 mmole CO_2/g dry wt/h
  - CO_2 upper uptake flux = +Infinity mmole CO_2/g dry wt/h

- Acetate lower uptake flux = 0
- Acetate upper uptake flux = 0

- Photon transport flux
- Lower photon flux = -54 mmole photon/g dry wt/h
- Upper photon flux = -5 mmole photon/g dry wt/h

MIXOTROPHIC:

- Fixed mixotrophic growth flux
- Growth lower flux = 0.0572 mmole biomass/g dry wt/h
- Growth upper flux = 0.0572 mmole biomass/g dry wt/h
- Carbon transport constraint
- CO_2 lower uptake flux = -8 mmole CO_2/g dry wt/h
- CO_2 upper uptake flux = +Infinity mmole CO_2/g dry wt/h
- Acetate lower uptake flux = -1.035 mmole acetate/g dry wt/h
- Acetate upper uptake flux = 0
- Photon transport flux
- Lower photon flux = -54 mmole photon/g dry wt/h
- Upper photon flux = -5 mmole photon/g dry wt/h

Heterotrophic condition infers growth in the dark with acetate uptake from the medium as the only carbon and energy source for growth. Autotrophic condition provides photosynthetic growth constraint in which CO_2 is the only available carbon for growth and light used as energy source (both CO_2 and photon transport have negative lower fluxes). Acetate was omitted from the *in silico* autotrophic medium and assigned zero flux (lower and upper bounds). In mixotrophic condition, acetate and CO_2 transport into model are the sources of available carbon (each have negative lower fluxes). Acetate and light provide the energy for growth (photon transport assigned negative lower flux). Growth in the three conditions required uptake of ammonia, phosphates and sulphates. Ammonia, phosphate and sulphate transport from the medium into model was modelled using the default lower and upper flux values in algaGEM (with unit of mmole/g dry wt/h) for these transport processes as shown in Table 3.3.

Table 3.3: Default flux values for ammonia, phosphates and sulphate uptake in the model.

Transport process	reaction index	Lower uptake flux (mmole/g dry wt/h)	Upper uptake flux (mmole/g dry wt/h)
Ammonia transport	39	-1000	1000
H_2S transport	40	-1000	1000
Sulphate transport	41	-1000	1000
Phosphate transport	47	-1000	0

All reactions with negative lower and positive upper fluxes represent reversible processes. To simulate gus production, the following reaction was added to the model:

$$A.A + tRNA + GTP \longrightarrow P + tRNA + GDP + pi \qquad (3.30)$$

Where, A.A refers to amino acids, tRNA refers to transfer RNA, GTP refers to guanine nucleotide trisphosphate. In the reaction, amino acid and GTP are substrates and tRNA serve to bound to and to transfer each amino acid into the polypeptide chain to form protein. The products of the reaction are shown on the right hand side of equation 3.30. P refers to the recombinant protein, GDP and pi refers to guanosine diphosphate and inorganic phosphate respectively. The hydrolysis of GTP into GDP and pi provides the energy for protein synthesis in which the amino acids are added through peptide bond formation. The tRNA on right hand side of equation 3.30 is unbound transfer RNA left after an amino acid is added into the protein. The addidtion of one amino acid into polypeptide of protein require one tRNA to transfer it, and one GTP hydrolysis. Each of the 20 amino acids has different number of occurrence in a protein. The number of occurrence of each amino acid (abundances) in the gus protein composition is presented on Table 6.3b (page 182).

The reaction in equation 3.30 is a lumped reaction that acts as a demand for the correct amounts of tRNAs, amino acids, and GTP in the production of gus protein. The objective function was defined as the flux through the gus production reaction (equation 3.30). The criterion of optimality was then set as the maximization of such flux.

Chapter 4 – Limitations to growth; Results and discussions

In this chapter, the autotrophic, heterotrophic and mixotrophic growth of *C. reinhardtii* cultures were characterized. In autotrophic condition, cultures were grown in minimal medium (a medium devoid of acetate or organic carbon source) under continuous white fluorescent light supplied at 54 µmol photons/m^2/s. The same conditions were implemented for mixotrophic growth of cultures except that the cultures were grown in TAP medium (a medium containing acetate). Heterotrophic cultures were grown in TAP medium and in continuously dark conditions, so that acetate was the only carbon and free-energy source for growth. In each condition, growth was permitted at a constant 25^{o}C and cultures were agitated in shake flasks rotating at constant speed of 90 rpm. Thus, by keeping the incubation temperature and mixing effect constant across the different conditions, other factors that limited the growth of cultures could be identified. Factors like light and duration of light, pH, carbon, nitrogen and energy limitations. We sought to quantify the limitations to growth so as to enable the design of strategy to optimize the microalgae growth.

4.1 Growth of cultures in minimal and TAP media

The compositions of TAP medium and minimal medium used for the propagation of cultures are listed on Table 3.1. TAP medium contains acetate and ammonium chloride as the sole carbon and nitrogen source respectively. Phosphates, sulphates, magnesium and calcium ions, and trace metal nutrients are provided in the medium to support heterotrophic, or mixotrophic growth of cultures. The medium was buffered against pH changes by tris and phosphate buffers. Minimal medium was used to provoke autotrophic growth as it had the same compositions as TAP, but was devoid of acetate. Growth of cultures in minimal medium under autotrophic conditions was the basis for the selection of photosynthetic-rescued strains (transformants) from the mutant strain (cc373 mt+) that do not grow in light, but strictly required acetate for growth.

4.1.1 Growth in autotrophic condition

Autotrophic cultures grow via photosynthesis utilizing free energy of light for photosynthetic CO_2 fixation as the only source of carbon. Previous authors (Collins and Bell, 2004, Moroney and Ynalvez, 2007) have demonstrated that *Chlamydomonas* cultures were capable to adapt and grow in very limiting CO_2 concentrations. In addition, cultures were reported to utilize respired CO_2 or CO_2 in the ambient air or CO_2 dissolved in the medium as HCO_3^- ions to meet their carbon needs through the use of highly efficient carbon concentrating mechanism that internally concentrate the substrate. In the current work, autotrophic growth in flasks was observed without the supply of exogenous CO_2.

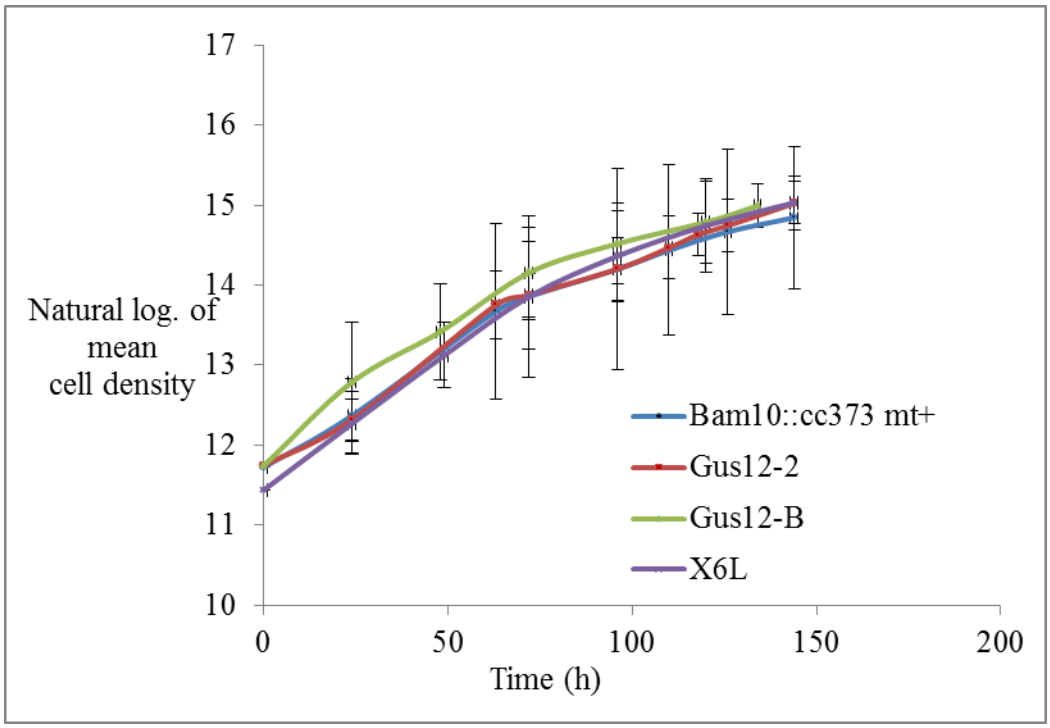

Figure 4.1: Autotrophic growth of Bam 10::cc 373 mt+, Gus12-2, Gus12-B and X6L cultures at 25^{o}C and 54 µmol photons/m^2/s maintained at 90 rpm. The mean cell density and standard deviation were determined from three biological replicates and two technical replicates each. The natural logarithm of mean cell density was plotted against time.

The growth curves of autotrophic cultures are shown in Figures 4.1 and 4.2. The maximum specific growth rates measured at the exponential phase of growth for autotrophic cultures

are presented in Table 4.1. Cultures were observed to grow for more than 200 h, fuelled by free energy of light and photosynthesis, resulting in high cell densities (usually >10 million cells per ml) of the autotrophic cultures (see Figure 4.2).

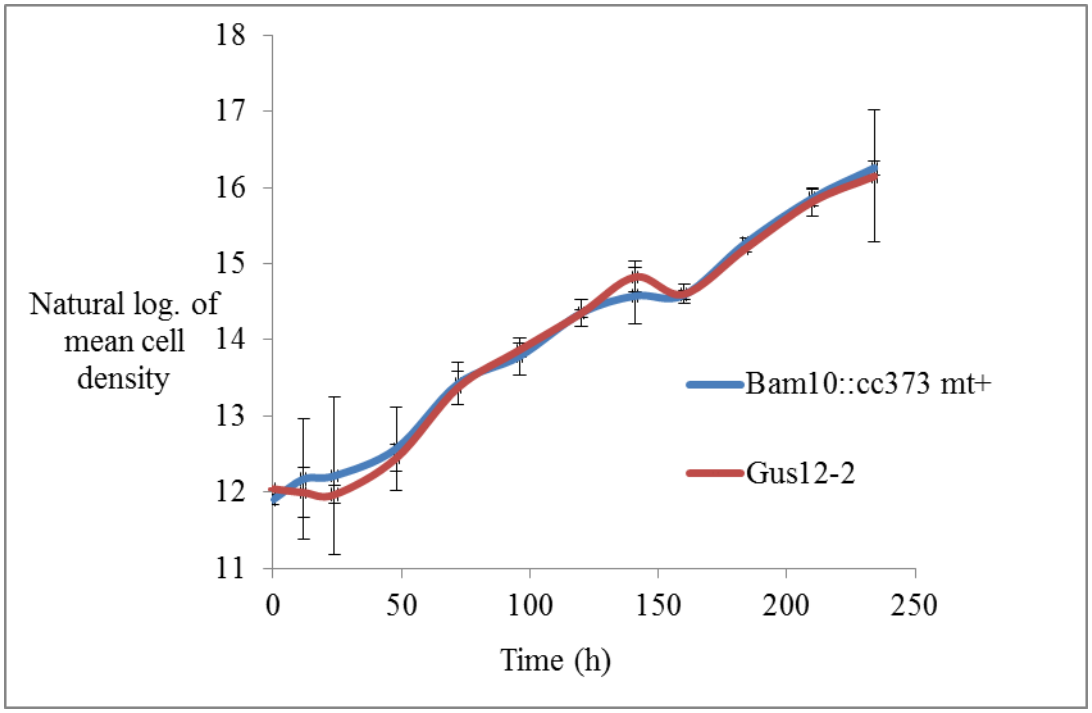

Figure 4.2: Autotrophic growth of Bam 10::cc 373 mt+ and Gus12-2 cultures at 25^{o}C and 54 µmol photons/m^{2}/s maintained at 90 rpm after 234 h incubation. The mean cell density and standard deviation were determined from three biological replicates and two technical replicates each. The natural logarithm of mean cell density was plotted against time.

The autotrophic condition was observed to support the persistence of cultures over long periods of time in minimal medium. For example, autotrophic cultures were observed to grow after more than 30 days in the liquid minimal medium, and also survive on minimal solid agar medium over more than 40 days. For long term storage, *C. reinhardtii* strains were maintained in minimal solid agar medium under autotrophic conditions (12 h light and 12 h dark periods), from which inoculum transfers were made into new minimal medium every four weeks.

4.1.2 Growth in heterotrophic condition

Typical growth curves for cultures propagated in heterotrophic condition are shown in Figure 4.3. One striking feature of growth under heterotrophic condition is that cultures reach the stationary phase quickly, typically at about 144 h. The duration of the stationary phase was short lasting about 24 - 48 h (see Figure 4.3), thereafter, cells entered death phase. Another feature of heterotrophic growth was that the final cell density achieved by the cultures was very low (about 3 million cells per ml) compared to the autotrophic or mixotrophic cultures. A third feature was that growth of cultures in heterotrophic condition presented a relatively slower growth rate than in autotrophic or mixotrophic growth condition (see Table 4.1). The lower final cell growth yield, shorter period in stationary phase may suggest stronger limitations to growth (stress) in heterotrophic cultures than in the other two conditions.

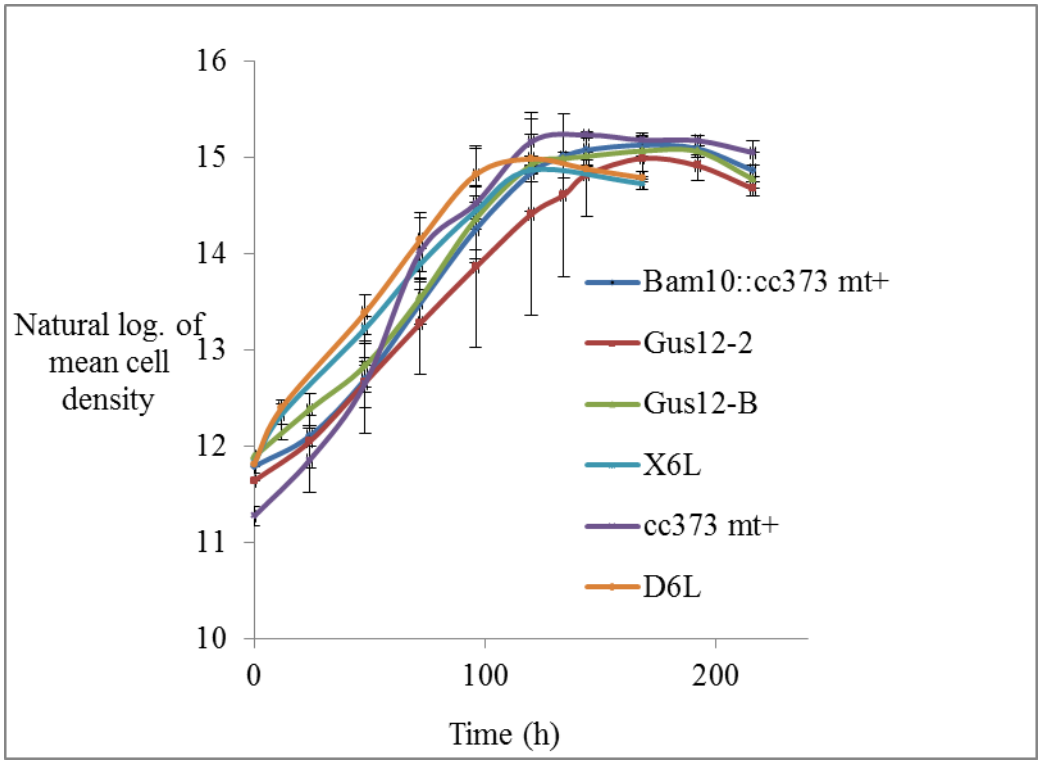

Figure 4.3: Heterotrophic growth of Bam10::cc373 mt+, Gus12-2, Gus12-B, cc373 mt+, X6L and D6L cultures in TAP liquid medium at 25^{o}C (90 rpm) in continuous dark condition. The mean cell density and standard deviation were determined from three biological and two technical replicates each. The natural logarithm of mean cell density was plotted against time.

4.1.3 Growth in mixotrophic condition

The growth curves of cultures cultivated under mixotrophic condition are shown in Figure 4.4. Growth in mixotrophic condition involves the simultaneous combination of autotrophic and heterotrophic growth in which CO_2 and acetate respectively, are the available carbon for growth. Additionally, the cells of mixotrophic cultures may use acetate and light as energy sources for growth. They may thus, take advantage of the combined benefits of two carbon and two energy sources. The result is that cells grow very fast under mixotrophic condition, reflected in the maximum specific growth rates shown in Table 4.1. The exponential phase was brief but intensive, lasting only until 72 h after culture start, but leading to high cell density of about 8 million cells per ml. It was followed by an extended period of virtually linear growth (Figure 4.4).

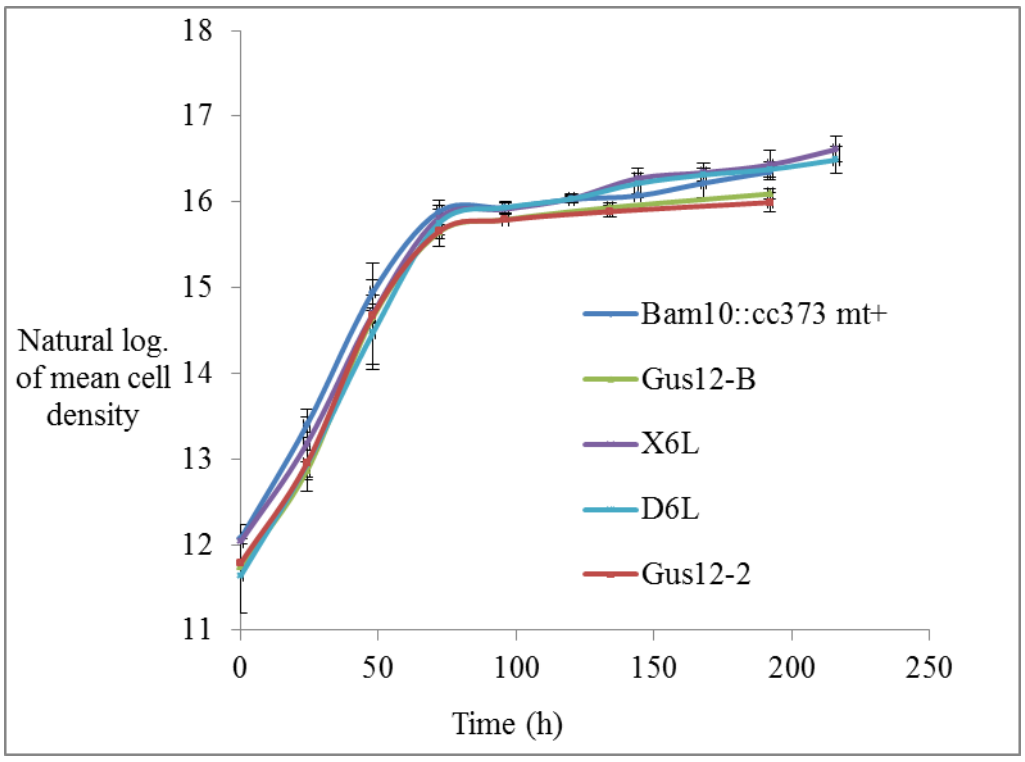

Figure 4.4: Mixotrophic growth of Bam10::cc373 mt+, X6L, D6L Gus12-2 and Gus12-B cultures in TAP liquid medium at 25°C and 90 rpm in continuous light condition (54 µmol photons/m^2/s). The mean cell density and standard deviation were determined for three biological replicates and two technical replicates each. The natural logarithm of mean cell density was plotted against time.

With the linear growth kinetics, these mixotrophic cultures then grew to very high cell densities (usually >10 million cells per ml). The cultures continued photosynthetic growth to high cell density comparable to autotrophic cultures. In addition, cultures grown in mixotrophic condition were observed to grow after more than 15 days in TAP liquid medium and persist over 30 days on TAP solid agar medium.

4.1.4 Identification of factors limiting growth rates and cell densities.

In this study, the culture growth was monitored and growth reflected by the increase in cell numbers with time. Growth curves were plotted as functions of cell density against time. Growth rates were described in terms of the specific growth rate. The maximum specific growth rate was determined during the exponential growth phase by taking the slope of the linear plot of the natural log of cell density against time. The slope of the linear plot was estimated as the maximum specific growth rate with units of h^{-1}. Examples of some of the semi-log plots are shown in Figures 4.1 – 4.5.

The maximum specific growth rates determined for the cultures propagated under autotrophic, heterotrophic and mixotrophic growth conditions are presented in Table 4.1. Depending on the strain, autotrophic maximum specific growth rates were between 0.030 – 0.033 h^{-1}, heterotrophic maximum specific growth rates between 0.022 – 0.029 h^{-1}, and mixotrophic maximum specific growth rate between 0.056 – 0.062 h^{-1} were observed. For mixotrophic cultures grown synchronously (in 12 h light and 12 h dark cycle periods) the growth rate results were also presented. The maximum specific growth rates between 0.047 – 0.050 h^{-1} were observed for these mixotrophic cultures. Comparatively, the Table 4.1 results confirm that cultures grown in heterotrophic condition present the slowest growth rate, and the fastest growth rates occur in mixotrophic cultures. The growth rate results were comparable to those reported by previous workers studying the growth of *C. reinhardtii* strains. (Boyle and Morgan, 2009) studying the central carbon metabolism in *C. reinhardtii* strain cc400 cw15 mt+ grown at 25^{o}C and 200 rpm, reported an autotrophic maximum specific growth rate of 0.059 h^{-1} for cultures in minimal medium at light intensity of 65 µmol photons/m^2/s.

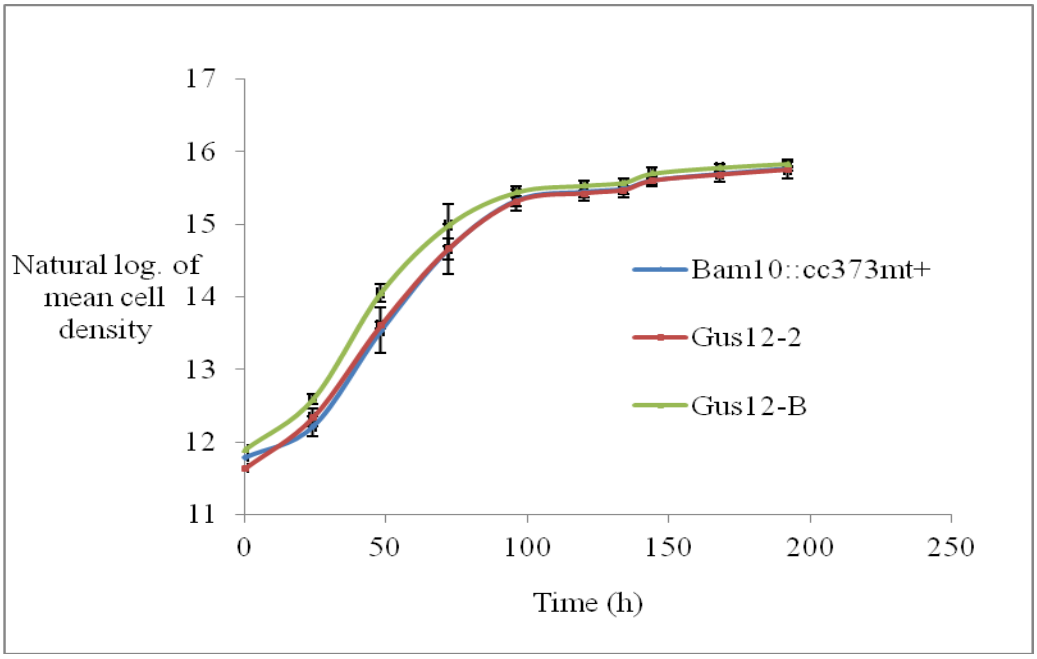

Figure 4.5: Mixotrophic cultures of Bam10::cc373 mt+, Gus12-2 and Gus12-B. The cultures were grown in TAP liquid medium at 25^{o}C and 90 rpm, synchronously in 12 h light (54 µmol photons/m^{2}/s) and 12 h dark cycles. The mean cell density and standard deviation were determined for three biological replicates and two technical replicates each. The natural logarithm of mean cell density was plotted against time.

At the same light intensity, the authors reported a mixotrophic maximum specific growth rate of 0.066 h^{-1} in TAP medium, and a heterotrophic maximum specific growth rate of 0.035 h^{-1} for growth on TAP medium. Janssen et al., (1999) reported autotrophic growth rate of 0.14 – 0.16 h^{-1} for *C. reinhardtii* grown at light intensity of 240 µmol photons/m^{2}/s in Sueoka high salt medium. The higher value of the maximum specific growth rates reported for the autotrophic and mixotrophic conditions by these authors reflects that growth rates depend on light intensity, type of strain and the growth medium composition used to propagate the cultures.

4.1.4.1 Effect of light on growth rates and cell densities

A comparison of heterotrophic and mixotrophic cultures (12 h light and 12 h dark cycles) was made to identify the effect of light. Both heterotrophic and mixotrophic cultures grew

in the acetate medium (TAP), but the growth rate of the heterotrophic culture was significantly lower.

Table 4.1: Maximum specific growth rate (μ_{max}) determined for Ba10::cc373 mt+, Gus12-2, Gus12-B, X6L, D6L and cc373 mt+ cultures at 25^{o}C and 90 rpm in autotrophic, heterotrophic and mixotrophic conditions. The maximum specific growth rates were determined during exponential growth phase by plotting the natural log of cell density against time. The slope of the linear plot was estimated as the maximum specific growth rate. The mean and standard deviation were determined from three biological replicates and two technical replicates each.

Strains	**Autotrophic (continuous light)**	**Heterotrophic (continuous dark)**	**Mixotrophic (continuous light)**	**Mixotrophic (12 h light and 12 h dark)**
	Mean μ_{max} ± sd (h^{-1}) x10^{-2}	Mean μ_{max} ± sd (h^{-1}) x 10^{-2}	Mean μ_{max} ± sd (h^{-1}) x 10^{-2}	Mean μ_{max} ± sd (h^{-1}) x10^{-2}
Bam10::cc373 mt+	3.06 ± 0.18	2.88 ± 0.11	5.85 ± 0.13	4.97 ± 0.48
Gus12-2	3.09 ± 0.25	2.44 ± 0.50	5.64 ± 0.20	4.71 ± 0.68
GUS12-B	3.03 ± 0.20	2.49 ± 0.38	5.81 ± 0.04	4.97 ± 0.28
X6L	3.31 ± 0.20	2.39 ± 0.20	5.96 ± 0.76	-
D6L	3.22 ± 0.10	2.23 ± 0.32	6.18 ± 0.17	-
cc373 mt+	-	4.12 ± 0.24	-	-

This limitation was due to growth in complete darkness i.e. lack of light in the heterotrophic condition. Typically, the μ_{max} values for heterotrophic cultures were ~50% of the maximum specific growth rate for mixotrophic cultures. When compared statistically, the mean values of maximum specific growth rates for heterotrophic and the mixotrophic Bam 10:: cc373 mt+, Gus 12-2 and Gus12-B were found to be significantly different ($p= 0.0004$) at 95% confidence, between heterotrophic and mixotrophic cultures. The results

show that by supplying light to heterotrophic cultures will increase specific growth rate by 2-fold! The lack of light in heterotrophic condition immensely reduced the growth rates and final cell densities reached in heterotrophic cultures (compare Figures 4.3 and 4.5).

4.1.4.2 Effect of duration of light on growth rates and cell densities

The specific growth rates of cultures (Bam10::cc373 mt+, Gus12-2 and Gus12-B) in the two types of mixotrophic conditions were compared to identify the effect of the duration of light on the conditions. The cultures grown synchronously in mixotrophic condition received 12 h light per 24 h, which is approximately, half the duration of light for the mixotrophic cultures grown in continuous light condition. The mean maximum specific growth rates were found to be significantly different between the 2 types of mixotrophic condition ($p= 0.002$) at 95% confidence. Also the result in Table 4.1 indicate that the reduction of the duration of light period by half (the synchronous mixotrophic condition) posted a 15% reduction in the mean μ_{max} values for mixotrophic growth. This suggests that the specific growth rates measured at the log-phases may be affected by halving the duration of light to the mixotrophic cultures. But if this effect may reduce the cell density of the mixotrophic cultures were unknown.

To address this question, the growth curves in Figure 4.4 (mixotrophic cultures in continuous light) and Figure 4.5 (mixotrophic cultures in 12 h light and 12 h dark cycles) were compared further. The mean inoculum cell densities of the propagated cultures (Figures 4.4 and 4.5) are shown in Table 4.2. The inoculum cell densities for the two types of mixotrophic culture were compared, but no significant difference in the mean inoculum cell density was observed ($p= 0.75$) at 95% confidence. The cell densities achieved by the two types of mixotrophic culture after 192 h incubation are presented in Table 4.3. The mean cell density was compared for the two mixotrophic condition. There was no significant difference in the mean cell density achieved after 192 h incubation ($p = 0.11$) at 95% confidence.

Table 4.2: Inoculum cell density of Bam::cc373 mt+, Gus12-2 and Gus12-B mixotrophic cultures grown in continuous light, or synchronously in 12 h light and 12 h dark cycles. The mean and standard deviation were determined for three biological replicates and two technical replicates each.

	Mixotrophic (continuous light)	**Mixotrophic (12 h light and 12 h dark)**
Strain	Mean inoculum cell Density ± sd (1×10^6 cells/ml)	Mean inoculum cell density ± sd (1×10^6 cells/ml)
Bam10::cc373 mt+	0.18 ± 0.02	0.13 ± 0.02
Gus12-2	0.13 ± 0.04	0.11 ± 0.02
Gus12-B	0.13 ± 0.03	0.15 ± 0.01

The result in Table 4.3 revealed that for cultures with similar inoculun concentrations, the achieved cell densities are not significantly different whether the mixotrophic cultures were grown continuously in light; or in a 12 h light and 12 h dark regime. The duration of light only affected the specific growth rate measured during the exponential phase. Overall, growing mixotrophic cultures in continuous light condition did not receive significant cell density increase over mixotrophic cultures grown in equal light and dark duration periods (see Figures 4.4 and 4.5). A reason for this may be due to the fact that approximately equal duration of light and dark periods is available for photosynthetic growth. Thus photosynthetic cells synthesize sugars and accumulate energy storage (e.g. starch) in the light period for biosynthetic reactions. In darkness, the energy stores are utilized for growth and to make more cellular materials. Growing cultures continuously in light may mean that at the other times, light is simply wasted or dissipated i.e. where the cells persist in the same circadian regulation.

Table 4.3: Cell densities of Bam::cc373 mt+, Gus12-2 and Gus12-B mixotrophic cultures grown in continuous light, or synchronously in 12 h light and 12 h dark cycles. The mean and standard deviation were determined for three biological replicates and two technical replicates each after 192 h incubation.

	Mixotrophic (continuous light)		**Mixotrophic (12 h light and 12 h dark)**	
Strain	Mean cell density ± sd (1 x 10^6 cells/ml)	Time (h)	Mean cell density ± sd (1 x 10^6 cells/ml)	Time (h)
Bam10::cc373 mt+	12.60 ± 0.35	192	7.03 ± 0.12	192
Gus12-2	8.83 ± 0.51	192	6.90 ± 0.41	192
Gus12-B	9.76 ± 0.31	192	7.52 ± 0.21	192

4.1.4.3 Effect of availability of carbon on growth rates and cell densities

The maximum specific growth rates results (see Table 4.1) obtained for autotrophic and mixtrophic cultures (in continuous light), were compared to identify the effect of added acetate. The result revealed a doubling in the growth rate of the mixotrophic cultures (contain acetate) compared to the autotrophic counterpact (no acetate). Generally, autotrophic cultures achieved ~55% of the mean maximum specific growth rate of the mixotrophic cultures. There was significant difference in the mean maximum specific growth rates ($p= 7 \times 10^{-8}$) at 95% confidence. Here, the reduction in autotrophic growth rate is due to the lack of additional source of carbon (acetate) in the minimal medium. Cultures grow relatively slowly in autotrophic than in mixotrophic condition. However, the free energy of light fuels photosynthetic growth in autotrophic cultures, reaching high cell densities comparable to mixotrophic cultures.

For example, a comparison of mean cell density achieved after 184 h (Figure 4.2) for autotrophic and 192 h (Figure 4.4) for mixotrophic cultures, revealed no significant difference in mean values ($p = 0.996$). The lack of acetate reduced the maximum specific

growth rates achieved in autotrophic cultures. However, the important factor for achieving a high autotrophic cell density is the supply of light.

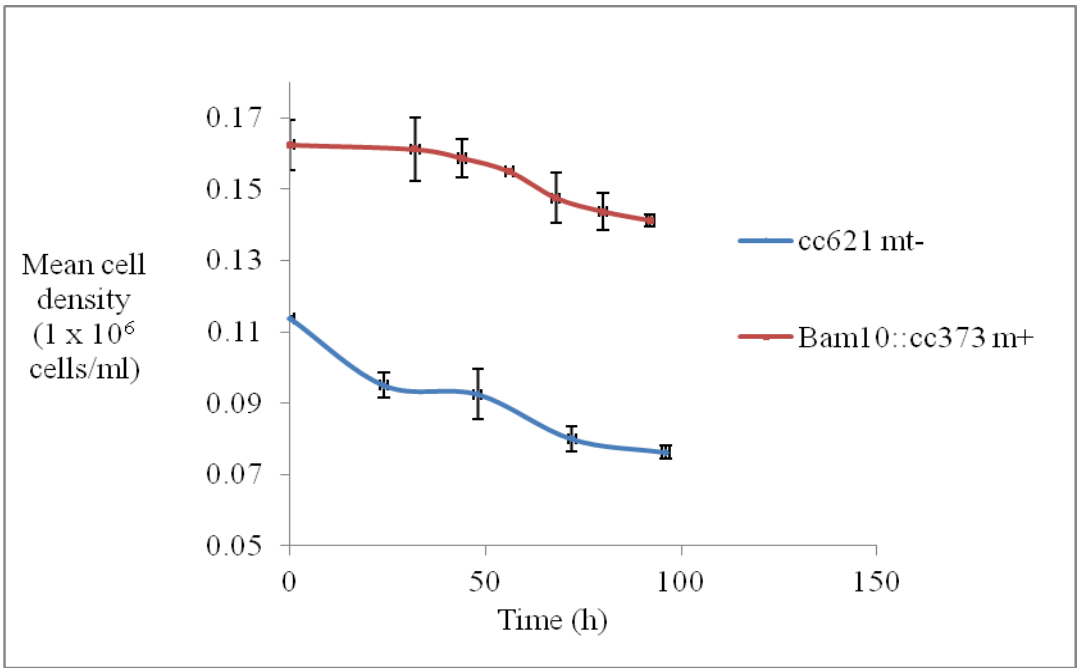

Figure 4.6: Profiles of Bam10::cc373 mt+ and cc621 mt- cultures propagated in minimal medium in dark conditions at 25^{o}C. The minimal medium is devoid of a carbon source. The mean values were determined for three biological replicates and two technical replicates of cell density each.

For heterotrophic cultures, lack of acetate strongly lowered growth rates and final cell densities. No growth was observed for cells inoculated into minimal medium in the dark (Figure 4.6). In these cases, the cultures never grew and inoculated cells die off due to lack of carbon and energy source. This implied a strict requirement on acetate (organic carbon) for growth to occur in heterotrophic condition. Cultures inoculated into minimal medium exhibited growth only if supplied with light (autotrophic condition). Therefore, light is another strict requirement for growth of cultures.

In summary, lack of light is the limiting factor reducing the growth rates of cultures, and the achievement of high cell densities (e.g. in heterotrophic, autotrophic and mixotrophic

cultures). The duration of light period may also affect growth rate of mixotrophic and autotrophic cultures. Lack of acetate is another strong limitation on growth rates and high cell density. The addition of acetate into autotrophic cultures significantly increased the growth rates as the cultures resumed mixotrophic growth. Light and acetate are energy sources for growth, and are were very important factors that affected growth rates and high cell densities.

4.1.4.4 Effect of availability of nitrogen to growth of cultures

In other experiments, the effect of availability of the nitrogen source (ammonium) on cell growth was tested. Growth was not observed for cell inoculum cultivated in ammonium-free TAP medium (Figure 4.7), indicating a strict requirement for a source of nitrogen for growth. Put together, the main requirements for the growth of *C. reinhardtii* cultures would include the availability of the carbon (acetate), energy (light) and nitrogen sources (ammonium). Limitations arising from any of these factors can reduce growth rates and cell densities.

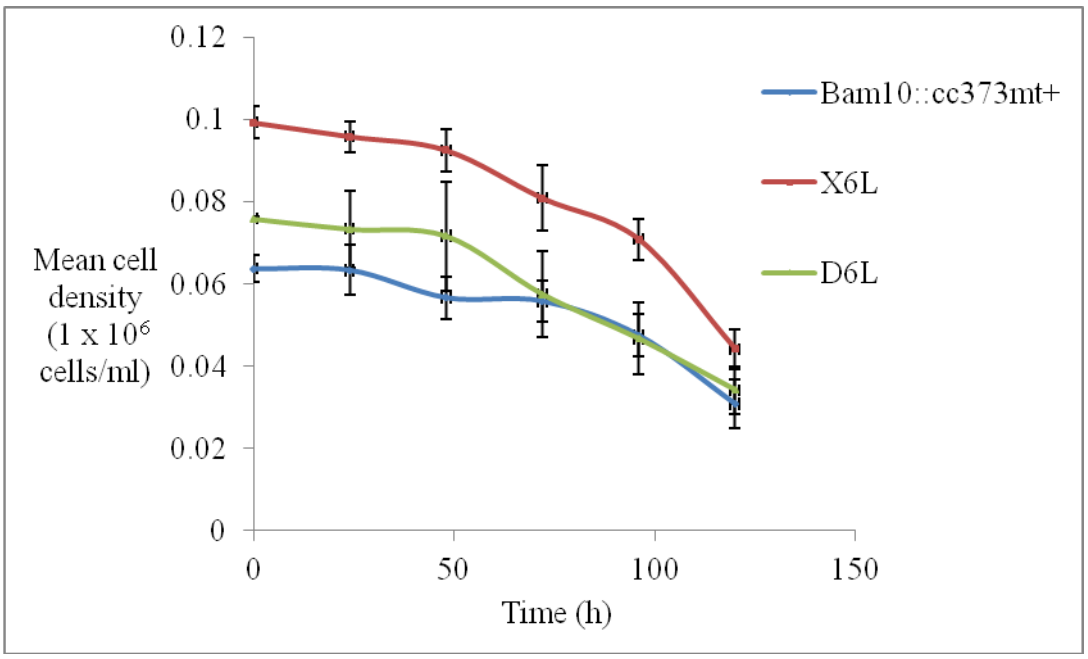

Figure 4.7: Profiles of Bam10::cc373 mt+, X6L and D6L cultures propagated in ammonium-free TAP medium in dark conditions at 25°C. The mean values were determined for three biological replicates and two technical replicates each.

4.2 Dependence of growth (cell density) on limiting factors

With the culture composition and all other conditions held constant in the experiments, then by varying only one condition one at a time, the dependence of growth on the varied factor was identified. The plot of cell densities against the varied factor was used to describe the dependence of growth on the factor. These analyses were used to determine the dependence of growth on acetate (carbon source), ammonium (nitrogen source), light (energy source) and on pH of the medium.

4.2.1 Effect of acetate concentrations on heterotrophic growth of *C. reinhardtii* cultures.

The effect of variable acetate concentration in medium on growth was determined. The heterotrophic cultures in TAP medium were grown in flasks containing different initial concentrations of acetate (0 – 26 mM). The composition of the culture and all other growth conditions were kept constant.

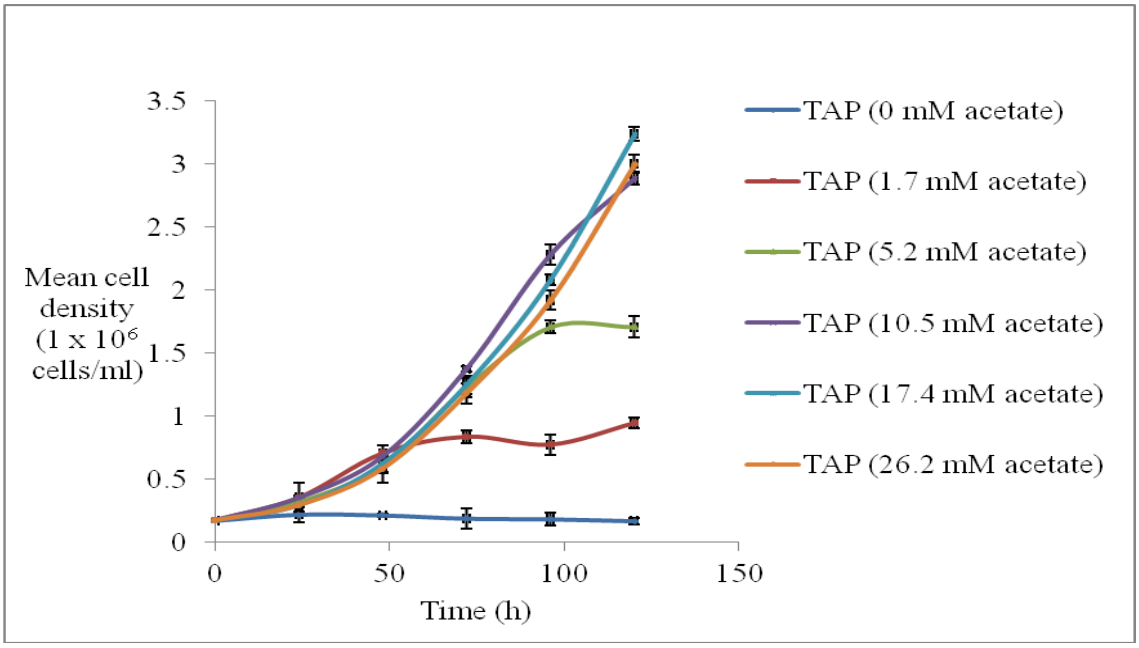

Figure 4.8: Heterotrophic growth plots (cell density against time) of Bam10::cc373 mt+ cultures grown in TAP medium containing different initial concentration of acetate. The mean cell density (cells/ml) was determined for three biological replicates and two technical replicates each.

The cultures were grown and the growth curves were plotted as cell density against time. The heterotrophic growth curves for these are shown in Figure 4.8. No growth was observed for cultures grown in the dark with 0 mM acetate.

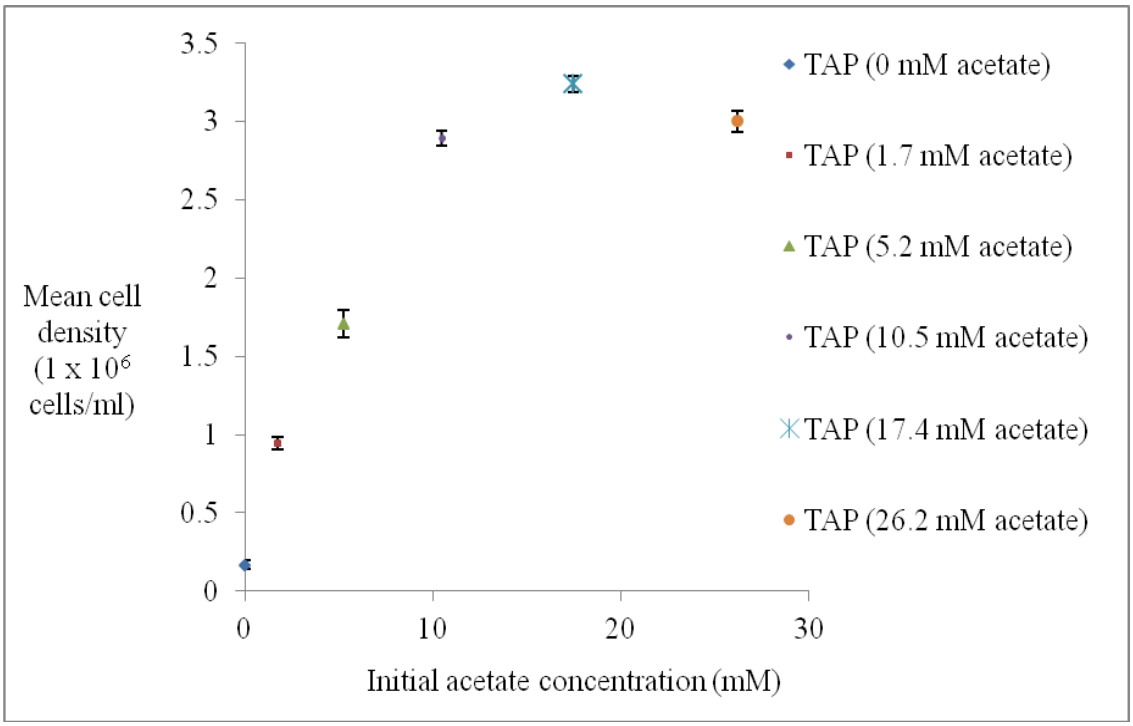

Figure 4.9: Cell densities of Bam 10::cc373 mt+ cultures after 120 h propagation in TAP medium containing different initial acetate concentration. The mean values and standard deviation for cell density were determined for three biological replicates and two technical replicates each.

Figure 4.9 describes the dependence of growth (cell densities) on acetate concentrations. No growth was observed for the heterotrophic cultures after 120 h incubation the medium containing 0 mM acetate (Figure 4.8). Different cell densities were achieved by cultures after 120 h propagation in TAP medium containing different initial acetate concentrations. The lowest cell density (<1 million cells/ml) was observed in TAP containing an 1.7 mM acetate. However, cell densities significantly increased in TAP medium containing higher initial acetate concentrations. For example, in the TAP with 17.4 mM acetate, cultures grew to ~3.2 million cells/ml. The results suggested that increasing acetate concentrations correlated with increased growth and higher cell densities. However, lower concentrations of the substrate limited growth of cultures.

4.2.2 Effect of ammonium concentrations on the growth of *C. reinhardtii* cultures

Similarly, the effects of varying only the ammonium concentrations were studied in order to identify and quantify ammonium concentrations that limit growth of mixotrophic cultures. These were grown synchronously (12 h light and 12 h dark cycles) in TAP medium containing different initial concentrations of ammonium chloride (0 – 14 mM).

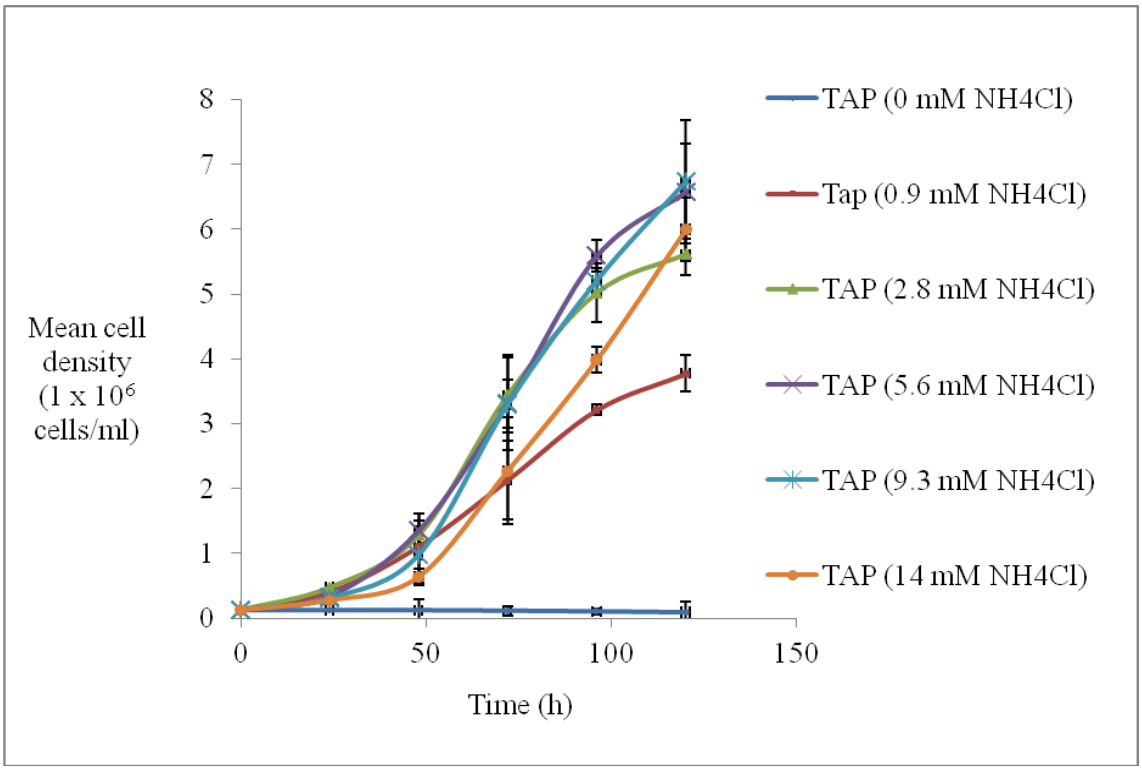

Figure 4.10: Mixotrophic growth curves of Bam10::cc373 mt+ cultures propagated in TAP medium containing different initial concentration of ammonium. The cultures were grown synchronously in 12 h light and 12 h dark cycles at 25^{o}C and light intensity 54 µmol photons/m^{2}/s. The mean values were obtained for cell density was determined from three biological replicates and two technical replicates each.

The growth curves are shown in Figure 4.10. In Figure 4.10, no growth was observed for cells cultivated in medium containing 0 mM ammonium. Figure 4.11 describes the dependence of the growth on ammonium concentrations in the medium. Different cell densities were observed for cultures after after 120 h propagation in TAP medium containing different initial ammonium concentrations. The lowest growth (~3.8 million

cells/ml) was observed in TAP containing 0.9 mM ammonium, and the highest yield (6.7 million cells/ml) in Tap containing 9.3 mM ammonium. The trend observed in Figure 4.11 shows that increasing ammonium concentrations increased the growth of cultures. The growth of the cultures was limited by low concentrations of this substrate.

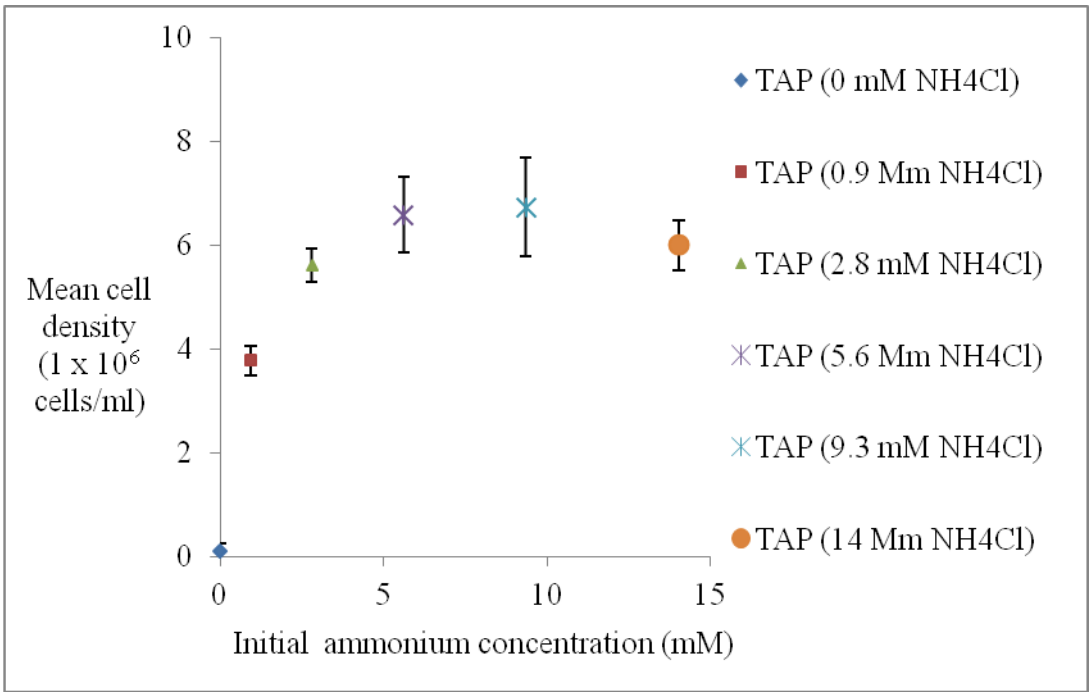

Figure 4.11: Cell densities of Bam 10::cc373 mt+ mixotrophic cultures after 120 h propagation in TAP medium containing different initial ammonium concentration. The mean values and standard deviation were determined for three biological replicates and two technical replicates each.

4.2.3 Effect of light intensity on the growth of *C. reinhardtii* cultures

The effect of light intensity on growth was studied by growing culture at various light intensities. The composition of components in the medium and the growth conditions were kept constant for each growth experiment, only the light intensity incident upon the cultures were varied. The cultures were propagated in TAP medium at light intensity of 0 (darkness), 16, 38, or 54 µmol photons/m^2/s respectively. The growth curves for these experiments are displayed in Figure 4.12. The cell densities achieved by cultures after 120 h propagation was dependent on the light intensity at which the cultures were grown. The

lowest growth (3.7 million cells per ml) was observed in cultures grown in TAP at zero light intensity (darkness). At light intensity of 16 µmol photons/m^2/s, the growth of cultures increased to ~5 million cells per ml. However, the highest at 120 h (~7.7 millon cells per ml) was achieved in cultures grown at 54 µmol photons/m^2/s. The results show that growth and cell densities achieved by cultures increases with increasing light intensity.

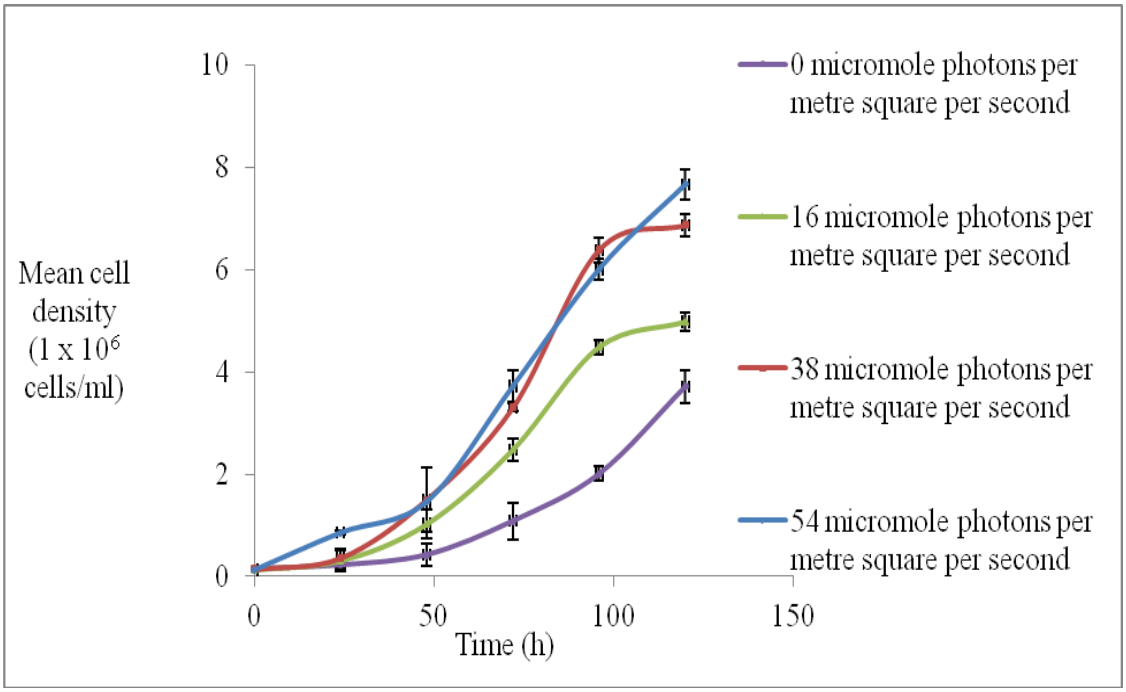

Figure 4.12: Growth curves of Bam10::cc373 mt+ cultures propagated in TAP medium (at 25°C) and supplied light at 0, 16, 38, or 54 µmol photons/m^2/s. The mean values were determined for three biological replicates and two technical replicates each.

The plot in Figure 4.13 shows the direct dependence of growth of cultures on light intensity. The highest specific growth rate (7.6 millon cells per ml) was observed for cultures grown at 54 µmol photons/m^2/s. The result confirms that growth yield of cultures could be affected by light intensity used to grow the culture. For the cultures grown at zero photon flux, growth was observed because of availability of acetate in the TAP medium. However, the growth yield in the dark condition was significantly reduced because of lack of light. Therefore an increase in light intensity incident upon cultures from 0 – 54 µmol photons/m^2/s increases the growth yields. If the light intensity is increased more than 54

µmol photons/m^2/s, the growth of cultures would rise until light-saturation of growth is reached.

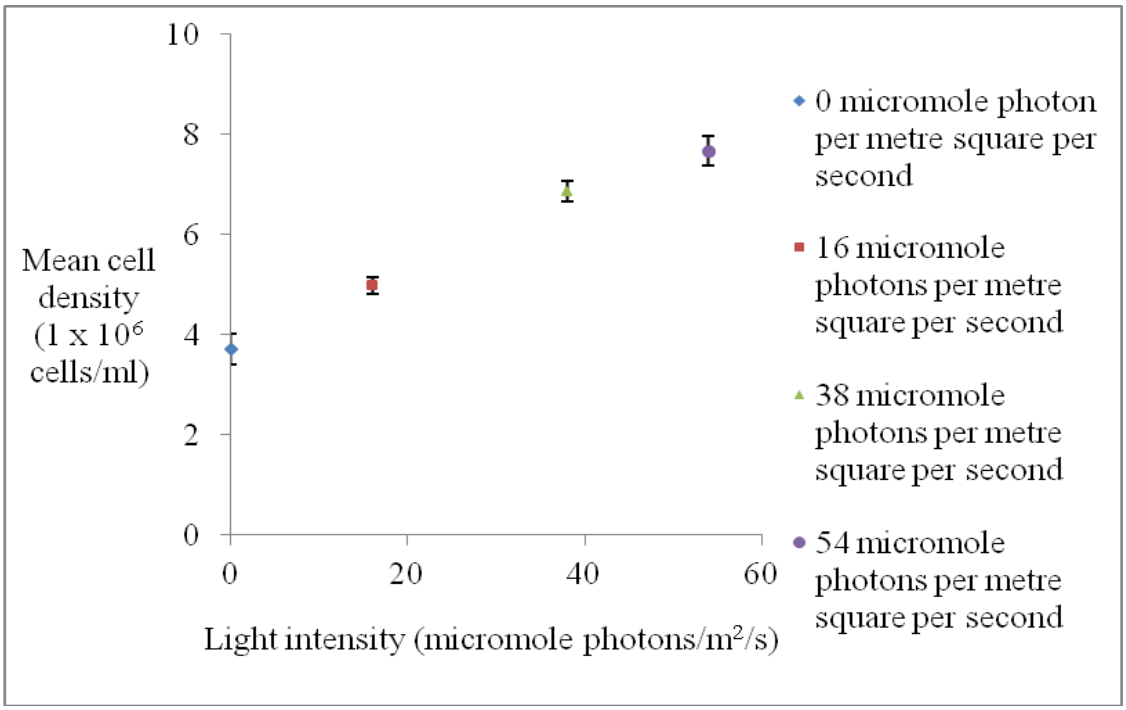

Figure 4.13: Cell densities of Bam 10::cc373 mt+ mixotrophic cultures in TAP medium after 120 h propagation at light intensity 0, 16, 38, or 54 µmol photons/m^2/s. The mean values and standard deviation for cell density were determined for three biological replicates and two technical replicates each.

4.2.4 Variations of growth with pH

The effect of pH on the growth of *C. reinhardtii* mixotrophic cultures is presented below. The mixotrophic cultures were grown synchronously in 12 h light and 12 h dark cycles in TAP medium various values of the initial pH (5.3, 6.3, 7.3, 8.3, or 9). The culture composition and other growth conditions were kept the same except for the initial pH. The growth curves of the cultures at the different initial pH are shown in Figure 4.14. The plot of cell density after 120 h propagation in TAP medium against initial pH is presented in Figure 4.15. No growth was observed for cultures grown in the medium at pH 5.3 or 9.3. The pH 5.3 and 9.3 represented acidic and alkaline pH that inhibited the growth of cultures.

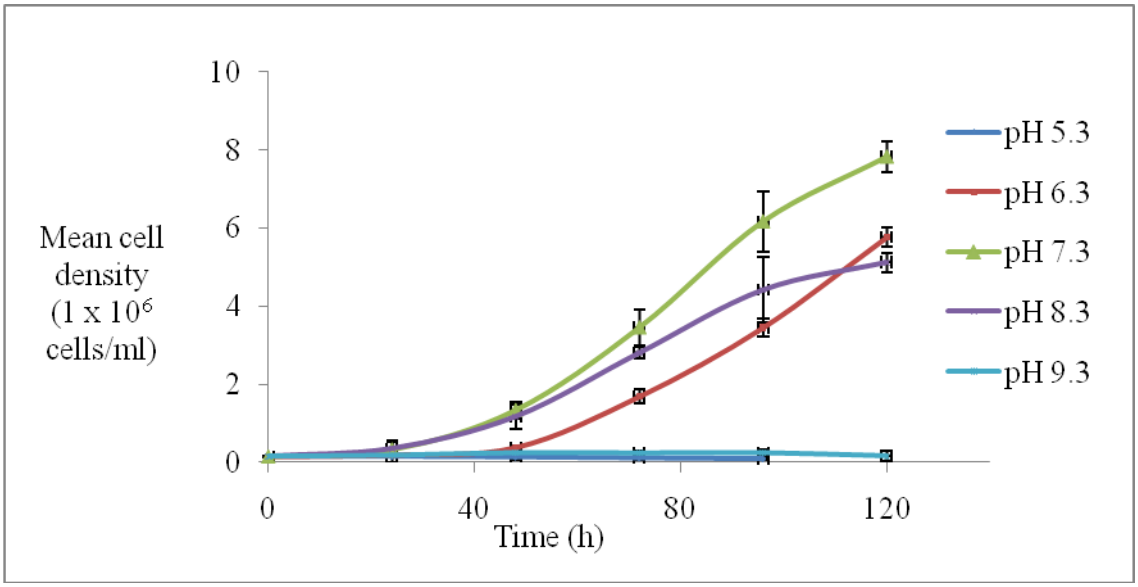

Figure 4.14: Mixotrophic growth of cc621 mt- cultures grown synchronously in a 12 h light and 12 h dark cycles (54 µmol photons/m^2/s) in TAP medium with different initial pH 5.3, 6.3, 7.3, 8.3 or 9.3. The mean values were determined for three biological and two technical replicates each.

The highest growth of cultures (7.8 million cells/ml) was obtained at pH 7.3. The optimum pH was about 7.3 as shown in Figure 4.15. For the cultures propagated at initial pH 6.3, or pH 8.3, growth were reduced to 5.7 million cells per ml, or 5.1 million cells per ml respectively. These results indicated the flexibility of *C. reinhardtii* cultures to grow at pH 6.3 or 8.3, but also a limitation on growth at these pH values. At values of pH < 6.3, or > 8.3, pH reduced growth further such that at pH 5.3 or pH 9.3 the growth of cultures was completely inhibited.

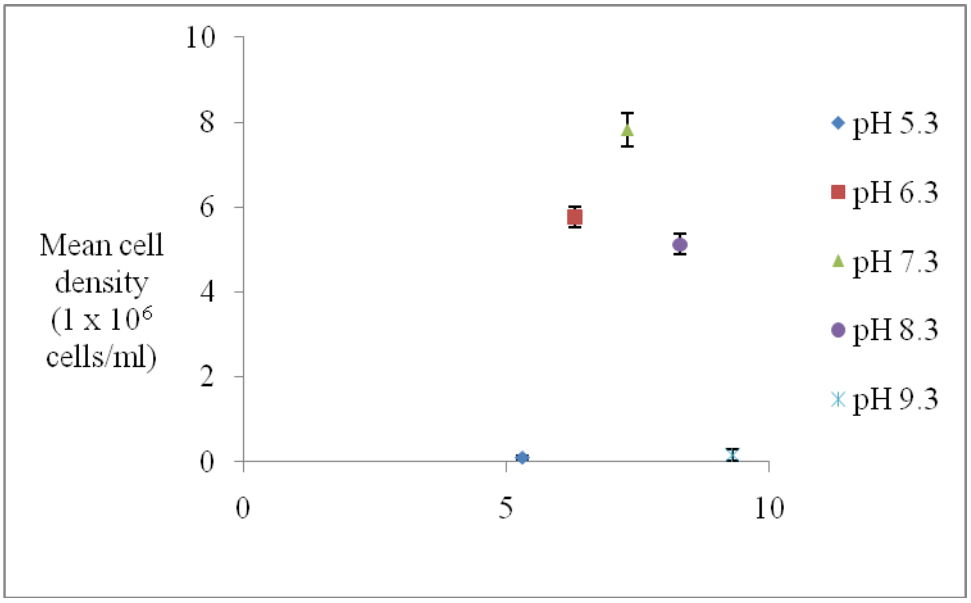

Figure 4.15: Cell densities of cc621 mt- mixotrophic cultures after 120 h propagation in TAP with various initial pH. The mean values and standard deviation were determined for three biological and two technical replicates each.

4.3 Effects of acetate on heterotrophic and mixotrophic culture pH

In the previous sections, factors that limited growth and growth rates in cultures were identified to include availability carbon, nitrogen substrates, availability of light and light intensity, and pH change. Here, significant fluctuations in pH during growth due to the consumption of acetate are discussed. The consumption of acetate in heterotrophic and mixotrophic growth was observed to increase the pH of the medium.

4.3.1 Acetate consumption increases the pH of growth medium.

An intriguing aspect in the heterotrophic and mixotrophic growth experiments was the observation that the initial pH of the medium increased from pH 7.3 during growth of *C. reinhardtii* cultures in the buffered TAP medium. The sharp rise in pH during growth corresponded with the concentration of acetate in the medium. For example, in Table 4.4, the pH changes recorded for the heterotrophic growth of Bam 10::cc373 mt+ cultures in media containing different concentration of acetate are displayed. The growth curves for the experiments are presented in Figure 4.8.

Table 4.4: The change in pH measured in TAP medium after 120 h heterotrophic growth of Bam10::cc373 mt+ cultures. The TAP contained different initial concentration of the acetate (1.7 – 26.2 mM) at start of the growth experiment. The mean and standard deviation errors were determined from three biological and two technical replicates each.

	Growth in TAP (1.7 mM acetate)	Growth in TAP (5.2 mM acetate)	Growth in TAP (10.5 mM acetate)	Growth in TAP (17.4 mM acetate)	Growth in TAP (26.2 mM acetate)
Mean increase in pH ± sd	0.2 ± 0.0	0.6 ± 0.02	0.8 ± 0.04	0.83 ± 0.03	0.85 ± 0.05
Time (h)	120	120	120	120	120

Furthermore, the pH change for autotrophic, heterotrophic, and mixotrophic cultures were compared in Table 4.5. Here, growth of cultures in heterotrophic and mixotrophic conditions resulted in at least one unit increase in pH of the growth medium from the initial pH 7.3. For the autotrophic cultures, growth resulted in a decrease of approximately 0.5 units from the initial pH 7.3 of the medium. The tris-minimal medium used for autotrophic growth contains no acetate. These results suggest the consumption of acetate in heterotrophic and mixotrophic conditions is the cause of the pH rise. On the other hand, the omission of acetate in the medium used to grow autotrophic cultures means a decrease in pH was observed instead, which may be due to the carbon dioxide consumption for growth.

Table 4.5: pH changes measured at 144 h growth of Bam10::cc373 mt+ cultures in TAP and tris-minimal media. The cultures were grown in continuous dark (heterotrophic); or in continuous light (mixotrophic); or synchronously in 12 h light and 12 h dark cycles (mixotrophic). The cultures in tris-minimal were grown in continuous light conditions (autotrophic). The mean and standard deviation were determined from three biological and two technical replicates each.

	Growth in tris-minimal (0 mM acetate) in continuous light	Growth in TAP (17 mM acetate) in continuous light	Growth in TAP (17 mM acetate) in continuous dark	Growth in TAP (17 mM acetate) 12 h light and 12 h dark cycles
Mean pH change ± sd	-0.5 ± 0.01	1.1 ± 0.02	1.0 ± 0.02	1.0 ± 0.02

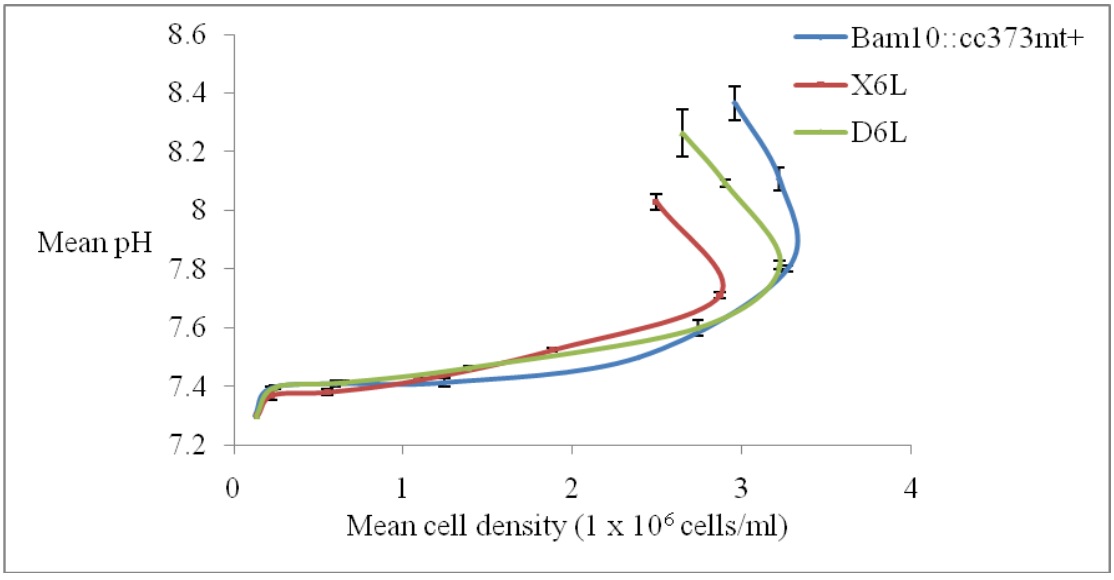

Figure 4.16: pH profiles of Bam10::cc373 mt+, X6L and D6L heterotrophic cultures grown in TAP in continuous darkness. The consumption of acetate was followed by increase in pH during growth. At stationary phase, acetate was completely consumed and pH rose to ~7.9. Cells lack carbon source to support growth and maintenance, influx of protons into cells resulted in further rise in pH to ~8.4 as cells entered death phase. The mean values of cell density and pH were determined from three biological replicates and two technical

replicates each. The experiment started by inoculum at pH 7.3, and the cell density and pH were measured as a function of time, and then plotted against each other in this Figure 4.16.

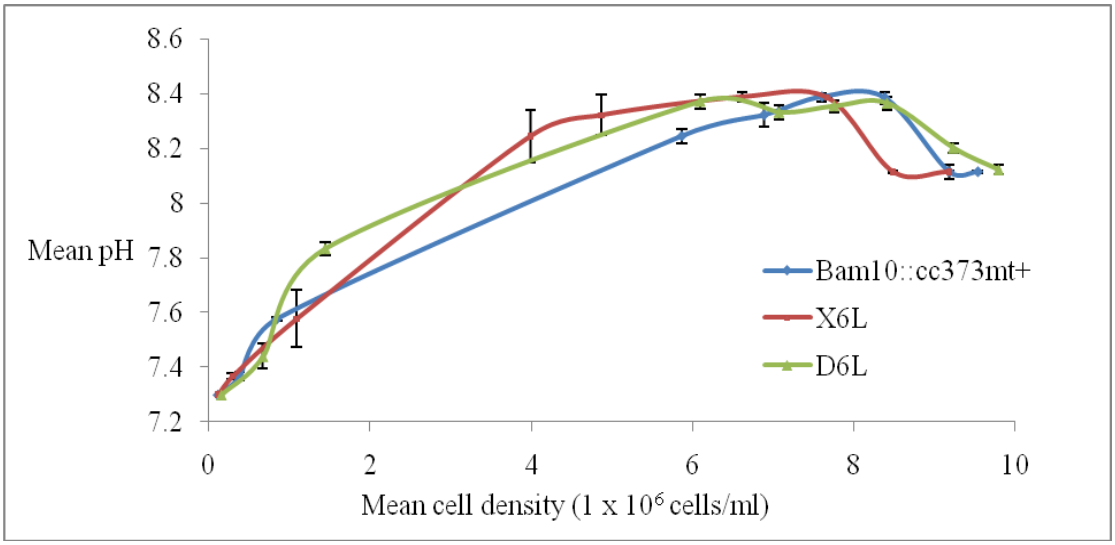

Figure 4.17: pH profiles of Bam10::cc373 mt+, X6L and D6L mixotrophic cultures grown in TAP in continuous light. The consumption of acetate was followed by increase in pH, and photosynthetic growth enabled cultures to achieve higher cell densities. Acetate was completely consumed from the dense cultures (6 - 7 million cells/ml) after 120 h incubation and the pH increased to ~8.4. Thereafter, photosynthetic growth was observed to gradually decrease the pH to ~8.1 at 192 h. The mean values of cell density and pH were determined from three biological replicates and two technical replicates each. The experiment started by inoculum at pH 7.3, and the cell density and pH were measured as a function of time, and then plotted against each other in this Figure 4.17.

In Figures 4.16, 4.17 and 4.18, the pH profiles for heterotrophic, mixotrophic and autotrophic cultures respectively, during growth were plotted against cell density to understand how pH change occurs in the medium relative to growth. In the heterotrophic (Figure 4.16) and mixotrophic conditions (Figure 4.17), the consumption of acetate was followed by culture growth and the rise in pH. In the heterotrophic cultures, after acetate was completely consumed from the medium, there was no more available carbon and energy to sustain growth of the dense cultures. The culture at approximately 2.9 – 3.4

million cells per ml entered a short stationary phase. Here, the rise was to ~pH 7.9, and the pH of the medium increased further to ~8.4 during the death phase.

For the mixotrophic cultures, the rise of pH was observed to about pH 8.4 (Figure 4.17). After acetate was completely consumed, photosynthesis ensured the growth of cultures continued to higher cell density followed by slight drop to ~pH 8.1. The difference between the mixotrophic and heterotrophic pH profile was the ability of mixotrophic cultures to continue photosynthetic growth in the absence of acetate, hence the drop in the pH of the medium observed in Figure 4.17.

For heterotrophic cultures, after acetate was consumed the cultures briefly entered stationary phase, followed by the death phase as the medium pH became more alkaline and limiting (Figure 4.16). In mixotrophic conditions, after acetate was consumed, the cultures remained photosynthetic, using light energy and fixing carbon dioxide to growth, biosynthesis of cellular material and cell maintenance functions. Consequently, the dense mixotrophic cultures (6 – 7 million cells per ml) continued growth in the medium, and the pH of the medium was observed to drop (see Figure 4.17). Equally for the same reasons, the growth of autotrophic cultures was accompanied by a small decrease in the pH by approximately -0.5 units as seen in Figure 4.18.

Acetate (or acetic acid) was reported to uncouple cellular membranes and stimulating the influx of H^+ ions from external medium into cells (Baronofsky et al., 1984, Tang et al., 1989). These authors showed that the influx of H^+ ions into cells rendered the external medium alkaline and that cells became internally acidified. In heterotrophic and mixotrophic cultures, the additional challenge for the cells may be the operation of internal pH homeostatic control that may demand extra energy to pump out excess protons. This has much implication for the growth of cultures consuming acetate. For heterotrophic cultures, after the acetate was consumed there was no exogenous carbon or energy to support biosynthesis, growth and cell maintenance such as internal pH homeostasis.

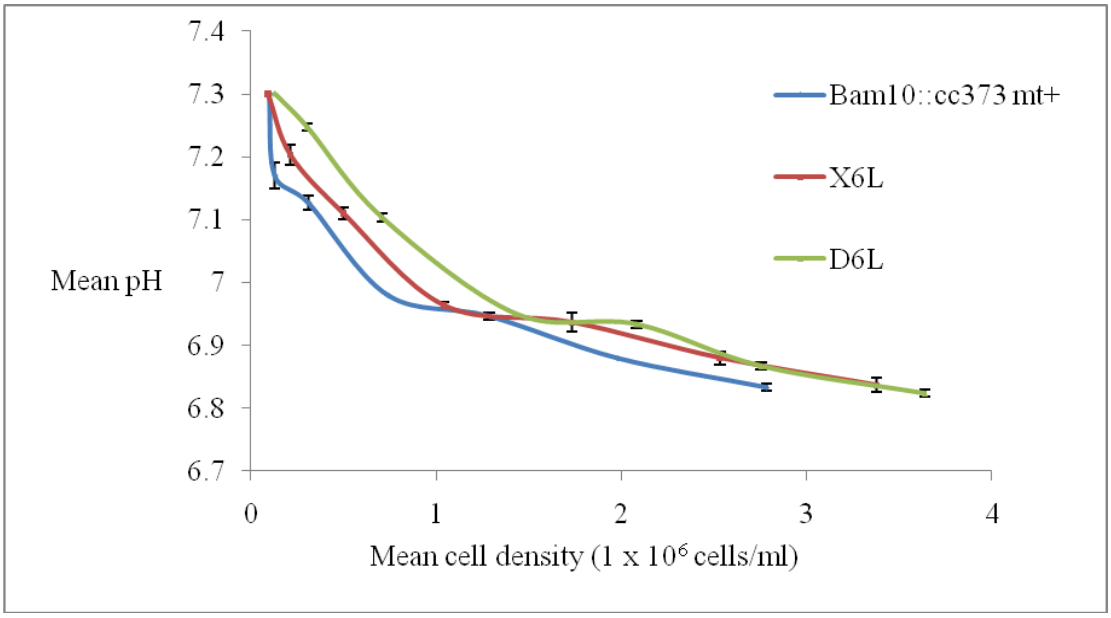

Figure 4.18: pH profiles of Bam10::cc373 mt+, X6L and D6L autotrophic cultures grown in tris-minimal (continuous light). The mean values of cell density and pH were determined from three biological replicates and two technical replicates each. The experiment started by inoculum at pH 7.3, and the cell density and pH were measured as a function of time, and then plotted against each other in this Figure 4.18.

4.3.2 Strategies to maximize growth in the heterotrophic condition

The implication of heterotrophic pH rise in the medium for large scale microalgae growth is profound. The heterotrophic condition represented the growth condition that is most limiting. As a result, the heterotrophic cultures exhibited more reduced growth and cell productivity than autotrophic or mixotrophic cultures. Additionally, heterotrophic cultures have low culture longevity (about 6 - 8 days after which cultures entered the death phase). The culture runs out of carbon, energy sources and the rise in pH was severe and detrimental to the growth of the cultures. Three experiments were performed to identify strategies that may effectively relieve the problems for heterotrophic cultures and significantly improve the cell density achievement, cell productivity and longevity of cultures.

In the first set of experiments, the heterotrophic cultures were grown in TAP medium. The acetate concentration in the medium was determined by the acetic acid assay method. The

growth was monitored until the cultures reach the stationary phase (about 144 h) at pH 8. The measured growth was ~3.7 million cells per ml, and the acetate depleted cultures were allowed to proceed to the death phase. This set of heterotrophic growth was the control (Figure 4.19).

In the second set of experiments, the heterotrophic growth of cultures in TAP medium was monitored (see Set 2 in Figure 4.19) till stationary phase was reached at 144 h, a point where the acetate was completely consumed from the medium. The measured cell density was ~3 million cells per ml. The acetate-deplete cultures were allowed to proceed to death phase at 187 h (pH 8.4). At this point, the cultures (~2.8 million cells per ml) were harvested by low speed centrifugation, washed twice with reverse osmosis water, and re-inoculated into fresh sterile TAP buffered at pH 7.30.

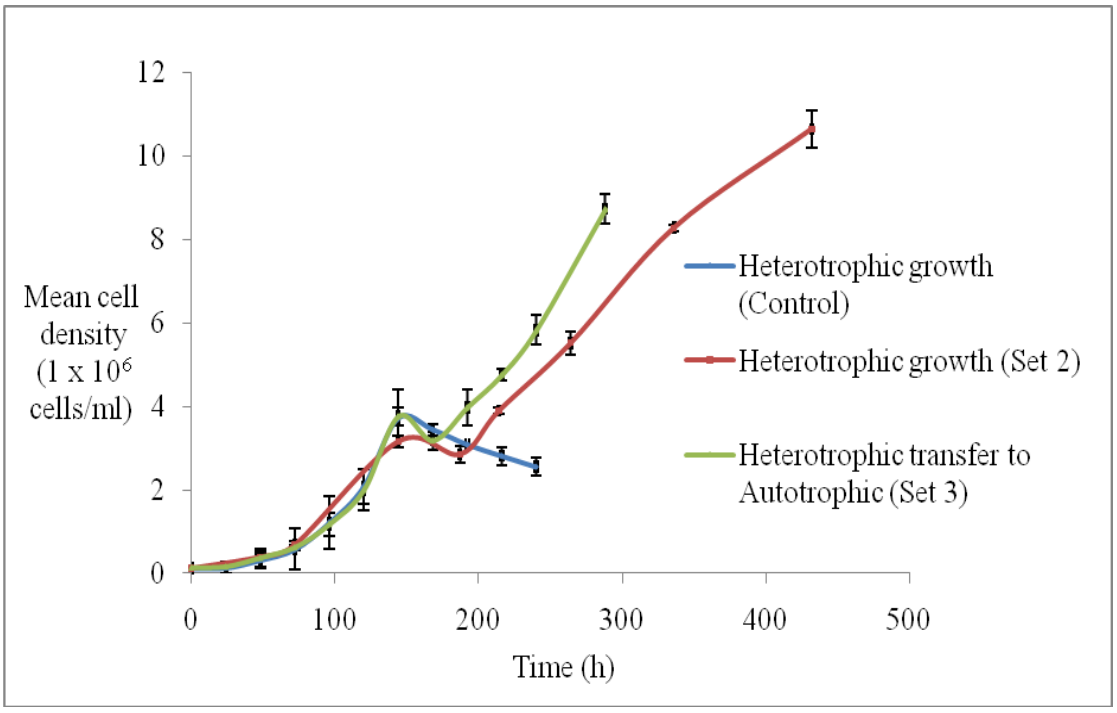

Figure 4.19: Heterotrophic growth of Gus12-2 cultures (control experiments), (Set 2 experiments) and (Set 3 experiments). The mean cell density values were determined from three biological and two technical replicates each.

The cultures were again propagated in the dark (heterotrophic condition) i.e. the heterotrophic growth culture was monitored. At different times: 264, 336 and 432 h

respectively, the cultures were harvested and re-supplemented with fresh TAP medium buffered at pH 7.30 and grown in heterotrophic conditions. The observed cell densities at 187, 264, 336 and 432 h were 2.8, 5.5, 8.3, and 10.7 million cells per ml respectively. The result demonstrated that by supplying exogenous acetate (TAP) into the carbon-depleted cultures, and provision of effective buffering of the medium around pH 7.30, heterotrophic cultures could achieve very high growth, cell productivity and longevity comparable to autotrophic and mixotrophic counterparts. This shows that the cultures in death phase could be revived and made to grow if the suitable supply of acetate was provided and the problem of high pH was addressed. At 432 h (18 days) of the heterotrophic condition, the heterotrophic cultures were actively growing (Set 2 of Figure 4.19) and at least a 3.4-fold increase in growth was observed.

In the third set of experiments (Set 3 in Figure 4.19), the heterotrophic cultures were grown to stationary phase at 144 h where acetate was consumed from the medium. The acetate-deplete stationary phase cultures were allowed to enter the death phase to 168 h (pH 8.2) with no available carbon and energy source. At the death phase, the flasks containing the cultures (~3.2 million cells per ml) were supplied light continuously at 54 µmol photons/m^2/s. Upon transfer into light, the cultures were observed to begin autotrophic growth within 24 hours. The resumption of growth was rapid and the cell density of cultures increased about 2.7-fold within a 120 h interval. The pH of the medium was observed to decrease to pH 7.76 within this interval. The absence of acetate and resumption of autotrophic growth ensured pH decrease to a more optimum level, and the growth of cultures to the high cell density characteristic of autotrophic and mixotrophic cultures. Light provided the free energy, and the photosynthetic growth was started. The resumption of autotrophic growth provided a means to fix CO_2 in the flask (or dissolved in the medium) into ultimately sugars and storage carbohydrates, providing the carbon blocks and energy for the biosynthesis of cellular materials, cell growth and cell maintenance. In addition, autotrophic growth led to decrease in pH of the culture medium.

4.4 Summary

The implications of the results presented here are much evident during growth of cultures where changes in the pH, concentration of substrates in the medium, or availability of adequate light to all areas in the dense culture are factors reducing the growth and cell productivity of microalgae cultures. The inclusion of buffers into medium aids to resist pH changes, however, pH changes do occur because growth as a very complex process involves the continuous interplay/interaction between the external environment of cells and metabolism within cells. For example the consumption of substrates from the medium, which are then subsequently metabolised within cells, generate precursors for cellular material, energy for growth and cell maintenance. The excretory waste venturing into the medium may be significant enough to cause fluctuations in pH from the optimum. Here, the consumption of acetate was found to cause a rise in pH during heterotrophic or mixotrophic growth. The resultant rise in pH was a strong limitation for heterotrophic cultures. Moreover, the consumption of the carbon and nitrogen substrates results in depletion in concentration. Cells strictly require carbon and nitrogen for growth, and the depletions are additional limitations that reduce growth.

The supply of light if not adequate enough poses another limitation that reduces growth. Generally as cells grow and multiply, the culture density increases in the medium. For the photosynthetic cultures, penetration of light into dense cultures could become limiting i.e. some areas within the culture may not receive the light adequately. In this chapter, light intensity incident upon the cultures was observed to affect culture growth and cell densities. The cultures receiving the lowest light intensity exhibited the lowest growth.

Overall, the comparisons showed that the heterotrophic condition was most-limiting condition for the growth of *C. reinhardtii* cultures. This growth condition was most limited in terms of carbon, energy, light and pH limitations. The challenges of heterotrophic cultures for economical and large scale growth of microalgae are profound. Therefore, two strategies that addressed some or the four limitations were identified to significantly improve the growth of the *C. reinhardtii* cultures. One of the strategies addressed the problems of lack of carbon, lack of energy and detrimental pH rises encountered in

heterotrophic condition, through continuous supply of the carbon and energy source while ensuring the medium pH was buffered around pH 7.30. The large improvement in cell densities, cell productivity, and longevity of the heterotrophic cultures by this strategy means that this method can be implemented for the cultures expressing recombinant proteins leading to increased productivity for the target protein and improved yield. The other strategy which involved transferring the cultures to autotrophic condition was equally effective in addressing the four limitations, and significantly improved the growth, cell productivity and longevity of the cultures. More importantly, scale up of the strategies should be possible. Therefore, economical and large scale operations for growing the microalgae cultures are feasible.

Chapter 5 – Limitations to recombinant protein production; Results and discussions

In the previous chapter, the growth of *C. reinhardtii* cultures were characterized in autotrophic, heterotrophic and mixotrophic conditions. Factors affecting the growth rates and cell densities were identified. The work in chapter 4 aimed for an understanding of the different growth profiles presented by *C. reinhardtii* cultures in the different growth condition, and the limitations affecting growth.

Chapter 5 is a continuation of the previous chapter, but additionally, the recombinant protein yields are determined for the different growth conditions. Also, the limitation to growth due to the expression of the foreign protein by *C. reinhardtii* under autotrophic, heterotrophic and mixotrophic conditions are determined. Chapter 5 results start with qualitative detection of the recombinant protein expression in cultures. Thereafter, the protein yields were quantified for the different growth conditions. The expression yield of *E. coli* β-glucuronidase (gus) in the transgenic strains Gus12-2 and Gus12-B are reported here.

In addition, the growth phenotypes were further characterized by comparing the cell size distribution and dry weight of cells in autotrophic, heterotrophic and mixotrophic conditions. The utilization of carbon substrates such as acetate in heterotrophic and mixotrophic conditions, CO_2 in autotrophic and mixotrophic conditions were determined, and used to estimate of carbon fluxes. The utilization of the nitrogen source (ammonium) was determined in autotrophic, heterotrophic and mixotrophic conditions. The total recombinant gus yield, the total protein yield for autotrophic, heterotrophic and mixotrophic conditions were compared. The protein burden (protein cost) on the growth of cultures due to expression of the recombinant gus was identified and quantified in the three conditions. Furthermore, the cellular ATP concentrations, total carbohydrate yield in the three conditions were compared.

5.1 Detection of gus expressed in strains

β-glucuronidases (EC.3.2.1.31) are enzymes that hydrolyse *β*-D glucuronides into glucuronates. Gus has been shown to be highly stable enzymes to degradation, heat, detergent treatment and require no cofactors for their activity (Jefferson, 1987). Plants and microalgae including *Chlamydomonas* lack gus activity. Therefore, the expression of foreign gus gene such as *E. coli* gus gene in *Chlamydomonas* may be useful for studying recombinant gus production in *Chlamydomonas*. Previously, recombinant gus expressed in plants have been used as a reporter of gene expression in plants, and to identify promoter function in the plants (Jefferson, 1989, Jefferson et al., 1986, Jefferson et al., 1987a). In current PhD work, the aim was to implement *C. reinhardtii* as the model of expression for the recombinant gus, determine the yields and identify strategy to optimize the yields.

The chloroplast transformation of *C reinhardtii* was performed by Leopoldo Hera Rodriguez who provided the Gus12-2 and Gus12-B strains expressing the recombinant gus (see method section 3.1). The Gus12-2 and Gus12-B strains were isolated by transforming the *gusA* gene from *E. coli* into the recipient strain cc373 mt+ (a photosynthetic mutant). Transformation was based on rescue of the defective *atpβ* gene in cc373 mt +. Rescue without the transgene provided the Bam10::cc373 mt+ control strain lacking *E. coli gusA.* Gus activity in *C. reinhardtii* cultures was used to confirm the expression of recombinant gus in the strains. Gus catalyse the hydrolysis of the glucuronide substrate (5-bromo-4-chloro-3-indoxyl glucuronide or *X-gluc*), through an intermediate, into a blue coloured precipitate product, 5’5’-dibromo-4’4’-dichloroindigo. The result of the enzyme assay performed at 37^{o}C on Gus12-2, Gus12-B, Bam10::cc373 mt+ cultures and on the sterile medium is presented in Figure 5.1. Gus12-2 and Gus12-B cultures were positive for gus activity described by the hydrolysis of the glucuronide substrate (*X-gluc)* into the final insoluble blue precipitate product after 24 h incubation at 37^{o}C. This confirmed that Gus12-2 and Gus12-B strains (gus transformants) retained the *E. coli gusA* gene after transformation.

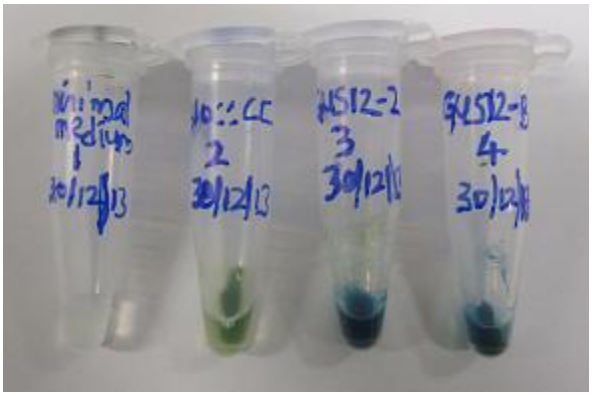

Figure 5.1: Qualitative detection of recombinant gus expression in *C. reinhardtii* strains. The 37^{o}C incubation assays of 30 µl cell sample with 40 µl of the substrate (5.75 mM *X-gluc*) was performed overnight (24 h) on: (tube 1) the sterile minimal medium (blank control); (tube 2) Bam 10::cc373 mt+ cell sample (negative control); (tube 3) Gus12-2 cell sample; (tube 4) Gus12-B cell sample. Detection of *β*-glucuronidase expression was confirmed by the enzymatic conversion of *X-gluc* to the insoluble blue-coloured precipitate (5'5'-dibromo-4'4'-dichloroindigo).

On the other hand, Bam10cc::373 mt+ culture sample was negative for gus activity because the strain lacked the *E. coli gusA* gene. Consequently, no hydrolysis of the glucuronide occurred in this test, and the assay retained the green colour of Bam10::cc373 mt+ culture. Assay on the sterile medium was negative as the medium remained colourless after 24 h incubation with the glucuronide at 37^{o}C. The assay was performed to rule out any false positive that may arise due to reactions of *X-gluc* with components of the medium or due to degradations in the assay.

Following the qualitative detection of recombinant gus activity in the Gus-12-2 and Gus12-B strains, the enzymatic activities were quantified, and the recombinant gus yield determined in autotrophic, heterotrophic and mixotrophic growth conditions. The results of these are presented and discussed later in sections of this chapter.

5.2 Cell size distributions

The growth of cultures was characterized by measuring the growth rates and cell sizes in autotrophic, heterotrophic and mixotrophic. The specific growth rates and cell sizes were measured during exponential growth phase in the three growth conditions.

Table 5.1: Cell sizes distribution and maximum specific growth rates (μ_{max}) of Bam 10::cc373 mt+, Gus12-2 and Gus12-B during exponential growth phase in autotrophic, heterotrophic and mixotrophic conditions. The maximum specific growth rates were determined during exponential growth phase (24 – 72 h) by plotting the natural log of cell density against time (See Appendix II, Figures A2.1, A2.2, A2.3). The slope of the linear plot was estimated as the maximum specific growth rate. The autotrophic and mixotrophic cultures were grown in continuous light at photon flux of 54 µmol photons/m^2/s. The mean and standard deviation were determined for six biological replicates and two technical replicates each.

	Autotrophic condition		**Heterotrophic condition**		**Mixotrophic condition**	
Strains	Mean cell Size ± sd (µm)	Mean μ_{max} ± sd (h^{-1}) x 10^{-2}	Mean cell size ± sd (µm)	Mean μ_{max} ± sd (h^{-1})x 10^{-2}	Mean cell size ± sd (µm)	Mean μ_{max} ± sd (h^{-1})x 10^{-2}
Bam10::cc373 mt+	8.5 ± 1.0	3.00 ± 0.2	10.1 ± 0.6	2.90 ± 0.01	8.9 ± 0.2	5.75 ± 0.1
Gus12-2	8.5 ± 0.2	3.12 ± 0.3	11.5 ± 0.9	2.42 ± 0.02	9.0 ± 0.2	5.72 ± 0.1
Gus12-B	8.7 ± 0.4	3.08 ± 0.2	11.6 ± 1.0	2.45 ± 0.04	9.1 ± 0.5	5.87 ± 0.04

The cell sizes were measured using the cellometer Auto T4 instrument. The specific growth rates and cell sizes for Bam10::cc373 mt+, Gus12-2 and Gus12-B cultures in the three conditions are presented on Table 5.1. The results in Table 5.1 show that cells in heterotrophic conditions were relatively larger than cells in autotrophic and mixotrophic conditions. The mean cell size of the cultures grown in the heterotrophic condition was found to be significantly different from the mean cell size of cultures grown in

autototrophic ($p = 0.033$) or mixotrophic ($p = 0.048$) condition at 95% confidence. However, there was no significant difference in the mean cell size of cultures grown in autotrophic or mixotrophic conditions. Assuming that the cells are approximately spherical, the formular for the volume of a sphere (equation 5.1) was used to estimate the cell volume in litres:

$$Cell\ volume = \left(\frac{4\pi\ X\ 10^{3}}{3\ X\ 10^{-18}}\right) X \left(\frac{d}{2}\right)^{3} \qquad (5.1)$$

Where π (*pi*) is approximately 3.14; d is the cell diameter (µm); the factor 10^{-18} in the denominator converts μm^3 into m^3. The factor 10^3 in the numerator, converts the volume unit into litre (L). Based on this calculation, the cell volumes were compared for the cultures grown in the three growth conditions and presented as Figure 5.2.

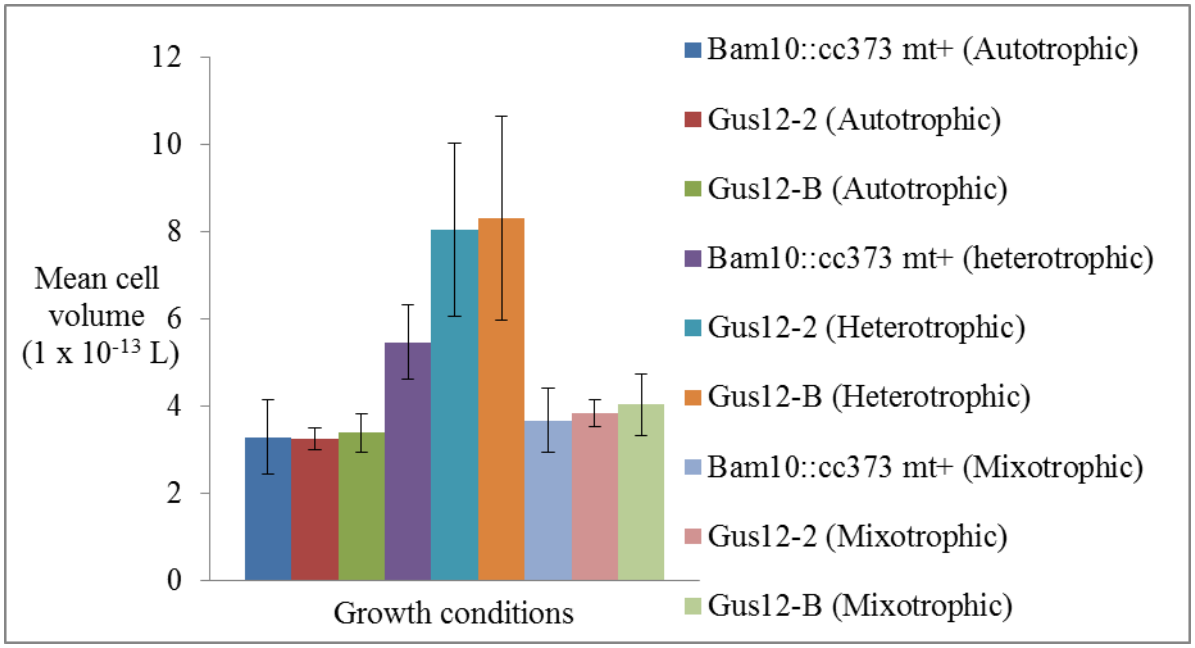

Figure 5.2: Mean cell volumes of cultures in autotrophic, heterotrophic and mixotrophic conditions. The mean cell volume and standard deviation were determined for six biological replicates and two technical replicates each.

The results in Figure 5.2 show the distribution of cell volumes for the three conditions based on the mean cell sizes (diameter) described. To understand the reason for the

relatively larger heterotrophic cells, the specific growth rates of the cultures at the exponential phase are presented in Table 5.1 and compared for the three conditions. The results confirm that heterotrophic cultures exhibit the slowest growth rates, typically ~ 0.024 h^{-1}. The autotrophic cultures at ~ 0.03 h^{-1} were slightly faster growing cultures than heterophic, while mixotrophic cultures exhibited the fastest growth rates about twice the growth rates of autotrophic or heterotrophic cultures. The mean μ_{max} value of heterotrophic cultures was observed to be significantly different from the mean μ_{max} value of autotrophic ($p = 0.04$) or mixotrophic ($p = 0.00005$). In addition, the mean μ_{max} values of autotrophic and mixotrophic cultures were significantly different ($p = 0.00002$) at 95% confidence.

Unicellular organisms have evolved to maximize growth (increase in cell number and cell mass) as an objective function (Molenaar et al., 2009). The unicellular organisms do not use energy to differentiate into different tissues but proliferate to gain growth advantage (Molenaar et al., 2009). The strategies to maximize growth may include rapid growth rate to achieve increase in cell numbers and accumulation of cellular materials resulting in increase in cell mass. The slowest growing cultures (heterotrophic), achieve relatively fewer of cell divisions, longer doubling time and lower cell density. The heterotrophic cell takes longer to divide resulting in relatively larger cell sizes before cell division. On the other hand, the fastest growing cultures (mixotrophic), achieve higher cell divisions, shorter doubling times and very high cell density. The maximization of growth may be achieved through rapid cell divisions and increase in cell numbers, resulting in relatively smaller cell sizes but higher cell density cultures. The growth rates of autotrophic cultures were significantly lower than those of mixotrophic cultures (Table 5.1) however the mean cell sizes were not significantly different in the two conditions. An explanation for this may be found from the cell cycle of *C. reinhardtii*.

In a study of the cell cycle of *C. reinhardtii*, the factors that affect the duration of the cell cycle time such as temperature, light intensity and the growth condition were described by (Vitova et al., 2011). Light intensity and temperature were reported as the major factors that controlled the duration of cell cycle time in *Chlamydomonas.* The cell cycle was reported to consist of two different phases by which microalgae cells divide depending on the growth conditions (a phase of growth commitment controlled by light intensity and

temperature; and another phase of growth commitment that is independent of light but controlled by the growth temperature). These authors demonstrated that an increase in growth temperature resulted in a corresponding decrease in the duration of cell cycle time. At the optimum growth temperature, the duration of cell cycle time was at a minimum (cells grow fastest). Upon further increase in growth temperature beyond the optimum, the cell cycle time increased. Increasing the light from low intensity to higher intensity was found to decrease the duration of the cell cycle time. An optimal growth condition also decreased the duration of cell cycle time. Since a parent cell divide at the end of the cell cycle into daughter cells, the number of the daughter cells produced would depend on whether the parent cell attained one or both growth commitments at the end of the cell cycle (Vitova et al., 2011). The number of daughter cells produced from a cell may determine the sizes of the produced cells. For example, one would expect that if four daughter cells are produced from a parent cell, the cells would be smaller, than if only two daughter cells are produced from the same parent cell.

In the current study, the growth temperature (25^{o}C) was constant for the three growth conditions. One may expect the effect of temperature to be similar in the three growth conditions. However, autotrophic and mixotrophic cultures were supplied light at the same intensity, therefore the total effect of light and temperature may be similar in the two conditions. Based on these assumptions, the cells in autotrophic and mixotrophic conditions may have attained the same number of growth commitments at the end of each cell cycle, and produced similar number of daughter cells hence the cells sizes were similar in both conditions. In contrast, the heterotophic cultures were grown in the dark suggesting that heterotrophic cells experienced longer duration of cell cycle time, and attained the growth commitment phase dependent on only temperature at the end of each cell cycle. This resulted in fewer number of cell division i.e. fewer daughter cells per cell cycle that were relatively larger in sizes than the cells in autotrophic or mixotrophic conditions. Autotrophic and mixotrophic conditions presented higher growth rates than heterotrophic condition because of the effect of light on the duration of cell cycle time (Vitova et al. 2011). However, the growth rate of mixotrophic cultures was significantly faster than autotrophic cultures suggesting that the mixotrophic condition may be a more optimal growth condition for *C. reinhardtii* cultures.

5.3 Dry cell weight determinations

The dry cell weight was determined for cultures in autotrophic, heterotrophic and mixotrophic conditions. Essentially, the method used involved drying the cell pellets until constant dry weight measurements were achieved. The measurement of dry cell weight determined for autotrophic, heterotrophic and mixotrophic cultures are presented in Table 5.2.

Table 5.2: Dry cell weight of Bam 10::cc373 mt+, Gus12-2 and Gus12-B cultures determined during the exponential growth phase in autotrophic, heterotrophic and mixotrophic conditions. The autotrophic and mixotrophic cultures were grown in continuous light at 54 µmol photons per m^2 per second. The mean and standard deviation were determined for three biological replicates and two technical replicates each.

Strains	Autotrophic condition Mean dry cell weight ± sd (g dry wt/cell) x 10^{-10}	Heterotrophic condition Mean dry cell weight ± sd (g dry wt/cell) x 10^{-10}	Mixotrophic condition Mean dry cell weight ± sd (g dry wt/cell) x 10^{-10}
Bam10::cc373 mt+	1.08 ± 0.02	1.5 ± 0.05	1.02 ± 0.08
Gus12-2	1.06 ± 0.07	1.52 ± 0.02	1.0 ± 0.05
Gus12-B	1.07 ± 0.09	1.5 ± 0.01	1.0 ± 0.03

The dry cell weight of heterotrophic cultures were relatively higher than autotrophic and mixotrophic cultures. The dry cell weight results on Table 5.2 were statistically compared. The cultures grown in the heterotrophic condition had mean dry cell weight values that are significantly different from those grown in autotrophic ($p = 0.000001$) or mixotrophic conditions ($p = 0.00000008$). However, there was no significant difference in the mean dry cell weight values for the autotrophic and mixotrophic cultures. The dry cell weight results correlated with the cell size distributions for the three growth conditions. The larger cell sizes in heterotrophic cultures were heavier suggesting that the slower growing heterotrophic cultures likely maximize growth by increasing cell size. The cultures achieve relatively lower final cell density, typically reaching ~3 - 4 million cells per ml (see Figure

4.3). Autotrophic (Figure 4.2) and mixotrophic cultures (Figure 4.4) on the other hand, maximize growth by increasing their cell numbers and achieve high cell densities greater than 10 million cells per ml.

To obtain estimates for the dry weight of cells per volume of cultures, the determined mean dry cell weight (g dry wt/cell) on Table 5.2 was used to multiply the cell density (number of cells/ml). This allowed the conversion of cell density from (number of cells/ml) into units of (g dry cell weight/ml). For example using this estimation, heterotrophic cultures achieve final cell density of 0.45×10^{-3} to 0.6×10^{-3} g dry cell weight/ml culture, whereas autotrophic and mixotrophic cultures achieve cell densities $> 1 \times 10^{-3}$ g dry cell weight/ml culture.

5.4. Acetate consumption, specific photosynthetic rate and ammonium utilization

The consumption of acetate, photosynthetic CO_2 fixation rate and ammonium utilization are presented here. During exponential phase, the uptake of acetate in heterotrophic and mixotrophic conditions, and the photosynthetic uptake of CO_2 in autotrophic and mixotrophic conditions were determined to get an estimate of carbon influx in the conditions. The consumption of ammonium in autotrophic, heterotrophic and mixotrophic conditions was measured to identify if consumption of the nitrogen source limited growth of *C. reinhardtii*.

5.4.1 Acetate consumption and specific acetate uptake rate

The acetate concentrations in TAP were followed by measuring the concentration of the substrate in the medium and calculating the concentration consumed during growth. The plot of acetate consumption with time is shown for example, for heterotrophic Bam10::cc373 mt+ and Gus12-2 cultures in TAP medium, where, acetate consumption from the medium was measured (Figure 5.3). The resultant decrease in acetate of the medium due to this consumption is shown in Figure 5.4.

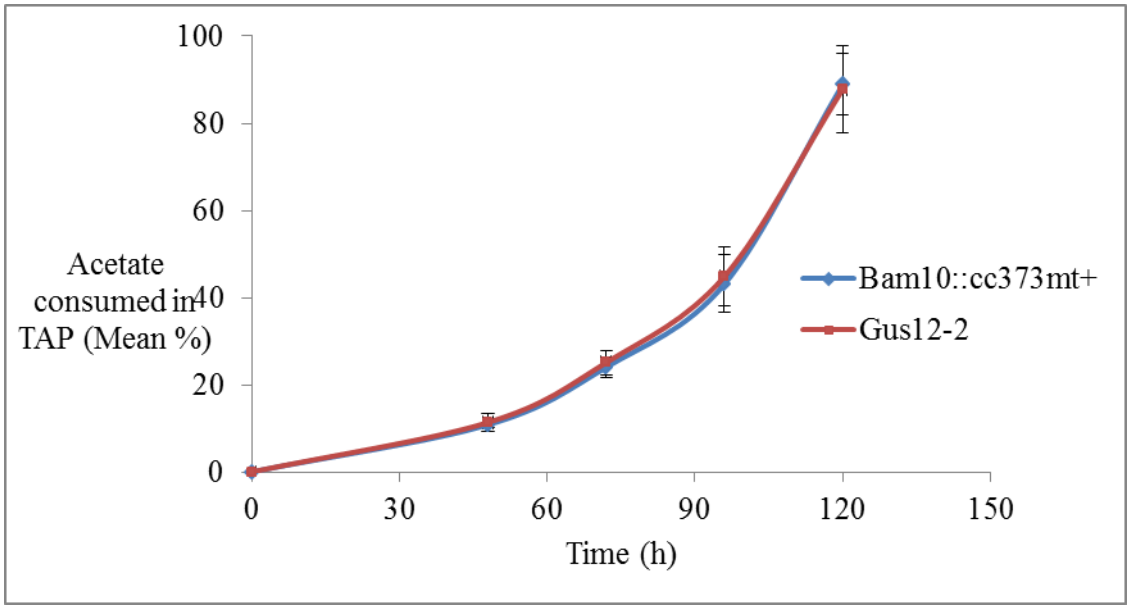

Figure 5.3: Acetate consumption profiles for heterotrophic Bam10::cc373 mt+ and Gus12-2 cultures growing in TAP medium containing 20.5 mM acetate. The mean percentage of acetate concentration consumed and standard deviation were determined from three biological and two technical replicates each

The acetate consumed from the medium depended on the cell density of the culture. The higher the cell density, the greater was the consumption of acetate as shown in Figure 5.5. Cultures in exponential phase experienced steady increase in growth, doubling in cell numbers, and doubling in acetate consumption with time (Figure 5.5). After 120 h incubation, ~90% (18 mM) of acetate was consumed from TAP medium (Figures 5.3 and 5.4). At 120 h, the concentration of the substrate remaining in the medium is ~2 mM. At this concentration, acetate was already very limiting and the growth of culture slowed down. Generally, heterotrophic cultures runs out of acetate completely after 144 – 168 h (refer to Figure 4.19), and enter the stationary phase followed by the death phase where cells die out due to lack of carbon, energy and pH effect. However, for the fast growing and highly dense mixotrophic cultures, acetate becomes completely consumed from the medium earlier, (usually at about 120 h), though the cultures continue photosynthetic growth far beyond this time.

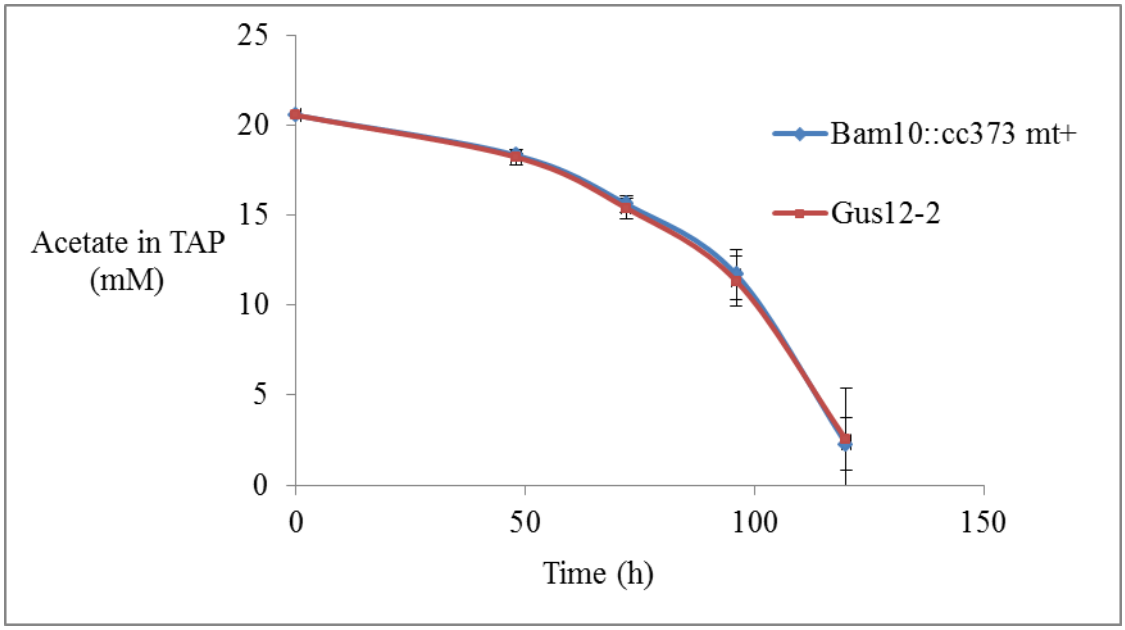

Figure 5.4: The decrease in acetate concentrations in TAP during heterotrophic growth of Bam10::cc373 mt+ and Gus12-2. The mean and standard deviation were determined from three biological replicates and two technical replicates each.

The specific acetate uptake rate determined for heterotrophic and mixotrophic cultures are reported in Table 5.3. The specific acetate uptake rate (mmoles acetate/g dry cell weight/h) was calculated using equation 3.18. The specific acetate uptake rate was used as an estimate for the organic carbon uptake rate per cell in heterotrophic and mixotrophic growth conditions. The mean specific acetate uptake rate was lower in mixotrophic condition than heterotrophic conditions (Table 5.3) due to the very large increase in the cell density of the mixotrophic cultures grown on the TAP.

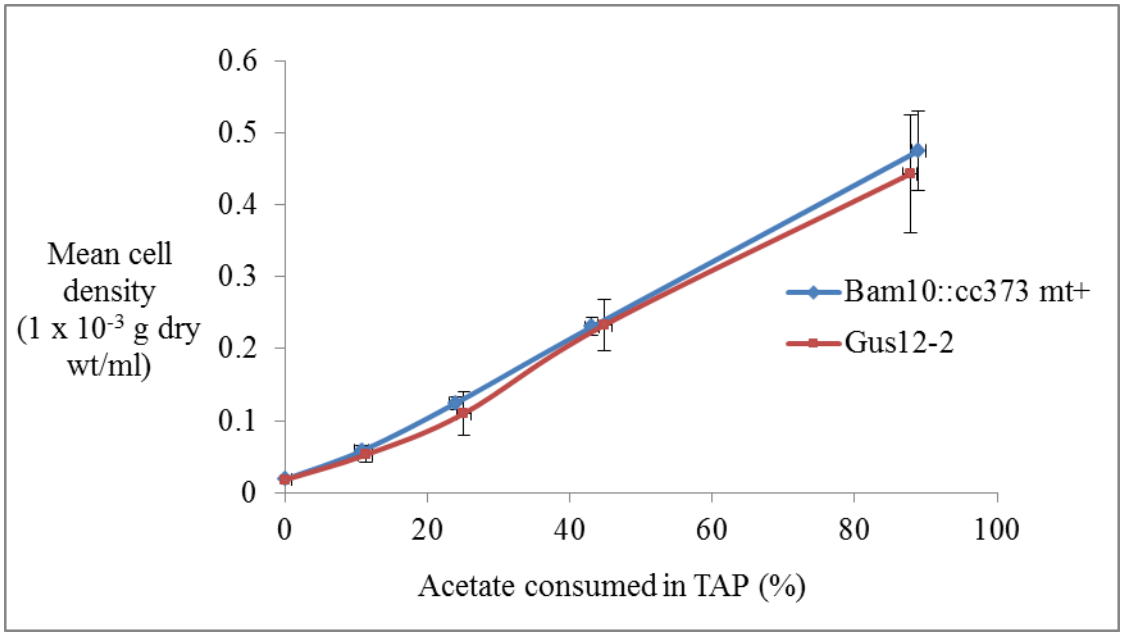

Figure 5.5: The growth profiles for heterotrophic Bam10::cc373 mt+ and Gus12-2 cultures in TAP medium containing initial 20.5 mM acetate. The mean and standard values were determined from three biological and two technical replicates each

Table 5.3: Specific acetate uptake rates in heterotrophic and mixotrophic cultures of Bam10::cc373 mt+ and Gus12-2. The mean and standard deviation were determined from six biological and two technical replicates.

Strains	**Heterotrophic** Mean specific acetate uptake rate ± sd (mmole acetate consumed/g dry wt/h)	**Mixotrophic** Mean specific acetate uptake rate ± sd (mmoles acetate consumed/g dry wt/h)
Bam10::cc373 mt+	1.61 ± 0.17	1.08 ± 0.1
Gus12-2	1.71 ± 0.29	1.03 ± 0.07

5.4.2 Specific photosynthetic CO_2 fixation rate (specific CO_2 fixation rate)

The photosynthetic rates were estimated using the oxygen electrode method. The photosynthetic rates were determined for exponential phase autotrophic and mixotrophic

cultures. Since the amount of oxygen moles evolved is approximately in ratio 1:1 with the amount of CO_2 moles fixed during photosynthetic activity, the photosynthetic rate (photosynthetic CO_2 fixation rate) was expressed as µmol CO_2 fixed/h. Photosynthetic growth depended also on the concentration of photosynthesizing cells, therefore, the specific photosynthetic rate or specific CO_2 fixation rate (µmol CO_2 fixed/g dry cell weight/h) was calculated using equation 3.23. The calculated specific CO_2 fixation rate was used as an estimate for inorganic carbon uptake rate for autotrophic and mixotrophic cultures. The specific CO_2 fixation rate determined for autotrophic and mixotrophic cultures are presented in Table 5.4.

Table 5.4: Specific CO_2 fixation rate for autotrophic and mixotrophic cultures of Bam10::cc373 mt+ and Gus12-2. The mean and standard deviation were determined for three biological and two technical replicates.

Strains	Autotrophic Mean specific CO_2 fixation rate ± sd (mmole CO_2 fixed/g dry wt/h)	Mixotrophic Mean specific CO_2 fixation rate ± sd (mmole CO_2 fixed/g dry wt/h)
Bam10::cc373 mt+	11.09 ± 0.73	7.99 ± 0.69
Gus12-2	11.74 ± 0.22	-

On the basis of carbon moles, the estimated total carbon flux in mixotrophic (~10 mmole carbon/g dry wt/h) and autotrophic condition (11 mmole carbon/g dry wt/h) are higher than in heterotrophic condition (~3.4 mmole carbon/g dry wt/h). Consequently, growth yield and recombinant protein yield might be more limited by a short-fall in carbon flux in the heterotrophic than in autotrophic or mixotrophic conditions.

5.4.3 Ammonium utilization

The ammonium utilization was determined by measuring the concentration of ammonium in the medium by the ninhydrin method. The ammonium consumed during growth was calculated. The ammonium concentration in the medium was measured for heterotrophic and autotrophic Gus12-2 cultures (144 h) to identify whether ammonium concentrations

were limiting the growth. The growth curves are shown in Figure 5.6. The result in Table 5.5 shows that the ammonium concentration was depleted by at least 50% in the autotrophic and heterotrophic Gus12-2 cultures at 144 h. This indicates that the substrate was consumed for growth. As ammonium concentrations become depleted in the medium, lower concentrations of the substrate may result in limitation to growth, as previously described in Figure 4.11.

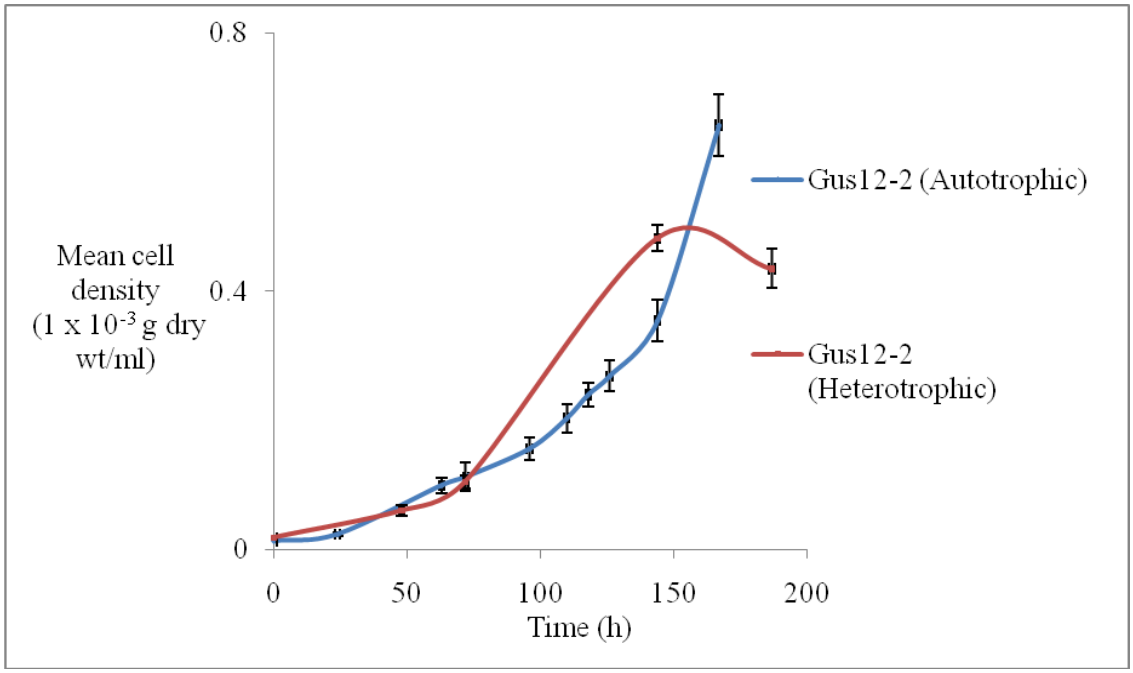

Figures 5.6: Autotrophic and heterotrophic growth curves for Gus12-2 cultures in minimal and TAP medium respectively. The autotrophic cultures were grown continuously in light at 54 µmol photons/m^2/s. The mean cell density was determined from three biological replicates and two technical replicates each

Similarly, the ammonium concentration of TAP medium used for culturing mixotrophic Bam10::cc373 mt+ was determined after 168 h growth (Figure 5.7). Here, about 57% (3.7 mM) of the ammonium was consumed by the culture (Table 5.6). The depletion of ammonium during growth highlights the need to address the nitrogen limitations that may arise during growth.

Table 5.5: Ammonium consumption by heterotrophic Gus 12-2 cultures (144 h), and by autotrophic Gus12-2 cultures (144 h). The initial ammonium concentration in TAP and minimal media was 9.5 mM. The mean and standard deviation were determined for three biological replicates and two technical replicates each.

		Gus12-2
144 h **Heterotrophic** growth in TAP medium (9.5 mM ammonium)	Ammonium consumed ± sd (mM)	5.15 ± 0.70
	Ammonium in medium ± sd (mM)	4.35 ± 0.72
	Ammonium Consumption ± sd (%)	54 ± 7.6
144 h **Autotrophic** growth in minimal medium (9.5 mM ammonium)	Ammonium consumed ± sd (mM)	4.8 ± 0.80
	Ammonium in medium ± sd (mM)	4.7 ± 0.80
	Ammonium Consumption ± sd (%)	50 ± 8.6

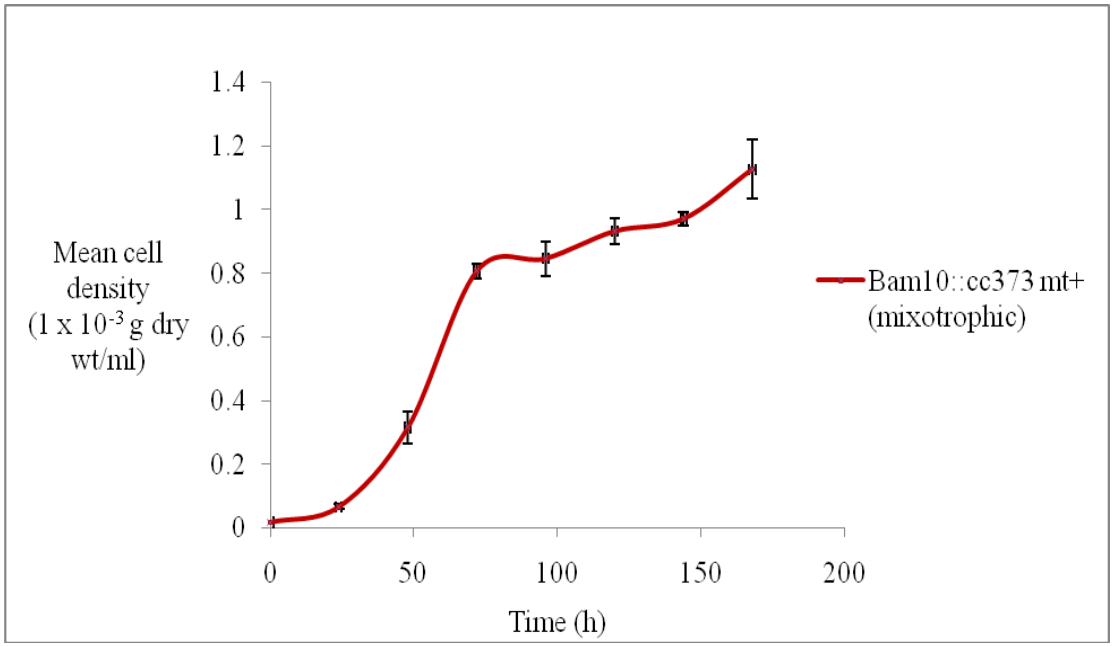

Figures 5.7: Mixotrophic growth of Bam10::cc373 mt+ cultures grown in TAP (and in continuous light at 54 µmol photons/m^2/s. The mean cell density was determined from three biological replicates and two technical replicates.

Table 5.6: Ammonium consumption by mixotrophic Bam10::cc373 mt+ cultures (168 h). The initial ammonium concentration in TAP medium was 8.5 mM. The mean and standard deviation were determined from three biological replicates and two technical replicates each.

		Bam10::cc373 mt+
168 h **Mixotrophic** growth in TAP medium (8.5 mM ammonium)	Ammonium consumed ± sd (mM)	4.8 ± 0.04
	Ammonium in medium ± sd (mM)	3.7 ± 0.04
	Ammonium Consumption ± sd (%)	57 ± 4.8

5.5 Recombinant gus yield and gus productivity in cultures

The recombinant gus yields were measured in autotrophic, heterotrophic and mixotrophic cultures. The detection of recombinant gus activity in Gus12-2 and Gus12-B strains was previously presented in Figure 5.1. Following the result, gus enzymatic activity was determined in the samples (culture supernatant and crude cell extract) using the methods described in section 3.6. No detectable measurement of recombinant gus activity was found in the culture supernatant. The enzyme activity was detected and measured in the crude cell extracts obtained from Gus12-2 and Gus12-B cultures. The results indicated that recombinant gus was accumulated internally in the cells and was not secreted into the medium. The results was supported by other findings that the chloroplast, as an expression platform for recombinant proteins correctly fold and accumulate the proteins (Coragliotti et al., 2011, Ishikura et al., 1999, Rasala et al., 2010). No detectable measurement of the recombinant gus activity was found in the Bam10::cc373mt+ strain, thus serving as the negative control.

At 37^{o}C, the gus catalysed hydrolysis of 4-nitrophenyl β-D-glucuronide into 4-nitrophenol and glucuronic acid, was measured by monitoring the absorbance of light by 4-nitrophenol at 405 nm. The total enzyme activity (nanomoles of 4-nitrophenol formed/minute) was determined. One unit of an enzyme is the amount of the enzyme that catalysed the formation of one nanomole of the product per minute at 37^{o}C. Therefore, the total gus activity was correlated into total gus units. According to Jefferson (1987), one unit of gus at 37^{o}C and pH 7 was approximately five nanogram of pure β-glucuronidase. Using this

information, total gus units were converted into total amount of gus (nanogram gus). Therefore, recombinant gus yield was expressed as the total amount of gus per cell (ng gus/g dry cell weight).

The recombinant gus yields were determined during exponential growth phase for the autotrophic, heterotrophic and mixotrophic cultures. The recombinant gus yields were compared in Figure 5.8. The lowest recombinant gus yield was obtained in the heterotrophic cultures.

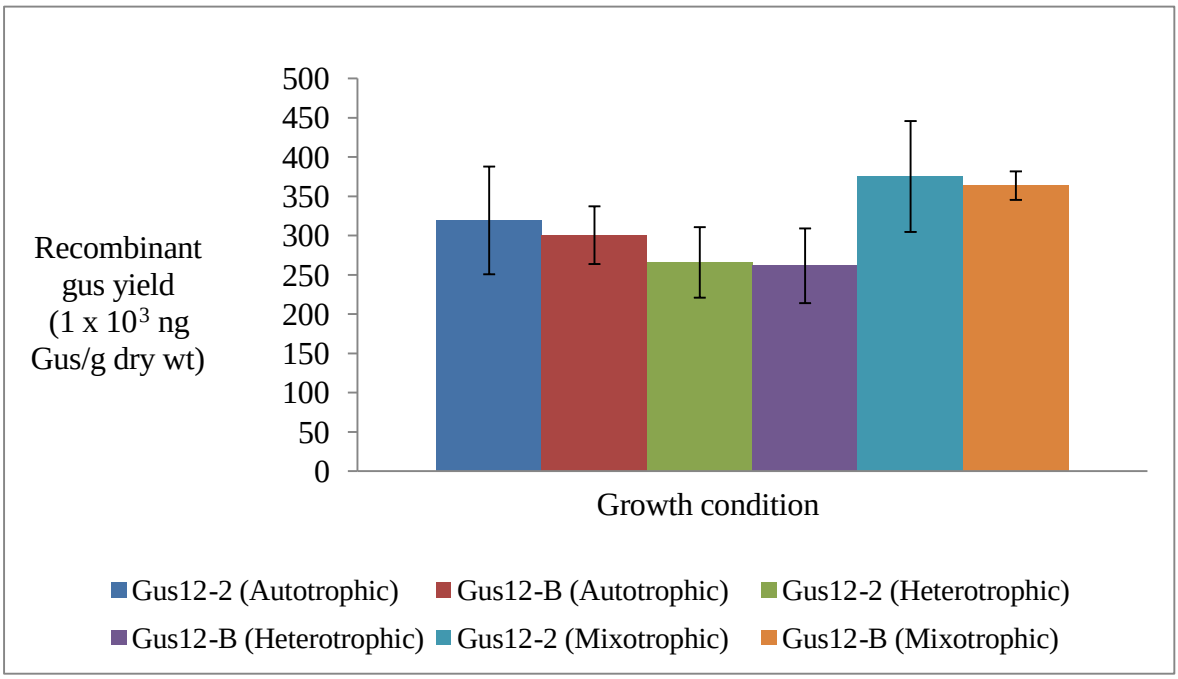

Figure 5.8: Recombinant gus yield during exponential growth phase of Gus12-2 and Gus12-B cultures in autotrophic, heterotrophic and mixotrophic conditions. The mean and standard deviation values were determined from six biological replicates and 2 technical replicates each. The autotrophic and mixotrophic cultures were grown in continuous light at 54 µmol photons/m^2/s.

The highest gus yield were obtained in mixotrophic cultures while autotrophic cultures had gus yield that was intermediate between those of mixotrophic and heterotrophic. The difference in the mean recombinant gus yield values were not significant for the three conditions. On the basis of percentage dry cell weight, the measured gus yields were

~0.027% dry cell weight (heterotrophic), ~0.032% dry cell weight (autotrophic) and ~0.038% dry cell weight (mixotrophic).

Overall, the measured recombinant gus yield was low. On the basis of total cellular protein (see Table 5.8), the gus yields in the current work were ~0.056% of the total cell protein (heterotrophic condition), ~0.062% of total cell protein (autotrophic) and ~0.065% of total cell protein (mixotrophic condition). These values were similar to the gus yield values reported by Ishikura et al. (1999). On the basis of percentage of total soluble proteins, these researchers reported recombinant gus yields expressed in *C. reinhardtii* chloroplast (0.01 and 0.08%). Generally, the reported yield of other foreign proteins expressed in *C. reinhardtii* chloroplast is low. For example, Komine et al. (2002) reported a yield of green fluorescent protein expressed in *C. reinhardtii* (0.05% of total soluble protein). Rasala et al. (2010) determined yields 0.1, 0.15, and 1% of total soluble protein for vascular endothelia growth factor (VEFR), high mobility group protein B1 (HMGB1), and fourteenth human fibronectin type III domain (14FN3) respectively. These proteins were expressed in *C. reinhardtii* chloroplast where *atpA* promoter and an *rbcL* 5'UTR combination was used to drive the transgene expression. However, when *psbA* promoter and an *rbcL* 5'UTR combination were used, the measured yield for VEGF, HMGB1 and 14FN3 were 2, 2.5 and 3% of soluble proteins respectively. This shows that the recombinant protein yield may also depend on the promoters used to drive the expression.

The maximum specific growth rates were determined at the exponential growth phase. During the exponential growth phase the natural log of cell density were plotted against time (see Appendix II). The slope of the linear plot was estimated as the maximum specific growth rate. The determined maximum specific growth rates in autotrophic, heterotrophic and mixotrophic conditions are included in Table 5.7.

Table 5.7: Maximum specific growth rates (μ_{max}), recombinant gus yield and gus productivity determined during exponential growth phase of Gus12-2 and Gus12-B cultures in autotrophic, heterotrophic and mixotrophic growth conditions. The autotrophic and mixotrophic cultures (Appendix II) were grown in continuous light conditions at 54 µmol photons/m^2/s. The mean and standard deviation were determined from six biological replicates and two technical replicates each.

		Gus12-2	**Gus12-B**
Heterotrophic	Mean total gus yield ± sd (ng Gus/g dry wt) x 10^5	2.66 ± 0.45	2.62 ± 0.75
	Mean μ_{max} ± sd (1 x 10^{-2} h^{-1})	2.42 ± 0.02	2.45 ± 0.04
	Mean gus productivity ± sd (ng Gus/g dry wt/h) x 10^3	6.44 ± 1.1	6.41 ± 1.82
Autotrophic	Mean total gus yield ± sd (ng Gus/g dry wt) x 10^5	3.20 ± 0.69	3.00 ± 0.37
	Mean μ_{max} ± sd (1 x 10^{-2} h^{-1})	3.12 ± 0.30	3.08 ± 0.2
	Mean gus productivity ± sd (ng Gus/g dry wt/h) x 10^3	9.97 ± 2.14	9.27 ± 1.13
Mixotrophic	Mean total gus yield ± sd (ng Gus/g dry wt)	3.75 ± 0.71	3.63 ± 0.18
	Mean μ_{max} ± sd (1 x 10^{-2} h^{-1})	5.72 ± 0.1	5.87 ± 0.04
	Mean gus productivity ± sd (ng Gus/g dry wt/h) x 10^3	21.34 ± 1.06	2.15 ± 4.05

Gus productivity was calculated for the exponential phase, as the product of maximum specific growth rate and recombinant gus yield. The gus productivity results are also included in the Table 5.7. A comparison of the gus productivity in the three growth conditions is shown Figure 5.9. The gus productivity was highest in the mixotrophic condition. Gus productivity was ~2-fold higher in mixotrophic cultures compared to autotrophic cultures but ~3-fold higher in mixotrophic than in the heterotrophic cultures.

Consequently, there was significant difference in the mean gus productivity between mixotrophic and autotrophic conditions ($p = 0.0009$), or between mixotrophic and heterotrophic conditions ($p = 0.00003$) at 95% confidence. In addition, the mean gus productivity in autotrophic and heterotrophic cultures was significantly different ($p = 0.012$) at 95% confidence.

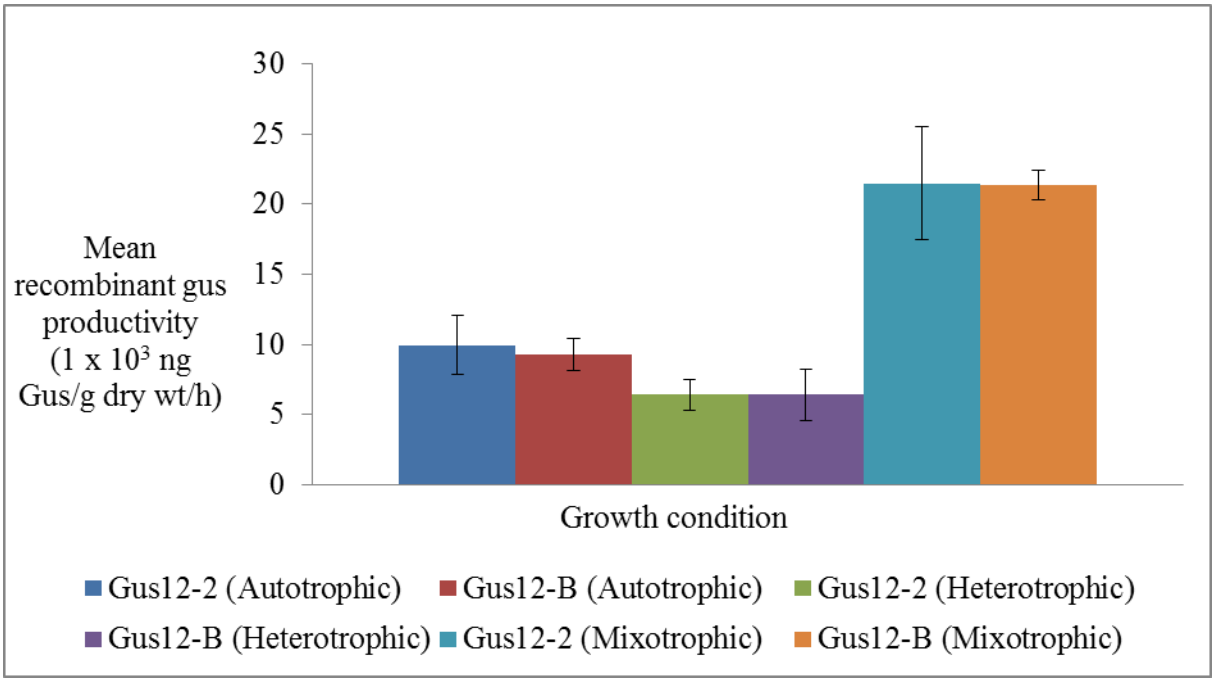

Figure 5.9: Gus productivity determined during exponential growth phase of Gus12-2 and Gus12-B cultures in autotrophic, heterotrophic and mixotrophic conditions. The mean and standard deviation were determined from six biological replicates and two technical replicates each. The autotrophic and mixotrophic cultures were grown in continuous light conditions at 54 µmol photons/m^2/s.

The analysis of productivity shows that the heterotrophic condition was the most limiting condition for recombinant gus production. During exponential phase, growth rate is fast and cultures achieve steady growth through regular cell divisions, and the rate of synthesis of proteins and other macromolecules may be assumed to be steady or pseudo-steady state. In this case, a measurement of productivity at the exponential phase provided clues about how fast the steady rate of synthesis of the proteins occurred in the three growth conditions. Mixotrophic cultures achieve the highest gus productivity because the

maximum specific growth rates are approximately twice those of autotrophic or mixotrophic cultures as shown in Table 5.7. Additionally, mixotrophic cultures expressed a slightly higher gus yield than the autotrophic and heterotrophic cultures.

5.6 Total protein yield and protein productivity in cultures

The total protein concentration was determined using the Biorad protein assay based on Bradford method (Bradford, 1976). The total protein was measured as the sum of the soluble proteins and insoluble proteins of the culture samples. The total protein yield (mg total protein/g dry cell weight) was calculated by dividing the total protein by the total number of cells. The total protein yield was determined during the exponential phase growth of cultures. The protein productivity was calculated as the product of the maximum specific growth rate and total protein yield. The measured maximum specific growth rates of the cultures are shown in the Table 5.7.

The total protein yield determined for autotrophic, heterotrophic and mixotrophic conditions are presented in Table 5.8, and compared in Figure 5.10. The results show that total protein yield varied between the three growth conditions. In heterotrophic condition, the total protein yield was about ~48% of the dry cell weight. In autotrophic condition, the total protein yield was ~54% of the dry cell weight. However, the mean difference in total protein yield was not significant in the two conditions (Figure 5.10). Total protein yield was higher in mixotrophic conditions (~60% of dry cell weight). The results reflected the pattern observed when recombinant gus yields (Figure 5.8) were compared across the three different growth conditions.

The total protein content on the basis of dry algae cell weight was reported to vary widely between 12 – 71% depending on the algae species (Becker, 2007, Brown, 1991). For example, in the freshwater microalgae, Samek et al. (2013) reported total protein yield of 43 – 52 % (*Scenedesmus quadricauda*), 22 – 55% (*Spirulina platensis*), and 49 – 53% (*Chlorella kessleri*), and 31 - 55% (*Chlorella sp.*). Becker (2007) reported 57% for *Dunaliella salina*, 51 - 58 % for *Chlorella vulgaris* and 48% for *Chlamydomonas*

reinhardtii. Thus it appears the protein content of the microalgae dry cell depends on the species of algae, but our results for *C. reinhardtii* (Table 5.8 and Figure 5.10) show that the total protein yield also depended on the growth conditions.

Table 5.8: Total protein yield and protein productivity in the exponential growth phase for autotrophic, heterotrophic and mixotrophic cultures. The autotrophic and mixotrophic cultures were grown in continuous light condition at 54 µmol photons/m^2/s. The mean and standard deviations were determined for three biological replicates and two technical replicates each.

		Gus12-2	Gus12-B	Bam10::cc373 mt+
Heterotrophic	Mean total protein yield ± sd (mg total protein/g dry wt)	493 ± 61	471 ± 22	472 ± 12
	Mean protein productivity ± sd (mg total protein/g dry wt/h)	12 ± 1.5	11.5± 0.5	13.67 ± 0.4
Autotrophic	Mean total protein yield ± sd (mg total protein/g dry wt)	511 ± 39	554 ± 38	569 ± 96
	Mean protein productivity ± sd (mg total protein/g dry wt/h)	16 ± 1.2	17 ± 1.2	17.1 ± 2.9
Mixotrophic	Mean total protein yield ± sd (mg total protein/g dry wt)	603 ± 37	577 ± 21	629 ± 35
	Mean protein productivity ± sd (mg total protein/g dry wt/h)	33 ± 1.2	34 ± 2.2	36.2 ± 2.06

The result of protein productivity in Figure 5.11 mirrors those of recombinant gus productivity (Figure 5.9) for the three growth conditions. The highest protein productivity was found in mixotrophic cultures. The results confirmed that mixotrophic conditions provide relatively higher protein yield and optimal protein productivity compared to heterotrophic or autotrophic condition. Heterotrophic condition provided the lowest protein productivity, and represented the limiting condition for protein and recombinant gus production.

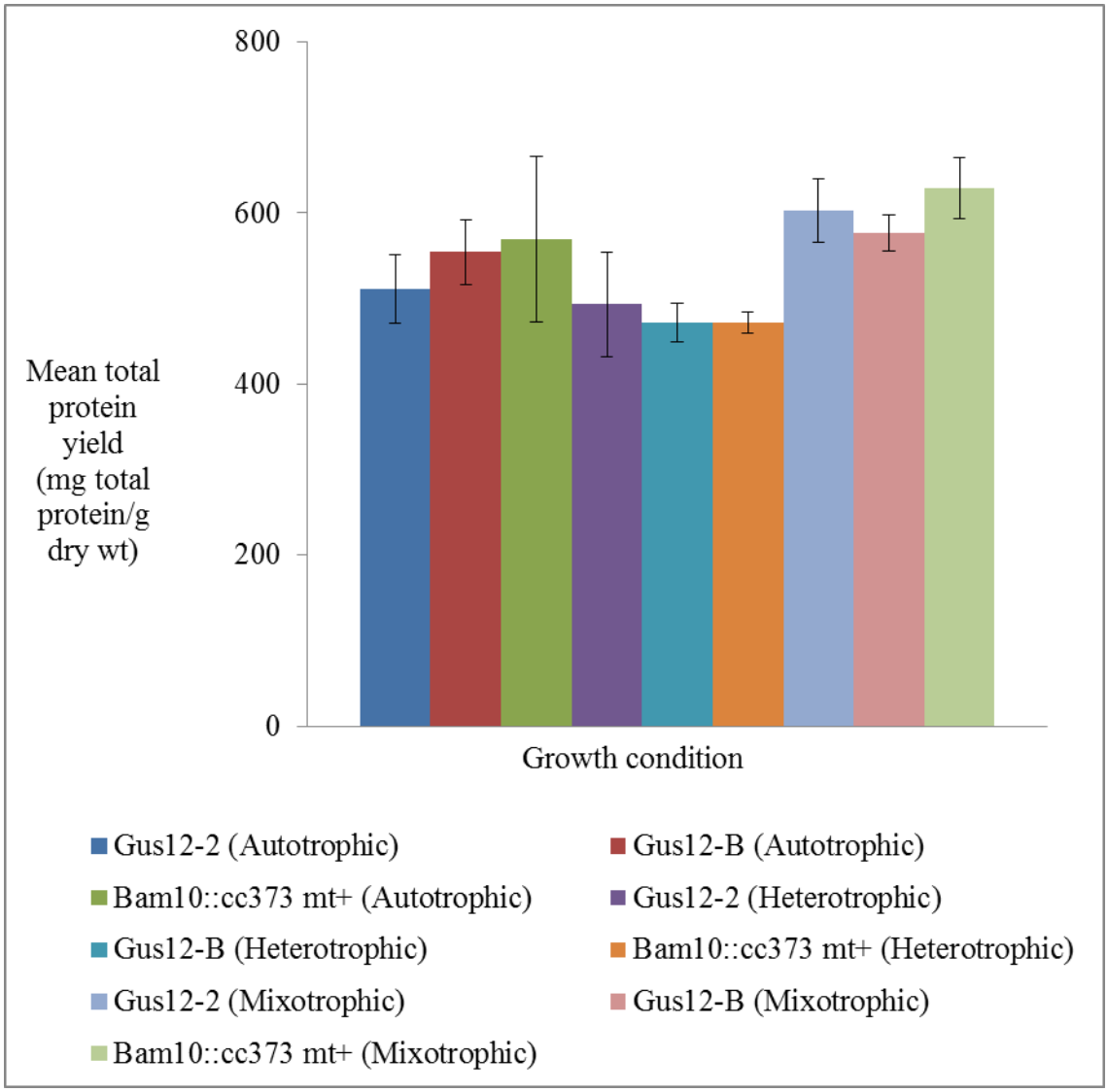

Figure 5.10: Total protein yield during exponential growth phase of Gus12-2, Gus12-B and Bam10::cc373 mt+ cultures in autotrophic, heterotrophic and mixotrophic conditions. The mean and standard deviation were determined from three biological replicates and 2 technical replicates each. The autotrophic and mixotrophic cultures were grown in continuous light condition at 54 µmol photons/m^2/s.

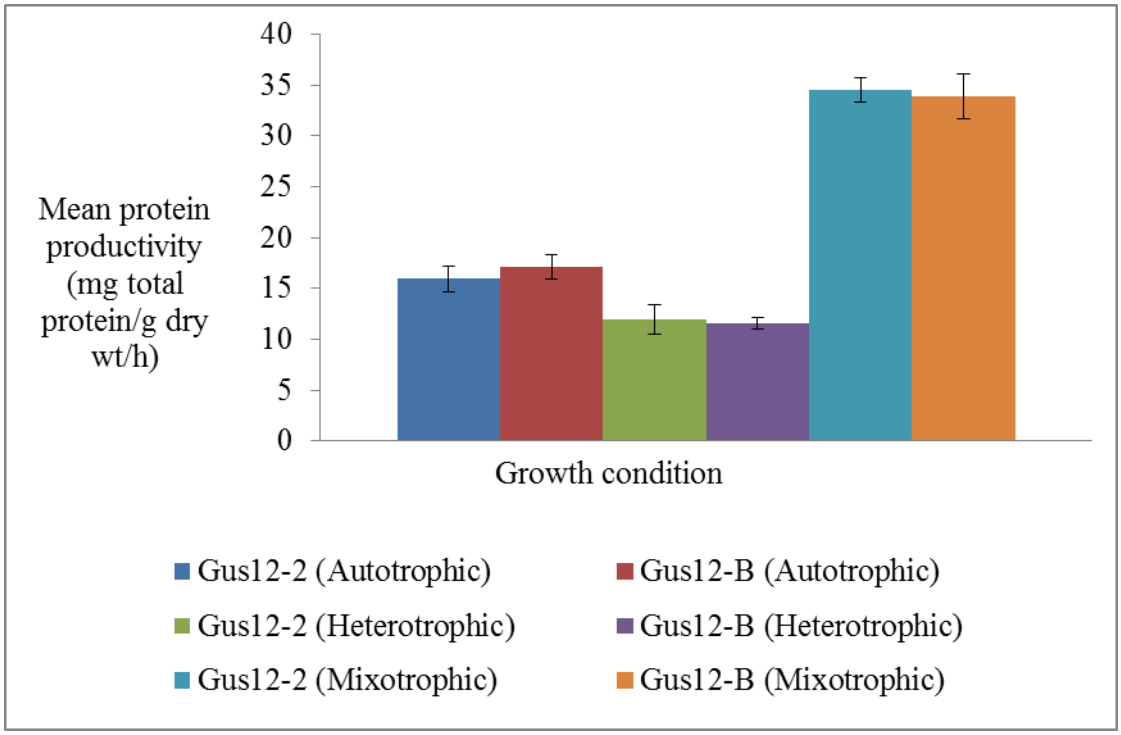

Figure 5.11: Total protein productivity determined during exponential growth phase of Gus12-2 and Gus12-B cultures in autotrophic, heterotrophic and mixotrophic conditions. The mean and standard deviation were determined from three biological and two technical replicates each. The autotrophic and mixotrophic cultures were grown in continuous light conditions at 54 µmol photons/m^2/s.

5.7 Protein burden (cost) for recombinant gus in *C. reinhardtii*

The limitation referred to as protein burden or protein cost (Dekel and Alon, 2005) for expressing proteins not needed for growth has been recognised for some time (Snoep et al., 1995, Dekel and Alon, 2005, Novick and Weiner, 1957, Koch, 1983). The protein burden is thought to arise due to diversion of cellular resources to produce 'extra proteins' not required for cell growth (Snoep et al., 1995, Koch 1983, Dekel and Alon 2005, Shachrai et al., 2010), or due to a competitive and dilution effect on the expression of endogenous proteins (Snoep et al., 1995). Also, since the production of proteins is a major energy demanding operation (Stouthamer, 1979), the expression of heterologous protein with no usefulness to a cell may suggest wastage to energy and may result in a cost (Marr, 1991). In this work, the maximum specific growth rates of the gus expressing strains (Gus12-2 and Gus12-B) were compared to those of the control (Bam10::cc373 mt+) to identify

whether growth rate of the transgenic strains were limited (reduced) by the production of recombinant gus. The protein burden represents a fractional reduction in growth rate of host cells (Snoep et al., 1995, Dekel and Alon, 2005, Shachrai et al., 2010). The protein cost was estimated during exponential phase using equation 5.2 described by Malakar and Venkatesh (2012):

$$Cost = \left(\frac{\mu_{\max\,(TRANSGENIC)} - \mu_{\max\,(CONTROL)}}{\mu_{\max\,(CONTROL)}} \right) \qquad (5.2)$$

Where, cost was expressed as a fractional decrease in growth rate, $\mu_{max\ (TRANSGENIC)}$ and $\mu_{max\ (CONTROL)}$ were the maximum specific growth rates of the transgenic strains (Gus12-2 and Gus12-B) and the control strain (Bam10::cc373 mt+) respectively.

Table 5.9: Maximum specific growth rate at exponential growth phase and estimated protein cost due to recombinant gus production in autotrophic, heterotrophic and mixotrophic conditions. The autotrophic and mixotrophic cultures were grown in continuous light conditions at 54 µmol photons/m^2/s. The mean and standard deviation were determined for six biological replicates and two technical replicates each.

	Autotrophic condition		Heterotrophic Condition		Mixotrophic Condition	
Strains	Mean μ_{max} ± sd (h^{-1}) x 10^{-2}	Mean Protein Cost ± sd (%)	Mean μ_{max} ± sd (h^{-1}) x 10^{-2}	Mean Protein Cost ± sd (%)	Mean μ_{max} ± sd (h^{-1}) x 10^{-2}	Mean Protein Cost ± sd (%)
Bam10::cc373 mt+	3.0 ± 0.2	0	2.9 ± 0.01	0	5.75 ± 0.1	0
Gus12-2	3.12 ± 0.3	3.8 ± 4.0	2.42 ± 0.02	-17.7 ± 1.1	5.72 ± 0.1	-0.3 ± 4.4
Gus12-B	3.08 ± 0.2	0.6 ± 4.8	2.45 ± 0.04	-15.1 ± 2.3	5.87 ±0.04	2.1 ± 3.9

The protein burden was estimated in autotrophic, heterotrophic and mixotrophic conditions and reported as percentage cost in Table 5.9. In autotrophic and mixotrophic conditions, there was no significant difference in the mean maximum specific growth rates for the gus expressing strains and the control strain. There was no detectable protein cost and the high standard deviation in the cost estimation suggests very wide fluctuations of the data about the mean for autotrophic and mixotrophic cultures.

On the other hand, the protein cost was observed in heterotrophic cultures because of the fractional reductions in the growth rate of the gus expressing strains compared to the control. The mean specific growth rates of Gus12-2 and Gus12-B were significantly different from the mean specific growth rates of Bam10::cc373 mt+ ($p = 0.003$) at 95% confidence. The calculated mean protein cost for the expression of recombinant gus in under heterotrophic condition was within 15 - 18% fractional reduction in growth rates. The growth of the gus expressing strains in heterotrophic condition was limited by the high protein burden. Protein burden was shown to depend on the environment the proteins are made, such as growth conditions and availability of nutrients (Shachrai et al., 2010, Malakar and Venkatesh, 2012). The autotrophic and mixotrophic conditions represented a more optimal growth conditions than the heterotrophic condition in terms of availability of free and unlimited energy (light) and photosynthetic ability. On the other hand, heterotrophic condition presented more limiting conditions to growth requirements.

No other researchers have published protein cost data for the expression of foreign protein in microalgae. But protein cost data exist for the expression of heterologous protein or the induction of proteins not needed for growth in bacteria. For example, (Novick and Weiner, 1957) demonstrated a 5% protein cost for the expression of *lac* proteins in *E. coli*. Koch (1983), studying the induction of the *lac* proteins in *E. coli*. reported protein cost of 5 – 10%. A protein cost of about 35% was measured by (Shachrai et al., 2010) for green fluorescent protein expressed in *E.coli* during very early exponential phase. More recently, Malakar and Venkatesh (2012) reported a protein cost of 15% for the IPTG induction of *lac* proteins in *E. coli*. Identifying and characterizing the protein cost for the production of recombinant proteins is important for understanding the allowable yield of the protein without cessation of growth. For example, Dong et al. (1995) showed that *E. coli* cells

stops growing when the protein cost becomes prohibitive. This coincides with an expression yield of recombinant proteins of about 30% of the total bacteria cell protein (Dong et al., 1995).

5.8 Cellular ATP concentration of cultures

The cellular ATP concentration may be used as an indicator of the free energy available for growth and cell maintenance. The total cellular ATP concentration of cultures was determined for exponential phase cultures using the ATP bioluminescence assay. The total cellular ATP concentration determined at the three growth conditions is shown in Table 5.10. The highest cellular ATP concentration was observed in autotrophic cultures (0.31 mM) while the lowest was in heterotrophic conditions (0.15 mM). The cellular ATP concentration in mixotrophic cultures was (0.21 mM). The heterotrophic cellular ATP concentration was comparable with the values reported by Rebeille and Gans (1988) for *C. reinhardtii* heterotrophic condition (0.14 - 0.25 mM).

Table 5.10: Total cellular ATP concentration determined for exponential growth phase cultures of Bam10::cc373 mt+ growing in autotrophic, heterotrophic and mixotrophic conditions. The autotrophic and mixotrophic cultures were grown in continuous light conditions at 54 µmol photons/m^2/s. The mean and standard deviation were determined from three biological replicates and two technical replicates each.

	Autotrophic (Mean total cellular ATP ± sd (mM))	Heterotrophic (Mean total cellular ATP ± sd (mM))	Mixotrophic (Mean total cellular ATP ± sd (mM))
Bam10::cc373mt+	0.31 ± 0.03	0.15 ± 0.01	0.21 ± 0.03

The cellular ATP concentration was highest in autotrophic conditions but lowest in heterotrophic condition (Figure 5.12). The difference in mean cellular ATP concentration was significant between autotrophic and heterotrophic ($p = 0.001$), or between autotrophic and mixotrophic conditions conditions ($p = 0.02$) at 95% confidence. Also, there was significant difference in the mean cellular ATP concentration between the mixotrophic and

heterotrophic conditions ($p = 0.02$). The results confirm that heterotrophic condition may be the most-limited condition in terms of energy (ATP concentration).

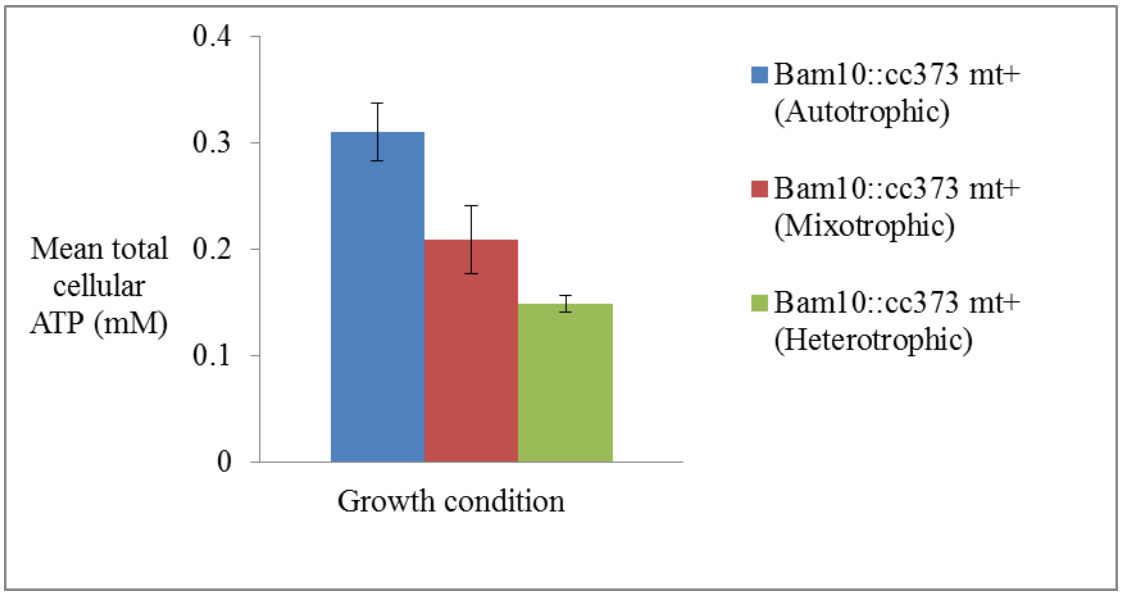

Figure 5.12: Cellular ATP concentrations during exponential growth phase for autotrophic, heterotrophic and mixotrophic cultures. The mean and standard deviation were determined from three biological replicates and two technical replicates each.

The autotrophic and mixotrophic cultures receive unlimited supply of free energy (light) and converted light energy into chemical energy (ATP) photosynthetic phosphorylation of ADP. Besides, the ability to fix CO_2 into sugars, provide intermediates for the biosynthesis of energy storages such as starch and for intermediary metabolisms, the extra incentives for producing cellular materials and growth. Therefore the cellular ATP concentration and the ATP pool may be higher in autotrophic or mixotrophic than in heterotrophic condition. In heterotrophic condition acetate is the only energy source, and the cultures are limited in the amount of the energy (ATP molecules) the cells can generate from the metabolism of acetate. Moreover, acetate may be expected to have some uncoupling effect (Baronofsky et al., 1984) or reduce the transmembrane pH difference, component of the proton motive force. For the heterotrophic culture, the cellular ATP concentration may be expected to be lower.

But mixotrophic cultures have significantly reduced cellular ATP concentrations than autotrophic cultures. Mixotrophic cultures experience the mix of autotrophic growth in light (unlimited free energy) and heterotrophic growth on acetate (the energy limited condition). Cellular ATP concentration is highly regulated (Rebeille and Gans, 1988), but the overall cellular ATP concentration in mixotrophic condition may represent an average balance for autotrophic and heterotrophic growth. Moreover, mixotrophic culture grows more rapidly and produce higher yields of proteins (energy (ATP) demanding processes) than the autotrophic or heterotrophic cultures.

5.9 Total carbohydrate yields in *C. reinhardtii* cultures

The total carbohydrate yield was determined during exponential growth phase for the autotrophic, heterotrophic and mixotrophic cultures. Total carbohydrate was determined using the phenol sulphuric acid assay method with glucose as the standard carbohydrate.

The total carbohydrate yield determined for autotrophic, heterotrophic and mixotrophic conditions are shown in Table 5.11. The total carbohydrate yield varied depending on the growth condition (see Figure 5.13). The total carbohydrate yield was highest in autotrophic condition (20 – 23% of dry cell weight) but lowest in mixotrophic condition (~13% of dry cell weight). There was significant difference in mean total carbohydrate yield between mixotrophic and autotrophic conditions ($p = 0.0000003$), and between mixotrophic and heterotrophic conditions ($p = 0.000002$). There was no significant difference in the mean total carbohydrate yield in autotrophic and heterotrophic conditions. The total carbohydrate yield was significantly reduced in mixotrophic condition because mixotrophic cultures grow very rapidly (at least twice the growth rates of autotrophic or heterotrophic cultures), and the quickly dividing cells require more energy to sustain the growth. Consequently, the cells use up the storage carbohydrate (starch) more rapidly to fuel the energy demands.

Table 5.11: Total carbohydrate yield determined during exponential growth phase of Bam10::cc373 mt+ and Gus12-2 cultures in autotrophic, heterotrophic and mixotrophic conditions. The autotrophic and mixotrophic cultures were grown in continuous light conditions at 54 µmol photons/m2/s. The mean and standard deviation were determined for three biological replicates and two technical replicates each.

	Autotrophic Mean total carbohydrate yield ± sd (mg carbohydrate/g dry weight)	Heterotrophic Mean total carbohydrate yield ± sd (mg carbohydrate/g dry weight)	Mixotrophic Mean total carbohydrate yield ± sd (mg carbohydrate/g dry weight)
Bam10::cc373 mt+	235 ± 17	202 ± 25	129 ± 9
Gus12-2	203 ± 44	178 ± 19	126 ± 1

Importantly, the results confirm that heterotrophic cultures channels acetate metabolism to synthesize sugars and accumulate starch. This may occur through gluconeogenesis pathways via acetyl CoA and oxaloacetate. For example, assimilated acetate may be converted into acetyl CoA in two steps catalysed by acetate kinase and phosphotransacetylase. Genes encoding the two enzymes have been identified in *C. reinhardtii* (Ingram-Smith et al., 2006). Different metabolic routes are available for the acetyl CoA. Acetyl CoA may feed into the glyoxylate cycle (Harris, 1989) consisting of a sequence of anaplerotic reactions to generate a molecule of succinate as a net product from two molecules of acetate. Unique enzymes isocitrate lyase (Bedhomme et al., 2009) and malate synthase (Nogales et al., 2004) for the operation of the glyoxylate cycle have now been identified in *C. reinhardtii*. The net succinate produced may enter the TCA cycle and be converted through series of reactions to oxaloacetate. Some oxaloacetate may be decarboxylated in the cytosol to form phosphoenolpyruvate, which may enter the gluconeogenesis pathway to form sugar phosphates and eventually through further conversions into storage compounds like starch. Acetyl CoA may also feed directly into

the TCA cycle for ATP generation and generation of reducing equivalents (NADH, $FADH_2$) for biosynthesis of other intermediary metabolites

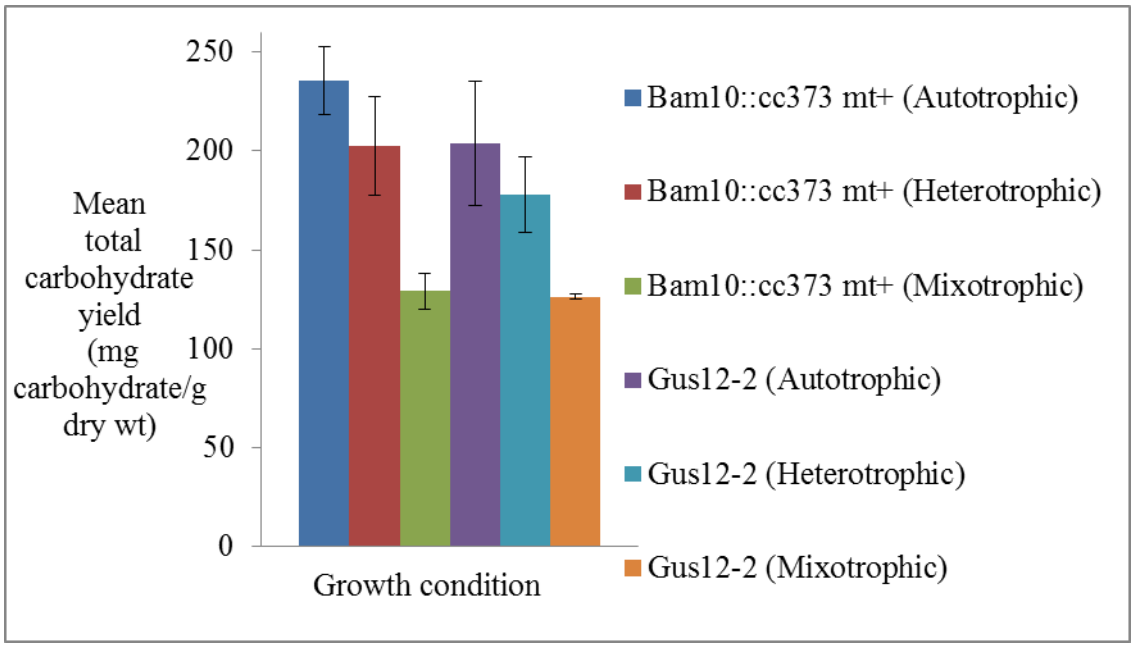

Figure 5.13: Total carbohydrate yield during exponential growth phase of Bam10::cc373 mt+ and Gus12-2 cultures grown under autotrophic, heterotrophic and mixotrophic conditions. The mean and standard deviations were determined for three biological and two technical replicates each.

Total carbohydrate yields in Table 5.11 were compared with values reported for *C. reinhardtii* and other microalgae. On the basis of dry cell weight, Becker (2007) reported total carbohydrate yield in *Chlorella vulgaris* (12-17%), *Chlorella pyrenoidosa* (26%), Spirogyra sp. (33 – 64%), *Dunaliella salina* (32%), and *Chlamydomonas reinhardtii* (17%). Total carbohydrate yield of 9% dry cell weight was determined for *C. reinhardtii* (Kightlinger et al., 2014). Between 38 - 50 % was reported for *C. reinhardtii* by Boyle and Morgan (2009). In addition, total carbohydrate of many microalgae species were shown by Becker (2007) and Brown (1991) to vary widely from 5 – 64% of dry cell weight. The total carbohydrate yield in the current study varied depending on the growth condition, and the results are consistent with those observed for *C. reinhardtii.*

5.9 Summary

In this work, recombinant gus expression in the chloroplast transformed *C. reinhardtii* strains (Gus12-2 and Gus12-B) was detected by enzymatic assays. An important finding in this work was the different dependence of cell sizes on the growth conditions. The exponential growth phase cultures in heterotrophic condition exhibited relatively larger cell sizes than those of autotrophic and mixotrophic conditions. Consequently, cells in heterotrophic cultures were heavier (on the basis of dry cell weight) than cells in autotrophic and mixotrophic cultures.

The estimated carbon fluxes for exponential phase was lowest in heterotrophic cultures (~ 3 mmole carbon/ g dry cell weight) as compared to mixotrophic and autotrophic cultures (~10 – 11 mmole carbon/g dry cell weight). The condition limited most for growth and protein production was the heterotrophic condition. Heterotrophic cultures were observed with a relatively lower gus yields and lower total protein yields than the autotrophic or mixotrophic cultures. Gus productivity and total protein productivity was significantly reduced in heterotrophic condition than in autotrophic or mixtotrophic conditions. At least a 2-fold increase in productivity was observed in mixotrophic cultures compared to autotrophic cultures. This indicated that the mixotrophic cultures may be more optimized for protein production than autotrophic cultures. Depletion in ammonium concentration during growth limited growth of cultures.

The protein burden for the expression of recombinant gus was determined in the three growth conditions. Autotrophic and mixotrophic conditions have no detectable protein cost on recombinant gus expression, whereas the protein burden for heterotrophic cultures was significant (15 – 18%). The results further confirm that the heterotrophic condition was the most limiting for recombinant gus expression. Since no protein data exist for microalgae, this finding is significant and may serve as a reference for future work on protein cost determinations. Protein cost analysis may be useful for example, to identify the limiting growth conditions for expression of different recombinant protein in the microalgae. The analysis may be developed further to identify the allowable yield of recombinant protein without cessation of cell growth under different conditions.

Furthermore, the comparison of cellular ATP concentrations, suggests that the heterotrophic condition as the most energy-limited condition.

Chapter 6 – Modelling: Results and Discussion

In chapters 4 and 5, the heterotrophic condition was identified as a condition in which both the growth of cultures and recombinant protein yield were reduced. The heterotrophic cultures were limited by insufficient supply of carbon, rise in pH, lack of light, energy (low ATP concentrations), and high protein cost. In chapter 4, strategies that addressed and reduced such limitations were identified, enabling the heterotrophic cultures to achieve optimal growth yield comparable to cultures grown in autotrophic and mixotrophic conditions. In chapter 5, the photosynthetic cultures were shown to represent an optimum for growth and protein production since these cells are able to convert light energy into chemical energy that can be utilized in the various metabolic operations of growth and cell maintenance. An over-riding strategy to optimize recombinant protein production in *C. reinhardtii* would be one that increased the cell density (so that a higher number of cells expressed the target protein), and also increased the yield of the target protein in each cell. In chapter 4, for example, a strategy that significantly improved the cell density achieved and productivity of heterotrophic cultures was provided. Here, by supplying cultures with acetate containing medium and adequate buffering of cultures in a series of fed-batch operations (to alleviate carbon, energy depletion and rising pH limitations), the heterotrophic growth yields were increased more than 3 folds.

In this Chapter 6, FBA modelling will be used to study steady-state fluxes that should be possible and optimal in the *C. reinhardtii* metabolic model (AgaGEM), and indeed to identify a flux pattern that maximizes gus production in the three conditions. Since at steady state, there was no net accumulation of metabolites in the network, the FBA will be used to obtain the description of gus yields from the stoichiometric matrix and steady state fluxes in the network. Since the heterotrophic condition was identified as the most-limiting condition for gus production, FBA methods were used to identify the fluxes that limit the heterotrophic gus yields in the network. Based on the modelling analysis, *in silico* strategy was implemented to overcome such metabolic limitations and improve the gus yields. The strategy was identified through FBA modelling, experimental verification and model improvement. The *in silico* outcome (strategy) was tested experimentally.

6.1 Flux balance analysis of gus production and calculation of yield.

The FBA simulation of gus production was performed for the heterotrophic, autotrophic and mixotrophic growth conditions. The FBA methods used in the simulations were described in method sections 3.14. The nitrogen source was ammonia (refer to Table 3.3). FBA was used to find an optimal steady state flux distribution (an optimal solution) that maximizes gus production under the given set of FBA constraints. The optimal steady-state flux that maximize gus production under heterotrophic, autotrophic and mixotrophic conditions are presented in Table 6.1a. Based on this optimal steady-state flux distribution for gus production and the total carbon flux through the network, the gus yield, was calculated using equation 6.1:

$$Y_{Protein} = \left(\frac{Predicted\ \ optimal\ \ flux\ \ for\ \max imal\ \ gus\ \ production}{Total\ \ carbon\ \ flux} \right) \qquad (6.1)$$

Here, $Y_{Protein}$ is the gus yield (mmole gus/mmole carbon). The numerator in equation 6.1 is the FBA predicted optimal flux for maximal gus production (mmole gus/g dry wt/h), and the denominator is the total uptake flux of carbon containing nutrients (mmole carbon substrate/g dry wt/ h). The carbon substrate was acetate in heterotrophic condition; CO_2 in autotrophic condition; and acetate and CO_2 in mixotrophic condition. The predicted gus yield was also expressed in terms of carbon yield of gus on the substrate (number of moles of carbon in gus per number of moles of carbon in substrate) using of equation 6.2:

$$Y_C = Y_{Protein} * \left(\frac{number\ of\ moles\ of\ \ carbon\ in\ gus\ protein}{number\ of\ moles\ \ of\ carbon\ in\ substrate} \right) \qquad (6.2)$$

Where Y_C is the carbon yield of gus on the substrate (g carbon in gus /g total carbon). Gus is a 68 kDa protein containing 603 amino acid residues (Jefferson et al., 1986). There are 3068 carbon atoms per mole of gus protein (Table 6.3b, and Table A3.1 (Appendix III)). The FBA predicted gus yield obtained in the simulation of heterotrophic, autotrophic and mixotrophic growth conditions are presented in Table 6.1b. The FBA gus yield was lowest in heterotrophic and highest in mixotrophic condition. The FBA predictions were consistent in relative terms with the experiments for the three growth conditions. However, the experimental yields were much lower than the ones predicted by FBA.

Table 6.1a: Predicted optimal steady-state flux for maximal gus production in heterotrophic, autotrophic and mixotrophic FBA simulations.

Condition	Carbon substrate	Total carbon flux through network (mmole carbon/g dry wt/h)	FBA optimal steady-state flux for maximal gus production (mmole gus /g dry wt/h) x 10^{-4}
Heterotrophic	Acetate	3.4	5
Autotrophic	CO_2	11	19
Mixotrophic	Acetate and CO_2	10	23

Table 6.1b: FBA predicted gus yield and experimental gus yield. The mean values of experimentally measured gus yield and standard deviation (with units of g gus protein/g dry cell wt) were determined from six biological replicates and two technical replicates each from Gus12-2 in heterotrophic, autotrophic and mixotrophic conditions. The experimental gus yield values were converted into units of g carbon in gus/g total carbon (Table A3.3 on Appendix III) for comparison with the FBA predicted gus yield.

Condition	FBA yield (g carbon in gus/g total carbon)	Mean Experimental yield ± sd (g gus protein/g dry cell wt) x 10^{-4}	Mean Experimental yield ± sd (g carbon in gus/g total carbon) x 10^{-4}
Heterotrophic	0.451	2.66 ± 0.45	2.10 ± 0.36
Autotrophic	0.530	3.20 ± 0.69	2.53 ± 0.55
Mixotrophic	0.700	3.75 ± 0.71	2.96 ± 0.56

6.2 Analysis of steady-state fluxes for protein production in heterotrophic condition.

Since the FBA predicted gus yields were reproducible and provided in relative terms, an approximate description of gus yields in the three conditions, further analysis was applied to identify the steady-state fluxes for maximal protein yield in the network. The amino acid composition of algae biomass, and the abundance of amino acid residues in gus are presented in Table 6.2a.

The amino acid compositions of algae dry biomass (Boyd, 1973) is shown in Table 6.2a. The data for three amino acids (tryptophan, asparagine and glutamine) in the algae biomass were not provided. Other sources for amino acid composition of algae biomass have incomplete data for most of the naturally 20 amino acids (Brown, 1991, Samek et al., 2013). The reason for this was that these authors could not determine some amino of the acids, however the report by Boyd (1973) provided determination for 17 amino acids from 16 fresh water algae species. Table 6.2a also include the abundance of amino acids (number of residues) in the gus protein (Jefferson et al., 1986). From this we find that amino acids such as valine, glycine, alanine, leucine, aspartate and glutamate are very abundance in gus. Compared with the amino acid composition in algae biomass, similar trend was observed i.e. glutamate, aspartate, alanine and leucine having higher concentration in algae biomass.

In a simple representation, protein production reactions (translation) involved the incorporation of the 20 amino acids to form the protein (equation 3.30). The translation process would require the 20 amino acids, energy (GTP) and tRNAs in the model. The products of the protein synthesis reaction are the gus, GDP, Pi and free tRNAs. Since translation is the hierarchical level where the major regulation occurs for the protein yield in *C. reinhardtii* (Eberhard et al., 2002, Rochaix, 1996), the total amino acid steady-state fluxes were analysed.

In the model, the predicted total steady-state flux of each amino acid is given by the summation of two combinations (amino acid flux diverted towards gus production, and the amino acid flux diverted towards other metabolic processes i.e. biomass formation).

Table 6.2a. Amino acids composition in algae dry biomass and in recombinant gus.

Amino acid	Amino acid composition of algae dry Biomass (Boyd, 1973) (g amino acid/100 g total protein)	No. of amino acids in gus sequence (Jefferson et al., 1986)
Asparagine	-	28
Tryptophan	-	19
Glutamine	-	32
Cysteine	0.93	9
Methionine	1.8	13
Histidine	2.06	19
Tyrosine	3.78	24
Proline	4.36	24
Isoleucine	4.54	29
Phenylalanine	4.85	25
Threonine	4.96	35
Serine	4.96	25
Valine	5.82	53
Glycine	6.05	46
Arginine	6.18	29
Lysine	6.97	27
Leucine	8.56	40
Alanine	8.66	46
Aspartate	12.18	40
Glutamate	13.34	40
TOTAL		***603 residues***

The amino acid steady-state fluxes for biomass formation and for gus production in the FBA simulation of heterotrophic condition are presented in Table 6.2b. Comparisons of fluxes in Table 6.2b shows that the amount of amino acids used for gus production (0.5 x 10^{-3} mmoles amino acids/g dry weight/h) was far lower than the amount used for biomass formation (50.9 x 10^{-3} mmoles amino acids/g dry weight/h).

Table 6.2b: Predicted amino acid steady-state fluxes in heterotrophic condition.

	Fixed heterotrophic growth flux (0.02446 h^{-1})	
Amino acids	Steady-state flux for biomass formation (mmole amino acid/g dry wt/h) x 10^{-6}	Steady-state flux for gus (mmole amino acid/g dry wt/h) x 10^{-6}
Glutamate	3376.451	33.1675
Alanine	3882.919	38.1426
Aspartate	3376.451	33.1675
Glycine	3882.919	38.1426
Serine	2110.282	20.7297
Threonine	2954.395	29.0216
Methionine	1097.347	10.7794
Cysteine	759.701	7.46269
Valine	4473.798	43.9469
Leucine	3376.451	33.1675
Isoleucine	2447.927	24.0464
Glutamine	2701.161	26.534
Arginine	2447.927	24.0464
Proline	2025.871	19.9005
Lysine	2279.104	22.3881
Histidine	1603.814	15.7546
Phenylalanine	2110.282	20.7297
Tyrosine	2025.871	19.9005
Tryptophan	1603.814	15.7546
Asparagine	2363.516	23.2172
TOTAL	**50900**	**500**

The steady-state flux value of 0.5 x 10^{-3} mmoles amino acids/g dry was obtained through FBA to maximize gus yield under the set of experimental constraints. High total steady state fluxes were observed for valine, alanine, glycine, leucine, valine and glutamate. Low total steady state fluxes were found with cysteine, methionine, histidine and tryptophan.

The value of the total steady-state fluxes mirrors the abundance of the different amino acids in the gus protein (Table 6.2a).

6.3 Identification of limiting amino acid for gus production.

In order to identify the limiting amino acids in the heterotrophic condition, FBA was run to compare the flux distributions associated with the synthesis of two highly differentially expressed endogenous protein of *C. reinhardtii*. In particular, separate FBA simulations were performed to maximize the production of ribulose-1, 5-bisphosphate carboxylase/oxygenase (rubisco) on the one hand, and ferroxidase on the other hand. Rubisco is a highly expressed protein in plants and algae (Ellis, 1979), while ferroxidase is one of the low expressed endogenous protein in *C. reinhardtii* (Hsieh et al., 2013). The amino acid sequence in gus, rubisco and ferroxidase are shown in Figures 6.1, 6.2 and 6.3 respectively. The abundance of the 20 amino acids in each of the proteins is shown in Table 6.3b.

MLRPVETPTREIKKLDGLWAFSLDRENCGIDQRWWESALQESRAIAVPGSFNDQFAD
ADIRNYAGNVWYQREVFIPKGWAGQRIVLRFDAVTHYGKVWVNNQEVMEHQGGY
TPFEADVTPYVIAGKSVRITVCVNNELNWQTIPPGMVITDENGKKKQSYFHDFFNYA
GIHRSVMLYTTPNTWVDDITVVTHVAQDCNHASVDWQVVANGDVSVELRDADQQ
VVATGQGTSGTLQVVNPHLWQPGEGYLYELCVTAKSQTECDIYPLRVGIRSVAVKG
EQFLINHKPFYFTGFGRHEDADLRGKGFDNVLMVHDHALMDWIGANSYRTSHYPY
AEEMLDWADEHGIVVIDETAAVGFNLSLGIGFEAGNKPKELYSEEAVNGETQQAHL
QAIKELIARDKNHPSVVMWSIANEPDTRPQGAREYFAPLAEATRKLDPTRPITCVNV
MFCDAHTDTISDLFDVLCLNRYYGWYVQSGDLETAEKVLEKELLAWQEKLHQPIIIT
EYGVDTLAGLHSMYTDMWSEEYQCAWLDMYHRVFDRVSAVVGEQVWNFADFAT
SQGILRVGGNKKGIFTRDRKPKSAAFLLQKRWTGMNFGEKPQQGGKQ

Figure 6.1: Amino acid sequence of gus (Jefferson et al., 1986).

MVPQTETKAGAGFKAGVKDYRLTYYTPDYVVRDTDILAAFRMTPQLGVPPEECGA
AVAAESSTGTWTTVWTDGLTSLDRYKGRCYDIEPVPGEDNQYIAYVAYPIDLFEEGS
VTNMFTSIVGNVFGFKALRALRLEDLRIPPAYVKTFVGPPHGIQVERDKLNKYGRGL
LGCTIKPKLGLSAKNYGRAVYECLRGGLDFTKDDENVNSQPFMRWRDRFLFVAEAI
YKAQAETGEVKGHYLNATAGTCEEMMKRAVCAKELGVPIIMHDYLTGGFTANTSL
AIYCRDNGLLLHIHRAMHAVIDRQRNHGIHFRVLAKALRMSGGDHLHSGTVVGKLE
GEREVTLGFVDLMRDDYVEKDRSRGIYFTQDWCSMPGVMPVASGGIHVWHMPALV
EIFGDDACLQFGGGTLGHPWGNAPGAAANRVALEACTQARNEGRDLAREGGDVIRS
ACKWSPELAAACEVWKEIKFEFDTIDKL

Figure 6.2: Amino acid sequence of ribulose-1,5-bisphosphate carboxylase/oxygenase large subunit of chloroplast (Maul et al., 2002, Taylor et al., 2001).

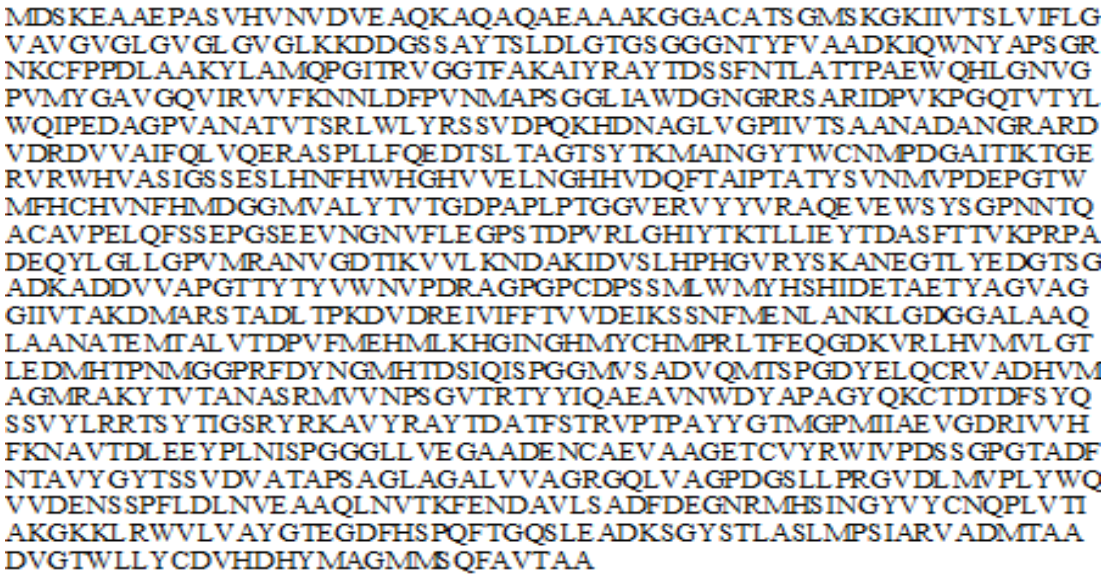

Figure 6.3: Amino acid sequence of *C. reinhardtiii* ferroxidase (La Fontaine et al., 2002).

The distribution of the amino acid total steady-states fluxes predicted by FBA for gus, rubisco and ferroxidase production is presented on Table 6.3a. Here, each amino acid total steady-state flux is the combined sum of the flux going for biomass formation, and flux for protein production. These steady-state fluxes are the result of the FBA simulations (calculation of steady state fluxes). The FBA was used to simulate maximized protein production at fixed growth. The abundance of amino acid residues in the protein sequences for gus, rubisco and ferroxidase is shown in Table 6.3b. The amino acid list in Table 6.3a show that some amino acids are required at high total steady state flux rates and some at low total steady-state flux rates in the network. In the three proteins of our example, high total steady-state fluxes were observed for alanine, glycine, and valine. These were the most abundant amino acids in the three proteins. Low required steady-states fluxes were found for example for cysteine, methionine, histidine and tryptophan. These were the least abundant in the proteins. Therefore, there were observable trends in gus, rubisco and ferroxidase production. Analyses of the steady state fluxes in the network was used for identifying the amino acids which carry low steady state fluxes (limiting amino acids) and those that carry high steady state fluxes in the network.

Table 6.3a: Total amino acid steady-state fluxes predicted through FBA under heterotrophic condition.

Gus model		**Rubisco model**		**Ferroxidase model**	
Amino acids	Amino acid total steady-state flux (mmole/g dry wt/h) x 10^{-6}	**Amino acids**	Amino acid total steady-state flux (mmole/g dry wt/h) x 10^{-6}	**Amino acids**	Amino acid total steady-state flux (mmole/g dry wt/h) x 10^{-6}
Cysteine	767.164	Tryptophan	869.052	Cysteine	582.837
Methionine	1108.126	Cysteine	1086.315	Tryptophan	762.171
Histidine	1619.568	Glutamine	1086.315	Histidine	1389.842
Tryptophan	1619.568	Methionine	1412.210	Phenylalanine	1434.676
Proline	2045.771	Histidine	1412.210	Glutamine	1479.509
Tyrosine	2045.771	Asparagine	1520.842	Lysine	1703.677
Serine	2131.011	Serine	1629.473	Methionine	1748.511
Phenylalanine	2131.011	Phenylalanine	2064	Isoleucine	1838.178
Lysine	2301.492	Tyrosine	2064	Arginine	1972.679
Asparagine	2386.733	Proline	2172.631	Glutamate	2152.014
Isoleucine	2471.973	Isoleucine	2281.263	Asparagine	2196.847
Arginine	2471.973	Lysine	2933.052	Tyrosine	2331.348
Glutamine	2727.694	Threonine	3150.315	Proline	2734.851
Threonine	2983.416	Glutamate	3258.947	Serine	3228.021
Glutamate	3409.618	Aspartate	3258.947	Leucine	3272.854
Aspartate	3409.618	Arginine	3367.578	Aspartate	3317.688
Leucine	3409.618	Valine	3802.105	Threonine	3766.024
Alanine	3921.061	Leucine	4019	Glycine	4886.865
Glycine	3921.061	Alanine	4888.421	Valine	5021.366
Valine	4517.744	Glycine	5322.947	Alanine	5380.035
TOTAL	**51400**	***TOTAL***	**51600**	***TOTAL***	**51200**

Table 6.3b: Abundance of amino acid residues in recombinant gus (Jefferson et al., 1986), endogenous rubisco (Maul et al., 2002, Taylor et al., 2001), and ferroxidase (La Fontaine et al., 2002) in *C. reinhardtii*.

Amino Acid	**Letter**	**Number of amino acid residues in gus**	**Number of amino acid residues in rubisco (*C. reinhardtii*)**	**Number of amino acid residues in ferroxidase (*C. reinhardtii*)**
Alanine	A	46	45	120
Arginine	R	29	31	44
Asparagine	N	28	14	49
Aspartate	D	40	30	74
Cysteine	C	9	10	13
Glutamine	Q	32	10	33
Glutamate	E	40	30	48
Glycine	G	46	49	109
Histidine	H	19	13	31
Isoleucine	I	29	21	41
Leucine	L	40	37	73
Lysine	K	27	27	38
Methionine	M	13	13	39
Phenylalanine	F	25	19	32
Proline	P	24	20	61
Serine	S	25	15	72
Threonine	T	35	29	84
Tryptophan	W	19	8	17
Tyrosine	Y	24	19	52
Valine	V	53	35	112
TOTAL	**20**	**603 residues**	**475 residues**	**1142 residues**

In order to identify the amino acids on Table 6.3a that can be considered limiting the protein production, a flux threshold value of α = 0.003mmoles amino acid/g dry wt/h was introduced. Amino acid with a total steady-state flux less than α was considered limiting, while amino acids with a total steady-state flux greater than α were considered non-limiting limiting. Based on this criterion, 14 amino acids were identified limiting for gus, 13 for ferroxidase, and 12 for rubisco production. The 14 putative limiting amino acids for gus production were cysteine, methionine, histidine, tryptophan, proline, tyrosine, serine, phenylalanine, lysine, asparagine, isoleucine, arginine, glutamine and threonine.

6.4 FBA predictions for increased gus yields

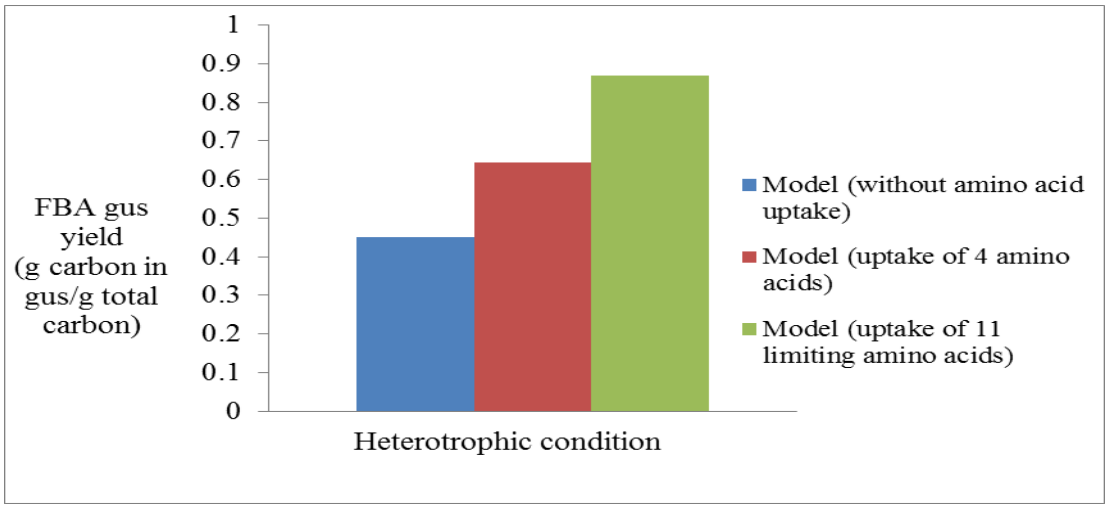

Figure 6.4: FBA predicted gus yield in heterotrophic condition for: (1) Model without amino acid uptake; (2) Model with uptake of 4 amino acids (arginine, leucine, proline, glutamine); (3) Model with uptake of 11 limiting amino acids (cysteine, histidine, tryptophan, tyrosine, serine, phenylalanine, lysine, asparagine, isoleucine, glutamine and threonine). In the model simulation without amino acid uptake, ammonium uptake was source of nitrogen. In the model simulation of uptake of 4 amino acids, or 11 putative limiting amino acids, ammonium and amino acids serve as nitrogen source.

Based on the identification of putative limiting amino acids for gus production, a new FBA simulation was performed this time allowing the uptake of such amino acids (cysteine, histidine, tryptophan, proline, tyrosine, serine, phenylalanine, lysine, asparagines,

isoleucine and arginine) from the *in silico* medium. In previous works, only four amino acids were reported to be taken up from the growth media by *C. reinhardtii*: arginine (Kirk and Kirk, 1978a, Kirk and Kirk, 1978b), leucine (Loppes, 1969), proline (Reynoso and Degamboa, 1982) and glutamine (Cain, 1965). Another FBA simulation was then performed based on these experimental findings where only arginine, leucine, proline and glutamine were allowed to enter the system. The allowed uptake rate was set to 0.03 mmoles/g dry wt/h for each of amino acid in the two FBA simulations. The predicted gus yields with 11 and 4 amino acids allowed to enter the system are shown in Figure 6.4. The results were compared with the predicted yield when no amino acid was taken from the *in silico* medium. The uptake of the 11 limiting amino acids from the medium resulted in a 1.9 fold increase in the predicted gus yield. Also, the supply of 4 amino acids increased FBA yield by ~1.4 fold.

6.5 Verification of FBA predictions of increased gus yields

To verify the FBA predictions, whether or not that recombinant gus yield in heterotrophic cultures can be significantly increased by exogenous supply of the 11 limiting amino acids, or the four amino acids (arginine, leucine, proline and glutamine), new sets of heterotrophic growth experiments were designed. In one set of such experiments, the Gus12-2 strain was grown in TAP medium supplemented with the 11 limiting amino acids (cysteine, histidine, tryptophan, tyrosine, serine, phenylalanine, lysine, asparagine, isoleucine, glutamine and threonine) each at 1 mM concentration. In a second set of growth experiments, the Gus12-2 strain was grown in TAP medium supplemented with arginine, proline, leucine and glutamine (each amino acid at 1 mM concentration). In a third set of experiments, the Gus12-2 strain was grown in TAP medium supplemented with 4 mM α-ketoglutarate (since α-ketoglutarate is a precursor for amino acids in cells). In a final set of growth experiments that served as the control, the Gus12-2 strain was grown in TAP medium. The heterotrophic growth curves are presented in Figure 6.5.

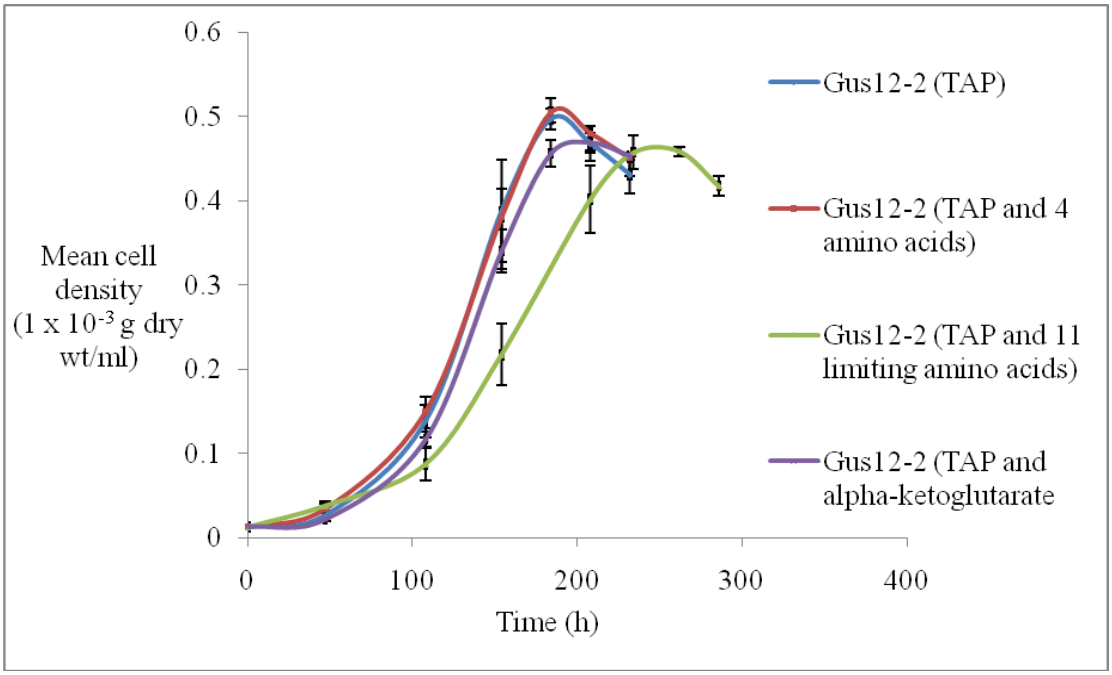

Figure 6.5: Heterorophic growth of Gus12-2 cultures: in TAP; in TAP supplemented with four amino acids (arginine, proline, leucine and glutamine each at 1 mM); in TAP supplemented with 11 limiting amino acids (cysteine, histidine, tryptophan, tyrosine, serine, phenylalanine, lysine, asparagine, isoleucine, glutamine and threonine each at 1 mM); and in TAP supplemented with 4 mM α-ketoglutarate. The mean cell density was determined from three biological and two technical replicates each.

The recombinant gus yields were measured in each set of experiments and the results are presented in Figure 6.6a (in units of g gus/g dry cell wt) and in Figure 6.6b (in units of g carbon in gus/g total carbon). On the basis of percentage dry cell weight, the experimentally determined gus yields were: (~0.09%) for the strains grown in TAP; (~0.12%) for strains grown in TAP supplemented with 4 amino acids; (~0.18%) for strains grown in TAP supplemented with 11 limiting amino acids; and (~0.13%) for strains grown in TAP supplemented with α-ketoglutarate. The growth experiments results verified the FBA predictions. A significant 1.35 fold increase in gus yield was observed when arginine, leucine, proline and glutamine were supplied to the heterotrophic cultures. An even higher 2.0 fold increase was observed when the 11 putative limiting amino acids were supplied. In the heterotrophic cultures supplemented with α-ketoglutarate, a 1.56 fold increase in recombinant gus yield was observed.

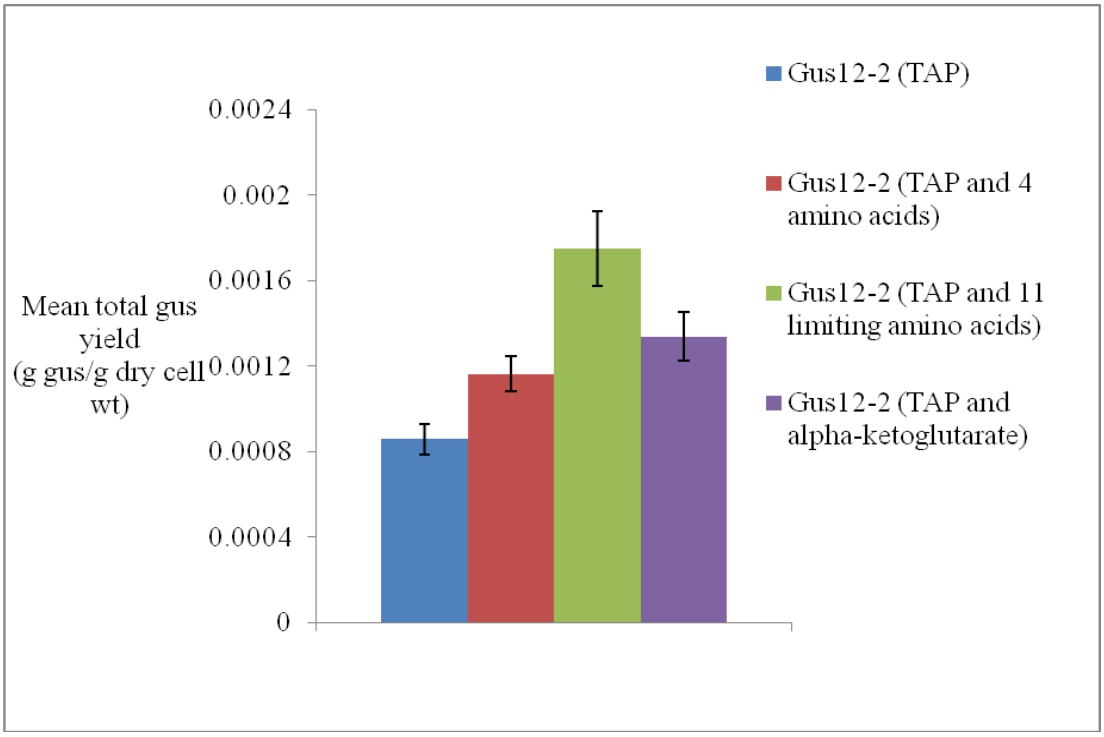

Figure 6.6a: Total gus yield (g gus/g dry cell wt) during exponential growth phase determined for heterotrophic Gus12-2 cultures grown: in TAP (control); in TAP containing four amino acids (arginine, proline, leucine and glutamine); in TAP supplemented with 11 limiting amino acids (cysteine, histidine, tryptophan, tyrosine, serine, phenylalanine, lysine, asparagine, isoleucine, glutamine and threonine); and in TAP containing α-ketoglutarate. The mean and standard deviation were determined from three biological and 2 technical replicates each.

The results highlighted amino acid limitation as a metabolic bottleneck for the recombinant gus production. The identification for example, of the limiting amino acid steady state fluxes was used to inform the design of the growth strategy that increased the gus yield. But important still, would be to identify the effects of individual amino acid uptake to the FBA gus yield. This is discussed in the next sections.

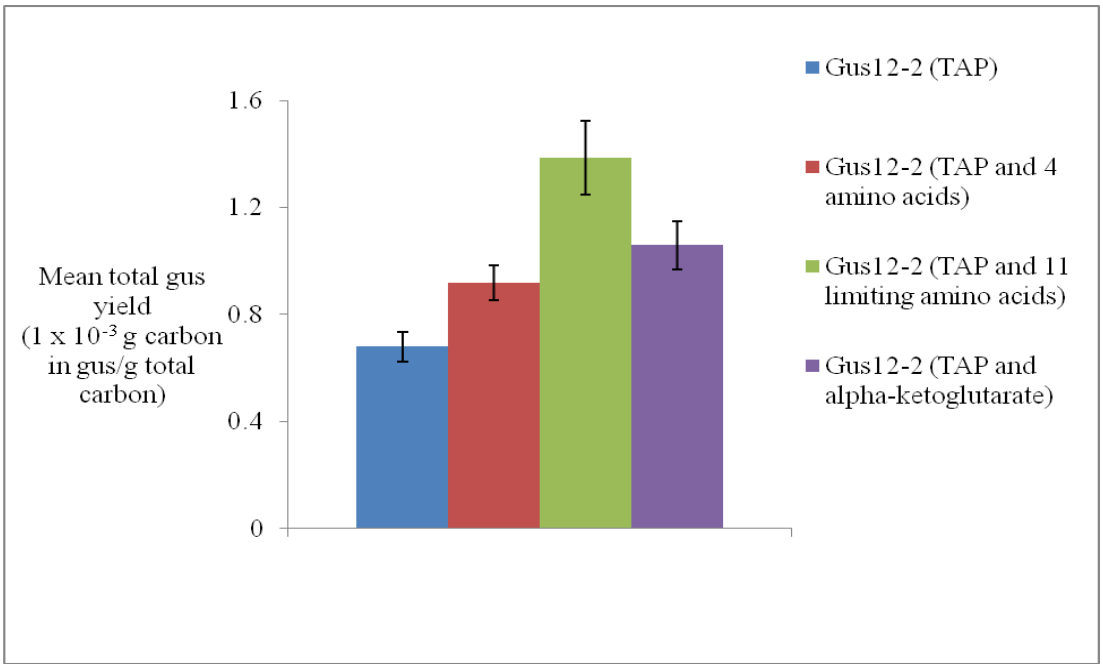

Figure 6.6b: Total gus yield (g carbon in gus/g total carbon) during exponential growth phase determined for heterotrophic Gus12-2 cultures grown: in TAP (control); in TAP containing four amino acids (arginine, proline, leucine and glutamine); in TAP supplemented with 11 limiting amino acids (cysteine, histidine, tryptophan, tyrosine, serine, phenylalanine, lysine, asparagine, isoleucine, glutamine and threonine); and in TAP containing α-ketoglutarate. The mean and standard deviation were determined from three biological and 2 technical replicates each.

6.6 Effect of amino acid uptake on gus yield

In this work, FBA was used to simulate the effect of adding individual amino acid uptake from the *in silico* medium. The FBA simulations were performed for gus production and rubisco production in heterotrophic condition. In this investigation, three sets of FBA simulations were performed. In the first set which we shall call FBA control, the FBA simulations of protein yield was performed with ammonium as the only nitrogen source. In the second set of FBA simulation (model II), the effect of the uptake of individual amino acid and ammonium uptake on protein yield was simulated. Here, the amino acid and ammonia serve as nitrogen sources. In the third set of FBA (model III), the effect of the uptake of individual amino acid without ammonia on the protein yield was simulated. In this case the amino acid was the only nitrogen source.

Table 6.4: FBA predicted gus yield for model II with ammonium and amino acid uptake; and model III with uptake of amino acid without ammonium. The fold change was calculated by dividing the gus yield in the model II or model III by gus yield of the FBA control.

Amino acids	Model (II) With uptake of ammonia and individual amino acid (g carbon in gus/g total carbon)	Fold Change	Model (III) with uptake of individual amino acid (g carbon in gus/g total carbon)	Fold change
Cysteine	0.463	1.027	0	0
Glycine	0.468	1.038	0	0
Histidine	0.472	1.048	0	0
Methionine	0.473	1.048	0	0
Serine	0.477	1.057	0	0
Alanine	0.479	1.062	0	0
Aspartate	0.481	1.066	0	0
Asparagine	0.483	1.070	0.0015	0.003
Lysine	0.484	1.073	0	0
Threonine	0.485	1.075	0	0
Isoleucine	0.489	1.083	0	0
Glutamate	0.492	1.090	0	0
Tryptophan	0.493	1.091	0	0
Tyrosine	0.493	1.093	0	0
Glutamine	0.494	1.094	0.0015	0.003
Proline	0.499	1.107	0	0
Valine	0.501	1.111	0	0
Arginine	0.502	1.113	0.0664	0.147
Leucine	0.506	1.123	0	0
Phenylalanine	0.544	1.206	0	0

The predicted yields of gus for the three FBA simulations were compared in Table 6.4. In the FBA control, the predicted yield of gus was 0.451 g carbon in gus/g total carbon (see Table 6.1b). The predicted gus yield for model II and model III are displayed in Table 6.4. The FBA gus yields (Table 6.4) of model II show that the uptake of ammonium and individual amino acid increased the protein yield, than if only ammonium was taken up (as in the FBA control).

The uptake of each individual amino acid in model II resulted in an increase in gus yield. The increase was reported as a fold change (ratio of gus yields in model II to gus yield in the control). The protein production is a lumped reaction that drains or place demand on amino acids. Some amino acids are made from ammonium, and if taken up with ammonium, this may further increase protein yield. Depending on the individual amino acid taken up, there could be between 1.027 – 1.206 fold changes (or 2.7 – 20.6% increase in gus yields). In the simulations, growth was kept fixed and protein production maximized. This way, the effect of adding an amino acid on gus yield was identified. For instance on Table 6.4, the effect of the uptake of each of the 20 amino acids with ammonium on the FBA gus yield (fold change) are listed. The combined effect of the 11 limiting amino acid on gus yield, would be a summation of the effect of each of the 11 amino acids. So if the 11 effects on the FBA gus yield from the 11 limiting amino acids are added up, this resulted in ~1.9 fold change (90% increase) in gus yield. Similarly, the combined effect of arginine, leucine, proline and glutamate uptake would be ~1.44 fold change (44% increase in FBA gus yield). In Table 6.4, we find that uptake of phenylalanine provide the highest increase in FBA gus yield (~21%) while the uptake of cysteine contribute the least increase to FBA gus yield (2.7%). Phenylalanine would be a better candidate to improve gus yield than cysteine.

Similarly, comparison of protein yields were performed for the FBA simulation of rubisco production and the results are presented in Table 6.5. The rubisco yield for the FBA control was 0.454 g carbon in rubisco/g total carbon uptake. In Table 6.5, the effect of individual uptake of 20 amino acids for model II is shown. The results on Table 6.4 and 6.5 are consistent and similar. For example, the uptake of phenylalanine produced the highest increase in the FBA yield of the proteins (~21% and ~19% respectively to gus and rubisco). In addition, we find that the uptake of amino acids that are very abundant in the protein sequences (e.g. valine, leucine) also significantly increased the FBA yields (10% and 12.5% respectively for rubisco; ~11% and 12% for gus). However, uptake of amino acids such as cysteine, histidine, methionine which are less abundant in rubisco or gus protein resulted in low increase in the FBA yield (see Tables 6.3b, 6.4, and 6.5).

Table 6.5: FBA predicted rubisco yield for model (II) with ammonium and amino acid uptake; and model (III) with uptake of amino acid without ammonium. The fold change was calculated by dividing the gus yield in the model II or model III by gus yield of the FBA control.

Amino acids	Model (II) With uptake of ammonia and individual amino acid (g carbon in rubisco/g total carbon)	Fold Change	Model (III) with uptake of individual amino acid (g carbon in rubisco/g total carbon)	Fold change
Cysteine	0.465	1.023	0	0
Glycine	0.467	1.027	0	0
Histidine	0.469	1.033	0	0
Tryptophan	0.474	1.043	0	0
Serine	0.476	1.047	0	0
Alanine	0.478	1.052	0	0
Methionine	0.478	1.053	0	0
Aspartate	0.479	1.055	0	0
Asparagine	0.480	1.058	00.0014	0.003
Threonine	0.483	1.064	0	0
Isoleucine	0.485	1.068	0	0
Glutamate	0.490	1.079	0	0
Lysine	0.491	1.082	0	0
Glutamine	0.492	1.083	0.0014	0.003
Tyrosine	0.493	1.085	0	0
Proline	0.498	1.095	0	0
Valine	0.500	1.100	0	0
Arginine	0.504	1.108	0.0646	0.142
Leucine	0.511	1.125	0	0
Phenylalanine	0.543	1.194	0	0

Factor that determined the effect of the uptake of an amino acid on the FBA yield may also depend on the number of carbon atoms contributed by the amino acid to the FBA carbon yield of a protein. The higher the total carbon atoms contributed, the higher will be the FBA yield. For example, phenylalanine has 25 residues in gus sequence (see Table 6.3b)

and each residue has 9 carbon atoms. A total number of 225 carbon atoms are contributed by phenylalanine in gus protein (see Table A3.1, Appendix section). Therefore, the uptake of phenylalanine resulted in a higher increase to FBA gus yield compared to glycine (92 carbon atoms), alanine (138 carbon atoms) or aspartate (160 carbon atoms).

The results underlined the importance of identifying the specific effect of an amino acid uptake on the FBA protein yield. Identification and understanding the effect of each amino acid uptake could be used to guide the design of culture media to include amino acids that improve gus yield. Culture media may then be supplemented with the amino acid or combinations of amino acids that significantly increase the yield for the protein. This FBA prediction could be tested rigorously by experiments (as in Figures 6.4, 6.6a, and 6.6b), and the candidate amino acids that optimizes the recombinant protein yield would be chosen.

The result of model III FBA simulations are included on Tables 6.4 and 6.5. A Zero FBA yield for gus or rubisco was predicted for the uptake of individual amino acids as the only nitrogen source. The uptake of asparagine and glutamine resulted in a 0.003 fold change in protein yield (about 99.7% reduction in protein yield compared to the FBA control). The uptake of arginine led to ~86% reduction in protein yield. The result suggests that ammonium is the main nitrogen substrate for growth, protein production and formation of many amino acids in the model. The use of amino acids as the only nitrogen source served no purposes for FBA protein production.

6.7 Amino acid as nitrogen source for the growth of cultures

In the experiments, *C. reinhardtii* cultures were grown in a nitrogen-free medium (ammonium-free, tris-free acetate medium) but supplemented with an amino acid as the sole source of nitrogen for growth. The experiments were designed to identify the amino acids that could be the sole nitrogen source for growth. For the successful amino acids, identification of their transporters into cells, characterizing and optimizing the expression

of the transporters would be promising areas of research in the future that may immensely contribute to the optimization of recombinant protein yield the cells.

The nitrogen-free medium was prepared and supplemented with an amino acid at a concentration of 10 mM. Though *C. reinhardtii* does not grow on tris, the omission of tris buffer ensured no nitrogenous compound was in the growth medium except the supplied amino acid. Twelve individual amino acids were tested in the growth medium (cysteine, histidine, tryptophan, serine, phenylalanine, lysine, threonine, isoleucine, valine, aspartate, arginine and glutamine). All cultures were grown in mixotrophic conditions (12 h light and 12 h dark cycles) at 54 µmol photons/m^2/s. Two control cultures were propagated: cultures grown in the ammonium-free, tris-free TAP medium without amino acid supplement (Control 1); and cultures grown in TAP medium with 9.35 mM ammonium chloride as the nitrogen source (Control 2). The growth curves of the mixotrophic cultures are presented in Figure 6.7.

No growth was observed for the cultures grown in the nitrogen-free acetate medium without amino acid (Control 1). In addition, no growth was observed for the mixotrophic cultures cultivated in the medium containing aspartate or threonine as the only nitrogen source. The results show that neither aspartate nor threonine is nitrogen sources for growth because of lack of uptake of the amino acids into cells.

Growth was extremely poor and inefficient for mixotrophic cultures grown in light on the TAP medium containing phenylalanine, valine, histidine, isoleucine, lysine, or tryptophan (Figure 6.7) as sole nitrogen source. Under mixotrophic condition, the uptake of these exogenous amino acids may be lacking, and failed to support growth. However under heterotrophic condition, growth was observed for the cultures grown in the dark on TAP medium containing ammonium source together with phenylalanine, histidine, isoleucine, lysine and tryptophan (see Figure 6.5). This revealed that ammonium is the sole nitrogen source for growth, and under this condition it is possible cells are able to take up phenylalanine, histidine, isoleucine, lysine or tryptophan as additional nitrogen source. The uptake of exogenous amino acids into *C. reinhardtii* cells are reported (Kirk and Kirk,

1978a, Kirk and Kirk, 1978b, Munoz-Blanco et al., 1990, Zuo et al., 2012). Many amino acids were reported to be deaminated extracellularly into 2-keto acids and ammonium (Munoz-Blanco et al., 1990), and the ammonium was taken up by cells. These amino acids included asparagine, alanine, serine, isoleucine, lysine, glutamine, valine, leucine, methionine, histidine and phenyalanine (Munoz-Blanco et al., 1990). Enzymes that catalyse the extracellular deamination of amino acids (L-amino oxidases) have been characterized (Piedras et al., 1992, Vallon et al., 1993). The uptake of arginine into *C. reinhardtii* cells was reported to be mediated by highly specific transport carrier (Kirk and Kirk, 1978a, Kirk and Kirk, 1978b). However, it may be possible also, that some amino acids have yet to be identified transport carriers. The transport of ammonium into cells involved the use of two types of transporters in *Chlamydomonas*: a low affinity high capacity transporter (Ullrich et al., 1984), and a high affinity low capacity transporter (Byrne et al., 1992, Franco et al., 1988). The authors reported that the expression of these transporters was induced by ammonium containing medium.

Growth was observed for mixotrophic cultures grown in TAP (control 2) with ammonium as the nitrogen source (Figure 6.7). Growth was also observed for mixotrophic cultures propagated in the medium supplemented with arginine or glutamine as the only nitrogen source (Figure 6.7), confirming reports for the growth of *C. reinhardtii* cultures on these amino acids as sole nitrogen source. Additionally, cysteine or serine supported growth effectively as sole nitrogen sources. Likely, deamination of these amino acids or the operation of specific transporters, for their uptake into cells was efficient and effective to support growth.

In Table 6.4, the predicted effect for the uptake of arginine was a 11.3% increase in FBA gus yield. The predicted effects for cysteine, serine and glutamine uptake on FBA gus yields are 2.7, 5.7, and 9.4% increase respectively. The combined effect of adding the uptake of the four amino acids would be about 29.1% increase in the FBA gus yield. Significant improvements to recombinant gus yield in cells might be made by supplementing TAP medium with these four amino acids. Then optimizing the enzyme

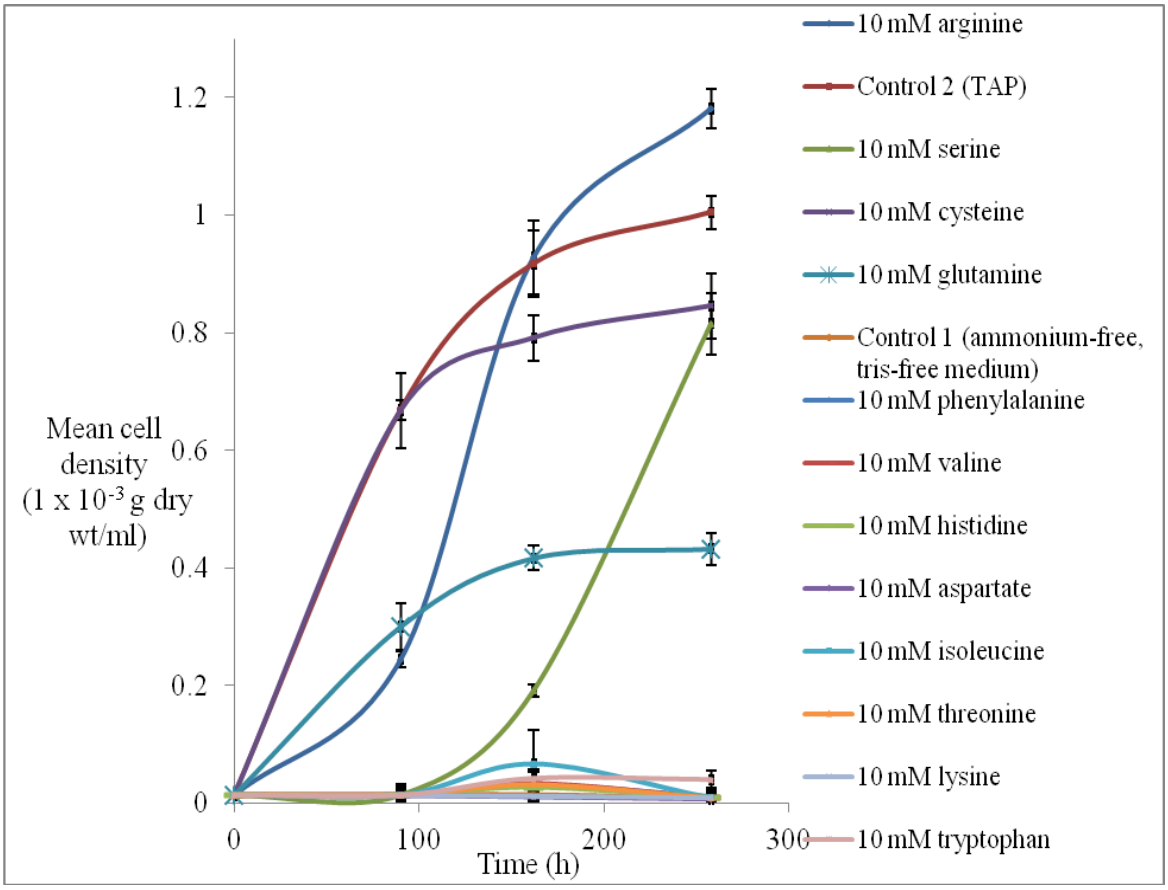

Figure 6.7: Growth profiles of Gus12-2 cultures grown synchronously in 12 h light and 12 h dark cycles at 54 µmol photons/m^2/s. Cultures were grown in ammonium-free tris-free acetate medium (control 1); TAP medium containing 9.35 mM ammonium (control 2); or in ammonium-free, tris-free acetate medium containing 10 mM of one of arginine, serine, cysteine, histidine, valine, phenyalanine, tryptophan, lysine, threonine, glutamine, aspartate, or isoleucine. The mean cell density was determined from three biological replicates and two technical replicates each.

(L-amino oxidase) expressions, and identifying, characterizing and optimizing expression for the specific carriers for these amino acids into cells, may be other important strategies needed to increase recombinant gus yield in the cells. These are aspects for future work that should be further exploited.

Chapter 7 - Conclusions and Future work

In the current study, systems biology approach was implemented that involved a range of quantitative experiments, analysis, FBA modelling, model predictions and verifications to identify limitations that affected growth of cultures, and steady-state fluxes for recombinant gus in the *C. reinhardtii* model. In the first part of the current work, the growth of *C. reinhardtii* cultures was characterized in autotrophic, heterotrophic and mixotrophic conditions to understand the major factors that affected achievement of high cell densities of cultures and growth rates. The lowest growth rates were observed in heterotrophic cultures. The autotrophic cultures exhibited higher growth rates than heterotrophic, but lower than the growth rates of mixotrophic cultures. The highest cell density were achieved in mixotrophic and autotrophic conditions, where both cultures propagated to cell densities >1 g dry cell weight per litre of culture. The cultures grown in these two conditions were observed with photosynthetic growth over extensive period of time usually > 20 days. On the other hand, heterotrophic condition provided the lowest cell density achievement by cultures. Generally, heterotrophic cultures grow up to 0.45 – 0.6 g dry cell weight per litre culture, but quickly reach stationary phase (6 – 8 days) and entered the death phase. The major factors that limited growth were the availability of carbon in the medium, supply of energy, lack of light and pH changes. Heterotrophic cultures did not grow in the dark without acetate as carbon substrate, indicating strict requirements for the substrate in this condition. Both heterotrophic and mixotrophic cultures grown in buffered TAP medium experienced high rises in pH due to the uncoupling effect of acetate on cell membranes. Internally, cells become acidified due to influx of protons from the medium and faced serious challenge for pH homeostasis intracellularly. The rise in pH was a stronger limitation for heterotrophic cultures because the cultures run out of the carbon source needed for energy supply for growth and cell maintenance.

Recombinant gus yields and protein yields were characterized in autotrophic, heterotropic and mixotrophic growth conditions. The lowest recombinant gus yields, gus productivity, total protein yield and protein productivity was observed in heterotrophic condition.

Recombinant gus yield, gus productivity, total protein yield and protein productivity was highest in mixotrophic cultures. In autotrophic condition, the gus yield and total protein yield were also higher than in heterotrophic condition. The results indicated that limitations to recombinant gus and protein yields in the microalgae was highest in the heterotrophic growth condition. Furthermore, there was no detectable protein cost for the expression of recombinant gus in autotrophic and mixotrophic cultures. The protein cost was high in heterotrophic cultures (15 – 18%). So far, no protein cost data has been published for the expression of foreign proteins in microalgae, though data exist for bacteria and yeast. The protein cost finding is important and is a relevant reference for the expression of heterologous proteins in *C. reinhardtii* under the different growth condition. Protein cost analysis may be further applied, for example, to estimate the allowable yield of recombinant protein in different condition without cessation of cell growth.

The analyses of cellular ATP concentration for cultures growing in the three growth conditions were performed. The highest cellular ATP concentration was observed in autotrophic cultures while the lowest was observed in heterotrophic cultures. Estimate of carbon flux in autotrophic, heterotrophic and mixotrophic conditions reveal that carbon flux was lowest in heterotrophic condition (~3 mmole carbon/g dry cell weight/h), but higher in mixotrophic (10 mmole carbon/g dry cell weight/h), and autotrophic conditions (11 mmole carbon/g dry cell weight/h). These results indicated that the heterotrophic condition is one that was the most-limited in terms of carbon and energy for growth and recombinant protein production.

A challenge for recombinant protein production in microalgae is the inherent and very low yield of the proteins. This study provided a platform to characterize the growth of *C. reinhardtii* and recombinant protein production in different growth conditions. The stated aim of the project was to address the low yield of recombinant protein, whether this was due to limitation that affected growth or suboptimal fluxes for the protein production. In this work, all the factors that limited the growth rates and high cell density achievement of cultures also affected recombinant protein yield. Of the three growth conditions,

heterotrophic growth was identified as the most-limiting condition for growth and recombinant gus protein production.

In the modelling work, FBA approaches were used to study steady state fluxes in the *C. reinhardtii* metabolic model (AlgaGEM) and to identify flux patterns that maximized gus production in the three conditions. At steady state there is no net accumulation of metabolites in the network, enabling the FBA analysis to obtain the description of gus yields only from steady state fluxes and stoichiometry of the reactions in the network. FBA was used to predict gus yields in autotrophic, heterotrophic and mixotrophic conditions and identified the heterotrophic condition as the most-limiting for gus production. Although, the FBA predicted gus yields was much higher than the gus yields determined from experiments, yet the predictions were consistent in relative terms to the experimentally determined yields across the three growth conditions. This consistency with patterns of experimental yields made the use of FBA possible to identify the amino acid fluxes that reduced heterotrophic gus yields metabolically in the model network. The FBA approaches could be applied to identify limiting amino acids for gus production in autotrophic and mixotrophic conditions.

A method for identifying, analysing and understanding the effect of the uptake of individual amino acids on recombinant protein yield was presented. Upon understanding the effect of the assimilation of an amino acid on the yield, growth cultures may be supplemented with an amino acid or combinations of amino acid so as to optimize the recombinant protein yield in the microalgae. Additionally, other strategies that may further increase recombinant protein yield were identified and proposed for future work towards recombinant protein research. These include the identifying, characterizing and optimizing the expression of the enzymes and specific carriers involved for amino acid transport into cells. A summary of the strategy to obtain 6-fold improvement in the amount of gus is discussed in the next section.

7.1 Strategy to achieve a 6-fold increase in recombinant gus

The main achievements and key results in this study, were the identification of the fed-batch growth strategy that increased the cell density of heterotrophic *C. reinhardtii* by > 3-fold, and a strategy that increased the yield of the recombinant gus in each cell by 2-fold. These are summarised as follows:

1. Heterotrophic cultures of the homoplasmic gus transformed strain (Gus12-2 or Gus12-B) must be grown in a modified TAP medium supplemented with ammonium and amino acids as nitrogen sources. The design of the modified TAP medium was predicted using FBA to simulate the effect of amino acids and ammonium uptake on maximal gus production. 11 amino acids were identified by FBA to limit gus production. These were cysteine, histidine, serine, asparagine, lysine, threonine, isoleucine,tryptophan, tyrosine, glutamine, and phenylalanine. These amino acids carry low steady state fluxes for the gus production. Their limitation was identified by analysing all amino acid total steady state flux distributions in the network calculated by FBA for maximized gus production.

2. The modified TAP medium was prepared by adding the 11 amino acids (each at 1 mM concentration) into TAP medium containing 9.35 mM ammonium. The FBA prediction of 1.9-fold increase in gus yield (see Figure 6.4) for heterotrophic cultures grown in the modified TAP medium was verified by experiment (Figures 6.6a, 6.6b).

3. In Figure 6.6a, the recombinant gus yields measured for the heterotrophic cultures grown in the modified TAP medium was 0.175% of dry cell weight, compared with the gus yield 0.085% of dry cell weight for the heterotrophic cultures grown in TAP medium (9.35 mM ammonium as sole nitrogen source). The results revealed that amino acid limitation was a metabolic bottleneck for gus production. By supplying these amino acids into TAP medium, the exogenous uptake of the amino acids and ammonium increased the steady state fluxes through the protein synthesis reactions leading to increased recombinant gus yield. Both ammonium and amino acids served as nitrogen sources for the gus production.

4. The factors reducing the growth and high cell density achievements of heterotrophic cultures were addressed and overcomed in order to increase the number of cells producing the optimized yield of recombinant gus. These limitations included availability of carbon

and energy sources (acetate), availability of nitrogen, detrimental pH rise and short culture longevity (viability). They were addressed in the following ways:

(a) The heterotrophic cultures were grown in the modified TAP prepared as in step 2, but in a fed-batch operation. The fed-batch operation is described next.

(b) Inoculated cultures should be allowed to reach~2.8 million cells/ml before harvesting by low speed centrifugation (*717 x* ***g*** for 5 minutes) to avoid disrupting or damaging cells. The pelleted cells can be washed twice by quick spins (*717 x* ***g*** for 30 seconds each) with reverse osmosis water to remove spent media.

(c) The pelleted cells should be fed into a new batch of sterile modified TAP medium buffered at pH 7.30. Growth should be propagated for the next 72 h in the medium to achieve a doubling in heterotrophic cell numbers to ~5.5 million cells/ml. Then the cells should be harvested as described in step 4b, and fed into another new sterile modified TAP buffered at pH 7.30.

(d) The fed-batch operation should be continued to triple the cell numbers within a 72 h period, to reach cell densities of ~8.3 million cells/ml, before harvesting, and feeding into a new sterile modified TAP medium buffered at pH 7.30 is performed.

(e) The cycle of fed-batch operations should be continued to attain cell densities >10 million cells/ml (>1.5 g dry wt/litre of culture), giving rise to >3-fold increase in cell density achieved by the heterotrophic cultures, than if the cells were grown in TAP medium in batch operation. At >10 million cells/ml, a much higher number of growing cells are achieved that produced twice the amount of gus. Put together, this represent a 6-fold increase in the amount of gus from cultures. The example of the approaches listed in step 4 (a - e) is in Figure 4.19. Here, the limiting effect of pH rise is greatly reduced by use of new medium buffered at optimum pH 7.30 every 72 h eriods. Additionally, the supply of modified TAP containing the amino acids in every 72 h, alleviates nitrogen depletion and increases recombinant gus yield. The culture longevity and viability is enhanced by the provision of favourable and optimal growth conditions. Cultures receive supply of acetate in the medium, and this removes depletion of the carbon and energy sources for growth and cell maintenance.

The scale up of the fed-batch operation is feasible. Industrially, it may be possible to operate the operation on a large-scale (100 – 1000 litre capacities) with bioreactors available in the market. Ideally, the process could be started in a 10 litre capacity bioreactor. As culture densities become very high (>20 million cells/ml or 3 g dry wt/litre of culture), the heterotrophic cultures may then be diluted by transferring and continuing the fed-batch operation into a 100 litre capacity bioreactor containing the modified TAP described above. The process could be further scaled-up to 1000 litres capacity depending on the demands for dry microalgae biomass and the target protein (recombinant gus). Microalgae dry biomass that may be obtained from the processing of a 1000 litre culture capacity at high cell densitiy of ~10 million cells/ml would be ~1500 g (1.5 kg dry biomass). The amount of recombinant gus that could recovered at this scale would be ~2.63 g. (~5.3 x 10^8 units of the enzyme).

An advantage of the fed-batch operation for heterotrophic cultures is that light is not needed for growth. At high culture densities, penetration of light becomes a strong limiting factor that reduces the growth of autotrophic and mixotrophic cultures. Attempts to increase and provide excessive light in order to ensure penetration could result in photo-inhibition of growth and oxidative damages to the cells. For the heterotrophic cultures in the fed-batch approaches and using the modified TAP (described above), the problems associated with high-titre densities of autotrophic and mixotrophic cultures would be avoided.

The combination of the quantitative experiments, analysis and the FBA modelling was a first in the field for recombinant protein expression research in microalgae. These approaches are transferable and applicable to other recombinant proteins expressed in the microalgae. Here, the work has provided a proof of the concept that systems biology analysis of networked processes that affect protein production in cells, may help make protein production more predictable. Collectively, this effort (quantitative experimentation, analyses and modelling) contributes immensely towards a predictable, robust and optimized production of recombinant proteins in microalgae.

References

Albert, R. (2007). Network inference, analysis, and modeling in systems biology. *Plant Cell,* 19**,** 3327 – 3338.

Alper, H., Miyaoku, K. and Stephanopoulos, G. (2005). Construction of lycopene-overproducing E-coli strains by combining systematic and combinatorial gene knockout targets. *Nature Biotechnology,* 23**,** 612 – 616.

Apic, G., Ignjatovic, T., Boyer, S. and Russell, R. B. (2005). Illuminating drug discovery with biological pathways. *Febs Letters*, 579**,** 1872 – 1877.

Apt, K. E. and Behrens, P. W. (1999). Commercial developments in microalgal biotechnology. *Journal of Phycology,* 35**,** 215 – 226.

Askenazi, M., Driggers, E. M., Holtzman, D. A., Norman, T. C., Iverson, S., Zimmer, D. P., Boers, M. E., Blomquist, P. R., Martinez, E. J., Monreal, A. W., Feibelman, T. P., Mayorga, M. E., Maxon, M. E., Sykes, K., Tobin, J. V., Cordero, E., Salama, S. R., Trueheart, J., Royer, J. C. and Madden, K. T. (2003). Integrating transcriptional and metabolite profiles to direct the engineering of lovastatin-producing fungal strains. *Nature Biotechnology,* 21**,** 150 – 156.

Barnes, D., Franklin, S., Schultz, J., Henry, R., Brown, E., Coragliotti, A. and Mayfield, S. P. (2005). Contribution of 5 '- and 3 '-untranslated regions of plastid mRNAs to the expression of *Chlamydomonas reinhardtii* chloroplast genes. *Molecular Genetics and Genomics,* 274**,** 625 – 636.

Baronofsky, J. J., Schreurs, W. J. A. and Kashket, E. R. (1984). Uncoupling by acetic-acid limits growth of and acetogenesis by *Clostridium-thermoaceticum*. *Applied and Environmental Microbiology,* 48**,** 1134 – 1139.

Becker, E. W. (2007). Micro-algae as a source of protein. *Biotechnology Advances,* 25**,** 207 – 210.

Becker, S. A., Feist, A. M., Mo, M. L., Hannum, G., Palsson, B. O. and Herrgard, M. J. (2007). Quantitative prediction of cellular metabolism with constraint-based models: the COBRA Toolbox. *Nature Protocols,* 2**,** 727 – 738.

Bedhomme, M., Zaffagnini, M., Marchand, C. H., Gao, X.-H., Moslonka-Lefebvre, M., Michelet, L., Decottignies, P. and Lemaire, S. D. (2009). Regulation by

Glutathionylation of Isocitrate Lyase from *Chlamydomonas reinhardtii*. *Journal of Biological Chemistry,* 284**,** 36282 – 36291.

Bielekova, B., Vodovotz, Y., An, G. and Hallenbeck, J. (2014). How implementation of systems biology into clinical trials accelerates understanding of diseases. *Frontiers in neurology,* 5**,** 102 – 102.

Bock, R. (2007). Plastid biotechnology: prospects for herbicide and insect resistance, metabolic engineering and molecular farming. *Current Opinion in Biotechnology,* 18**,** 100 – 106.

Boele, J., Olivier, B. G. and Teusink, B. (2012). FAME, the Flux Analysis and Modeling Environment. *Bmc Systems Biology,* 6.

Boogerd, F. C., Bruggeman, F. J., Hofmeyr, J.-H. S. and Westerhoff, H. V. (2007). 1 - Towards philosophical foundations of Systems Biology: Introduction. *In:* Boogerd, F. C., Westerhoff, H. V., Bruggeman, F. J., and Hofmeyr, J.-H. S. (eds.) *Systems Biology.* Amsterdam: Elsevier.

Bowers, G. N., McComb, R. B., Christensen, R. G. and Schaffer, R. (1980). High-purity 4-nitrophenol: purification, characterization, and specification for use as a spectrophotometric reference material. *Clinical Chemistry,* 26, 724 – 729.

Boyd, C. E. (1973). Amino-acid composition of freshwater algae. *Archiv Fur Hydrobiologie,* 72**,** 1 – 9.

Boyle, N. R. and Morgan, J. A. (2009). Flux balance analysis of primary metabolism in *Chlamydomonas reinhardtii*. *Bmc Systems Biology,* 3.

Boynton, J. E., Gillham, N. W., Harris, E. H., Hosler, J. P., Johnson, A. M., Jones, A. R., Randolphanderson, B. L., Robertson, D., Klein, T. M., shark, K. B. and Sanford, J. C. (1988). Chloroplast transformation in *Chlamydomonas* with high-velocity microprojectiles. *Science,* 240**,** 1534 – 1538.

Boynton, J. E., Harris, E. H., Burkhart, B. D., Lamerson, P. M. and Gillham, N. W. (1987). Transmission of mitochondrial and chloroplast genomes in crosses of *Chlamydomonas*. *Proceedings of the National Academy of Sciences of the United States of America,* 84**,** 2391 – 2395.

Bradford, M. M. (1976). Rapid and sensitive method for quantitation of microgram quantities of protein utilizing principle of protein-dye binding. *Analytical Biochemistry,* 72**,** 248 – 254.

Brown, M. R. (1991). The amino-acid and sugar composition of 16 species of microalgae used in mariculture. *Journal of Experimental Marine Biology and Ecology*, 145**,** 79 – 99.

Brown, T. J. and Geen, G. H. (1974). Effect of light quality on carbon metabolism and extracellular release of *Chlamydomonas-reinhardtii* dangeard. *Journal of Phycology*, 10**,** 213 – 220.

Bruggeman, F. J. and Westerhoff, H. V. (2007). The Nature of Systems Biology. *Trends Microbiol* 15, 45 – 50.

Butcher, E. C., Berg, E. L. and Kunkel, E. J. (2004). Systems biology in drug discovery. *Nature Biotechnology*, 22**,** 1253 – 1259.

Byrne, T. E., Wells, M. R. and Johnson, C. H. (1992). circadian-rhythms of chemotaxis to ammonium and of methylammonium uptake in *Chlamydomonas*. *Plant Physiology*, 98**,** 879 – 886.

Cain, B. J. (1965). Nitrogen utilization in 38 freshwater chlamydomonad algae. *Canadian Journal of Botany*, 43**,** 1367.

Casas-Mollano, J. A., Van Dijk, K., Eisenhart, J. and Cerutti, H. (2007). SET3p monomethylates histone H3 on lysine 9 and is required for the silencing of tandemly repeated transgenes in *Chlamydomonas*. *Nucleic Acids Research*, 35**,** 939 – 950.

Chang, C., Alber, D., Graf, P., Kim, K. and Seibert, M. (2007). Addressing unknown constants and metabolic network behaviors through petascale computing: understanding H-2 production in green algae. *Journal of Physics:Conference Series*, 78, 012011.

Chebolu, S. and Daniell, H. (2009). Chloroplast-Derived Vaccine Antigens and Biopharmaceuticals: Expression, Folding, Assembly and Functionality. *Plant-Produced Microbial Vaccines*, 332, 33 – 54.

Chisti, Y. (2007). Biodiesel from microalgae. *Biotechnology Advances*, 25**,** 294 – 306.

Chlamydomonas Resource Centre. Available: http://www.chlamy.org [Accessed 4 November 2014].

Cho, C. R., Labow, M., Reinhardt, M., Van Oostrum, J. and Peitsch, M. C. (2006). The application of systems biology to drug discovery. *Current Opinion in Chemical Biology*, 10**,** 294 – 302.

Collins, S. and Bell, G. (2004). Phenotypic consequences of 1,000 generations of selection at elevated CO_2 in a green alga. *Nature*, 431**,** 566 – 569.

Coragliotti, A. T., Beligni, M. V., Franklin, S. E. and Mayfield, S. P. (2011). Molecular Factors Affecting the Accumulation of Recombinant Proteins in the *Chlamydomonas reinhardtii* Chloroplast. *Molecular Biotechnology,* 48**,** 60 – 75.

Corriveau, J. L. and Coleman, A. W. (1988). Rapid screening method to detect potential biparental inheritance of plastid DNA and results for over 200 angiosperm species. *American Journal of Botany,* 75**,** 1443 – 1458.

Cournac, L., Mus, F., Bernard, L., Guedeney, G., Vignais, P. & Peltier, G. (2002). Limiting steps of hydrogen production in *Chlamydomonas reinhardtii* and *Synechocystis* PCC 6803 as analysed by light-induced gas exchange transients. *International Journal of Hydrogen Energy,* 27**,** 1229 – 1237.

Crouch, S. P. M., Kozlowski, R., Slater, K. J. and Fletcher, J. (1993). The use of ATP bioluminescence as a measure of cell-proliferation and cytotoxicity. *Journal of Immunological Methods,* 160**,** 81 – 88.

Culture Collection of Algae (SAG). Available: http://www.uni-goettingen.de/en/184982.html [Accessed 10 October 2013].

Culture Collection of Algae and Protozoa (CCAP). Available: http://www.ccap.ac.uk [Accessed 10 October 2013].

Dal'molin, C. G. D. O., Quek, L.-E., Palfreyman, R. W. and Nielsen, L. K. (2011). AlgaGEM - a genome-scale metabolic reconstruction of algae based on the *Chlamydomonas reinhardtii* genome. *Bmc Genomics,* 12.

Available: http://www.biomedcentral.com/1471-2164/12/S4/S5 [Accessed June 15 2014].

Day, A. and Goldschmidt-Clermont, M. (2011). The chloroplast transformation toolbox: selectable markers and marker removal. *Plant Biotechnology Journal,* 9**,** 540 – 553.

Debuchy, R., Purton, S. and Rochaix, J. D. (1989). The argininosuccinate lyase gene of *Chlamydomonas reinhardtii*-An important tool for nuclear transformation and for correlating the genetic and molecular maps of the Arg7 locus. *Embo Journal,* 8**,** 2803 – 2809.

Dekel, E. and Alon, U. (2005). Optimality and evolutionary tuning of the expression level of a protein. *Nature,* 436**,** 588 – 592.

Dekel, E., Mangan, S. and Alon, U. (2005). Environmental selection of the feed-forward loop circuit in gene-regulation networks. *Physical Biology,* 2**,** 81 – 88.

Devinoy, E., Thepot, D., Stinnakre, M. G., Fontaine, M. L., Grabowski, H., Puissant, C., Pavirani, A. and Houdebine, L. M. (1994). High-level production of human growth-

hormone in the milk of transgenic mice - the upstream region of the rabbit whey acidic protein (wap) gene targets transgene expression to the mammary-gland. *Transgenic Research,* 3**,** 79 – 89.

Devisser, J., Hoekstra, R. F. and Vandenende, H. (1996). The effect of sex and deleterious mutations on fitness in Chlamydomonas. *Proceedings of the Royal Society B-Biological Sciences,* 263**,** 193 – 200.

Dong, H. J., Nilsson, L. and Kurland, C. G. (1995). Gratuitous overexpression of genes in *Escherichia coli* leads to growth-inhibition and ribosome destruction. *Journal of Bacteriology,* 177**,** 1497 – 1504.

Doran, P. M. (2006). Foreign protein degradation and instability in plants and plant tissue cultures. *Trends in Biotechnology,* 24**,** 426 – 432.

Dove, A. (2001). The bittersweet promise of glycobiology. *Nature Biotechnology,* 19**,** 913 – 917.

Dove, A. (2002). Uncorking the biomanufacturing bottleneck. *Nature Biotechnology,* 20**,** 777 – 779.

Duarte, N. C., Becker, S. A., Jamshidi, N., Thiele, I., Mo, M. L., Vo, T. D., Srivas, R. & Palsson, B. O. (2007). Global reconstruction of the human metabolic network based on genomic and bibliomic data. *Proceedings of the National Academy of Sciences of the United States of America,* 104**,** 1777 – 1782.

Dubois, M., Gilles, K. A., Hamilton, J. K., Rebers, P. A. and Smith, F. (1956). Colorimetric method for determination of sugars and related substances. *Analytical Chemistry,* 28**,** 350 – 356.

Dunahay, T. G. (1993). Transformation of *Chlamydomonas reinhardtii* with silicon-carbide whiskers. *Biotechniques,* 15**,** 452 – 455.

Eberhard, S., Drapier, D. and Wollman, F. A. (2002). Searching limiting steps in the expression of chloroplast-encoded proteins: relations between gene copy number, transcription, transcript abundance and translation rate in the chloroplast of *Chlamydomonas reinhardtii*. *Plant Journal,* 31**,** 149 – 160.

Edwards, J. S., Ibarra, R. U. and Palsson, B. O. (2001). *In silico* predictions of *Escherichia coli* metabolic capabilities are consistent with experimental data. *Nature Biotechnology,* 19**,** 125 – 130.

Ellis, R. J. (1979). Most abundant protein in the world. *Trends in Biochemical Sciences,* 4**,** 241 - 244.

Ellstrand, N. C. (2001). When transgenes wander, should we worry? *Plant Physiology,* 125**,** 1543 – 1545.

Fell, D. A. and Small, J. R. (1986). Fat synthesis in adipose-tissue - an examination of stoichiometric constraints. *Biochemical Journal,* 238**,** 781 – 786.

Fischer, R., Liao, Y. C., Hoffmann, K., Schillberg, S. and Emans, N. (1999). Molecular farming of recombinant antibodies in plants. *Biological Chemistry,* 380**,** 825 – 839.

Fletcher, S. P., Muto, M. and Mayfield, S. P. (2007). Optimization of recombinant protein expression in the chloroplasts of green algae. *Transgenic Microalgae as Green Cell Factories,* 616**,** 90 – 98.

Franco, A. R., Cardenas, J. and Fernandez, E. (1988). 2 different carriers transport both ammonium and methylammonium in *Chlamydomonas reinhardtii*. *Journal of Biological Chemistry,* 263**,** 14039 – 14043.

Franklin, S., Ngo, B., Efuet, E. and Mayfield, S. P. (2002). Development of a GFP reporter gene for *Chlamydomonas reinhardtii* chloroplast. *Plant Journal,* 30**,** 733 – 744.

Franklin, S. E. and Mayfield, S. P. (2004). Prospects for molecular farming in the green alga *Chlamydomonas reinhardtii*. *Current Opinion in Plant Biology,* 7**,** 159 – 165.

Gantar, M. and Svircev, Z. (2008). Microalgae and cyanobacteria: Food for thought. *Journal of Phycology,* 44**,** 260 – 268.

Gevorgyan, A., Bushell, M. E., Avignone-Rossa, C. and Kierzek, A. M. (2011). SurreyFBA: a command line tool and graphics user interface for constraint-based modeling of genome-scale metabolic reaction networks. *Bioinformatics,* 27**,** 433 – 434.

Gorman, D. S. and Levine, R. P. 1965. Cytochrome f and plastocyanin- Their sequence in photosynthetic electron transport chain of *Chlamydomonas reinhardi*. *Proceedings of the National Academy of Sciences of the United States of America,* 54**,** 1665 – 1669.

Grafahrend-Belau, E., Klukas, C., Junker, B. H. and Schreiber, F. (2009). FBA-SimVis: interactive visualization of constraint-based metabolic models. *Bioinformatics,* 25**,** 2755 – 2757.

Grant, D. and Chiang, K. S. (1980). Physical mapping and characterization of *Chlamydomonas* mitochondrial-DNA molecules - Their unique ends, sequence homogeneity, and conservation. *Plasmid,* 4**,** 82 – 96.

Gray, M. W. and Boer, P. H. (1988). Organization and expression of algal (*Chlamydomonas-reinhardtii*) mitochondrial-DNA. *Philosophical Transactions of the Royal Society of London Series B-Biological Sciences,* 319**,** 135 – 147.

Gresshoff, P. M. (1981). amide metabolism of *chlamydomonas-reinhardi*. *Archives of Microbiology,* 128**,** 303 – 306.

Grima, E. M., Fernandez, F. G. A., Camacho, F. G. and Chisti, Y. (1999). Photobioreactors: light regime, mass transfer, and scaleup. *Journal of Biotechnology,* 70**,** 231-247.

Grima, E. M., Sevilla, J. M. F., Perez, J. A. S. and Camacho, F. G. (1996). A study on simultaneous photolimitation and photoinhibition in dense microalgal cultures taking into account incident and averaged irradiances. *Journal of Biotechnology,* 45**,** 59 – 69.

Grobbelaar, J. U. (1994). Turbulence in mass algal cultures and the role of light-dark fluctuations. *Journal of Applied Phycology,* 6**,** 331 – 335.

Grobbelaar, J. U. (2003). Algal Nutrition-Mineral Nutrition. *In:* Richmond, A. (ed.) *Handbook on microalgal culture:Biotechnology and Applied Phycology,* Oxford, Blackwell Publishing Ltd. 95 – 115.

Grobbelaar, J. U. (2010). Microalgal biomass production: challenges and realities. *Photosynthesis Research,* 106**,** 135 – 144.

Gruissem, W. and Tonkyn, J. C. (1993). Control mechanisms of plastid gene-expression. *Critical Reviews in Plant Sciences,* 12**,** 19 – 55.

Gudmundsson, S. and Thiele, I. (2010). Computationally efficient flux variability analysis. *Bmc Bioinformatics,* 11.

Harris, E. H. (1989). *The Chlamydomonas Sourcebook: A Comprehensive guide to biology and laboratory use,* New York, Academic Press, Inc. 1 – 780.

Hiatt, A., Cafferkey, R. and Bowdish, K. (1989). Production of antibodies in transgenic plants. *Nature,* 342**,** 76 – 78.

Hodson, R. C., Williams, S. K. and Davidson, W. R. (1975)**.** Metabolic control of urea catabolism in *Chlamydomonas reinhardi* and *chlorella pyrenoidosa***.** *Journal of Bacteriology,* 121**,** 1022 – 1035.

Hoppe, A., Hoffmann, S., Gerasch, A., Gille, C. and Holzhuetter, H.-G. (2011). FASIMU: flexible software for flux-balance computation series in large metabolic networks. *Bmc Bioinformatics,* 12.

Hsieh, S. I., Castruita, M., Malasarn, D., Urzica, E., Erde, J., Page, M. D., Yamasaki, H., Casero, D., Pellegrini, M., Merchant, S. S. and Loo, J. A. (2013). The Proteome of Copper, Iron, Zinc, and Manganese Micronutrient Deficiency in *Chlamydomonas reinhardtii*. *Molecular and Cellular Proteomics,* 12**,** 65 – 86.

Hutner, S. H. (1949). Some approaches to the study of the metal requirements of microorganisms. *Science,* 110**,** 548 – 549.

Ingram-smith, C., Martin, S. R. and Smith, K. S. (2006). Acetate kinase: not just a bacterial enzyme. *Trends in Microbiology,* 14**,** 249 – 253.

Ishikura, K., Takaoka, Y., Kato, K., Sekine, M., Yoshida, K. and Shinmyo, A. (1999). Expression of a foreign gene in *Chlamydomonas reinhardtii* chloroplast. *Journal of Bioscience and Bioengineering,* 87**,** 307 – 314.

Janssen, M., Kuijpers, T. C., Veldhoen, B., Ternbach, M. B., Tramper, J., Mur, L. R. and Wijffels, R. H. (1999). Specific growth rate of *Chlamydomonas reinhardtii* and *Chlorella sorokiniana* under medium duration light dark cycles: 13-87 s. *Journal of Biotechnology,* 70**,** 323 – 333.

Jefferson, R. A. (1987). Assaying Chimeric Genes in Plants: The GUS gene Fusion System. *Plant molecular biology reporter,* 5**,** 387 – 405.

Jefferson, R. A. (1989). The gus reporter gene system. *Nature,* 342**,** 837 – 838.

Jefferson, R. A., Burgess, S. M. & Hirsh, D. (1986). Beta-glucuronidase from *Escherichia coli* as a gene-fusion marker. *Proceedings of the National Academy of Sciences of the United States of America,* 83**,** 8447 – 8451.

Jefferson, R. A., Kavanagh, T. A. and Bevan, M. W. (1987a). Beta-glucuronidase (gus) as a sensitive and versatile gene fusion marker in plants. *Journal of Cellular Biochemistry***,** 57 – 57.

Jefferson, R. A., Kavanagh, T. A. and Bevan, M. W. (1987b)**.** Gus fusions - beta-glucuronidase as a sensitive and versatile gene fusion marker in higher-plants. *Embo Journal,* 6**,** 3901 – 3907.

Jones, D. L., Owen, A. G. and Farrar, J. F. (2002). Simple method to enable the high resolution determination of total free amino acids in soil solutions and soil extracts. *Soil Biology & Biochemistry,* 34**,** 1893 – 1902.

Kalisky, T., Dekel, E. and Alon, U. (2007). Cost-benefit theory and optimal design of gene regulation functions. *Physical Biology,* 4**,** 229 – 245.

Kanehisa, M., Goto, S., Sato, Y., Kawashima, M., Furumichi, M. and Tanabe, M. (2014). Data, information, knowledge and principle: back to metabolism in KEGG. *Nucleic Acids Research,* 42, D199 – D205.

Kell, D. B. and Westerhoff, H. V. (1986). Metabolic control-theory - its role in microbiology and biotechnology. *Fems Microbiology Letters,* 39**,** 305 – 320.

Khannapho, C., Zhao, H., Bonde, B. K., Kierzek, A. M., Avignone-Rossa, C. A. and Bushell, M. E. (2008). Selection of objective function in genome scale flux balance analysis for process feed development in antibiotic production. *Metabolic Engineering,* 10**,** 227 – 233.

Kightlinger, W., Chen, K., Pourmir, A., Crunkleton, D. W., Price, G. L. and Johannes, T. W. (2014). Production and characterization of algae extract from *Chlamydomonas reinhardtii*. *Electronic Journal of Biotechnology,* 17, 14 – 18.

Kim, H. U., Sohn, S. B. and Lee, S. Y. (2012). Metabolic network modeling and simulation for drug targeting and discovery. *Biotechnology Journal,* 7**,** 330 – 342.

Kindle, K. L. (1990). High-frequency nuclear transformation of *Chlamydomonas reinhardtii*. *Proceedings of the National Academy of Sciences of the United States of America,* 87**,** 1228 – 1232.

Kindle, K. L., Richards, K. L. and Stern, D. B. (1991). Engineering the chloroplast genome - techniques and capabilities for chloroplast transformation in *chlamydomonas reinhardtii*. *Proceedings of the National Academy of Sciences of the United States of America,* 88**,** 1721 – 1725.

Kindle, K. L., Schnell, R. A., Fernandez, E. and Lefebvre, P. A. (1989). Stable nuclear transformation of chlamydomonas using the chlamydomonas gene for nitrate reductase. *Journal of Cell Biology,* 109**,** 2589 – 2601.

Kirk, D. L. and Kirk, M. M. (1978a). Amino-acid and urea uptake in 10 species of chlorophyta. *Journal of Phycology,* 14**,** 198 – 203.

Kirk, D. L. and Kirk, M. M. (1978b). Carrier-mediated uptake of arginine and urea by *chlamydomonas reinhardtii*. *Plant Physiology,* 61**,** 556 – 560.

Kitano, H. (2002). Systems biology: A brief overview. *Science,* 295**,** 1662 – 1664.

Klein, U., Salvador, M. L. and Bogorad, L. (1994). Activity of the *Chamydomonas* chloroplast rbcl gene promoter is enhanced by a remote sequence element. *Proceedings of the National Academy of Sciences of the United States of America,* 91**,** 10819 – 10823.

Koch, A. L. (1983). The protein burden of *lac* operon products. *Journal of Molecular Evolution,* 19**,** 455 – 462.

Komine, Y., Kikis, E., Schuster, G. and Stern, D. (2002). Evidence for in vivo modulation of chloroplast RNA stability by 3 '-UTR homopolymeric tails in *Chlamydomonas reinhardtii*. *Proceedings of the National Academy of Sciences of the United States of America,* 99**,** 4085 – 4090.

Kreeger, P. K. and Lauffenburger, D. A. (2010). Cancer systems biology: a network modeling perspective. *Carcinogenesis,* 31**,** 2 – 8.

La Fontaine, S., Quinn, J. M., Nakamoto, S. S., Page, M. D., Gohre, V., Mosely, J. L., Kropat, J. and Merchant, S. (2002). Copper-dependent iron assimilation pathway in the model photosynthetic eukaryote *Chlamydomonas reinhardtii*. *Eukaryotic Cell,* 1**,** 736 – 757.

Lakshmanan, M., Koh, G., Chung, B. K. S. and Lee, D. Y. (2014). Software applications for flux balance analysis. *Briefings in Bioinformatics,* 15**,** 108 – 122.

Lee, D. Y. and Fiehn, O. (2008). High quality metabolomic data for *Chlamydomonas reinhardtii. Plant Methods,* 4, 7

Lee, S. J., Lee, D. Y., Kim, T. Y., Kim, B. H., Lee, J. W. and LEE, S. Y. (2005). Metabolic engineering of Escherichia coli for enhanced production of succinic acid, based on genome comparison and in silico gene knockout simulation. *Applied and Environmental Microbiology,* 71**,** 7880 – 7887.

Lee, S., Phalakornkule, C., Domach, M. M. and Grossmann, I. E. (2000). Recursive MILP model for finding all the alternate optima in LP models for metabolic networks. *Computers & Chemical Engineering,* 24**,** 711 – 716.

Lee, Y. K. and Low, C. S. (1992). Productivity of outdoor algal cultures in enclosed tubular photobioreactor. *Biotechnology and Bioengineering,* 40**,** 1119 – 1122.

Leoncikas, V., Wu, H., Ward, L. T., Kierzek, A. M. and Plant, N. J. (2014). Predicting the metabolic landscape of poor prognosis breast cancer. *International Journal of Molecular Medicine,* 34**,** S28 – S28.

Lien, T. and Knutsen, G. (1976). Synchronized cultures of a cell wall-less mutant of *Chlamydomonas reinhardii*. *Archives of Microbiology,* 108**,** 189 – 194.

Liu, Z. P., Wang, Y., Zhang, X. S. and Chen, L. (2012). Network-based analysis of complex diseases. *Iet Systems Biology,* 6**,** 22 – 33.

Loppes, R. (1969). A new class of arginine-requiring mutants in *Chlamydomonas reinhardi*. *Molecular and General Genetics,* 104**,** 172 – 177.

Mahadevan, R. and Schilling, C. H. (2003). The effects of alternate optimal solutions in constraint-based genome-scale metabolic models. *Metabolic Engineering,* 5**,** 264 – 276.

Malakar, **P. and Venkatesh, K. V.** (2012). Effect of substrate and IPTG concentrations on the burden to growth of *Eschericia coli* on glycerol due to the expression of *lac* proteins. *Applied Microbiology and Biotechnology,* 93, 2543 – 2549.

Manichaikul, A., Ghamsari, L., Hom, E. F. Y., Lin, C. W., Murray, R. R., Chang, R. L., Balaji, S., Hao, T., Shen, Y., Chavali, A. K., Thiele, I., Yang, X. P., Fan, C. Y., Mello, E., Hill, D. E., Vidal, M., Salehi-Ashtiani, K. and Papin, J. A. (2009). Metabolic network analysis integrated with transcript verification for sequenced genomes. *Nature Methods,* 6**,** 589 – 592.

Manuell, A., Beligni, M. V., Yamaguchi, K. and Mayfield, S. P. (2004). Regulation of chloroplast translation: interactions of RNA elements, RNA-binding proteins and the plastid ribosome. *Biochemical Society Transactions,* 32**,** 601 – 605.

Manuell, A. L., Beligni, M. V., Elder, J. H., Siefker, D. T., Tran, M., Weber, A., Mcdonald, T. L. and Mayfield, S. P. (2007). Robust expression of a bioactive mammalian protein in *Chlamydomonas* chloroplast. *Plant Biotechnology Journal,* 5**,** 402 – 412.

Marr, A. G. (1991). Growth-rate of *Eschericia coli*. *Microbiology Reviews*, 55, 316 – 333.

Maul, J. E., Lilly, J. W., Cui, L. Y., Depamphilis, C. W., Miller, W., Harris, E. H. and Stern, D. B. (2002). The *Chlamydomonas reinhardtti* plastid chromosome: Islands of genes in a sea of repeats. *Plant Cell,* 14**,** 2659 – 2679.

Mayfield, S. P., Cohen, A., Danon, A. and Yohn, C. B. (1994). Translation of the psbA messenger-RNA of *Chlamydomonas reinhardtii* requires a structured RNA element contained within the 5' untranslated region. *Journal of Cell Biology,* 127**,** 1537 – 1545.

Mayfield, S. P. and Franklin, S. E. (2005). Expression of human antibodies in eukaryotic micro-algae. *Vaccine,* 23**,** 1828 – 1832.

Mayfield, S. P., Franklin, S. E. and Lerner, R. A. (2003). Expression and assembly of a fully active antibody in algae. *Proceedings of the National Academy of Sciences of the United States of America,* 100**,** 438 – 442.

Mayfield, S. P., Manuell, A. L., Chen, S., Wu, J., Tran, M., Siefker, D., Muto, M. and Marin-Navarro, J. (2007). *Chlamydomonas reinhardtii* chloroplasts as protein factories. *Current Opinion in Biotechnology,* 18**,** 126 – 133.

Mayfield, S. P., Yohn, C. B., Cohen, A. and Danon, A. (1995). Regulation of chloroplast gene-expression. *Annual Review of Plant Physiology and Plant Molecular Biology,* 46**,** 147 – 166.

Melis, A. and Happe, T. (2004). Trails of green alga hydrogen research - from Hans Gaffron to new frontiers. *Photosynthesis Research,* 80**,** 401 – 409.

Merchant, S. S., Prochnik, S. E., Vallon, O., Harris, E. H., Karpowicz, S. J., Witman, G. B., Terry, A., Salamov, A., Fritz-Laylin, L. K., Marechal-Drouard, L., Marshall, W. F., Qu, L. H., Nelson, D. R., Sanderfoot, A. A., Spalding, M. H., Kapitonov, V. V., Ren, Q. H., Ferris, P., Lindquist, E., Shapiro, H., Lucas, S. M., Grimwood, J., Schmutz, J., Cardol, P., Cerutti, H., Chanfreau, G., Chen, C. L., Cognat, V., Croft, M. T., Dent, R., Dutcher, S., Fernandez, E., Fukuzawa, H., Gonzalez-Ballester, D., Gonzalez-Halphen, D., Hallmann, A., Hanikenne, M., Hippler, M., Inwood, W., Jabbari, K., Kalanon, M., Kuras, R., Lefebvre, P. A., Lemaire, S. D., Lobanov, A. V., Lohr, M., Manuell, A., Meir, I., Mets, L., Mittag, M., Mittelmeier, T., Moroney, J. V., Moseley, J., Napoli, C., Nedelcu, A. M., Niyogi, K., Novoselov, S. V., Paulsen, I. T., Pazour, G., Purton, S., Ral, J. P., Riano-Pachon, D. M., Riekhof, W., Rymarquis, L., Schroda, M., Stern, D., Umen, J., Willows, R., Wilson, N., Zimmer, S. L., Allmer, J., Balk, J., Bisova, K., Chen, C. J., Elias, M., Gendler, K., Hauser, C., Lamb, M. R., Ledford, H., Long, J. C., Minagawa, J., Page, M. D., Pan, J. M., Pootakham, W., Roje, S., Rose, A., Stahlberg, E., Terauchi, A. M., Yang, P. F., Ball, S., Bowler, C., Dieckmann, C. L., Gladyshev, V. N., Green, P., Jorgensen, R., Mayfield, S., Mueller-Roeber, B., Rajamani, S., Sayre, R. T., Brokstein, P., et al. (2007). The Chlamydomonas genome reveals the evolution of key animal and plant functions. *Science,* 318**,** 245 – 251.

Michaelis, G., Vahrenholz, C. and Pratje, E. (1990). Mitochondrial-DNA of *Chlamydomonas reinhardtii* - The gene for apocytochrome-b and the complete functional map of the 15.8 kb DNA. *Molecular & General Genetics,* 223**,** 211 – 216.

Mihara, S. and Hase, E. (1971). Studies on the vegetative life cycle of *Chlamydomonas reinhardi* dangeard in synchronous culture. 1. Some characteristics of cell cycle. *Plant and Cell Physiology,* 12**,** 225 – 236.

Mitra, M. & Melis, A. (2008). Optical properties of microalgae for enhanced biofuels production. *Optics Express,* 16**,** 21807 – 21820.

Mo, M. L., Jamshidi, N. & Palsson, B. O. (2007). A genome-scale, constraint-based approach to systems biology of human metabolism. *Molecular Biosystems,* 3**,** 598 – 603.

Molenaar, D., Van Berlo, R., De Ridder, D. and Teusink, B. (2009). Shifts in growth strategies reflect tradeoffs in cellular economics. *Molecular Systems Biology,* 5, 323

Moore, S. & Stein, W. H. (1954). A modified ninhydrin reagent for the photometric determination of amino acids and related compounds. *Journal of Biological Chemistry,* 211**,** 907 - 913.

Moroney, J. V. and Ynalvez, R. A. (2007). Proposed carbon dioxide concentrating mechanism in *Chlamydomonas reinhardtii*. *Eukaryotic Cell,* 6**,** 1251 – 1259.

Munoz-Blanco, J., Hidalgo-Martinez, J. and Cardenas, J. (1990). Extracellular deamination of L-amino-acids by Chlamydomonas-reinhardtii cells. *Planta,* 182**,** 194 – 198.

Murabito, E., Simeonidis, E., Smallbone, K. and Swinton, J. (2009). Capturing the essence of a metabolic network: A flux balance analysis approach. *Journal of Theoretical Biology,* 260**,** 445 – 452.

Nakamura, Y., Gojobori, T. and Ikemura, T. (1999). Codon usage tabulated from the international DNA sequence databases; its status 1999. *Nucleic Acids Research,* 27**,** 292 – 292.

Navlakha, S. and Bar-Joseph, Z. (2011). Algorithms in nature: the convergence of systems biology and computational thinking. *Molecular Systems Biology,* 7, 546

Neufeld, R. J. and Zajic, J. E. (1982). A technique for monitoring biomass levels and cell-adhesion in hexadecane fermentations. *Biotechnology Letters,* 4**,** 701 – 704.

Neupert, J., Karcher, D. and Bock, R. (2009). Generation of *Chlamydomonas* strains that efficiently express nuclear transgenes. *Plant Journal,* 57**,** 1140 – 1150.

Nevoigt, E. (2008). Progress in metabolic engineering of *Saccharomyces cerevisiae*. *Microbiology and Molecular Biology Reviews,* 72**,** 379 – 412.

Newman, S. M., Boynton, J. E., Gillham, N. W., Randolphanderson, B. L., Johnson, A. M. & Harris, E. H. (1990). Transformation of chloroplast ribosomal-RNA genes in *Chlamydomonas* - Molecular and genetic-characterization of integration events. *Genetics,* 126**,** 875 – 888.

Newman, S. M., Gillham, N. W., Harris, E. H., Johnson, A. M. & Boynton, J. E. (1991). Targeted disruption of chloroplast genes in *Chlamydomonas reinhardtii*. *Molecular & General Genetics,* 230**,** 65 – 74.

Nogales, J., Guijo, M. I., Quesada, A. and Merchan, F. (2004). Functional analysis and regulation of the malate synthase from *Chlamydomonas reinhardtii*. *Planta,* 219**,** 325 – 331.

Novick, A. and Weiner, M. (1957). Enzyme induction as an all-or-none phenomenon. *Proceedings of the National Academy of Sciences of the United States of America,* 43**,** 553 – 566.

Oberhardt, M. A., Yizhak, K. and Ruppin, E. (2013). Metabolically re-modeling the drug pipeline. *Current Opinion in Pharmacology,* 13**,** 778 – 785.

Oliver, S. G. (2006). From genomes to systems: the path with yeast. *Philosophical Transactions of the Royal Society B-Biological Sciences,* 361**,** 477 – 482.

Orth, J. D., Thiele, I. and Palsson, B. O. (2010). What is flux balance analysis? *Nature Biotechnology,* 28**,** 245 – 248.

Papini, M., Salazar, M. and Nielsen, J. (2010). Systems Biology of Industrial Microorganisms. *In:* Wittmann, C. and Krull, R. (eds.) *Biosystems Engineering I.* Springer Berlin Heidelberg.

Papoutsakis, E. T. (1984). Equations and calculations for fermentations of butyric-acid bacteria. *Biotechnology and Bioengineering,* 26**,** 174 – 187.

Park, J. H., Lee, S. Y., Kim, T. Y. and Kim, H. U. (2008). Application of systems biology for bioprocess development. *Trends in Biotechnology,* 26**,** 404 – 412.

Piedras, P., Pineda, M., Munoz, J. and Cardenas, J. (1992). Purification and characterization of an L-amino-acid oxidase from Chlamydomonas-reinhardtii. *Planta,* 188**,** 13 – 18.

Pineda, M., Fernandez, E. and Cardenas, J. (1984). Urate oxidase of *chlamydomonas-reinhardii*. *Physiologia Plantarum,* 62**,** 453 – 457.

Pirt, S. J. (1986). Tansley review no-4 - The thermodynamic efficiency (quantum demand) and dynamics of photosynthetic growth. *New Phytologist,* 102**,** 3 – 37.

Pirt, S. J., Lee, Y. K., Richmond, A. and Pirt, M. W. (1980). Photosynthetic efficiency of *Chlorella* biomass growth with reference to solar-energy utilization. *Journal of Chemical Technology and Biotechnology,* 30**,** 25 – 34.

Popescu, C. E. and Lee, R. W. (2007). Mitochondrial genome sequence evolution in chlamydomonas. *Genetics,* 175**,** 819 – 826.

Porra, R. J., Thompson, W. A. and Kriedemann, P. E. (1989). Determination of accurate extinction coefficients and simultaneous-equations for assaying chlorophyll-a and chlorophyll-b extracted with 4 different solvents - verification of the concentration of chlorophyll standards by atomic-absorption spectroscopy. *Biochimica et Biophysica Acta,* 975**,** 384 – 394.

Proschold, T., Harris, E. H. and Coleman, A. W. (2005). Portrait of a species: *Chlamydomonas reinhardtii*. *Genetics,* 170**,** 1601 – 1610.

Puigbo, P., Guzman, E., Romeu, A. and Garcia-Vallve, S. (2007). Optimizer: a web server for optimizing the codon usage of DNA sequences. *Nucleic Acids Research,* 35**,** W126 – W131.

Pulz, O. (2001). Photobioreactors: production systems for phototrophic microorganisms. *Applied Microbiology and Biotechnology,* 57**,** 287 – 293.

Purton, S. (2007). Tools and techniques for chloroplast transformation of *Chlamydomonas*. *In:* Leon, R., Galvan, A. and Fernandez, E. (eds.) *Transgenic Microalgae as Green Cell Factories.* New York, Landes Bioscience and Springer Science+Business Media LLC., 616, 34 – 45.

Quist, D. and Chapela, I. H. (2001). Transgenic DNA introgressed into traditional maize landraces in Oaxaca, Mexico. *Nature,* 414**,** 541 – 543.

Raghunathan, A., Shin, S. and Daefler, S. (2010). Systems approach to investigating host-pathogen interactions in infections with the biothreat agent *Francisella*. Constraints-based model of *Francisella tularensis*. *Bmc Systems Biology,* 4.

Randolphanderson, B. L., Boynton, J. E., Gillham, N. W., Harris, E. H., Johnson, A. M., Dorthu, M. P. and Matagne, R. F. (1993). Further characterization of the respiratory deficient dum-1 mutation of chlamydomonas-reinhardtii and its use as a recipient for mitochondrial transformation. *Molecular & General Genetics,* 236**,** 235 – 244.

Ranganathan, S., Suthers, P. F. and Maranas, C. D. (2010). OptForce: An Optimization Procedure for Identifying All Genetic Manipulations Leading to Targeted Overproductions. *Plos Computational Biology,* 6.

Rasala, B. A., Muto, M., Lee, P. A., Jager, M., Cardoso, R. M. F., Behnke, C. A., Kirk, P., Hokanson, C. A., Crea, R., Mendez, M. and Mayfield, S. P. (2010). Production of therapeutic proteins in algae, analysis of expression of seven human proteins

in the chloroplast of *Chlamydomonas reinhardtii*. *Plant Biotechnology Journal,* 8**,** 719 – 733.

Rebeille, F. and Gans, P. (1988). Interaction between chloroplasts and mitochondria in microalgae - role of glycolysis. *Plant Physiology,* 88**,** 973 – 975.

Reynoso, G. T. and Degamboa, B. A. (1982). Salt tolerance in the fresh-water algae chlamydomonas-reinhardii - effect of proline and taurine. *Comparative Biochemistry and Physiology a-Physiology,* 73**,** 95 – 99.

Rocha, I., Maia, P., Evangelista, P., Vilaca, P., Soares, S., Pinto, J. P., Nielsen, J., Patil, K. R., Ferreira, E. C. and Rocha, M. (2010). OptFlux: an open-source software platform for in silico metabolic engineering. *Bmc Systems Biology,* 4.

Rochaix, J. D. (1995). *Chlamydomonas reinhardtii* as the photosynthetic yeast. *Annual Review of Genetics,* 29**,** 209 – 230.

Rochaix, J. D. (1996). Post-transcriptional regulation of chloroplast gene expression in Chlamydomonas reinhardtii. *Plant Molecular Biology,* 32**,** 327 – 341.

Rochaix, J. D. (2002). The three genomes of *Chlamydomonas*. *Photosynthesis Research,* 73**,** 285 – 293.

Rochaix, J. D., Mayfield, S., Goldschmidt-Clermont, M. & Erickson, J. (1988). Molecular biology of chlamydomonas. *In:* SHAW, C. H. (ed.) *Plant molecular Biology: a practical approach,* Oxford, England, IRL Press Ltd. 253 – 276.

Rokem, J. S., Lantz, A. E. and Nielsen, J. (2007). Systems biology of antibiotic production by microorganisms. *Natural Product Reports,* 24**,** 1262 – 1287.

Rosenberg, J. N., Oyler, G. A., Wilkinson, L. and Betenbaugh, M. J. (2008). A green light for engineered algae: redirecting metabolism to fuel a biotechnology revolution. *Current Opinion in Biotechnology,* 19**,** 430 – 436.

Ruf, S., Karcher, D. and Bock, R. (2007). Determining the transgene containment level provided by chloroplast transformation. *Proceedings of the National Academy of Sciences of the United States of America,* 104**,** 6998 – 7002.

Sager, R. and Granick, S. (1953). Nutritional studies with *Chlamydomonas-reinhardi*. *Annals of the New York Academy of Sciences,* 56**,** 831 – 838.

Salvador, M. L., Suay, L., Anthonisen, I. L. and Klein, U. (2004). Changes in the 5 '-untranslated region of the rbcL gene accelerate transcript degradation more than 50-fold in the chloroplast of *Chlamydomonas reinhardtii*. *Current Genetics,* 45**,** 176 – 182.

Samek, D., Misurcova, L., Machu, L., Bunka, F. and Fisera, M. (2013). Influencing of amino acid composition of green freshwater algae and cyanobacterium by methods of cultivation. *Turkish Journal of Biochemistry-Turk Biyokimya Dergisi,* 38**,** 360 – 368.

Sauer, U., Heinemann, M. and Zamboni, N. (2007). Genetics - Getting closer to the whole picture. *Science,* 316**,** 550 – 551.

Schellenberger, J., Que, R., Fleming, R. M. T., Thiele, I., Orth, J. D., Feist, A. M., Zielinski, D. C., Bordbar, A., Lewis, N. E., Rahmanian, S., Kang, J., Hyduke, D. R. and Palsson, B. O. (2011). Quantitative prediction of cellular metabolism with constraint-based models: the COBRA Toolbox v2.0. *Nature Protocols,* 6**,** 1290 – 1307.
Available: http://opencobra.sourceforge.net/ [Accessed 15 June 2014].

Sedmak, J. J. and Grossberg, S. E. (1977)**. Rapid, sensitive, and versatile assay for protein using coomassie brilliant blue G250.** *Analytical Biochemistry,* 79**,** 544 – 552.

Shachrai, I., Zaslaver, A., Alon, U. and Dekel, E. (2010). Cost of Unneeded Proteins in *E. coil* Is Reduced after Several Generations in Exponential Growth. *Molecular Cell,* 38**,** 758 – 767.

Shepherd, H. S., Boynton, J. E. and Gillham, N. W. (1979). Mutations in 9 chloroplast loci of *chlamydomonas* affecting different photosynthetic functions. *Proceedings of the National Academy of Sciences of the United States of America,* 76**,** 1353 – 1357.

Shimogawara, K., Fujiwara, S., Grossman, A. and Usuda, H. (1998). High-efficiency transformation of Chlamydomonas reinhardtii by electroporation. *Genetics,* 148**,** 1821 – 1828.

Silver, P. A. and Way, J. C. (2007). Molecular systems biology in drug development. *Clinical Pharmacology & Therapeutics,* 82**,** 586 – 590.

Sinclair, C. G., and Kristiansen, B. (1987). *Fermentation kinetics and modelling,* Milton Keyes, Open University Press, 1 – 113.

Snoep, J. L., Van Der Weijden, C. C., Andersen, H. W., Westerhoff, H. V. and Jensen, P. R. (2002). DNA supercoiling in *Escherichia coli* is under tight and subtle homeostatic control, involving gene-expression and metabolic regulation of both topoisomerase I and DNA gyrase. *European Journal of Biochemistry,* 269**,** 1662 – 1669.

Snoep, J. L., Yomano, L. P., Westerhoff, H. V. and Ingram, L. O. (1995). Protein burden in Zymomonas mobilis: negative flux and growth control due to overproduction of glycolytic enzymes. *Micobiology,* 141, 2329 – 2337.

Sonnleitner, B., Locher, G. and Fiechter, A. (1992). Biomass determination. *Journal of Biotechnology,* 25**,** 5 – 22.

Sookoian, S. and Pirola, C. J. (2013). Systems Biology Elucidates Common Pathogenic Mechanisms between Nonalcoholic and Alcoholic-Fatty Liver Disease. *Plos One,* 8.

Staub, J. M., Garcia, B., Graves, J., Hajdukiewicz, P. T. J., Hunter, P., Nehra, N., Paradkar, V., Schlittler, M., Carroll, J. A., Spatola, L., Ward, D., Ye, G. N. and Russell, D. A. (2000). High-yield production of a human therapeutic protein in tobacco chloroplasts. *Nature Biotechnology,* 18**,** 333 – 338.

Samek, D., Misurcova, L., Machu, L., Bunka, F. and Fisera, M. (2013). Influencing of amino acid composition of green freshwater algae and cyanobacterium by methods of cultivation. *Turkish Journal of Biochemistry,* 38, 360 – 368.

Stouthamer, A. H. (1979). The search for correlation between theoretical and experimental growth yields. *In:* Quayle, J. R. (ed.) *International Review of Biochemistry,* Baltimore, University Park Press, 21, 1 - 47.

Su, Z. L., Qian, K. X., Tan, C. P., Meng, C. X. and Qin, S. (2005). Recombination and heterologous expression of allophycocyanin gene in the chloroplast of *Chlamydomonas reinhardtii*. *Acta Biochimica et Biophysica Sinica,* 37**,** 709 – 712.

Suay, L., Salvador, M. L., Abesha, E. and Klein, U. (2005). Specific roles of 5 ' RNA secondary structures in stabilizing transcripts in chloroplasts. *Nucleic Acids Research,* 33**,** 4754 – 4761.

Sueoka, N. (1960). Mitotic replication of deoxyribonucleic acid in *Chlamydomonas reinhardi*. *Proceedings of the National Academy of Sciences of the United States of America,* 46**,** 83 – 91.

Sugita, M. and Sugiura, M. (1996). Regulation of gene expression in chloroplasts of higher plants. *Plant Molecular Biology,* 32**,** 315 – 326.

Surzycki, R., Greenham, K., Kitayama, K., Dibal, F., Wagner, R., Rochaix, J.-D., Ajam, T. and Surzycki, S. (2009). Factors effecting expression of vaccines in microalgae. *Biologicals,* 37**,** 133 – 138.

Syrett, P. J. (1962). Nitrogen assimilation. *In:* LEWIN, R. A. (ed.) *Physiology and Biochemistry of Algae,* New York, Academic Press, 171 – 188.

Tam, L. W. and Lefebvre, P. A. (1993). Cloning of flagellar genes in *Chlamydomonas-reinhardtii* by DNA insertional mutagenesis. *Genetics,* 135**,** 375 – 384.

Tang, I. C., Okos, M. R. and Yang, S. T. (1989). Effects of pH and acetic-acid on homoacetic fermentation of lactate by clostridium-formicoaceticum. *Biotechnology and Bioengineering,* 34**,** 1063 – 1074.

Taylor, T. C., Backlund, A., Bjorhall, K., Spreitzer, R. J. and Andersson, I. (2001). First crystal structure of rubisco from a green alga, *Chlamydomonas reinhardtii*. *Journal of Biological Chemistry,* 276**,** 48159 – 48164.

Ter Kuile, B. H. and Westerhoff, H. V. (2001). Transcriptome meets metabolome: hierarchical and metabolic regulation of the glycolytic pathway. *Febs Letters,* 500**,** 169 – 171.

Terry, K. L. and Raymond, L. P. (1985). System-design for the autotrophic production of microalgae. *Enzyme and Microbial Technology,* 7**,** 474 – 487.

Thacker, A. and Syrett, P. J. (1972). Assimilation of nitrate and ammonium by *Chlamydomonas-reinhardi*. *New Phytologist,* 71**,** 423 – 433.

Ullrich, W. R., Larsson, M., Larsson, C. M., Lesch, S. and Novacky, A. (1984). Ammonium uptake in lemna-gibba g-1, related membrane-potential changes, and inhibition of anion uptake. *Physiologia Plantarum,* 61**,** 369 – 376.

Vaistij, F. E., Goldschmidt-Clermont, M., Wostrikoff, K. and Rochaix, J. D. (2000). Stability determinants in the chloroplast psbB/T/H mRNAs of *Chlamydomonas reinhardtii*. *Plant Journal,* 21**,** 469 – 482.

Vallon, O., Bulte, L., Kuras, R., Olive, J. and Wollman, F. A. (1993). Extensive accumulation of an extracellular L-amino-acid oxidase during gametogenesis of Chlamydomonas-reinhardtii. *European Journal of Biochemistry,* 215**,** 351 – 360.

Varma, A. and Palsson, B. O. (1994). Metabolic flux balancing - basic concepts, scientific and practical use. *Bio-Technology,* 12**,** 994 – 998.

Villoslada, P., Steinman, L. and Baranzini, S. E. (2009). Systems Biology and Its Application to the Understanding of Neurological Diseases. *Annals of Neurology,* 65**,** 124 – 139.

Vitova, M., Bisova, K., Hlavova, M., Kawano, S., Zachleder, V. and Cizkova, M. (2011). *Chlamydomonas reinhardtii*: duration of its cell cycle and phases at growth rates affected by temperature. *Planta,* 234**,** 599 – 608.

Wagner, A. & Fell, D. A. (2001). The small world inside large metabolic networks. *Proceedings of the Royal Society B-Biological Sciences,* 268**,** 1803 – 1810.

Walker, T. L., Purton, S., Becker, D. K. and Collet, C. (2005). Microalgae as bioreactors. *Plant Cell Reports,* 24**,** 629 – 641.

Wang, X., Brandsma, M., Tremblay, R., Maxwell, D., Jevnikar, A. M., Huner, N. and Ma, S. (2008). A novel expression platform for the production of diabetes-associated autoantigen human glutamic acid decarboxylase (hGAD65). *Bmc Biotechnology*, 8.

Weissman, J. C., Goebel, R. P. & Benemann, J. R. (1988). Photobioreactor design - mixing, carbon utilization, and oxygen accumulation. *Biotechnology and Bioengineering*, 31**,** 336 – 344.

Westerhoff, H. V. and Alberghina, L. (2005). Systems Biology: Did we know it all along? *In:* Alberghina, L. and Westerhoff, H. V. (eds.) *Systems Biology: Definitions and Perspectives.* Berlin, Springer-Verlag, 3 – 9.

Winder, C. L., Dunn, W. B., Schuler, S., Broadhurst, D., Jarvis, R., Stephens, G. M. and Goodacre, R. 2008. Global metabolic profiling of *Escherichia coli* cultures: An evaluation of methods for quenching and extraction of intracellular metabolites. *Analytical Chemistry*, 80**,** 2939 – 2948.

Woessner, J. P., Masson, A., Harris, E. H., Bennoun, P., Gillham, N. W. & Boynton, J. E. (1984). Molecular and genetic-analysis of the chloroplast atpase of *Chlamydomonas*. *Plant Molecular Biology*, 3**,** 177 – 190.

Yang, H., Roth, C. M. and Ierapetritou, M. G. (2009). A Rational Design Approach for Amino Acid Supplementation in Hepatocyte Culture. *Biotechnology and Bioengineering*, 103**,** 1176 – 1191.

Zuo, Z., Rong, Q., Chen, K., Yang, L., Chen, Z., Peng, K., Zhu, Y., Bai, Y. and Wang, Y. (2012). Study of amino acids as nitrogen source in Chlamydomonas reinhardtii. *Phycological Research*, 60**,** 161 – 168.

Appendix I – Standard calibration curves

(a)

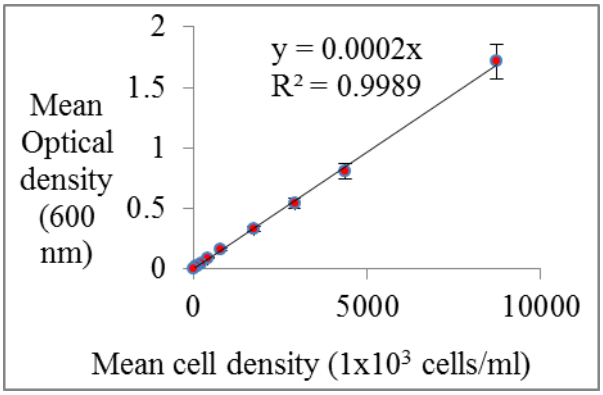

(b)

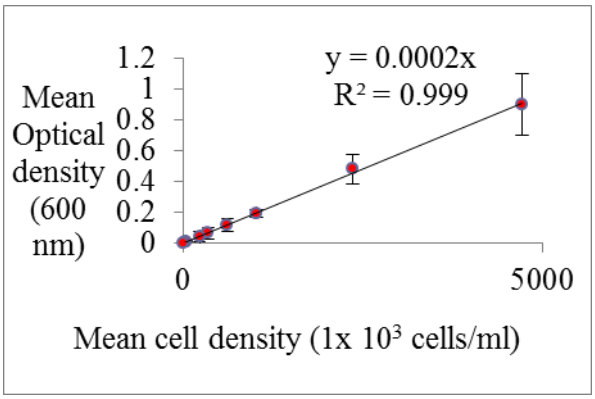

(c)

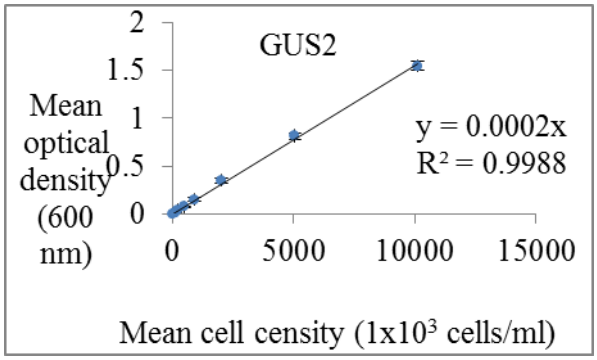

(d)

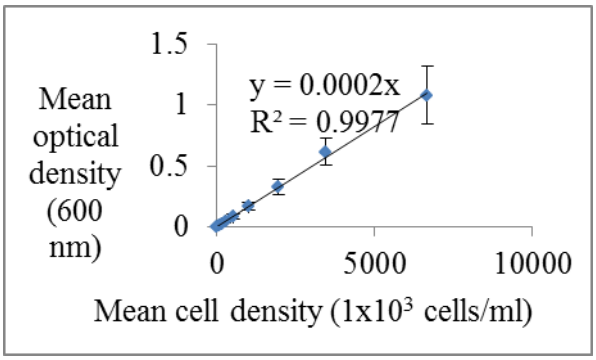

(e)

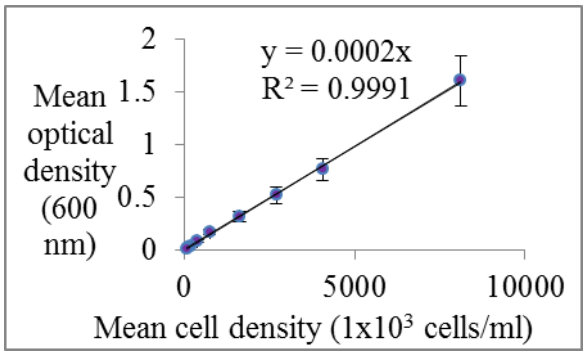

Figure A1.1: Standard calibration of optical density at 600 nm and cell density (cells/ml) of mixotrophic cultures: (a) X6L, (b) D6L, (c) cc621 mt- , (d) GUS12-2, and (e) GUS12-B. The mean values and standard deviation were determined from three biological replicates and two technical replicates each.

(a)

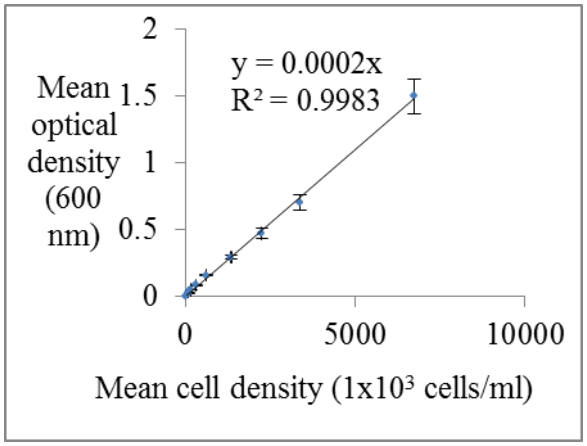

(b)

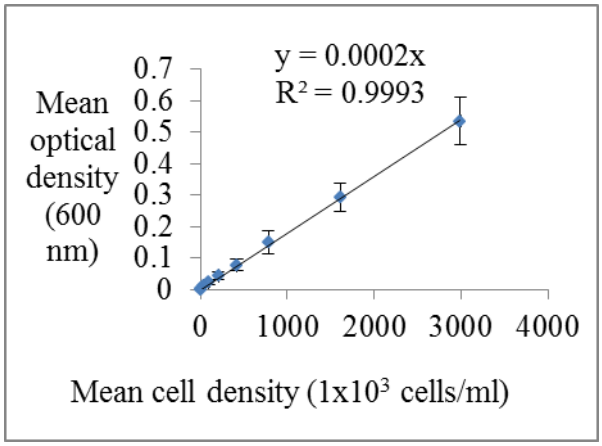

(c)

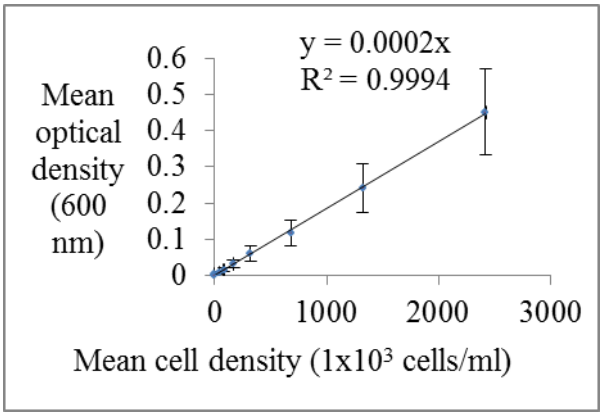

(d)

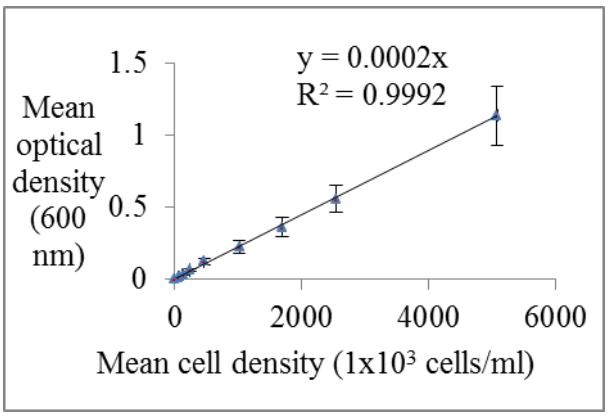

Figure A1.2: Standard calibration of optical density at 600 nm and cell density (cells/ml) of autotrophic cultures: (a) X6L, (b) D6L, (c) Gus12-2, and (d) Gus12-B. The mean values and standard deviation were determined from three biological replicates and two technical replicates each.

(a)

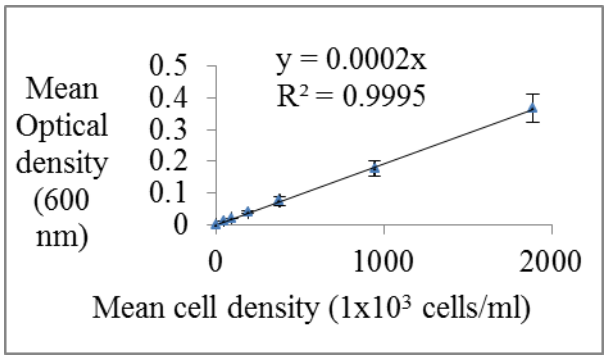

(b)

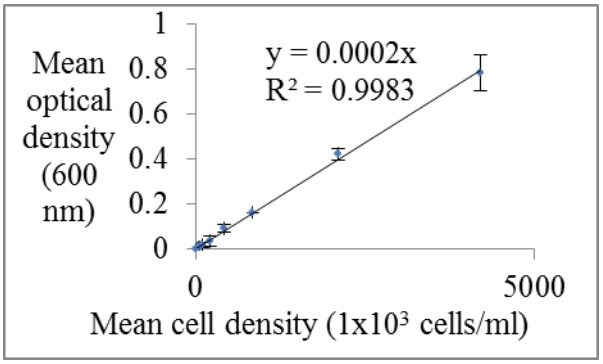

(c)

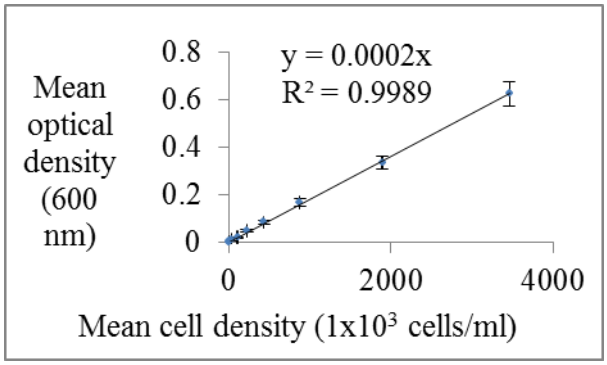

(d)

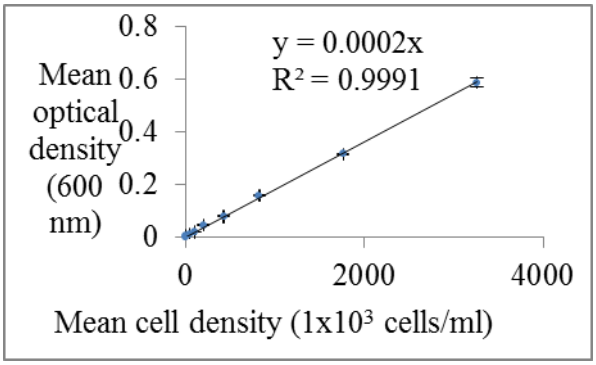

(e)

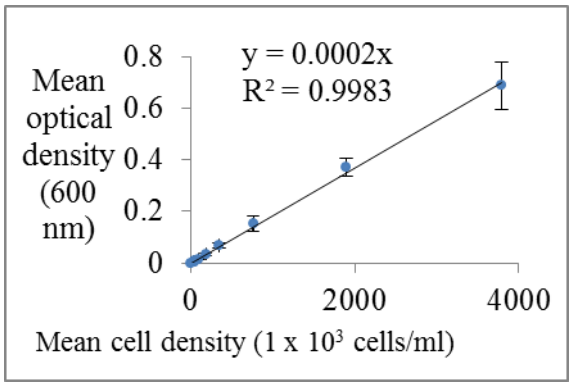

(f)

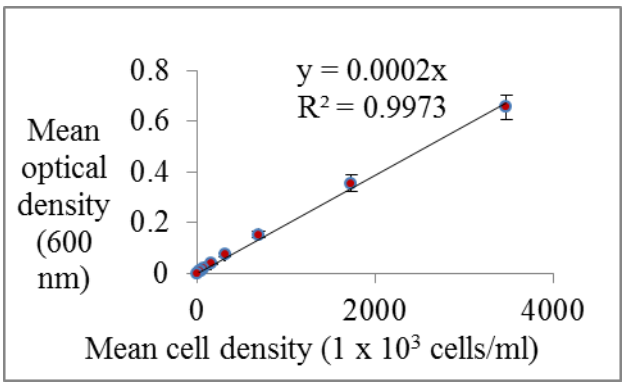

Figure A1.3: Standard calibration of optical density at 600 nm and cell density (cells/ml) of heterotrophic cultures: (a) cc373mt+, (b) cc621 mt-, (c) Gus12-2, (d) Gus12-B, (e) X6L, and (f) D6L. The mean values and standard deviation were determined from three biological replicates and two technical replicates each.

Appendix II – Semi-log growth curves

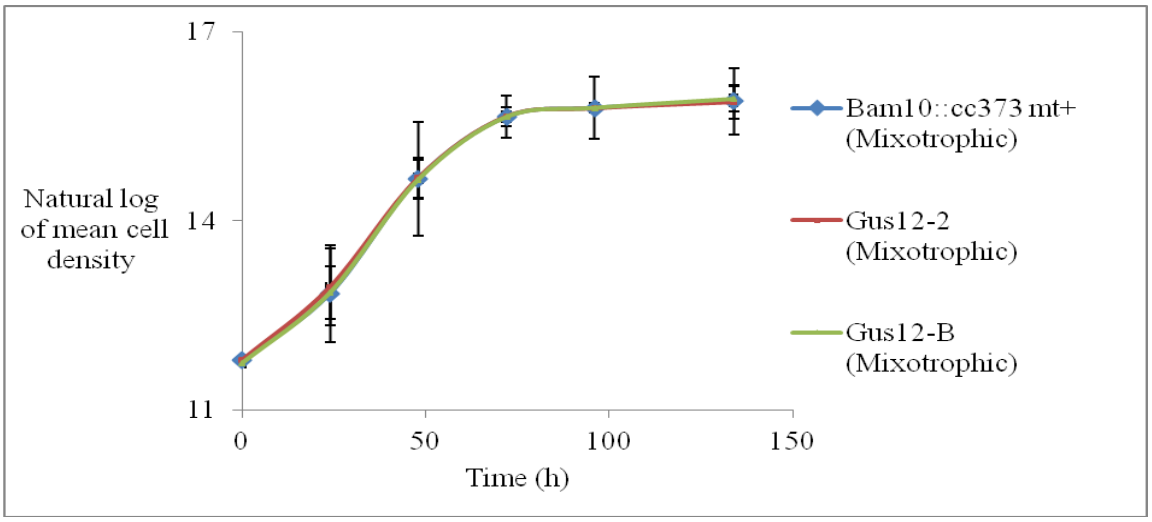

Figure A2.1: Mixotrophic cultures of Bam10::cc373 mt+, Gus12-2 and Gus12-B grown in TAP medium at 54 µmol photons/m^2/s. The mean cell density was determined for six biological replicates and two technical replicates each.

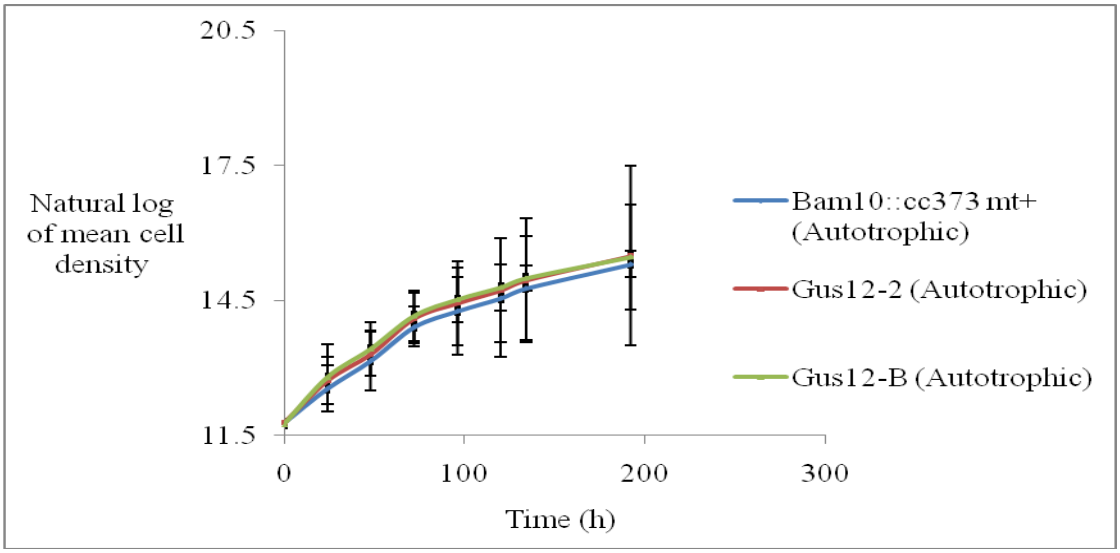

Figure A2.2: Autotrophic cultures of Bam10::cc373 mt+, Gus12-2 and Gus12-B grown in minimal medium at 54 µmol photons/m^2/s. The mean cell density was determined for six biological replicates and two technical replicates each.

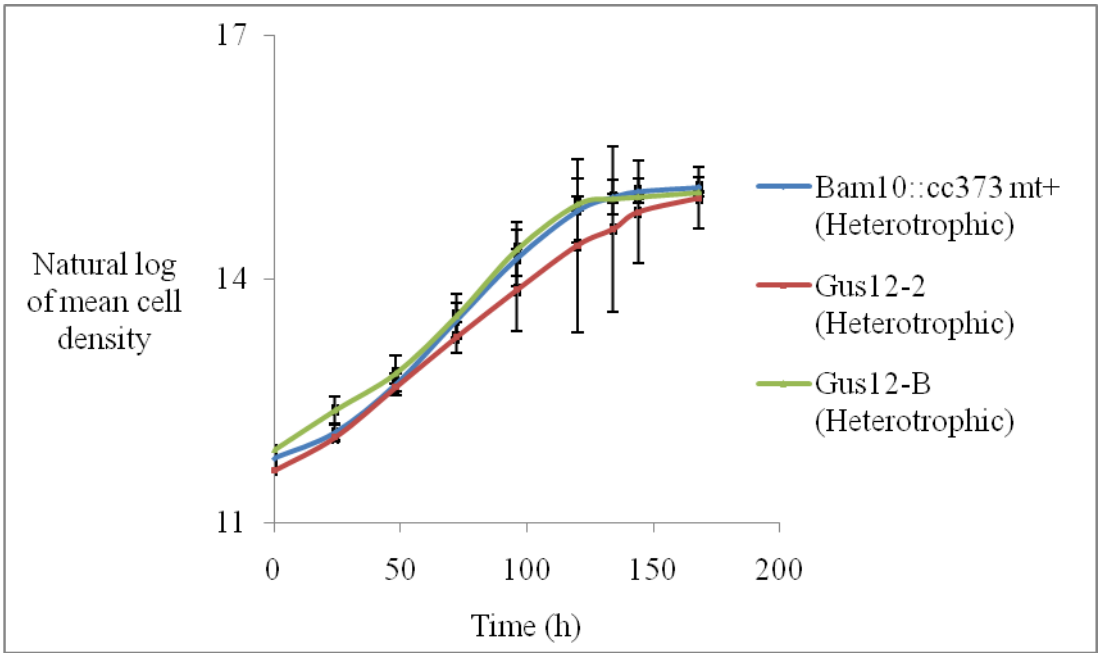

Figure A2.3: Heterotrophic cultures of Bam10::cc373 mt+, Gus12-2 and Gus12-B grown in TAP medium in the dark. The mean cell density was determined for six biological replicates and two technical replicates each.

Appendix III– Correlations

Table A3.1: Total number of carbon atoms provided by amino acids in gus, rubisco and ferroxidase. The abundance of each amino acid in the protein sequences are shown in Table 6.3b.

GUS		RUBISCO		FERROXIDASE	
Amino acids	Total number of carbon atoms	**Amino acids**	Total number of carbon atoms	**Amino acids**	Total number of carbon atoms
Cysteine	27	Cysteine	30	Cysteine	39
Methionine	65	Serine	45	Glutamine	165
Serine	75	Glutamine	50	Histidine	186
Glycine	92	Asparagine	56	Tryptophan	187
Asparagine	112	Methionine	65	Methionine	195
Histidine	114	Histidine	78	Asparagine	196
Proline	120	Tryptophan	88	Serine	216
Alanine	138	Glycine	98	Glycine	218
Threonine	140	Proline	100	Lysine	228
Aspartate	160	Threonine	116	Glutamate	240
Glutamine	160	Aspartate	120	Isoleucine	246
Lysine	162	Isoleucine	126	Arginine	264
Isoleucine	174	Alanine	135	Phenylalanine	288
Arginine	174	Glutamate	150	Aspartate	296
Glutamate	200	Lysine	162	Proline	305
Tryptophan	209	Phenylalanine	171	Threonine	336
Tyrosine	216	Tyrosine	171	Alanine	360
Phenylalanine	225	Valine	175	Leucine	438
Leucine	240	Arginine	186	Tyrosine	468
Valine	265	leucine	222	Valine	560
TOTAL	**3068**		**2344**		**5431**

The experimental gus yield was correlated from units of (g gus protein/ g dry cell wt) into units of (g carbon in gus/ g carbon) for comparison with FBA gus yield. There are 603 amino acid residues in gus protein (Jefferson et al., 1986). The number of carbon, hydrogen, oxygen, nitrogen, sulphur atoms that make up each amino acid residue of gus protein is shown in Table A3.2.

Table A3.2: Number of carbon, hydrogen, oxygen, nitrogen, sulphur atoms in each amino acid residue of gus protein sequence.

		Number of atoms per amino acid residue				
Amino Acids	Number of amino acid residues	Carbon	Hydrogen	Oxygen	Nitrogen	Sulphur
Alanine	46	3	7	2	1	
Arginine	29	6	14	2	3	
Asparagine	28	4	8	3	2	
Aspartate	40	4	6	4	1	
Cysteine	9	3	6	2	1	1
Glutamine	32	5	10	3	2	
Glutamate	40	5	8	4	1	
Glycine	46	2	5	2	1	
Histidine	19	6	9	2	3	
Isoleucine	29	6	13	2	1	
Leucine	40	6	13	2	1	
Lysine	27	6	15	2	2	
Methionine	13	5	11	2	1	1
Phenylalanine	25	9	11	2	1	
Proline	24	5	9	2	1	
Serine	25	3	7	3	1	
Threonine	35	4	9	3	1	
Tryptophan	19	11	12	2	2	
Tyrosine	24	9	11	3	1	
Valine	53	5	11	2	1	
TOTAL	**603**					

This was used to calculate the empirical formular of gus protein normalised to one carbon mole (C_1 $H_{1.494}$ $O_{0.2959}$ $N_{0.2624}$ $S_{0.0071}$). The empirical formular was used to calculate the empirical molecular weight 17.92g/mol carbon. The empirical formular of microalgae biomass normalised to one carbon mole were determined and reported as C_1 $H_{1.80}$ $O_{0.432}$ $N_{0.143}$ with empirical molecular weight of 22.714 g/mol carbon by Pirt et al. (1980); and C_1 $H_{1.83}$ $O_{0.48}$ $N_{0.11}$ $P_{0.01}$ with empirical molecular weight of 23.36 g/mol carbon by Grobbelaar (2003). The results from these authors were consistent, with carbon making up between 53% and 51% of dry microalgae biomass respectively. The value reported by Pirt et al (1980) was used for *C. reinhardtii* (the microalgae) in this thesis.

Since the empirical molecular formular of gus protein and microalgae biomass (17.92 g/mol carbon and 22.714 g/mol carbon respectively) contain one carbon mole each, the experimental gus yield was converted into unit of g carbon in gus/g total carbon in equation A3.1:

$$\left(\frac{g\ gus}{g\ dry\ weight}\right) * \left(\frac{17.92\ mole\ carbon}{22.714\ mole\ carbon}\right) \qquad \text{A3.1}$$

Table A3.3: The experimental gus yield in units of g gus protein/g dry wt were correlated into units of g carbon in gus/g total carbon. The mean values of experimental measured gus yield and standard deviation were determined from six biological replicates and two technical replicates each from Gus12-2 in heterotrophic, autotrophic and mixotrophic conditions.

Growth Condition	Mean Experimental yield ± sd (g gus /g dry wt) x 10^{-4}	Mean Experimental yield ± sd (g carbon in gus/g total carbon) x 10^{-4}
Heterotrophic	2.66 ± 0.45	2.10 ± 0.36
Autotrophic	3.20 ± 0.69	2.53 ± 0.55
Mixotrophic	3.75 ± 0.71	2.96 ± 0.56

Appendix IV– Commands to run Cobra Scripts

The Cobra Toolbox version 2.0 (Schellenberger et al., 2011) was freely downloaded from http://opencobra.sourceforge.net/ and used in the Matlab environment. Flux balance analysis simulations were performed using the Cobra tool box software running in MatLab environment. The Cobra Toolbox incorporates a linear programing solver (glpk), the sbml library (libsbml) and the sbml Toolbox for the analysis and simulation of the sbml models within MatLab. The following commands were used to execute the main tasks at the core of the *in silico* analysis presented in this thesis. Each command invokes either a Cobra script, or an in-house written script (i.e. a script that was written to address specific concerns). The code of the in-house written script is provided at the end of Appendix IV.

Loading the model in MatLab

```
% This invokes a Cobra script
CbA = loadCbModel();
```

This command allows the user to browse the file-system for the sbml file containing the metabolic reconstruction of interest (in our case AlgaGEM.xml). The sbml file is loaded and converted in a MatLab structure (CbA).

Pre-processing the model

```
CbA.id = 'AlgaGEM';
```

This command adds an identification field to the model (the MatLab structure CbA). Such identification was necessary for some further steps along the analysis that are dependent on the specifics of the model.

Re-orienting the exchange reactions

It is good practice to have the exchange reactions oriented from the inside to the outside of the system. The reason is that, by doing so, the uptake of a nutrient will be characterized by

a negative flux and the secretion of a product by a positive flux. This sign convention is consistent with the measurement of the species' concentrations in the extracellular environment. For example the uptake of acetate is detected because of a negative change of its level in the growing medium, while the secretion of target protein is characterised by a positive change of its level. The command to re-orientate the exchange reactions is:

```
% This invokes an in-house written script
CbA = revertExchRxns (CbA);
```

The model CbA will now have the exchange reactions properly oriented.

Adding the recombinant protein to the model

A reaction accounting for the production of the target protein needs to be added to the model. This was done in three main steps. First, the list of bounded tRNA, unbounded tRNA and the GDP/GTP/Pi moiety has to be retrieved from the model. This was done by executing the following command:

```
% This invokes an in-house written script
[tRNA_AA, tRNA, GTP_GDP_P] = retrieve_tRNA_AA_GXP(CbA);
```

Secondly, the composition of the target protein (e.g. recombinant protein composition) will be loaded from a text file. This was done by executing the command:

```
% This invokes an in-house written script
[ProtComp, warn] = retrieveProteinComposition ();
```

Finally, the reaction accounting for the production of the target protein was added to the model. This was done by executing the command:

```
% This invokes an in-house written script
CbA = AddProteinProduction(CbA, tRNA, tRNA_AA, GTP_GDP_P,
ProtComp);
```

Defining the growing medium

The growing medium was defined *in silico* by specifying a set of nutrients that are allowed to enter the system. For such nutrients, the corresponding transport (exchange) reactions were allowed to carry a negative flux by adjusting their lower bound.

The general command was the following:

```
CbA.lb(reaction_index) = -Inf;
```

where reaction_index is the index that the reaction of interest has in the model. The list of transport (exchange) reactions and their reaction index in the cobra model (CbA) are shown in Table 3.2.

Using experimental values

To find a flux pattern representative of the genome-scale metabolic trafficking under specific condition, we fixed the flux value of some exchange reactions to its corresponding experimental value. This was done by setting both the upper bound (ub) and lower bound (lb) of such reactions using the following commands:

```
CbA.lb(reaction_index) = experimental_value;
CbA.ub(reaction_index) = experimental_value;
```

Making predictions on the protein production

To predict the protein production rate we first set the objective function so as to coincide with the rate of the corresponding added reaction:

```
CbA.c(find(CbA.c ~= 0)) = 0;
CbA.c(target_protein_reaction_index) = 1;
```

The field, **c** of the model CbA is a vector containing the weights of each reaction in the objective function. Such weights were all set to zero, apart from the weight corresponding to the production of the target protein which was set to 1. Secondly an FBA was run through the following command:

```
% This invokes a COBRA script
FBAsolution = optimizeCbModel(CbA,'max');
```

FBAsolution is a MatLab structure containing all the relevant information of the FBA solution, such as the optimal value of the objective function (in our case the maximal theoretical rate of the target protein production) and the corresponding flux pattern. The theoretical maximal protein production rate can be performed whether (some of) the exchange fluxes have been set to their experimental value or not. Of course, the interpretation of the FBA solution is different in the two cases.

Codes of the in-house written scripts

revertExchRxns.m

```
function CbModel = revertExchRxns (CbModel)

% Turn the exchange reactions inside -> out

for j = 1:length(CbModel.rxns)
    reactants = find(CbModel.S(:,j) < 0);
    if isempty(reactants)
        CbModel.S(:,j) = -CbModel.S(:,j);
        aux = CbModel.ub(j);
        CbModel.ub(j) = -CbModel.lb(j);
        CbModel.lb(j) = -aux;
    end
end
```

retrieve_tRNA_AA_GXP.m

```
function [tRNA_AA, tRNA, GTP_GDP_P] = retrieve_tRNA_AA_GXP(Model)
```

```
    tRNA_AA = containers.Map;
    tRNA = containers.Map;
    GTP_GDP_P = containers.Map;

    switch(Model.id)

        case 'ymn' % S. cerevisiae (yeast 7.0)
            % Code not reported

        case 'ecmn' % E. coli
            % Code not reported

        case 'CHOmn' % CHO cells
            % Code not reported

        case 'iLC915' % P. pastoris
            % Code not reported

        case 'algaGEM' % AlgaGEM

            tRNA_AA('A') = 'S_L_45_Alanyl_45_tRNA[c]';
            tRNA_AA('R') = 'S_L_45_Arginyl_45_tRNA_40_Arg_41_[c]';
            tRNA_AA('N') = ...
'S_L_45_Asparaginyl_45_tRNA_40_Asn_41_[c]';
            tRNA_AA('D') = 'S_L_45_Aspartyl_45_tRNA_40_Asp_41_[c]';
            tRNA_AA('C') = 'S_L_45_Cysteinyl_45_tRNA_40_Cys_41_[c]';
            tRNA_AA('Q') = 'S_L_45_Glutamyl_45_tRNA_40_Gln_41_[c]';
            tRNA_AA('E') = 'S_L_45_Glutamyl_45_tRNA_40_Glu_41_[c]';
            tRNA_AA('G') = 'S_Glycyl_45_tRNA_40_Gly_41_[c]';
            tRNA_AA('H') = 'S_L_45_Histidyl_45_tRNA_40_His_41_[c]';
            tRNA_AA('I') = 'S_L_45_Isoleucyl_45_tRNA_40_Ile_41_[c]';
            tRNA_AA('L') = 'S_L_45_Leucyl_45_tRNA[c]';
```

```
                tRNA_AA('K') = 'S_L_45_Lysyl_45_tRNA_40_Lys_41_[c]';
                tRNA_AA('M') = 'S_L_45_Methionyl_45_tRNA[c]';
                tRNA_AA('F') = ...
                           'S_L_45_Phenylalanyl_45_tRNA_40_Phe_41_[c]';
                tRNA_AA('P') = 'S_L_45_Prolyl_45_tRNA_40_Pro_41_[c]';
                tRNA_AA('S') = 'S_L_45_Seryl_45_tRNA_40_Ser_41_[c]';
                tRNA_AA('T') = 'S_L_45_Threonyl_45_tRNA_40_Thr_41_[c]';
                tRNA_AA('W') = ...
'S_L_45_Tryptophanyl_45_tRNA_40_Trp_41_[c]';
                tRNA_AA('Y') = 'S_L_45_Tyrosyl_45_tRNA_40_Tyr_41_[c]';
                tRNA_AA('V') = 'S_L_45_Valyl_45_tRNA_40_Val_41_[c]';


                tRNA('A') = 'S_tRNA_40_Ala_41_[c]';
                tRNA('R') = 'S_tRNA_40_Arg_41_[c]';
                tRNA('N') = 'S_tRNA_40_Asn_41_[c]';
                tRNA('D') = 'S_tRNA_40_Asp_41_[c]';
                tRNA('C') = 'S_tRNA_40_Cys_41_[c]';
                tRNA('Q') = 'S_tRNA_40_Gln_41_[c]';
                tRNA('E') = 'S_tRNA_40_Glu_41_[c]';
                tRNA('G') = 'S_tRNA_40_Gly_41_[c]';
                tRNA('H') = 'S_tRNA_40_His_41_[c]';
                tRNA('I') = 'S_tRNA_40_Ile_41_[c]';
                tRNA('L') = 'S_tRNA_40_Leu_41_[c]';
                tRNA('K') = 'S_tRNA_40_Lys_41_[c]';
                tRNA('M') = 'S_tRNA_40_Met_41_[c]';
                tRNA('F') = 'S_tRNA_40_Phe_41_[c]';
                tRNA('P') = 'S_tRNA_40_Pro_41_[c]';
                tRNA('S') = 'S_tRNA_40_Ser_41_[c]';
                tRNA('T') = 'S_tRNA_40_Thr_41_[c]';
                tRNA('W') = 'S_tRNA_40_Trp_41_[c]';
                tRNA('Y') = 'S_tRNA_40_Tyr_41_[c]';
                tRNA('V') = 'S_tRNA_40_Val_41_[c]';
```

```
            GTP_GDP_P('GTP') = 'S_GTP[c]';
            GTP_GDP_P('GDP') = 'S_GDP[c]';
            GTP_GDP_P('PI') = 'S_Orthophosphate[c]';

        otherwise

            fprintf('Model %s is not currently available',Model.id);
    end
```

retrieveProteinComposition.m

```
function [ProtComp,warn] = retrieveProteinComposition()

% Select the file containing the AA composition of the protein
[FileName,PathName,~] = ...
    uigetfile('.txt','Chose the file containing the amino-acid
sequence');
fileID = fopen([PathName,FileName]);

% Extract the content of the file.
C = textscan(fileID,'%c');
C = C{1};
C = (C(:))';

% Check the file is well formatted
warn = [];
AA = regexp(C,'([^A-Z]+)','tokens','lineanchors');
if ~isempty(AA)
    warn = 'Invalid file';
end
```

AddProteinProduction.m

```
% This function will check the amino acid sequence of the
% recombinant protein (ProtComp) and add a new reaction to
% the COBRA model that accounts for the production of the
% target protein.

function CbModel =
AddProteinProduction(CbModel,tRNA,tRNA_AA,GTP_GDP_P,ProtComp)

Aminoacids = ['A','R','N','D','C','Q','E','G','H','I' ...
              'L','K','M','F','P','S','T','W','Y','V'];

%-------------------------------------------------------------
% Preparing the COBRA model (CbModel) to host the
% recombinant protein production pseudo-reaction.

CbModel.rxns{end+1} = 'RPPbyUser';
CbModel.rev(end+1) = 0;
CbModel.lb(end+1) = 0;
CbModel.ub(end+1) = +Inf;
CbModel.rules(end+1) = CbModel.rules(end);
CbModel.genes{end+1} = 'RPPGene';
CbModel.grRules{end+1} = 'RPPGene';
CbModel.rxnGeneMat(length(CbModel.rxns),length(CbModel.genes)) = 1;
CbModel.rxnNames{end+1} = 'RPPbyUser';
CbModel.subSystems{end+1} = {};

if (isfield(CbModel, 'rxnReferences'))
  CbModel.rxnReferences{end+1} = '';
End

if (isfield(CbModel, 'rxnECNumbers'))
```

```
  CbModel.rxnECNumbers{end+1} = '';
End

if (isfield(CbModel, 'rxnNotes'))
  CbModel.rxnNotes{end+1} = '';
end

CbModel.c(end+1) = 0;



%-------------------------------------------------------------
% Setting the stoichiometry of the new reaction
% based on the protein composition (ProtComp)

SumGTP = 0;

for i=1:length(Aminoacids)

    % Checking the number of occurrances of aminoacid i
    % in the protein sequence
    AA_indexes = strfind(ProtComp,Aminoacids(i));
    if isempty(AA_indexes)
        AAOccurrencies = 0;
    else
        AAOccurrencies = length(AA_indexes);
    end
    SumGTP = SumGTP + AAOccurrencies;

    % retrieve the index of tRNA(i)
    if ~isempty(tRNA)
        tRNA_id = tRNA(Aminoacids(i));
        matches = strcmp(tRNA_id,CbModel.mets);
```

```
        [~,tRNA_index] = ismember(1,matches);
        CbModel.S(tRNA_index,length(CbModel.rxns)) = AAOccurrencies;
    end

    % retrieve the index of tRNA_AA(i)
    tRNA_AA_id = tRNA_AA(Aminoacids(i));
    matches = strcmp(tRNA_AA_id,CbModel.mets);
    [~,tRNA_AA_index] = ismember(1,matches);
    CbModel.S(tRNA_AA_index,length(CbModel.rxns)) = -AAOccurrencies;

end

% Retrieving the index of GTP, GDP and Pi
GTP_id = GTP_GDP_P('GTP');
GDP_id = GTP_GDP_P('GDP');
PI_id = GTP_GDP_P('PI');

matches = strcmp(GTP_id,CbModel.mets);
[~,GTP_index] = ismember(1,matches);
matches = strcmp(GDP_id,CbModel.mets);
[~,GDP_index] = ismember(1,matches);
matches = strcmp(PI_id,CbModel.mets);
[~,PI_index] = ismember(1,matches);

CbModel.S(GTP_index,length(CbModel.rxns)) = -SumGTP;
CbModel.S(GDP_index,length(CbModel.rxns)) = SumGTP;
CbModel.S(PI_index,length(CbModel.rxns)) = SumGTP;
```